JOINT TRANSPORTATION
RESEARCH PROGRAM
INDIANA DEPARTMENT OF TRANSPORTATION
AND PURDUE UNIVERSITY

Development of SPT-Torque Test Correlations for Glacial Till

Monica Prezzi, Seth Scheilz, Rodrigo Salgado, Nayyar Zia Siddiki

SPR-3317 • Report Number: FHWA/IN/JTRP-2014/05 • DOI: 10.5703/1288284315499

RECOMMENDED CITATION

Prezzi, M., Scheilz, S., Salgado, R., & Siddiki, N. Z. (2014). *Development of SPT-torque test correlations for glacial till* (Joint Transportation Research Program Publication No. FHWA/IN/JTRP-2014/05). West Lafayette, IN: Purdue University. http://dx.doi.org/10.5703/1288284315499

AUTHORS

Monica Prezzi, PhD
Professor of Civil Engineering
Lyles School of Civil Engineering
Purdue University
(765) 494-5034
mprezzi@purdue.edu
Corresponding Author

Rodrigo Salgado, PhD
Professor of Civil Engineering
Lyles School of Civil Engineering
Purdue University

Seth Scheilz
Graduate Research Assistant
Lyles School of Civil Engineering
Purdue University

Nayyar Zia Siddiki, PhD, PE
Geotechnical Operations Manager
Division of Geotechnical Services
Indiana Department of Transportation

ACKNOWLEDGMENTS

This research was funded with the support provided by the Indiana Department of Transportation through the Joint Transportation Research Program at Purdue University. The authors would like to thank the agency for the support. The authors are very grateful for the support received from the Project Administrator Samy Noureldin and the Study Advisory Committee, composed of Athar Khan, Tom Harris, Nayyar Zia, Malek Smadi, and Keith Hoernschemeyer, throughout the duration of the project and for their valuable comments and suggestions. Special thanks are also due to Jonathan Paauwe and Joey Franzino and the INDOT drilling crew, Dennis Torrance, Steve Dubac, and Marsell Smith, for their incredible help and support throughout the duration of this project and for performing the in situ tests required for this project. Thanks are also due to Nayyar Zia and Athar Khan for their support and valuable comments and to our students Hector Flores, Jintae Lee, Yanbei Zhang, and Faraz Tehrani for their help with this research project.

JOINT TRANSPORTATION RESEARCH PROGRAM

The Joint Transportation Research Program serves as a vehicle for INDOT collaboration with higher education institutions and industry in Indiana to facilitate innovation that results in continuous improvement in the planning, design, construction, operation, management and economic efficiency of the Indiana transportation infrastructure. https://engineering.purdue.edu/JTRP/index_html

Published reports of the Joint Transportation Research Program are available at: http://docs.lib.purdue.edu/jtrp/

NOTICE

COPYRIGHT

Print ISBN: 978-1-62260-462-3
ePUB ISBN: 978-1-62260-463-0

TECHNICAL REPORT STANDARD TITLE PAGE

1. Report No.	2. Government Accession No.	3. Recipient's Catalog No.
FHWA/IN/JTRP-2014/05		

4. Title and Subtitle	5. Report Date
Development of SPT-Torque Test Correlations for Glacial Till	June 2014
	6. Performing Organization Code

7. Author(s)	8. Performing Organization Report No.
Monica Prezzi, Seth Scheilz, Rodrigo Salgado, Nayyar Zia Siddiki	FHWA/IN/JTRP-2014/05

9. Performing Organization Name and Address	10. Work Unit No.
Joint Transportation Research Program Purdue University 550 Stadium Mall Drive West Lafayette, IN 47907-2051	11. Contract or Grant No. SPR-3317

12. Sponsoring Agency Name and Address	13. Type of Report and Period Covered
Indiana Department of Transportation State Office Building 100 North Senate Avenue Indianapolis, IN 46204	Final Report
	14. Sponsoring Agency Code

15. Supplementary Notes
Prepared in cooperation with the Indiana Department of Transportation and Federal Highway Administration.

16. Abstract

Torque tests, which are performed immediately after a standard penetration test (SPT), have grown in popularity since its conception in Brazil during the early 1990s. Purdue University developed the first automated torqueing hardware prototype in 2010. SPT, SPT-Torque and cone penetration test (CPT) field testing were performed in glacial till soils at four different sites in northern Indiana and one site in southern Indiana. Index tests were performed for the soil samples collected at each of these sites. Relationships between the torque ratio (the measured torque divided by the corrected SPT blow count) vs. soil type, and unit side resistance vs. normalized SPT blow count (N1,60) and normalized CPT cone resistance (qc,1) were explored for these soils. For saturated clay soils, development of a relationship between unit side resistance and undrained shear strength was also attempted. Reliable correlations based on the torque ratio were not achieved based on the data collected for all the different soils tested. However, reasonably high coefficients of determination were obtained for the normalized equations developed for clays and saturated non-plastic silt. Low coefficients of determination were obtained for saturated and unsaturated sandy soils. The low coefficients of determination values are attributed to the small population dataset for sandy soils and the difficulty of adequately determining the degree of saturation for unsaturated non-plastic soil types due to the soil structure destruction with sampling. Overall, it was found that the relationships are strong for clay and saturated non-plastic silt and it is recommended that further data be collected to continue to strengthen all relationships, especially those for sand and unsaturated non-plastic silt.

17. Key Words	18. Distribution Statement
SPT, torque, SPT-T, glacial till, field testing, correlations, undrained shear strength, side resistance	No restrictions. This document is available to the public through the National Technical Information Service, Springfield, VA 22161.

19. Security Classif. (of this report)	20. Security Classif. (of this page)	21. No. of Pages	22. Price
Unclassified	Unclassified	176	

Form DOT F 1700.7 (8-69)

EXECUTIVE SUMMARY

DEVELOPMENT OF SPT-TORQUE TEST CORRELATIONS FOR GLACIAL TILL

Introduction

The standard penetration test (SPT) is the most commonly used *in situ* test for site investigation. The test procedure consists of driving a standard split-spoon sampler into the ground and measuring the number of blows required for penetration of the sampler at specific depths. Disturbed samples are retrieved and used for soil identification in the field and for performing index tests in the laboratory. Over time, many sources of errors were identified regarding the SPT equipment and testing procedure. The SPT-Torque test (SPT-T) is a modification of the original SPT procedure and consists of rotating the standard sampler while torque is measured after it is driven the required 0.45 meters. Purdue University developed the first automated torqueing hardware prototype in 2010 as part of this INDOT/JTRP-funded research project.

Glacial deposits are found across the majority of the state of Indiana. Glacial till is a highly variable soil due to the type of source material that it is composed of and the vast area that it covers. The developed SPT-Torque equipment was selected by INDOT for use in glacial till soils found within the state of Indiana. By performing torque tests, additional *in situ* data is collected, thereby improving engineering design.

In this research, data collected from side-by-side field testing (SPT, SPT-T and CPT) at various sites in the state of Indiana were used in the development of blow count, torque, and cone resistance correlations for Indiana soils.

Study Objectives

The main objectives of the proposed research were to (1) develop SPT-Torque hardware and software that are compatible with INDOT SPT equipment; (2) collect *in situ* SPT-Torque data for multiple sites composed of glacial till; (3) develop relationships between laboratory and field test data, including cone penetration test results; and (4) properly train INDOT personnel on how to operate the fabricated equipment to reduce site investigation, design, and construction costs to INDOT. The research focused on the development of SPT-T interpretation methods and shear strength correlations for glacial tills, beyond development of the SPT-T equipment itself.

Findings

Development of various correlations between the blow count number, cone resistance, torque ratio, and shear strength were explored based on the data collected for different Indiana soils. Reasonably high coefficients of determination were obtained for the normalized equations developed for clayey soils and saturated non-plastic silt. Low coefficients of determination were obtained for saturated and unsaturated sandy soils. The low coefficients of determination values are attributed to the small population dataset for sandy soils and the difficulty of adequately determining the degree of saturation for unsaturated non-plastic soil types due to the soil structure destruction with sampling. Overall, it was found that the relationships are stronger for clay and saturated non-plastic silt, and hence it is recommended that further data be collected to continue to strengthen all relationships, especially those for sand and unsaturated non-plastic silt.

Implementation

Use of the SPT-T equipment is recommended in connection with SPT site investigations done by INDOT for sites with fine-grained soils for which the developed correlations between torque measurements and shear strength are reliable. Additional data can be collected in the context of INDOT projects to verify and refine the correlations provided in this report. If fabrication of other SPT-T hardware is required by INDOT, improvements can be made to the current SPT-Torque prototype. Use of a more expensive but lighter alloy material can be explored in order to reduce the current size and weight of the hardware while at the same time keeping it sturdy. A storage box could be fabricated to safely transport and store the hardware when not in use by the INDOT drilling crew. A cost-benefit analysis could be done to determine the cost of production of additional SPT-T units versus benefits due to better site investigations and geotechnical design.

CONTENTS

LIST OF TABLES

LIST OF FIGURES

1. INTRODUCTION

1.1 Introduction

The standard penetration test (SPT) is the most commonly used *in situ* test for site investigation. The test procedure consists of counting the number of hammer blows required for penetration of a split-spoon sampler into the ground surface at given depths, and then retrieving disturbed samples that are used for soil identification in the field and for performing index tests in the laboratory. Over time, many sources of errors were identified regarding the SPT equipment and testing procedure. Correction factors are used to alleviate concerns regarding normalization of measurements made with different equipment and operators. Equipment errors are due to different hammer type and efficiency, hammer drop mechanism, sampler type, and borehole diameter. Operating errors are related to how operators use the equipment during testing.

The first SPT-Torque (SPT-T) test was developed in Brazil by Ranzini (1988). Basically, the SPT-T test modified the original SPT procedure by applying a torque at the ground surface after the sampler was driven 0.45 meters. The SPT-T test is similar to the vane shear test in that the testing device is inserted into the ground at the desired depth and rotated while torque is measured at the ground surface. The SPT-T measurements obtained in conjunction with the SPT are used to calculate at each depth the test is performed the resistance offered by the soil surrounding the sampler to the measured torque. When the process of torque measurement is automated, as is the case with the SPT-Torque hardware developed by Purdue University, the human error is removed from the torque test procedure. Therefore, this additional measurement is helpful in the sense that it increases the reliability of the SPT test since the measurement of torque is independent of operator-related factors and of the dynamic processes that influence blow counts. As a result, measurement of torque provides some assurance on the quality of the SPT blow N numbers measured, and permits better estimation of soil properties. The time required to perform SPT-T tests is minimal and does not reduce the productivity of site investigations done using the SPT.

The developed SPT-Torque hardware and software was selected by INDOT for use in glacial till soils found within the state of Indiana. Glacial till soils were formed during the Pleistocene epoch of the Quaternary Period when ice covered up to 30% of the Earth's surface (Milligan, 1976). Glaciers cover approximately 10% of the Earth's surface at the present time. During cooling trends, glaciers moved toward the Equator from the North and South Poles and retreated during warming periods. Most major glacial advances (common names used to identify glacial advances in the United States: Nebraskan, Kansan, Illinoian, and Wisconsin) depositing glacial till occurred during this time. Illinoian and Wisconsin advances are found in Indiana, with the Wisconsin deposits generally being thicker and overlaying the Illinoian deposits.

Glacial deposits are found across the majority of the state of Indiana. The Illinoian ice made the greatest advance southward with the boundary reaching the Ohio River in southeast Indiana. The Illinoian boundary lies north of Evansville and Bloomington, and east of New Albany. The Wisconsin boundary is north of the Illinoian boundary. The Wisconsin boundary lies north of Terre Haute and Martinsville and south of Richmond. Indianapolis and West Lafayette, where Purdue University is situated, are located on the regionally named Tipton Till Plain, which consists of glacial till from the Illinoian and Wisconsin advances. Wisconsin deposits cover the Illinoian deposits across the Tipton Till Plain. The northern quarter of Indiana consists of morainal and outwash plains from the Great Lakes during the retreating of the glaciers during the warming trends.

Glacial till is a highly variable soil due to the type of source material that it is comprised of and the vast area that it covers. Glacial till soil particles vary across many orders of magnitude, being comprised of soil particles ranging from clay to cobbles and boulders. The variability of glacial till particle sizes depends on the following factors: parent material, distance travelled from the source, and transportation and depositional method, including the type of glacier(s) and/or meltwater. As the distance from the parent material increases, the soil particles begin to transition from coarse-grained soils to fine-grained soils. Generally, the natural state of glacial till is over-consolidated due to the weight of the overlying glacier that is removed at some point in time, has a low compressibility and is a hard and dense soil that has a large bearing capacity (Loiselle & Hurtubise, 1976).

Research on the SPT-T has been very limited, and there is no data on the SPT-T in connection with glacial tills. Accordingly, the main goals of the present study were to develop reliable correlations between blow count, torque measurements, and cone penetration resistance for the glacial till found in Indiana. The correlations proposed in this research can be used to obtain soil parameters needed in pile design, slope stability analyses, and many other geotechnical design applications that INDOT engineers and consultants face routinely.

1.1.1 Problem Statement

The number of blows, "blow count" or "N_{SPT}," are counted and recorded at specified depths in the soil profile when the split-spoon sampler is driven during the SPT. The blow count can vary significantly due to many different factors, some of which were outlined in the previous section. For example, when the blow count is recorded as 10 blows and is miscounted by 1 blow the percent error is 10%. The percent error of miscounting 1 blow increases as the total blow count decreases. The misrepresentation of the blow count can have significant effects on analyses that use relationships relating the blow count to the undrained shear strength. By

performing torque tests, additional *in situ* data is collected, thereby reducing the dependency on blow count measurements for engineering design.

Correlations between SPT blow counts (without torque measurement) and glacial till properties is at best limited. In this research, data collected from side-by-side field testing (SPT, SPT-T and CPT) at various sites in the state of Indiana were used in the development of blow count, torque and cone resistance correlations for glacial till soils. With these relationships, the Indiana Department of Transportation (INDOT) engineers will be able to design deep foundations more efficiently when glacial till soils are encountered within the state of Indiana.

1.1.2 Research Objectives

The four main project objectives are listed below:

- Develop SPT-Torque hardware and software that are compatible with INDOT equipment.
- Collect *in situ* SPT-Torque data for multiple sites comprised of glacial till.
- Develop relationships between laboratory and field test data, including cone penetration test results.
- Properly train INDOT personnel on how to operate the fabricated equipment.

1.1.3 Scope of Work

This report presents the results of the research performed on the development of SPT-Torque correlations. The scope of work includes a detailed literature review, instrumentation development of SPT-Torque hardware, data acquisition software development, site selection and *in situ* torque field testing and CPT testing, laboratory testing of disturbed split-spoon and undisturbed Shelby tube samples, analysis of results, conclusions and recommendations. Details regarding these topics are presented in subsequent chapters.

1.2 Organization of the Report

The report consists of seven chapters covering the equipment development and results from the SPT-Torque research.

Chapter 1 is an introduction of the research on the SPT-Torque.

Chapter 2 is a review of previously published literature, focusing mainly on previous research projects using results of the SPT-Torque tests.

Chapter 3 pertains to details of the development of software and SPT-Torque hardware used during field testing.

Chapter 4 pertains to the five sites that were selected for field testing. Detail is provided regarding the number of borings, SPT-Torque tests performed, CPT soundings, and undisturbed samples collected.

Chapter 5 shows the results of the laboratory tests that were performed on the disturbed samples from the split-spoon sampler and the undisturbed samples from Shelby tubes. Disturbed and undisturbed samples were used to perform index property tests to provide soil classification.

Chapter 6 contains the analysis of the relationships developed for the various soils that were encountered during the field investigations with the results from the SPT-Torque tests and CPT soundings performed at the field sites and laboratory testing.

Chapter 7 provides the conclusions of the report and recommendations for further research.

1.3 Chapter Summary

Chapter 1 presents an overview of the development of the standard penetration test with and without the addition of torque measurements and of the main characteristics of glacial till soils. The research objectives highlight the need for the development of the SPT-Torque hardware and software to collect *in situ* data for the purpose of developing correlations to better predict parameters needed for engineering design.

2. LITERATURE REVIEW

2.1 SPT-Torque Introduction

The Standard Penetration Test (ASTM D 1586 (ASTM, 2007b)) has been used in the geotechnical field for many decades. This test consists of dropping a 63.5 kg hammer from a height of 76 cm to drive a metal, split-spoon soil sampler 45 cm into the bottom of a soil boring in three 15-cm increments and recording the number of blows needed to drive the sampler each of the three 15 cm increments. The number of blows for the second and third 15-cm increments is added, and the resulting number is commonly referred to as the "blow count or N_{SPT} value." Over time, adjustments have been made to reduce or minimize the source of many errors found with the original SPT practice. In the past two decades, additional data has been obtained when SPTs are performed by rotating clockwise the sampler after the sampler has been driven 45 cm into the ground.

The original concept of torqueing an SPT sampler was developed in Brazil (Ranzini, 1988) in the late 1980s with manual application of a torque to the string of drill rods (Bullock, 1999; Bullock & Schmertmann, 2003; Cottingham, 2009; Decourt & Quaresma, 1991; Hicks, 2001; Lutenegger & Kelley, 1998; Peixoto & Carvalho, 1999; Rausche et al., 1995; Winter et al., 2005). All published research performed by the previously mentioned authors used the same method of manual rotation for collecting torque data. The original hardware used by Decourt and Quaresma (1991) for performing the SPT-Torque consisted of a mechanical torquemeter with kg-m torque units. The peak and residual torque values were visually observed and recorded during the manual rotation of the torquemeter.

Bullock (1999) developed a data acquisition system that recorded the measured torque as a function of the rotation angle. The system used a laptop and a torque cell that contained two Wheatstone bridge configurations. A Wheatstone bridge configuration allows for a direct relationship between the strain and the applied torque using a calibration factor. This system was used in later research performed by Hicks (2001), Bullock and Schmertmann (2003), Bullock et al. (2005a, 2005b), and Cottingham (2009). Most of the testing performed by these authors used standard drilling methods, but rotary wash drilling with casing was used for one project (Bullock et al., 2005b). The reason for using the rotary wash and casing was to minimize soil disturbance from other boreholes that were open at the same time a given borehole was being drilled.

There is great uncertainty in SPT measurements. There are several sources of errors associated with the SPT procedure and equipment that can be taken into account before interpretation of test results. The blow count numbers measured in the field are corrected as follows:

$$N_{60} = C_h C_r C_s C_d N_{SPT} \tag{2.1}$$

where N_{60} = blow count for 60% hammer energy efficiency (Blows), C_h = hammer correction (unitless), C_r = rod length correction (unitless), C_s = sampler correction (unitless), and C_d = borehole diameter correction (unitless), N_{SPT} = measured *in situ* blow count (Blows). C_h corrects for the type of hammer because different hammers have different energy efficiency. C_r corrects for the rod length since measured N values performed with a rod length less than 10 meters has artificially high N values and must be corrected. C_s corrects for a sampler that accommodates a sampler liner and is used without the liner. Without the liner, the sampler allows for internal relief, and the measured N value is artificially low. C_d corrects for the diameter of the borehole. As the diameter increases, the measured N value becomes artificially low due to a decrease in confinement at the base of the borehole and must be corrected.

Based on a modification of work performed by Terzaghi and Peck (1967), Kulhawy and Mayne (1990) proposed the following N_{60} vs. undrained shear strength s_u correlation:

$$\frac{s_u}{P_a} = 0.06 N_{60} \tag{2.2}$$

where s_u = undrained shear strength, P_a = reference stress (100 kPa), N_{60} = blow count for 60% hammer energy efficiency. According to Hara et al. (1974), N_{60} is related to s_u as:

$$\frac{s_u}{P_a} = 0.29 (N_{60})^{0.72} \tag{2.3}$$

Generally, measured N values for soft clayey soils are low. For example, the percent error for ten blows when the N value is measured incorrectly by 1 blow is 10%. As the blow count decreases, the percent error increases. When the N value is used in either Equation 2.2 or 2.3 or a similar relationship, the error is being compounded, and this may lead to conservative or unconservative undrained shear strength estimates that are then used for engineering design. The addition of torque measurements to the SPT provides further data that allows engineers to do design for clayey soils without relying only on potentially questionable blow count data. The additional step of performing a torque test minimal time or cost, thus not lengthening the normal time needed or increasing the proposed budget for a standard site investigation.

For clay, CPT tip resistance is related to undrained shear strength as shown:

$$q_c = N_k s_u + \sigma_v \tag{2.4}$$

where q_c = CPT tip resistance, N_k = Cone factor, s_u = undrained shear strength and σ_v = total vertical stress. Salgado (2008) provides a table summarizing soil type, testing method, index properties and cone factor. Equation 2.4 is the bearing capacity equation used for in foundation design. Values of the cone factor for clayey soils range from 9 to 12.

2.2 Preliminary SPT-Torque Results (Development of Torque Ratio)

In 1991, the first Standard Penetration Test Torque (SPT-Torque) test was performed in Brazil with no test-specific fabricated equipment (Decourt & Quaresma, 1991). The tests were performed by manually applying torque to the string of drilling rods using a standard torquemeter; the same equipment that was typically used to perform vane shear tests. The authors collected peak and residual torque values by visual observation of the torquemeter gauge. The peak torque value was commonly reached within a visually observed ½ revolution for the tests performed. The residual torque, which was visually observed by applying torque for several continuous revolutions, represents the strength of the remolded soil at large strains (Decourt & Quaresma, 1994).

Decourt and Quaresma (1994) defined the torque ratio T_R as:

$$T_R = \frac{T}{N_{72}} \tag{2.5}$$

where T = measured torque (kgf-m), and N_{72} = blow count for 72% hammer energy efficiency. The torque ratio is conceptually similar to the friction ratio (sleeve friction resistance/cone resistance) defined for the Cone Penetration Test (CPT) and used to categorize soil behavior type. The similarity results from the fact that the torque measurement and sleeve friction resistance capture the soil resistance along the radial surface area of the split-spoon sampler and cone sleeve, respectively, and the blow count and cone tip resistance capture the soil resistance at the split-spoon sampler shoe and cone

tip, respectively; however, one is a dynamic test while the other is a quasi-static test. As these authors collected T_R data for different types of soil, the data were added to the pre-existing T_R data to enlarge the data set. The data can potentially be used to propose soil behavior charts.

Common practice in Brazil is to adjust the N values to a corrected hammer efficiency of 72 percent (Decourt & Quaresma, 1994), while common practice in the United States is to adjust to a corrected hammer efficiency of 60 percent (Kelley & Lutenegger, 1999). Caution should be used when comparing the data set from Decourt and Quaresma (1994), Decourt (1998), Peixoto and Carvalho (1999), and Peixoto et al. (2000) due to the differences in hammer efficiency. Decourt and Quaresma (1994) introduced the concept of critical depth defined as the depth at which the weight of the drilling rods equals the weight of the hammer. Measured hammer efficiencies tend to increase until the critical depth is reached because the secondary waves returning to the surface interfere less with the primary waves generated by the hammer impact as the depth increases. Lower hammer efficiencies increase N values, thus lowering the torque ratios due to the inverse relationship between the two variables. However, because there is a limited torque ratio data set in the published literature (see Table 2.1), T_R correlations can only be used for site specific soil types (Peixoto et al., 2003). Except for a few soil types published by Decourt (1998), the majority of soils in Table 2.1, ranging from fine-grained soils to sandy soils, have a torque ratio that falls within the range of 0.75–2.0.

2.3 Development of Soil Setup along Sampler and Pile Interfaces

Bullock (1999) performed research for the Florida Department of Transportation to develop relationships between soil setup along the split-spoon sampler and soil setup along driven piles. Setup is the measure of soil strength gain over time due to pore pressure dissipation in fine-grained soils. The research consisted of driving

TABLE 2.1
Published torque ratios for various soil types

Soil Type	T_{R72}[a]	T_{R60}[b]	T_{R60}[c]	Reference
Fine Sand Above the Water Table	1.02	0.85	8.34	Decourt and Quaresma (1994)
Fine Sand Below the Water Table	0.71	0.59	5.80	Decourt and Quaresma (1994)
Lower Bound Sedimentary Sands	~0.3	~0.25	~2.45	Decourt (1998)
Soil from the Tertiary Sedimentary Basin of Sao Paulo	~1.2	~1.0	~9.81	Decourt (1998)
Saprolitic Soils-SP	~2.0	~1.67	~16.35	Decourt (1998)
Collapsible Porous Clays	2.5–5.0	2.1–4.2	20.44–40.88	Decourt (1998)
Soft Marine Clays of Santos	3.0–4.0	2.5–3.3	24.53–32.70	Decourt (1998)
Upper Bound Sedimentary Sands	~10.0	~8.3	~81.75	Decourt (1998)
Sandy Silty Clay with Organic Material	1.57–1.65	1.31–1.38	12.83–13.49	Peixoto and Carvalho (1999)
Sandy Silty Clay without Organic Material	1.18–1.28	0.98–1.07	9.65–10.46	Peixoto and Carvalho (1999)
Silty Clay with Organic Material	1.12	0.93	9.16	Peixoto and Carvalho (1999)
Silty Clay without Organic Material	0.76	0.63	6.21	Peixoto and Carvalho (1999)
Sandy Clay with Organic Material	1.28	1.07	10.46	Peixoto and Carvalho (1999)
Sandy Clay without Organic Material	0.91	0.76	7.44	Peixoto and Carvalho (1999)
Sandy Silty Clay with Gravel	1.12	0.93	9.16	Peixoto and Carvalho (1999)
Sandy Silty Clay without Gravel	1.32	1.10	10.79	Peixoto and Carvalho (1999)
Silty Clay with Gravel	0.68	0.57	5.56	Peixoto and Carvalho (1999)
Silty Clay without Gravel	0.96	0.80	7.85	Peixoto and Carvalho (1999)
Sandy Clay with Gravel	1.17	0.98	9.56	Peixoto and Carvalho (1999)
Sandy Clay without Gravel	1.20	1.0	9.81	Peixoto and Carvalho (1999)
Sandy Silt with Gravel	1.66–1.89	1.38–1.58	13.57–15.45	Peixoto and Carvalho (1999)
Sandy Silt without Gravel	1.27–1.56	1.06–1.30	10.38–12.75	Peixoto and Carvalho (1999)
Clayey Sandy Silt with Gravel	1.20–1.32	1.0–1.1	9.81–10.79	Peixoto and Carvalho (1999)
Clayey Sandy Silt without Gravel	0.93–1.33	0.78–1.11	7.60–10.87	Peixoto and Carvalho (1999)
Sandy Silt with Mica	1.27–1.39	1.06–1.16	10.38–11.36	Peixoto and Carvalho (1999)
Sandy Silt without Mica	1.62–1.68	1.35–1.40	13.24–13.73	Peixoto and Carvalho (1999)
Clayey Sandy Silt with Mica	1.34–2.47	1.12–2.06	10.95–20.19	Peixoto and Carvalho (1999)
Clayey Sandy Silt without Mica	0.92–1.71	0.77–1.43	7.52–13.98	Peixoto and Carvalho (1999)
Sandy Clayey Silt with Mica	1.36–1.87	1.13–1.56	11.12–15.28	Peixoto and Carvalho (1999)
Sandy Clayey Silt without Mica	1.35–1.57	1.13–1.31	9.24–15.29	Peixoto and Carvalho (1999)
Sandy Silty Clay	0.8–1.0	0.67–0.83	6.54–8.18	Peixoto et al. (2000)
Sandy Clayey Silt	1.0–2.0	0.83–1.67	8.18–16.35	Peixoto et al. (2000)

[a]Torque Ratio has torque units of kg_f-m and energy efficiency of 72%.
[b]Torque Ratio has torque units of kg_f-m and energy efficiency of 60%.
[c]Torque Ratio has torque units of N-m and energy efficiency of 60%.

precast concrete piles into various Florida soils and comparing the setup factors from load tests against the results from SPT-Torque tests. The driven piles were tested over a set schedule to determine set-up effects. SPT-Torque tests were performed with staged and unstaged schedules. A staged test is defined as a determined number of SPT-Torque tests performed with a determined timeline that models pile setup over a logarithmic scale time frame. An unstaged test consists of only one additional SPT-Torque test performed after the initial test, which is performed immediately following the SPT driving. The square, prestressed concrete piles were instrumented along the entire length of the pile with strain gauges, and an Osterberg Cell (O-Cell) was cast into the base of the piles (Bullock et al., 2005a). The data collected from strain gauges placed along the entire pile length were used to analyze the transition of the load from the pile onto the in situ soil layers during the pile load test. The study found that the SPT-Torque can be used in a practical manner to estimate setup factors for fine-grained clayey soils. The research was furthered by Hicks (2001) by comparing staged tests versus unstaged tests. A limiting factor in Hicks (2001) is that the staged testing requires many tests over a period of time that mirrors the logarithmic time scale currently used for pile setup design. The logarithmic scale used for the SPT-Torque tests had a reference time of 5 minutes. The SPT-Torque reference time was modeled to the results of a driven pile with a reference time of 1 day (Bullock et al., 2005b). This staged testing procedure requires that borings at the test site remain open for at least 18 hours, which reduces site exploration productivity. The amount of time needed for staged tests limits the number of tests that can be performed for any project that has a rigid or limiting schedule.

The Wisconsin Department of Transportation funded two projects to further understand relationships between setup along the sampler interface and setup of piles (Komurka et al., 2003; Winter et al., 2005). Winter et al. (2005) modified the method used by Hicks (2001) by reducing the time allowed for setup along the sampler interface to a maximum of two hours. Results indicated that the SPT-Torque underestimated the setup of piles and that the two hour maximum criterion did not allow enough time to properly capture the setup effects along the sampler interface, making the SPT-Torque a poor site exploration tool for determining driven pile setup factors.

Lutenegger and Kelley (1998) performed load tests on steel pipe piles. Open and close-ended steel pipe piles were tested in tension, and the load tests results were compared with the unit side resistance results from the SPT-Torque testing. Setup of 30 days was allowed before the tensile tests were performed.

2.4 Side Shear Resistance Relationships

Ranzini (1994) proposed the following relationship between measured torque and unit side resistance:

$$f_s = \frac{T}{(41.226L - 0.032)} \tag{2.6}$$

where f_s = unit side resistance (kPa), T = measured torque (kN-m), and L = penetration length of the split-spoon sampler (m).

Rausche et al. (1995) was the first to perform SPT-Torque research in the United States. Lutenegger and Kelley (1998) performed extensive research testing the SPT-Torque procedure in New England. These authors' research proposed the following relationship between unit side resistance and torque:

$$f_s = \frac{2T}{\pi d^2 L} \tag{2.7}$$

where f_s = unit side resistance (kPa), T = measured torque (kN-m), d = diameter of split-spoon sampler (m), and L = penetration length of the split-spoon sampler (m). There are two assumptions made in this relationship. First, unit side resistance relating to the soil-split-spoon sampler interface located on the inside of the sampler is neglected based on the idea that many of the SPT samplers used within the United States can be driven without a sampler liner, which is the current Indiana Department of Transportation practice, allowing for internal relief (Lutenegger & Kelley, 1998). The second assumption neglects any contribution of end bearing resistance because of the minimal end bearing area; this is related to the first assumption since due to the internal relief, there is no soil plugging in the sampler and thus the end bearing capacity is insignificant (Lutenegger & Kelley, 1998).

From the Lutenegger and Kelley (1998) initial research, it was found that the unit side resistance calculated using Equation 2.7 can be related to the blow count N_{60} using an empirical factor:

$$f_s = \alpha_s N_{60} \tag{2.8}$$

where f_s = unit side resistance (kPa), α_s = empirical factor (unitless), and N_{60} = blow count for 60 percent hammer energy efficiency. Table 2.2 presents α_s for fine-grained, coarse-grained, residual and glacial till soils from SPT-Torque tests performed at twelve sites. The relationships for the four different soils at four sites are plotted in Figure 2.1.

The relationship represented by Equation 2.8 is dependent on soil type. The unit side resistance is calculated and then plotted versus the corresponding energy-corrected blow counts to determine the soil specific empirical factor α_s, which can be used for pile design (Kelley & Lutenegger, 2004). Lutenegger (2009) found empirical factors for fine-grained soils that are generally higher than those for coarse-grained soils; similarly, those for displacement piles are higher than those for nondisplacement piles.

Similar to Figure 2.1, data from Winter et al. (2005) are plotted in Figure 2.2 with the relationships published by Kelley and Lutenegger (2004). All data, except for some organic clay and silt data points, fall near or

TABLE 2.2
Summary of empirical factors α_s (Kelley & Lutenegger, 2004)

Site Number	Site	α_s[a]	Description of Soil
		Fine-Grained	
1	NGES,[b] Amherst, MA	7.4	Varved clay
2	NGES,[b] Houston, TX	6.6	Montgomery clay over Beaumont clay
3	NGES,[b] Evanston, IL	6.2	Blodgett deposit clay
4	South Deerfield, MA	3.7	Varved clay
		Coarse-Grained	
5	Plattsburgh, NY	3.6	Fine to medium sand with trace silt
6	Plymouth, MA	2.6	Fine to medium sand
7	North Amherst, MA	5.4	Silty sand overlain by sandy silt
3	NGES,[b] Evanston, IL	4.2	Fine sand
4	South Deerfield, MA	3.2	Sand overlain by silty sand overlain by silt, trace sand
		Residual	
8	McLean, AL	5.4	Sandy silt to silty sand overlain by a thinner layer of clayey silt to silty clay
9	NGES,[b] Spring Villa, AL	6.9	Sandy silt to silty sand overlain by a thinner layer of clayey silt to silty clay
10	Atlanta, GA	5.1	Sandy silt to silty sand overlain by a thinner layer of clayey silt to silty clay
11	Rome, GA	8.6	Sandy silt to silty sand overlain by a thinner layer of clayey silt to silty clay
		Glacial Till	
12	Cohasset, MA	1.5	Clayey sand and silty clay with some gravel

[a]Factor provides f_s (kPa) when it is multiplied by N_{60}.
[b]NGES = National Geotechnical Experimentation Sites.

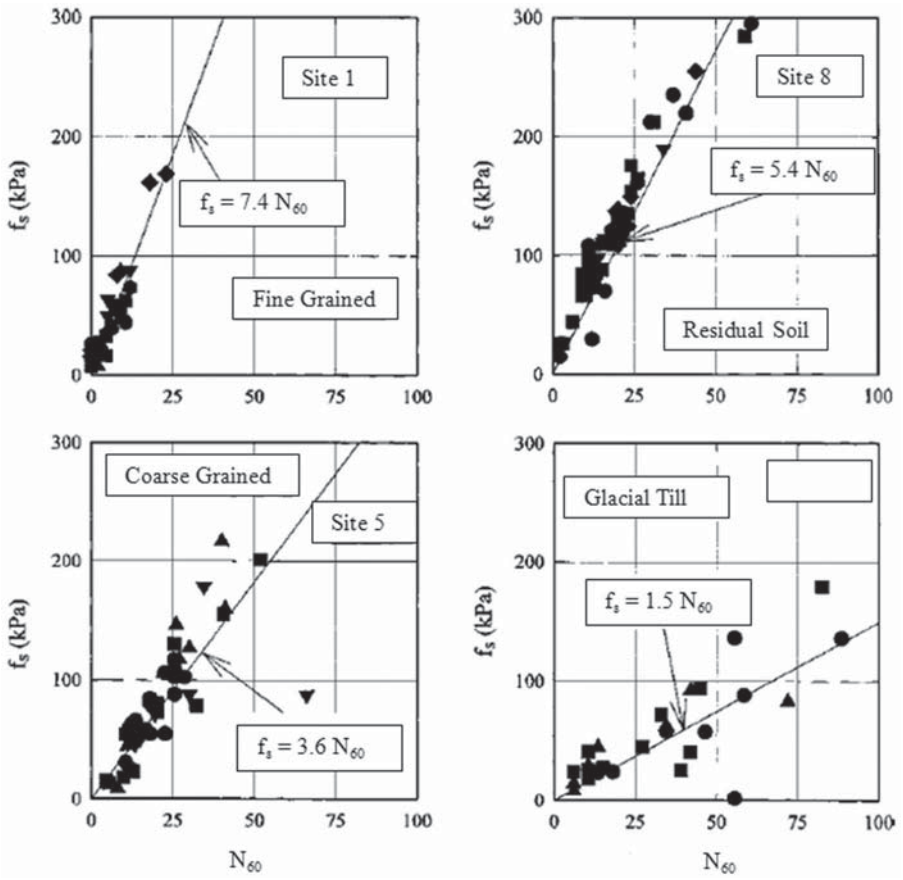

Figure 2.1 Unit side resistance versus standard penetration test N_{60} values for selected soil types (after Kelley & Lutenegger, 2004).

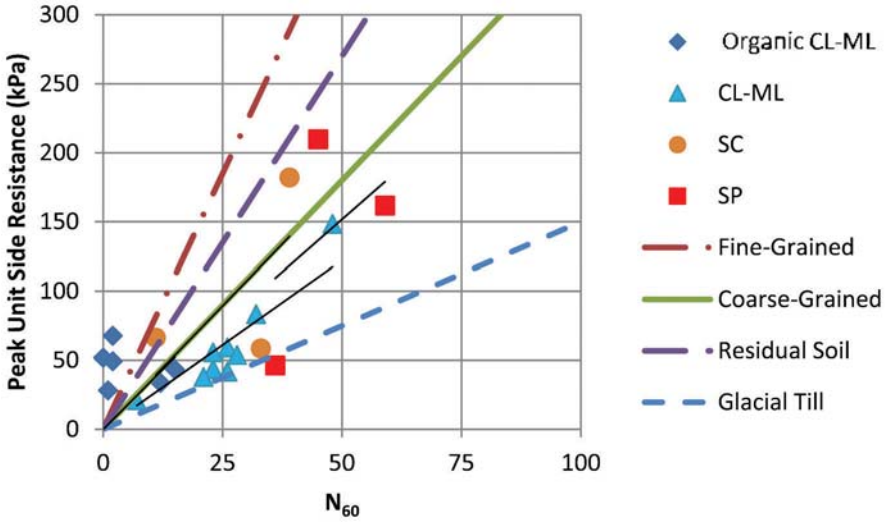

Figure 2.2 Unit side resistance versus standard penetration test N_{60} for various soils (Winter et al., 2005).

within the relationships published by Kelley and Lutenegger (2004). Table 2.3 presents the raw data that is shown in Figure 2.2. Table 2.4 presents the empirical factors for the Winter et al. (2005) data.

Many different correlations have been developed to try to capture the relationship between blow count and unit shaft resistance. There is a large variation among all of the different correlations due to two factors: pile data and SPT data (Lutenegger, 2009). The pile data vary for three reasons. The first reason is the type of piles, which have different geometries and installation methods, and are installed in different materials. Secondly, the chosen method of analysis of load test results determines important factors, such as the ultimate load capacity (different methods lead to different results). The final reason for pile data variation is due to lack of published data for highly instrumented pile load tests. Many pile load tests collect a minimal amount of data along the pile shaft that is analyzed by interpolating or extrapolating the data. If along the length of a pile, there is a limited amount of collected data or potential for data collection at the soil-pile interface, then, typically, the unit shaft resistance is calculated as the average value obtained along the entire pile length. Due to lack of instrumentation and/or soil property data, the assumption of a homogenous, single soil layer is made. This assumption can lead to the neglect of contributing soil layer and lenses with differing unit shaft resistance. Factors that affect SPT data variation are discussed in Section 2.1.

TABLE 2.3
Data presented in Figure 2.2 (Winter et al., 2005)

Soil Type	N_{60}	Peak Unit Side Resistance (kPa)
Organic CL-ML	0	51.90
Organic CL-ML	1	28.20
Organic CL-ML	2	49.31
Organic CL-ML	2	67.79
Organic CL-ML	12	33.66
Organic CL-ML	15	43.37
CL-ML	26	59.27
CL-ML	23	43.57
CL-ML	23	55.73
CL-ML	26	41.70
CL-ML	28	53.86
CL-ML	21	37.92
CL-ML	7	21.06
CL-ML	32	83.45
CL-ML	48	148.41
SC	39	182.07
SC	11	66.40
SC	33	58.60
SP	36	46.25
SP	59	161.67
SP	45	209.79

Note: CL-ML is silty clay, SC is clayey sand and SP is poorly-graded sand.

2.5 Factors that Influence the SPT-Torque Testing and Performance

Rod length has an insignificant influence on the SPT-Torque test (Peixoto et al., 2007). Peixoto et al. (2007) tested with drill rods in the horizontal and vertical orientations and determined that the torque loss from the top of the boring to the bottom of the boring is less

TABLE 2.4
α_s values of various soil types for blow count versus peak unit side resistance relationships (Winter et al., 2005)

Soil Type	α_s[a]
Organic CL/ML	3.4838
CL/ML	2.4465
SC*	3.5756
SP*	3.0350

*Note: α values based on limited data.
[a]Factor provides f_s (kPa) when multiplied by N_{60}.

than the smallest torque increment of mechanical torquemeters used in common practice. As the torque increases, the drill rod influence decreases (Peixoto et al., 2007). Maximum torque values commonly measured in soft, clayey soils are approximately equal to the torque loss due to drill rods. Because of this phenomenon, the torque loss may be significant, and caution should be taken when using the SPT-Torque test in soft, clayey soils.

Further research by Peixoto et al. (2010) investigated the buckling potential of the string of drill rods. Peixoto et al. (2010) found that the self-weight of the rods is not the controlling factor related to buckling. The controlling factor for buckling is the slenderness ratio, which is the parameter normally used when considering the design of structural columns. The slenderness ratio is defined as the effective length divided by the radius of gyration. A slenderness ratio of 200 is commonly used for analyses where steel is the material being loaded in axial compression of the drill rods. Based on this ratio, buckling can occur at spans of just 2 meters. It may be necessary to provide supports to prevent the drill rods from buckling during the SPT-Torque test when extremely stiff or hard soils are encountered at the base of the split-spoon sampler and little or no lateral support for the drill rods is present. Rotation speed is not an important factor, as long as human mistakes can be limited (Peixoto et al., 2008).

For site exploration with multiple borings, it is recommended that the lateral spacing between borings be at least 3 meters (Hicks, 2001). This distance helps to reduce any soil disturbance from stress relief, soil removal, and ground vibrations (Hicks, 2001).

2.6 Tested Soil Types

The testing by Decourt and Quaresma (1991) with the original SPT-Torque equipment was performed in residual soils composed of saturated and unsaturated saprolites of granite and gneiss formations. Additional testing by Decourt and Quaresma (1994) was performed in the sedimentary soils of the Tertiary Sedimentary Basin in Brazil. Peixoto and Carvalho (1999) performed SPT-Torque tests in Brazilian residual soils and collapsible soils. Further testing of residual soils was performed in the Piedmont Province and Southern Piedmont region located in the Appalachian Mountains of the Eastern United States (Kelley & Lutenegger, 1999; Cottingham, 2009). Fine sand and silty clay was studied in Florida by considering the development of relationships between setup factors for precast concrete piles and SPT-Torque test results (Bullock, 1999; Hicks, 2001; Bullock & Schmertmann, 2003; Bullock et al., 2005a). Organic clay, silty clay and silty sand were studied in Wisconsin by exploring the development of relationships between setup factors for driven piles and SPT-Torque test results (Winter et al., 2005). Glacial till and loess, among others, are lesser studied soils (Kelley & Lutenegger, 2004; Lutenegger, 2008). Soils comprised mainly of gravel have not been the primary soil for any studies, but Peixoto and Carvalho (1999) concluded that gravel found within clayey soils decreased the torque ratio for the given data set based on an increase in the blow count with no increase in the measured torque.

2.7 Chapter Summary

Chapter 2 outlines the development of the SPT-Torque testing procedure in Brazil during the late 1980's (Ranzini, 1988). A manual torque was applied after a traditional SPT (ASTM D 1586 (ASTM, 2007b)) test was performed in many different soil types. The data was first analyzed using the Torque Ratio defined as the measured or observed torque divided by the recorded blow count. Bullock (1999) and Hicks (2001) studied and compared setup factors from driven precast concrete piles and SPT-Torque tests. Winter et al. (2005) further studied setup factors and concluded that a two-hour time period did not provide enough time to properly develop a relationship between the pile and SPT-T setup factors. Lutenegger and Kelley (1998) proposed an equation for calculating the unit side resistance based on the measured torque, split-spoon sampler diameter and driven penetration length of the split-spoon sampler. Further research, by Kelley and Lutenegger (2004), lead to the development of an empirical equation relating unit side resistance and the recorded N_{60} value. Peixoto et al. (2007) found that the torque loss is minimal and not significant for most soils; however, in soft clayey soils the maximum torque is approximately equal to the torque loss and caution must be taken when soft clayey soils are encountered.

3. INSTRUMENTATION DEVELOPMENT

3.1 Data Acquisition System Development

The Data Acquisition System (DAQ System) and its components described herein were manufactured by Anita Machine & Tool, Inc. of Lafayette, Indiana and Stoeller Automation, Inc. of Frankfort, Indiana. The software was written using C# from the Visual Studio 2010 package. The software interacts with three National Instrument (NI) modules contained in an NI chassis via a USB connection. Data from the **SPT-Torque Hardware** are collected by the NI modules and chassis located in the **Control Box Hardware** and stored by the software. The DAQ System records the strain which is converted to torque using a calibration factor based on a full-bridge configuration of the strain gauges (see Appendix A for calibration data relating torque versus measured strain). A digital encoder is used to determine the angle of rotation and rotation velocity as the string of drill rods are rotated by the SPT-Torque hardware.

3.1.1 Software Components and Operation

Figure 3.1 shows the user interface of the SPT-Torque software. First the units must be selected. The software allows for operation using units common in

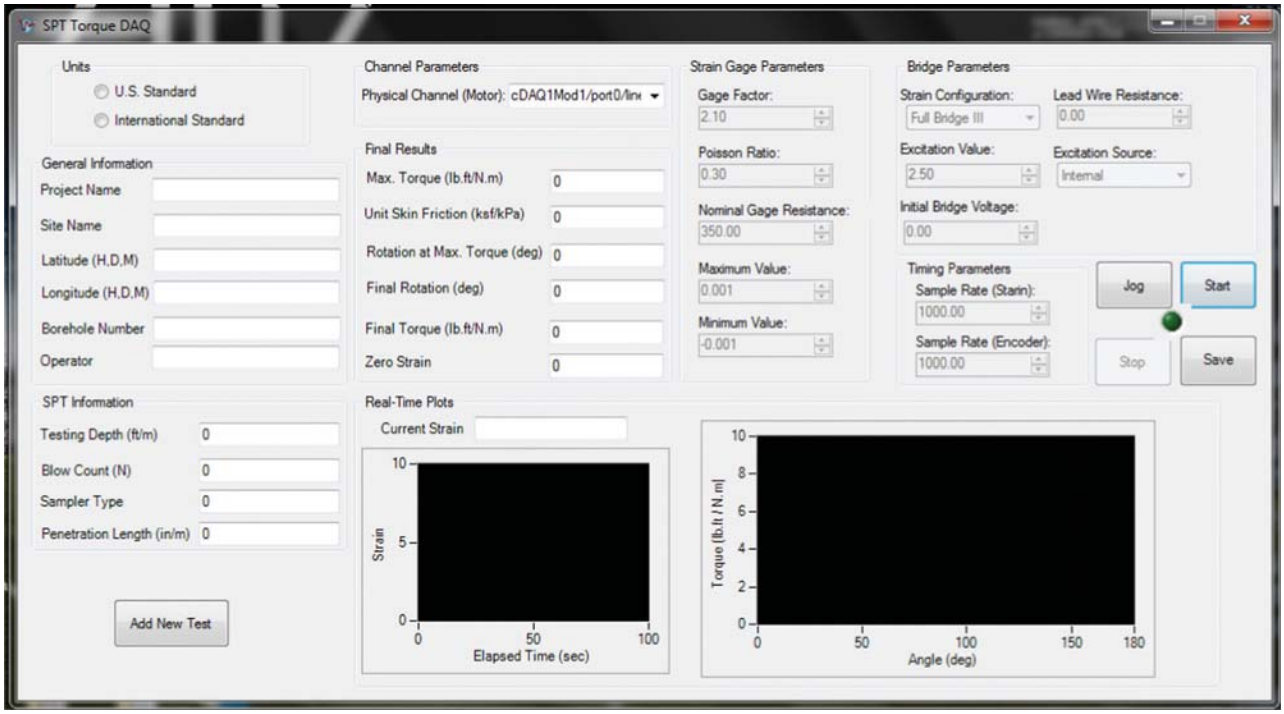

Figure 3.1 Software user interface.

the United States or the International Standard. Once the units have been selected, the **General Information** specific to the testing site is recorded. Unless changed by the operator, this information remains the same for additional tests performed in a given boring. Next, the sample depth, blow count, sample type and penetration length are recorded in the **SPT Information** section. This information is specific to the SPT sampler driven at the current depth interval. The **SPT Information** (testing depth, blow count, sample type and penetration length) is traditionally recorded in the boring log by INDOT personnel. Then the channel that controls the motor on the SPT-Torque hardware must be selected from the drop-down box. The **Strain Gauge Parameters**, **Bridge Parameters**, and **Timing Parameters** are set based on the strain gauge type and configuration. These values are summarized in Table 3.1.

The motor must be jogged before starting a test. The term jog refers to the process of rotating the SPT-Torque shaft counterclockwise to its original position (See the **SPT-Torque Hardware** Section 3.2.1 regarding the functionality of the original and ending positions and the **Control Box Hardware** Section 3.2.2 regarding the jogging procedure). First, the operator selects the **Jog** button on the right side of the software interface and then jogs the motor using the **Control Box Hardware**. Once jogging is complete, the operator selects the **Stop** button on the interface. The hardware is then ready to perform the torque test. The **Start** button is selected next, and the software takes a baseline reading by averaging the initial strain values for a period of ten seconds. The net strain is calculated by subtracting the real time strain values from the average baseline value recorded over the ten-second period. The net strain is used to calculate the torque. The torque and other important values are recorded in the **Final Results** section. All values in the **Final Results** section are directly recorded from the hardware except the unit side resistance value. The unit side resistance is calculated based on Equation 2.7, presented in Chapter 2:

$$f_s = \frac{2T}{\pi d^2 L} \tag{2.7}$$

where f_s = unit side resistance (kPa), T = measured torque (kN-m), d = diameter of split-spoon sampler (m), and L = penetration length of split-spoon sampler (m).

TABLE 3.1
Strain gauge, bridge and timing parameters used in the SPT-Torque software

Strain Gauge Parameters		Bridge Parameters		Timing Parameters	
Gauge Factor	2.10	Strain Configuration	Full Bridge III	Sample Rate (Strain)	1000.00
Poisson Ratio	0.30	Lead Wire Resistance	0.00	Sample Rate (Encoder)	1000.00
Nominal Gage Resistance	350.00	Excitation Value	2.50		
Maximum Value	0.001	Excitation Source	Internal		
Minimum Value	−0.001	Initial Bridge Voltage	0.00		

The interface contains two figures that present the data in real time located in the **Real-Time Plots** section. The first figure plots time in seconds on the x-axis versus measured net strain on the y-axis. The second figure plots rotation angle in degrees on the x-axis versus torque in pound-feet or Newton-meters, according to the unit selection on the y-axis. After the **Stop** button is selected, the current test is saved in XML format in a temporary file. To perform multiple tests in the same boring, the **Add New Test** button located in the lower left corner of the interface is selected to perform an additional test after the completion of the current test. This will clear the **SPT Information** and **Final Results** sections. The temporary output file is updated after each subsequent test is completed in a given boring. Once all testing is complete in a given boring, selecting the **Save** button on the right side of the software interface allows the operator to save the data from all tests in an output file with XML format.

3.2 Hardware Development

The **SPT-Torque Hardware** was machined by Anita Machine & Tool, Inc. located in Lafayette, Indiana under the direction of Purdue University. The **Control Box Hardware** was assembled by Stoeller Automation, Inc. located in Frankfort, Indiana. The **SPT-Torque Hardware** is the first known instrumentation that rotates the string of drill rods in an automated manner. This process helps to regulate the rotation velocity of the drill rods and remove any human error that was incorporated in the torque testing when performed manually.

3.2.1 SPT-Torque Hardware

The **SPT-Torque Hardware** shown in Figure 3.2 consists of a 187.5 watt motor from Sterling Electric, Inc. located in Irvine, California. The motor rotates the string of drill rods in a clockwise direction by rotating the SPT-Torque shaft connected to the **Drill Rod Adaptor**, as shown in Figure 3.3. The hardware is lifted by the drilling rig using the overhead cable. Then, the adjustable clamp, located on the back of the SPT rig, holds the hardware by the truck mounting rod. The strain gauges are mounted on the exterior of the SPT-Torque shaft at a 45 degree angle from the vertical axis. This orientation creates an "X" on the rod also known as a full-bridge type III configuration, as shown in Figure 3.4. Two gauges measure elongation of the SPT-Torque shaft, while the other two gauges measure the contraction of the shaft. This configuration allows for the gauges to act as a torque cell, and the output voltage is directly proportional to the torque.

The **Drill Rod Adaptor** is a modified drill rod. The adaptor and **SPT-Torque Hardware** have matching connection ends that allow for eight 1.27 mm × 5.1 mm coarse threaded bolts to be placed through the SPT-Torque connection. Coarse threaded nuts are used to ensure a tight connection between the **SPT-Torque**

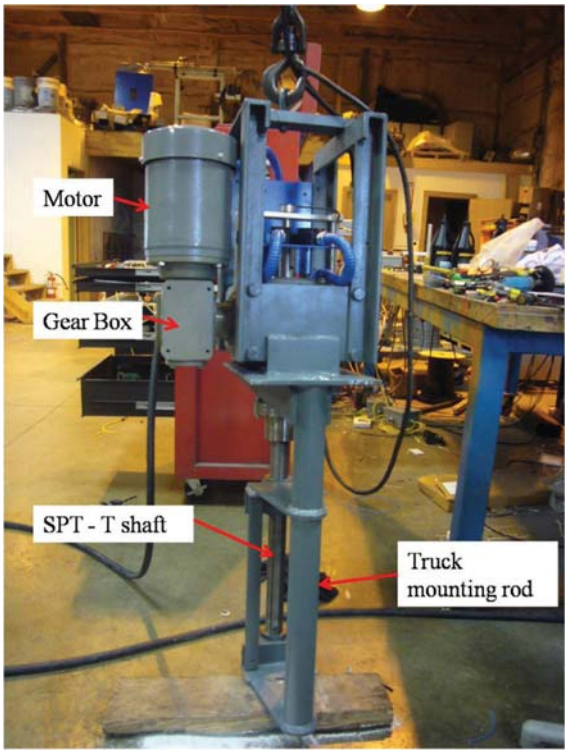

Figure 3.2 SPT-Torque hardware.

Hardware and the **Drill Rod Adaptor**. It is critical that the **Drill Rod Adaptor** is not loosened during the driving of the split-spoon sampler. The hammer impact can loosen the drill rod adaptor, leading to poor results because the hardware will have to tighten the connection before rotation can be applied to the sampler.

The SPT-Torque original position limit switch is shown in Figure 3.5, while the ending position limit switch is shown in Figure 3.6. The rotating shaft has a slot cut into it. A key is placed in this slot to engage the two limit switches. Once the jogging process is complete (counterclockwise rotation), the key applies a normal compressive force on the limit switch plunger in the

Figure 3.3 Drill rod adaptor.

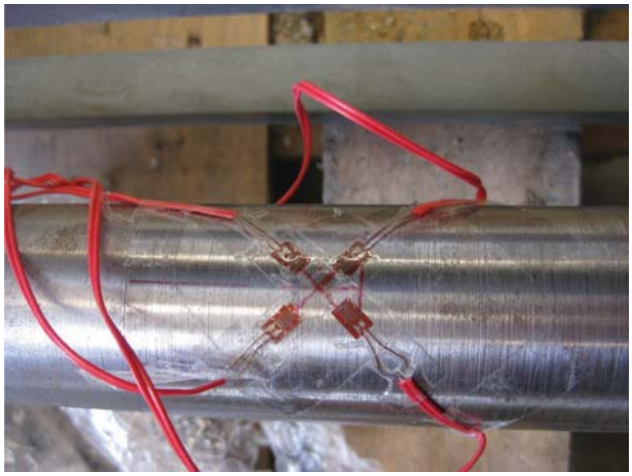

Figure 3.4 Full-bridge type III strain gauge configuration.

original position. After the clockwise rotation begins, the shaft can rotate until the ending position is reached. Again, the key applies a normal compressive force on the limit switch plunger. The normal forces applied on the limit switches start and stop the rotation, respectively. The limit switches allow for a maximum shaft rotation of 310 degrees. The maximum rotation speed is for a frequency of 60 Hz (= 174 deg/min). A 20 Hz (=58 deg/min) frequency was found suitable for the soils tested in this research.

3.2.1.1 SPT-Torque hardware calibration. Figure 3.7 demonstrates how to calibrate the strain gauges mounted on the shaft surface of the **SPT-Torque Hardware**. The **SPT-Torque Hardware** is placed in a horizontal position, and a lever arm is bolted to the base of the hardware connection. The weight of the lever arm, bucket and additional weights placed inside of the bucket are used to calculate the moments that are

Figure 3.5 Original position limit switch engaged.

Figure 3.6 Ending position limit switch engaged.

applied to the SPT-Torque shaft. As the moments increase, the strain gage values are recorded. The data are plotted against the respective moment values to determine the calibration factor used in the software for proper torque calculation during field testing. Further details regarding the SPT-Torque calibration can be found in Appendix A.

3.2.2 Control Box Hardware

The **Control Box Hardware** acts as the link between the SPT-Torque hardware and the computer software. Figure 3.8 shows the front of the **Control Box Hardware**. The **Control Box Hardware** allows for the operator to manually control the SPT-Torque hardware. The "**On Button**" provides power to the **SPT-Torque Hardware**. The "**Emergency Stop Button**" immediately locks out all power to the **SPT-Torque Hardware** should an emergency arise. The four buttons

Figure 3.7 SPT-Torque calibration.

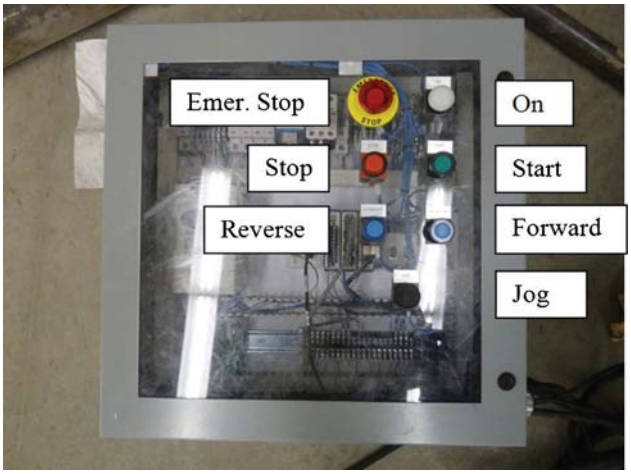

Figure 3.8 Control box exterior.

below the previously two mentioned buttons can be controlled by the software. The operator uses the "**Jog Button**" simultaneously with the "**Reverse Button**" to rotate the motor counterclockwise to its original position.

The inside of the **Control Box Hardware** is shown in Figure 3.9. National Instrument hardware is used to collect data from the **SPT-Torque Hardware**. An NI cDAQ 9172 chassis is used to house the three modules. The NI 9472 module outputs digital signals and acts as a power source for the quadrature encoder. The NI 9411 module collects digital input signals from the quadrature encoder. The encoder measures the rotational velocity and the direction of rotation of the drill rods. The NI 9219 module collects analog input signals from the full-bridge III configuration. All data are sent from the chassis to the computer software via a USB connection.

3.3 Chapter Summary

Chapter 3 described the **SPT-Torque Hardware** and software required for data collection during field testing. The **SPT-Torque Hardware** was developed to be compatible with the INDOT drill rig while rotating the drill rods 310 degrees after driving the split-spoon sampler into the ground. The **Control Box Hardware** relays real-time data from the **SPT-Torque Hardware** to the computer where the data is collected and viewed in the software. The software records the data in the **Final Results** section, and the measured data is plotted in **Real-Time Plots** for the operator to better understand the results as the SPT-Torque test is being performed.

4. SITE SELECTION FOR FIELD TESTING

4.1 Indiana Geology

Figure 4.1 shows the distribution of glacial deposits across the north-central United States. A non-glaciated region in southwest Wisconsin and northwest Illinois can be observed in detail. The geology of Indiana varies greatly across the state in the north to south direction.

Figure 4.2, a landform map of Indiana, shows the distribution of glacial deposits found within the state. The Illinoian glacial ice made the greatest advance southward, with the boundary located at the Ohio River in southeast Indiana. The boundary extends from Evansville north toward Bloomington, and east toward New Albany. The Wisconsin boundary is located north of the Illinoian boundary. The Wisconsin boundary runs north of Terre Haute and Martinsville and south of Richmond. Indianapolis and West Lafayette (where Purdue University is located) lie on the regional zone known as the Tipton Till Plain which consists of glacial till from the Illinoian and Wisconsin advances. Wisconsin deposits overlie the Illinoian deposits in the Tipton Till Plain and vary in thickness from approximately 30 meters near the Illinois-Indiana state line to approximately 25 meters near Kokomo, Indiana (Bleuer, 1991). The northern portion of Indiana consists of morainal and outwash plains from the Great Lakes deposited by the retreating glaciers during the warming episodes.

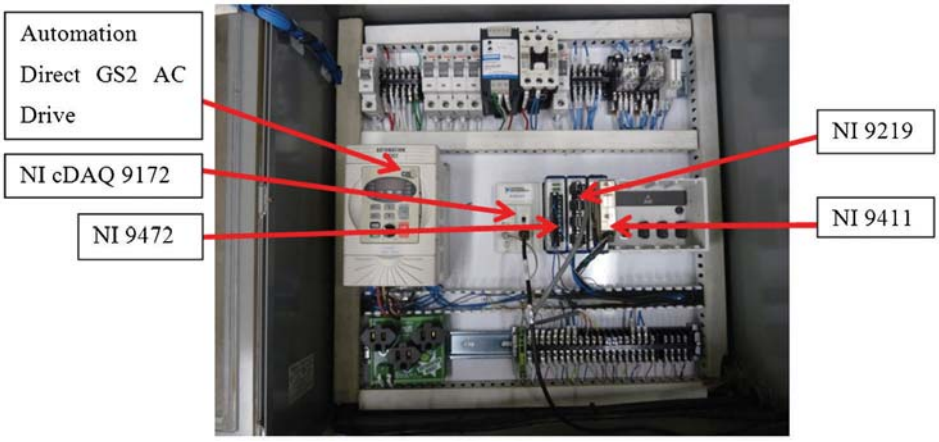

Figure 3.9 Control box interior.

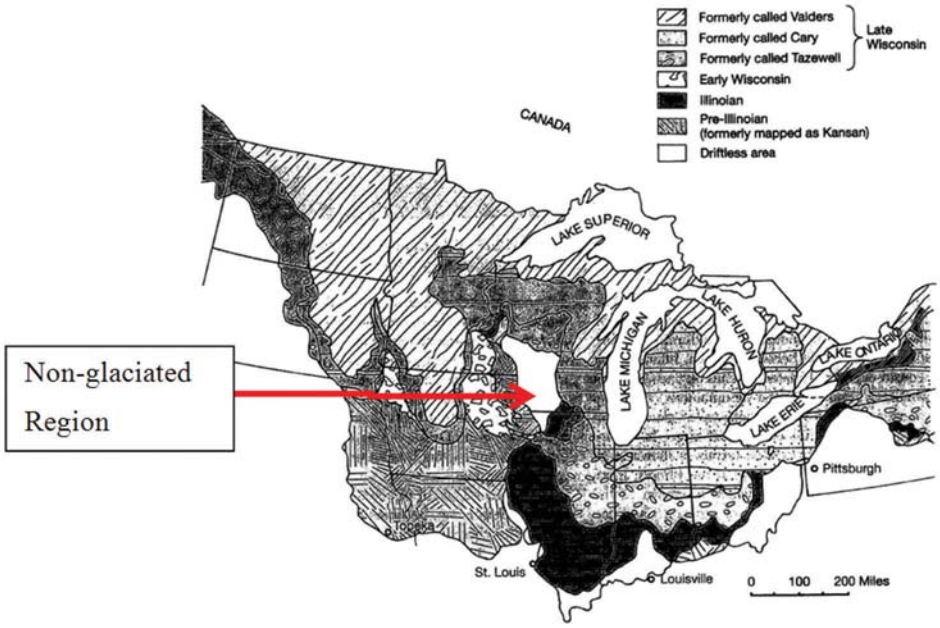

Figure 4.1 Distribution of glacial deposits in the north-central United States (West, 1995).

4.2 Site Locations

SPT-Torque testing and Cone Penetration Testing (CPT) were performed at five sites in four counties: Carroll, Clinton, Greene and Tippecanoe counties (shown in Figure 4.3, Map of Indiana counties). Two counties, Carroll and Tippecanoe, are located in north-central Indiana, one (Clinton) in central Indiana and one (Greene) in southern Indiana. All field testing in Carroll, Clinton and Tippecanoe Counties was performed at the Indiana Department of Transportation maintenance units by the INDOT drilling crew. The field testing in Greene County was performed along the expansion of Interstate 69. This allowed for more detailed planning of boring location, spacing, and other research considerations relative to the field testing criteria and eliminated the need for traffic control. Field testing performed on or near a highway hinders traffic flow and limits the amount of time available for SPT-Torque and CPT testing. The time between the completion of subsequent SPT-Torque tests is approximately twelve to fifteen minutes for tests performed at 1.52 meter intervals. The time period varies slightly for two reasons: first, the drilling speed of the hollow-stem augers depends on the soil type and soil properties, such as density and stiffness; and secondly, the amount of time needed to reach the maximum torque while shearing along the sampler interface. All SPT drilling was performed by the INDOT drilling crew. All SPT tests were performed using an automatic hammer, an unlined 50.8 millimeters outer-diameter split-spoon sampler with hollow-stem augers that have an inner diameter of 82.55 millimeters and an outer diameter of 165.1 millimeters. The CPT soundings were performed by Purdue University personnel. Two Hogentogler analog cones with an outer diameter of 36.6 millimeters were used for testing. The soundings were pushed with a penetration rate of 20 mm/s.

The blow count values were correct using Equation 2.1. The values used for each correction are listed below:

C_h = 60 percent for Flora and Lafayette Maintenance Units (personal communication with Jon Paauwe)

= 70 percent for Frankfort and Romney Maintenance Units (personal communication with Jon Paauwe)

= Measured efficiency was taken before each SPT at the Koleen site (measured average for all tests was 59.1 percent)

C_r = 0.75, if rod length $<$ 4 m; 0.85, if 4 m $<$ rod length $<$ 6 m;

= 0.95, if 6 m $<$ rod length $<$ 10 m; 1.0, if rod length $>$ 10 m

C_s = 1.2 (Split-spoon sampler with no liner)

C_d = 1.0 (standard borehole diameter)

4.2.1 The Flora Maintenance Unit (Carroll County)

The Flora Maintenance Unit (FMU) is located 1.6 kilometers south of the town of Flora on the east side of Indiana State Route 75. The glacial till deposit at the site is approximately 45 meters thick consisting of Wisconsin and Illinoian deposits with bedrock consisting of the Borden Group of Mississippian Age. A satellite image of the Flora site is shown in Figure 4.4. A total of 12 SPT-Torque tests were performed at the Flora Maintenance Unit on August 9, 2011. Figure 4.5 shows the plan view with an approximate spacing of 3 meters between the SPT borings and CPT soundings. Tests were performed in three intervals of 1.07–1.52 meters, 2.59–3.05 meters, and 4.12–4.57 meters in four

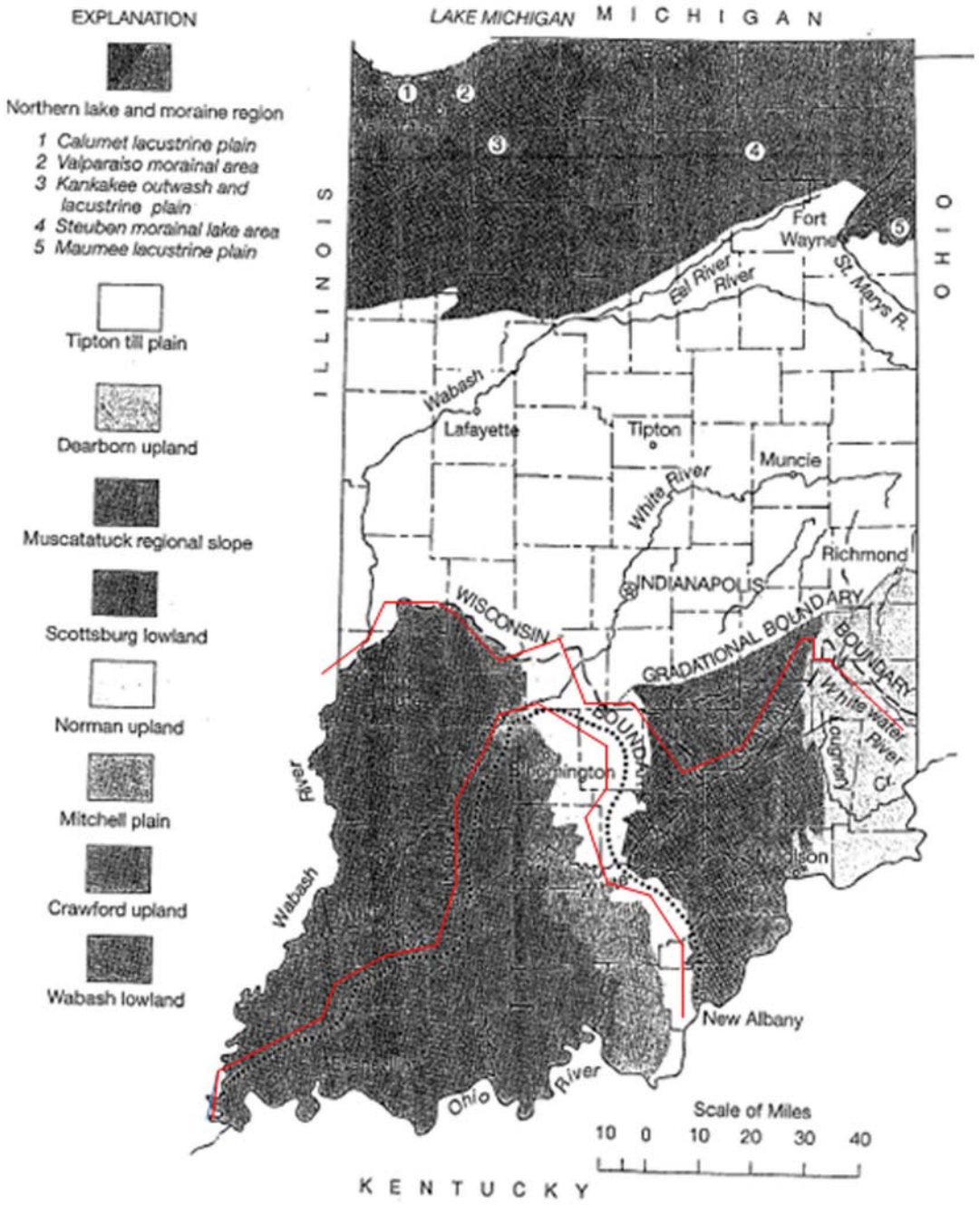

Figure 4.2 Glacial boundaries in Indiana (West, 1995).

separate borings, FMU borings 1–4. The four boring logs are presented in Figures F.1, F.3, F.5, and F.7 in Appendix F. The borings could not be advanced to the next interval due to heave occurring at the bottom of the hole. Groundwater was pushing sand upward and preventing the split spoon sampler from reaching the necessary depth for the next sample. The area received approximately 3.8 centimeters of rainfall the night before drilling. The excess rainfall could affect the typical groundwater level and contribute to the sand heave issue. The ground surface elevation is 216.16 meters. The groundwater table, represented with a blue line in Figures F.2, F.3, F.6, and F.8 in Appendix F, was measured at 2.74 meters below the ground surface. Previous ground water levels from past years are not available to verify this observation. Five Shelby tubes were pushed to collect undisturbed soil samples at depth intervals that correspond to the SPT-Torque tests. Two tubes were collected from FMU boring 5 and three tubes were collected from FMU boring 6. Again the heave issue was encountered during the collection of undisturbed samples. Four CPT soundings were performed to a depth ranging from 8.99 to 11.13 meters on February 22, 2012. Figures F.2, F.3, F.6, and F.8 in

Figure 4.3 Map of Indiana counties.

Figure 4.4 Satellite view of the Flora site from Google Earth.

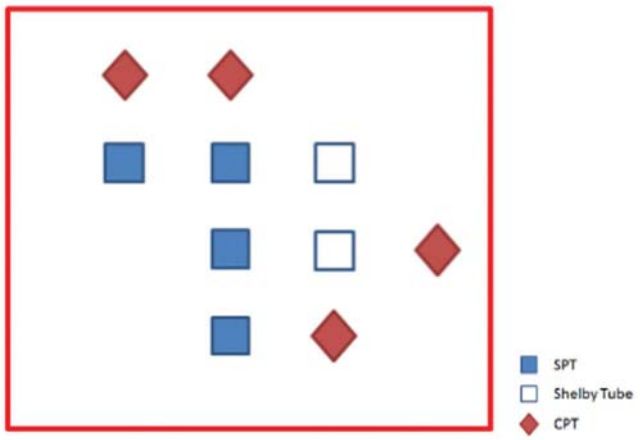

Figure 4.5 3-meter approximate spacing between SPT borings and CPT soundings at the Flora site.

Appendix F present the four SPT borings and CPT soundings from the Flora Maintenance Unit.

4.2.2 The Lafayette Maintenance Unit (Tippecanoe County)

The Lafayette Maintenance Unit (LMU) is located eight kilometers north of the city of West Lafayette on the east side of Indiana State Route 43. The glacial till deposits at the site are approximately 60 meters thick consisting of Wisconsin and Illinoian deposits with bedrock consisting of New Albany Shale from the Devonian Age. However, the site lies near the Wabash River; therefore, outwash deposits are present in the vicinity as well. A satellite image of the Lafayette site is shown in Figure 4.6. Six SPT-Torque tests were performed in one boring, LMU boring 1 on September 1, 2011. The boring log is presented in Figure F.9 in Appendix F. The six tests were performed at a depth interval of 1.52 meters. The ground surface elevation is 175.91 meters. The ground water table, represented by a blue line in Figure F.10, was observed at 6.71 meters below the ground surface. The boring was terminated at 9.15 meters. Five Shelby tubes were pushed in five individual borings, LMU borings 2–6. Figure 4.6 shows the plan view with an approximate spacing of 3 meters between of the SPT boring and CPT sounding. Stiff and dense soil prevented the proper pushing of the Shelby tubes in one continuous boring, and therefore undisturbed samples were taken at shallow depths not exceeding 1.83 meters below the ground surface. One CPT sounding was performed to a depth of 4.97 meters on February 23, 2012. Figure F.10 in Appendix F presents the SPT boring and CPT sounding from the Lafayette Maintenance Unit.

4.2.3 The Frankfort Maintenance Unit (Clinton County)

The Frankfort Maintenance Unit (FRMU) is located 1.6 kilometers west of the city of Frankfort on the south side of Indiana State Route 28. The glacial till deposit

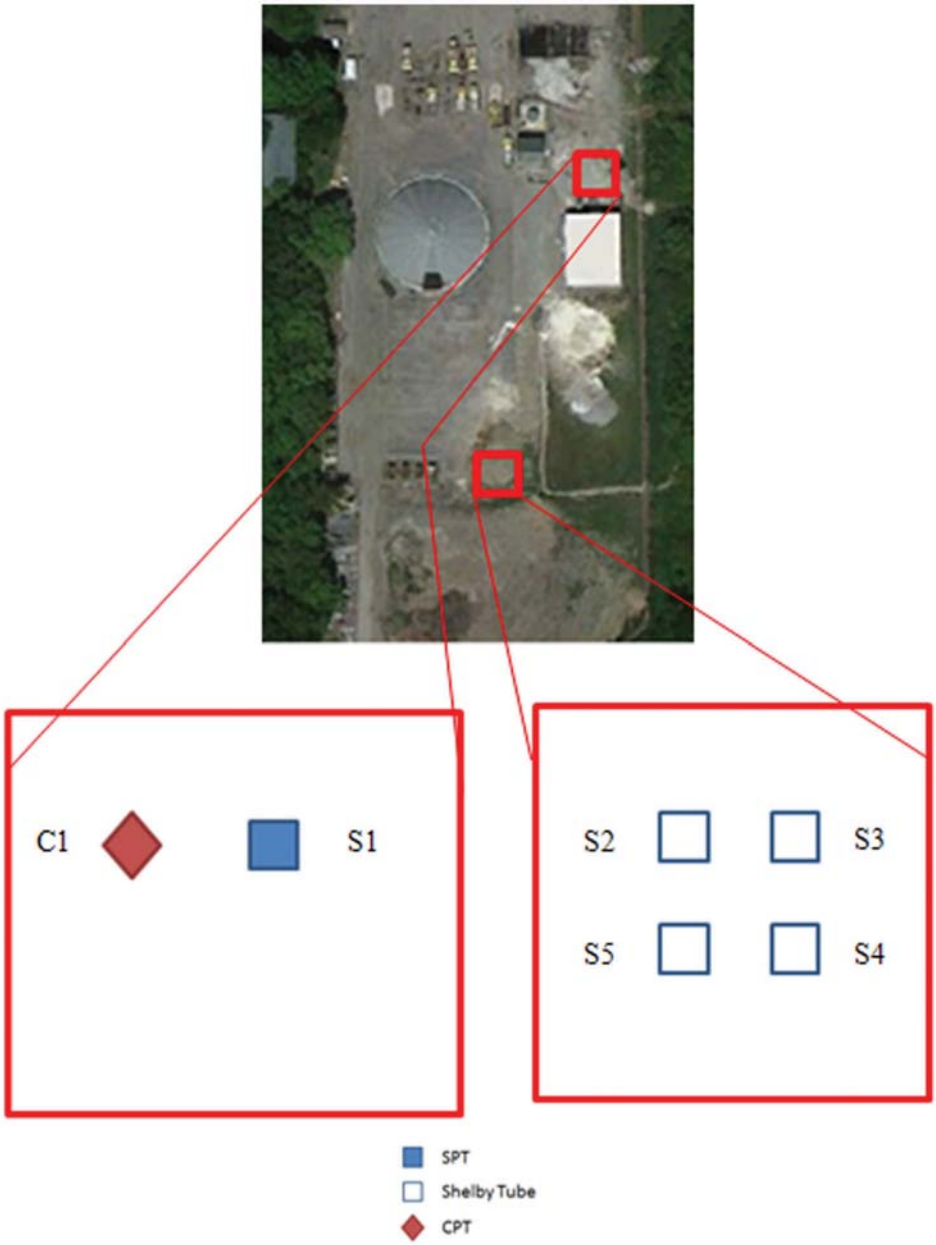

Figure 4.6 Satellite view of the Lafayette site from Google Earth. 3-meter approximate spacing between SPT borings and CPT soundings at the Lafayette site.

at the site is approximately 85 meters thick consisting of Wisconsin and Illinoian deposits with bedrock consisting of New Albany Shale from the Devonian Age. A satellite image of the Frankfort site is shown in Figure 4.7. Twenty-three torque tests were performed in seven borings in the period from January 4–6, 2012. Figure 4.7 presents the plan view with an approximate spacing of 3 meters between the SPT borings and CPT soundings. Two borings were terminated at a depth of 6.10 meters, and the last five were terminated at a depth of 4.57 meters due to sand heave preventing the drill crew from reaching the proper testing depth. The seven boring logs are presented in Figures F.11, F.13, F.15, F.17, F.19, F.21, and F.23 in Appendix F with a ground surface elevation of 264.33 meters. The groundwater table, represented by a blue line in Figures F.12, F.14, F.16, F.18, F.20, F.22, and F.24 in Appendix F, was observed at 3.81 meters below the ground surface. All tests were performed at 1.52 meter intervals. Four Shelby tubes were pushed to collect undisturbed samples, two tubes in FRMU 2 and 9, respectively. Seven CPT soundings that were performed to a depth ranging from 2.74 to 9.14 meters on April 5, 9 and 10, 2012. Figures F.12, F.14, F.16, F.18, F.20, F.22, and F.24 in Appendix F present seven SPT borings and CPT soundings from the Frankfort Maintenance Unit.

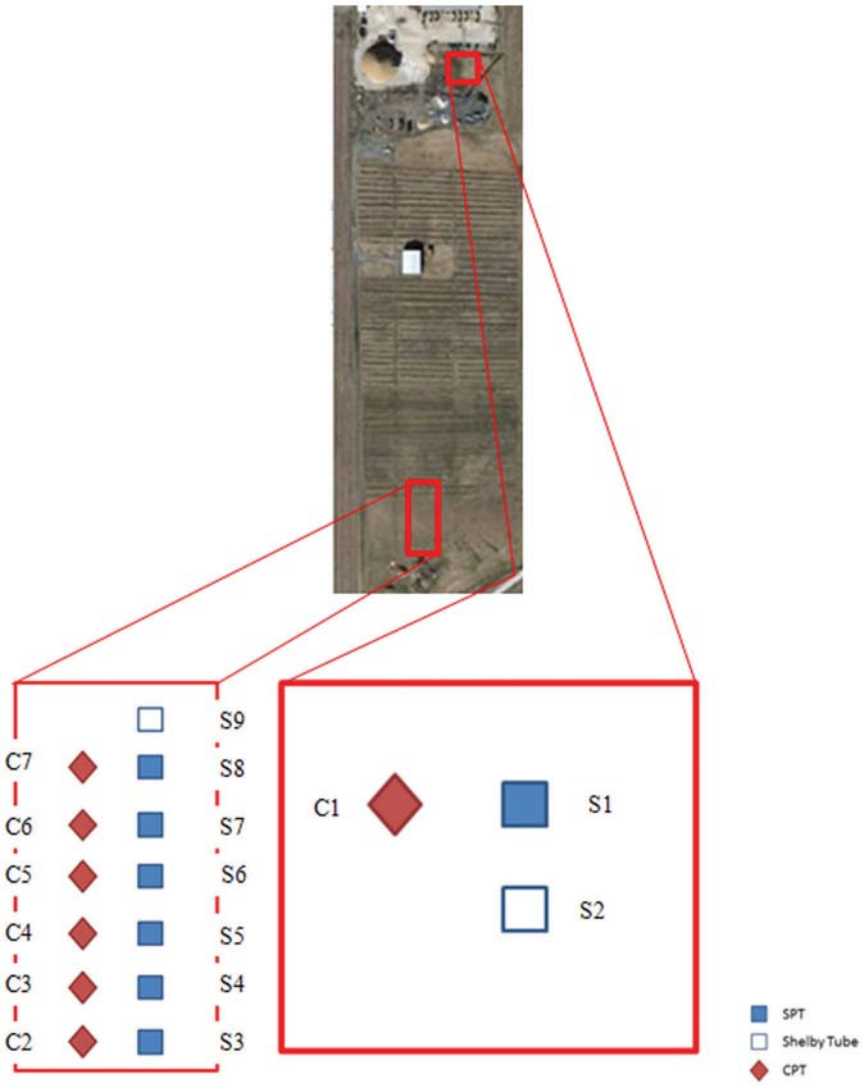

Figure 4.7 Satellite view of the Frankfort site from Google Earth. 3-meter approximate spacing between SPT borings and CPT soundings at the Frankfort site.

4.2.4 The Romney Maintenance Unit (Tippecanoe County)

The Romney Maintenance Unit (RMU) is located 2.4 kilometers south of the community of Romney on the west side of U.S. Highway 231. The glacial till deposit at the site is approximately 30 meters thick consisting of Wisconsin and Illinoian deposits with bedrock consisting of the Wabash Formation from the Silurian Age. A satellite image of the Romney site is shown in Figure 4.8. A total of twenty-five SPT-Torque tests were performed in six borings from January 9–10, 2012. Figure 4.9 presents the plan view with an approximate spacing of 3 meters between the SPT borings and CPT soundings. The six boring logs are presented in Figures F.25, F.27, F.29, F.31, F.33, and F.35 in Appendix F with a ground surface elevation of 233.23 meters. The groundwater table, represented by a blue line in Figures F.26, F.28, F.30, F.32, F.34, and F.36 in Appendix F, was observed at 5.49 meters below the ground surface. One boring was terminated at a depth of 7.62 meters, while the other SPT-Torque borings were terminated at a depth of 6.10 meters. All tests were performed at 1.52 meter intervals. Two Shelby tube samples were taken at the site, one tube from RMU 8 and one tube from RMU 9. Hard and dense soils prevented pushing of the Shelby tubes below the depth of 1.68 meters. Six CPT soundings that were performed to a depth ranging from 6.95 to 10.67 meters on March 1, 6, and 26, 2012. Figures F.26, F.28, F.30, F.32, F.34, and F.36 in Appendix F present the six SPT borings and CPT soundings from the Romney Maintenance Unit.

4.2.5 The Koleen Interstate 69 Expansion Site (Greene County)

The Koleen site (KS) is located 1.1 kilometers south of the community of Koleen on the west side of County Road 600 East which intersects County Road 400

Figure 4.8 Satellite view of the Romney site from Google Earth.

South. The glacial deposit at the site is approximately 15 meters thick consisting of Illinoian deposits along the bedrock boundary consisting of the Raccoon Creek Group from the Pennsylvania Age and the Buffalo Wallow Group of the Mississippian Age. A satellite image of the Koleen site is shown in Figure 4.10. A total of twenty-eight SPT-Torque tests were performed in four borings from July 16–19, 2012. Figure 4.11 shows the plan view with an approximate spacing of 3 meters between the SPT borings and CPT soundings. The ground surface is 158.84 meters. No groundwater table was observed due to the low permeability of the fine-grained soil present at the site. The boring logs are presented in Figures F.37, F.39, F.41, and F.43 in Appendix F. The groundwater table, represented by a blue line in Figures F.38, F.40, F.42, and F.44 in Appendix F, is at an approximate depth of 2.29 meters below the ground surface. This depth was estimated based on the degree of saturation of the collected soil samples. Three borings were terminated at a depth of 9.15 meters, and the fourth boring was terminated at

Figure 4.10 Satellite view of the Koleen site from Google Earth.

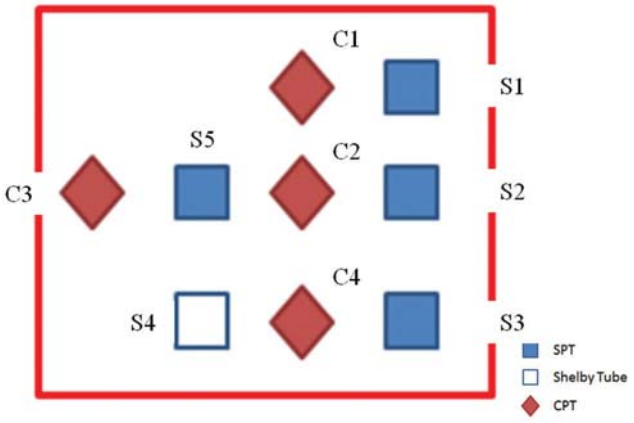

Figure 4.11 3-meter approximate spacing between SPT borings and CPT soundings at the Koleen site.

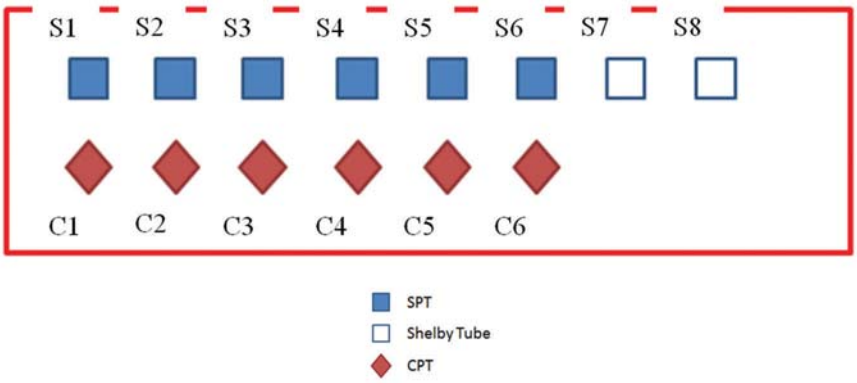

Figure 4.9 3-meter approximate spacing between SPT borings and CPT soundings at the Romney site.

15.24 meters. All tests were performed at 1.52 meter intervals. Four Shelby tube samples were taken at the site from KS 4. Four CPT soundings were performed to a depth ranging from 7.92 to 16.85 meters on July 17–20, 2012. Figures F.38, F.40, F.42, and F.44 in Appendix F present the four SPT borings and CPT soundings from the Koleen site.

4.3 Chapter Summary

Chapter 4 provided details regarding all SPT-Torque and CPT field testing performed at the Flora Maintenance Unit in Carroll County, the Lafayette and Romney Maintenance Units in Tippecanoe County, the Frankfort Maintenance Unit in Clinton County and the Koleen Interstate 69 expansion site in Greene County. Further field data relating to the five sites are presented in Appendix D and Appendix F.

5. LABORATORY TESTING

5.1 Testing Program

The laboratory testing was performed in the Geotechnical Soil Laboratories at Purdue University. The testing program consisted of index testing. The index testing is comprised of many individual tests. Index testing is commonly used to classify the type of soil from a given sample. Disturbed samples from split-spoon samplers or undisturbed samples from Shelby tubes can be used for index testing. Separation criteria include soil type (sand, silt, and clay); degree of saturation relating to saturated or unsaturated soil response; and plasticity which mirrors the division based on soil type (non-plastic sand, non-plastic silt or plastic clay). Relationships identifying correlations between the *in situ* torque tests ($N_{1,60}$, $q_{c,1}$ and f_s) are developed according to soil type, degree of saturation and non-plastic/plastic divisions. Further details relating the identified relationships between the measured *in situ* torque and tip resistance results and laboratory test results are discussed in Chapter 6, "Results and Analysis."

5.2 Index Testing

Index testing plays an important role in classifying soil collected in the field. Index testing is used to determine the type of soil, the percentages of the coarse-grained and fine-grained material (from sieve analysis and hydrometer tests) and water content of a given soil sample. From these tests, grain size distribution curves can be obtained. Additional tests (Atterberg limits) can be performed to determine the soil plasticity of fine-grained soils. The data from these tests are used in accordance with the Unified Soil Classification System (ASTM D2487 (ASTM, 2010b)).

5.2.1 Sieve Analysis Test

The sieve analysis (ASTM D6913 (ASTM, 2009)) is a composite test that separates soil particles based on the particle diameter. The amount of sample needed is dependent on the largest particle size found within the sample. Individual sieves are selected based on the desired break points of particles. Commonly, the sieves are selected to separate soil types such as coarse-grained soils, gravel and sand, from fine-grained soils, silt and clay. The sieve set is placed in a mechanical shaker with a sufficient sample size. Once the soil has been separated, the amount of soil retained by weight on each sieve, as a percentage of the total sample weight, is recorded. These percentages retained are used with the Unified Soil Classification System (USCS) to classify the soil sample. The wet sieving method is used if fine-grained soil flocculates into peds after the sample has been air dried. The addition of water will cause the peds of fine-grained material to break down to single soil particles and pass through each individual sieve. Once all sieves have been washed, the sieves are oven dried and the percentage of coarse-grained and fine-grained soils are determined as stated above. Refer to ASTM D6913 (ASTM, 2009) for the detailed procedure regarding "Sieve Analysis Testing."

Figure 5.1 presents a photograph of a sieve set that was used for sieve testing. The following sieves were used for all sieve testing: #10, #20, #40, #60, #100, #140, #200, and the pan. If it was determined that gravel was present in the soil sample, a #4 sieve was placed on top of the #10 sieve before testing began. Figure 5.2 presents a photograph of the soil sample placed in the top sieve just before the wet sieving process began.

Figure 5.1 Photograph of a sieve set used to determine the soil gradation.

Figure 5.2 Photograph of the soil before starting the wet sieving process.

5.2.2 Hydrometer Test

Soil particles that are collected in the pan at the bottom on the sieve set are fine-grained soils, silt and clay. The particle size of this soil is determined using a hydrometer (ASTM D422 (ASTM, 2007a)). The soil (50 grams) is mixed with a dispersing agent, (Sodium Hexametaphosphate) that will prevent the flocculation of individual soil particles suspended in water, as shown in Figure 5.3. The mixing equipment and the process of determining the solution density with the hydrometer are shown in Figure 5.4. As time passes and the soil settles out of the solution, the density of the water-soil solution will decrease. The density is used with correction factors to determine the particle diameter and percent passing values. Refer to ASTM D422 (ASTM, 2007a) for the detailed procedure regarding hydrometer testing.

Figure 5.3 Photograph of 50 grams of soil passing a #200 sieve with 5 grams of anti-flocculation agent, Sodium Hexametaphosphate.

5.2.3 Water Content Test

The water content test (ASTM D2216 (ASTM, 2010a)) is normally performed when other index tests or shear strength tests are performed. Water content is defined as the weight of water divided by the weight of solids and calculated as a percentage. A small sample of soil is taken from a larger soil specimen. The weight of the soil sample is recorded both before and after placing the sample in an oven for a period of 24 hours. The oven is kept at a temperature of 110°C to evaporate the water in the soil. The difference of the weight before and after the test is equal to the weight of water. The weight of water and weight of solids after the evaporation is used to calculate the water content. Refer to ASTM D2216 (ASTM, 2010a) for the detailed procedure regarding water content determination. Figure 5.5 presents a photograph of a soil sample in a water content container. Figure 5.6 presents water content containers that are placed in the drying oven.

5.2.4 Atterberg Limits Test

Atterberg Limits (ASTM D4318 (ASTM, 2010c)) are used to determine different phase limits of a soil sample. The liquid limit test (Figure 5.7) and the plastic limit test (Figure 5.8) are the two common limits that are determined for engineering design. The liquid limit determines the water content limit at which the soil begins to act as a liquid when energy is applied to soil that has been separated by a grooving tool. The plastic limit determines the water content limit of the soil at which the soil begins to crack due to lack of plasticity. In both cases, the water content is determined when each respective limit is reached. The water content is determined as previously described in 5.2.3 and shown in Figure 5.5 and Figure 5.6. The difference between these two limits is known as the plasticity index. The plasticity index and the liquid limit are used to classify fine-grained soils such as silt and clay by using the Unified Soil Classification System. Refer to ASTM D4318 (ASTM, 2010c) for the detailed procedure regarding Atterberg limit testing.

5.3 Chapter Summary

Chapter 5 presented details relating to the index testing performed on the disturbed and undisturbed samples collected at the five sites listed in Chapter 4. The index testing comprised of water content, sieve analysis, Atterberg limits and hydrometer analysis were used to classify the soil type of the disturbed samples. Additionally, index testing provided the percent fines passing the #200 sieve and the plasticity index is used to develop the relationships presented in Chapter 6. Further laboratory data relating to the five sites are presented in Appendix D.

Figure 5.4 A photograph, on the left, of the soil solution being amalgamated with the electric mixer and a photograph, on the right, of the hydrometer placed in the soil solution.

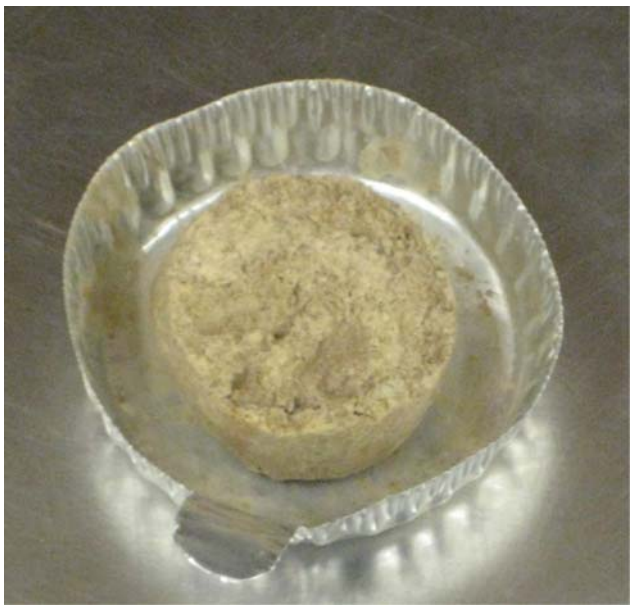

Figure 5.5 Photograph of a soil sample in a water content container.

Figure 5.6 Photograph of water content tests placed in the drying oven.

Figure 5.7 Photograph of a liquid limit test.

Figure 5.8 Photograph of a plastic limit test.

6. RESULTS AND ANALYSIS

6.1 Field Test Results and Analysis

SPT-Torque and CPT field testing were performed at five sites located in four counties: Flora in Carroll County, Frankfort in Clinton County, Koleen in Greene County, and Lafayette and Romney in Tippecanoe County. SPT-Torque tests were performed at 1.52 meter intervals until boring termination. CPT tests were performed adjacent to the SPT borings either to the depth of SPT-Torque boring termination or cone penetration refusal. All SPT, CPT, torque testing and laboratory testing for the five sites are presented in Appendix D with the data used for the development of the relationships presented in Appendix E. Figure 6.1 presents an ideal SPT-Torque curve. The torque increases until the peak torque is reached and then continues to decrease until a continuous horizontal critical-state torque is observed for non-plastic soils or a residual-state torque is observed for plastic soils. The computer software records the largest torque value as the peak torque. The critical-state or residual-state torque is determined by visual observation and recording of the corresponding torque value.

6.1.1 Torque Ratio

The torque ratio is defined as the ratio of the measured torque to the blow count. Torque data has units of N-m. The measured *in situ* blow counts are corrected to N_{60}, as shown in Equation 2.1. Torque ratios were calculated by dividing the torque by the respective blow count. Table 6.1 presents ranges of peak and critical-state torque ratios for non-plastic soils and peak- and residual-state torque ratios for plastic soils. Three groupings are shown that represent the range of torque ratios for all samples, regardless of the degree of saturation and then by accounting for the saturated or unsaturated condition.

All torque ratios have the same orders of magnitude and prevent observable differences between the categories. The calculation of torque ratios does not adequately capture any differences between the soil types or the fines percentage found within the soil for

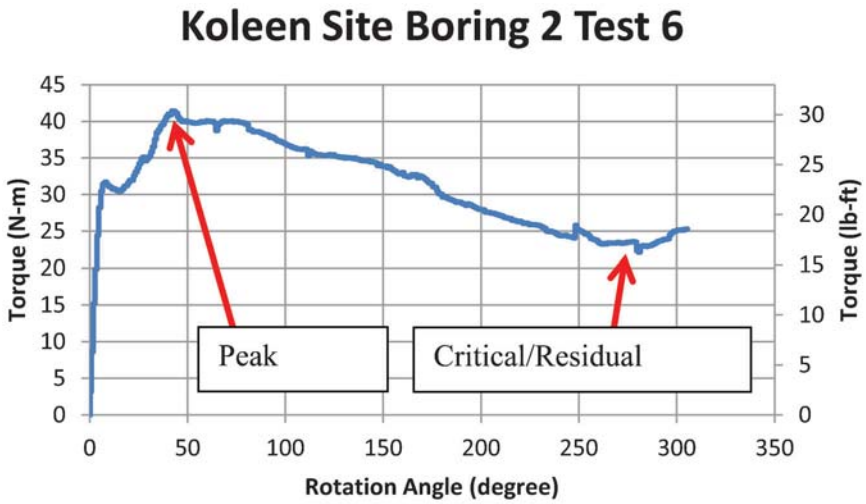

Figure 6.1 Koleen site boring 2 test performed at a depth of 8.69–9.15 meters.

soil classification purposes. Torque ratios were not used for engineering design due to the overlap of torque ratio values for various soils.

6.1.2 Standard Penetration Test N_{60} Values

Recorded blow counts were corrected to a 60 percent hammer efficiency based on Equation 2.1 from Chapter 2:

$$N_{60} = C_h C_r C_s C_d N_{SPT} \tag{2.1}$$

All $N_{1,60}$ values are presented in Appendix D with the corresponding depth, soil classification, $q_{c,1}$, water content, Atterberg limits, and sieve analysis gradation.

6.1.3 Peak and Critical/Residual Unit Side Resistance from Torque Tests

The unit side resistance values are calculated using Equation 2.7, which is shown below. The peak and critical/residual unit side resistance are selected from the collected *in situ* data. The peak unit side resistance is the largest recorded data point. The critical/residual unit side resistance is determined by reviewing the data and identifying the constant unit side resistance at large deformation strains which develop due to the large split-spoon sampler rotations.

$$f_s = \frac{2T}{\pi d^2 L} \tag{2.7}$$

TABLE 6.1
Ranges of peak and residual-state torque ratios for various soil types

Soil Type	Peak T_R[a]	Critical/Residual T_R[a]	Unsaturated Peak T_R[a]	Saturated Peak T_R[a]	Unsaturated Critical or Residual T_R[a]	Saturated Critical or Residual T_R[a]
CL	4.58–32.96	1.06–27.14	4.58–28.20	4.99–32.96	3.19–23.54	1.06–27.14
CL-ML	2.37–10.55	1.96–9.07	6.38	2.37–10.55	5.89	1.96–9.07
ML	3.52–13.67	3.43–10.10	7.93–9.16	3.52–13.67	6.46–7.52	3.43–10.10
SC	13.90	11.69	13.90	N/A	11.69	N/A
SC–SM	4.09–21.01	3.11–16.02	4.09–21.01	14.47	3.11–16.02	10.38
SM	1.64–13.24	1.64–11.61	1.64–13.24	6.29–10.06	1.64–11.61	2.37–7.44
SP-SC	7.28–31.88	5.15–25.83	7.28–10.79	14.80–31.88	5.15–10.14	9.24–25.83
SP-SM	4.50–12.51	2.62–8.99	4.50–12.51	N/A	2.62–8.99	N/A
SP	7.36–17.00	6.54–15.53	N/A	7.36–17.00	N/A	6.54–15.53
SW-SC	6.05	5.15	6.05	N/A	5.15	N/A
SW-SM	9.65	8.91	N/A	9.65	N/A	8.91
GW	0.63	0.39	0.63	N/A	0.39	N/A

[a]Torque has torque units of N-m and Blow count corresponds to N_{60}.

Note: CL is Clay, CL-ML is silty clay, ML is silt, SC is clayey sand, SC-SM is silty clayey sand, SM is silty sand, SP-SC is poorly-graded sand with clay, SP-SM is poorly-graded sand with silt, SP is poorly-graded sand, SW-SC is well-graded sand with clay, SW-SM is well-graded sand with silt, GW is well-graded gravel.

6.1.4 Cone Penetration Test Tip Resistance

The cone penetration tip resistance was determined by averaging the data collected over a 0.45 meter distance (length of the split-spoon sampler) at the depth corresponding to the SPT-Torque test in the adjacent boring. All $q_{c,1}$ are presented in Appendix D with the corresponding depth, soil classification, $N_{1,60}$, water content, Atterberg limits, and sieve analysis gradation.

6.2 Laboratory Testing Analysis

The laboratory testing was performed in the Geotechnical Soil Laboratories at Purdue University. The testing program consisted of index testing. Index testing is commonly used to classify the type of soil from a given sample. Disturbed samples from a split-spoon sampler or undisturbed samples from a Shelby tube can be used for index testing. Index tests help classify the soil type and develop properties which are used to separate the various soils. Separation criteria include soil type (sand, silt, and clay); degree of saturation relating to saturated or unsaturated soil mechanics; and plasticity which mirrors the division based on soil type (non-plastic sand, non-plastic silt or plastic clay). Relationships identifying correlations between the *in situ* torque tests and laboratory results were developed once the divisions were made.

6.3 Field Test Results

Traditionally, the blow count, percent recovery of soil, and soil type are logged at each depth at which an SPT test is performed. With the addition of the torque testing, the following data are recorded with the traditional information: the maximum torque, the unit side resistance and the rotation angle of the maximum torque. The peak unit side resistance depends on the maximum torque, diameter of the split-spoon sampler and the penetration length, as shown in Equation 2.7. After the maximum torque, the torque decreases until a continuous horizontal critical-state torque is observed for non-plastic soils or a residual-state torque is observed for plastic soils. The critical/residual torque is used in Equation 2.7 to calculate the critical/residual unit side resistance. Relationships are developed between the peak and critical/residual unit side resistance and more traditional *in situ* tests, SPT (Section 6.3.1) and CPT (Section 6.3.2), for sand, non-plastic silt, and clay soil types. Additionally, the undrained shear strength is estimated using Equation 2.4 and related to the unit side resistance. The unit side resistance is related to the undrained shear resistance under a specific loading condition for the clay and silt relationships due the build-up of excess pore pressures during the process of applying torque to the sampler. Since the pore pressure can dissipate immediately in sand, the unit side resistance is related to its drained shear resistance.

6.3.1 $N_{1,60}$ versus Unit Side Resistance Relationships

Figure 2.1 in Chapter 2 presents the relationships between N_{60} and the unit side resistance originally published by Kelley and Lutenegger (2004) based on Equation 2.8 provided in Chapter 2; values of α_s are shown in Table 6.2 for fine-grained, coarse-grained, residual and glacial till soils. Figure 2.2 presents the relationship based on data for Wisconsin soils published in Winter et al. (2005), provided in Table 2.4.

$$f_s = \alpha_s N_{60} \tag{2.8}$$

N_{60} values can be normalized with respect to the vertical effective stress as:

$$N_{1,60} = N_{60}\sqrt{\frac{P_a}{\sigma'_v}} \tag{6.1}$$

where $N_{1,60}$ = normalized blow count with 60 percent hammer energy efficiency (Blows), N_{60} = blow count for 60 percent hammer energy efficiency (Blows), σ'_v = vertical effective stress (kPa), and P_a = reference stress (100 kPa).

Equation 2.8 was modified by normalizing the unit side resistance by the vertical effective stress and incorporating $N_{1,60}$, therefore creating a unitless equation for non-plastic silt and sand:

$$\frac{f_s}{\sigma'_v} = aN_{1,60} \tag{6.2a}$$

where f_s = unit side resistance (kPa), σ'_v = vertical effective stress (kPa), a = fitting parameter (unitless) and $N_{1,60}$ = normalized blow count for 60 percent hammer energy efficiency (Blows) and a unitless equation for clay:

$$\frac{f_s}{\sigma'_v} = aN_{1,60}\sqrt{OCR} \tag{6.2b}$$

where OCR = overconsoliation ratio. OCR values for the Koleen site were determined from 1-D consolidation tests performed from undisturbed samples collected at the site previously by INDOT. Limited OCR values are available for the Flora and Frankfort sites due to the difficulty of obtaining undisturbed samples in the field. The OCR is incorporated into the developed equation for clay soils to account for stress

TABLE 6.2
Empirical factors for unit side resistance versus standard penetration test N_{60} values for selected soil types (Kelley & Lutenegger, 2004)

Soil Type	α_s[a]
Fine-Grained	7.4
Coarse-Grained	3.6
Residual Soil	5.4
Glacial Till	1.5

[a]Factor provides f_s (kPa).

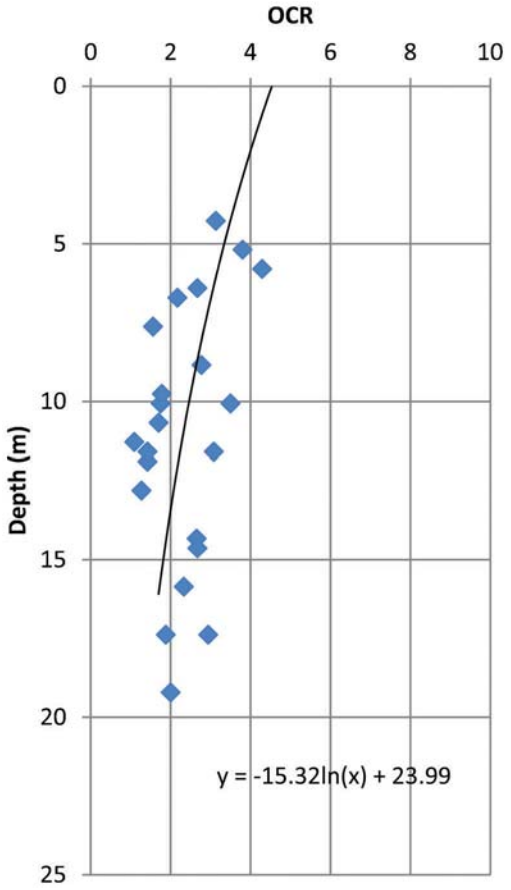

Figure 6.2 INDOT 1-D consolidation data with relationship for the Koleen site.

history. Figure 6.2 presents the INDOT 1-D consolidation data for the Koleen site, and Table 6.3 lists the data in tabular form with the 1-D consolidation plots shown in Appendix C.

Figure 6.3 presents the developed relationship between $N_{1,60}$ and peak unit side resistance for saturated clay, and Figure 6.4 presents the developed relationship between $N_{1,60}$ and residual unit side resistance for saturated clay. Figure 6.5 presents the developed relationship between $N_{1,60}$ and peak unit side resistance for saturated non-plastic silt, and Figure 6.6 presents the developed relationship between $N_{1,60}$ and critical unit side resistance for saturated non-plastic silt. Figure 6.7 presents the developed relationship between $N_{1,60}$ and peak unit side resistance, and Figure 6.8 presents the developed relationship between $N_{1,60}$ and critical unit side resistance for saturated sand. The coefficient of determination R^2 predicts the reliability of the developed relationships. The previous studies presented in Chapter 2 (Kelley & Lutenegger, 2004; Winter et al., 2005) do not provide the coefficient of determination for their relationships between N_{60} and the peak unit side resistance. Table 6.4 provides values of the fitting parameter, a, and the coefficient of determination for the six plots shown in Figures 6.3–6.8. The data used to develop the relationships and determine the respective

TABLE 6.3
INDOT 1-D consolidation data for the Koleen site

Depth (m)	OCR
4.27	3.13
5.79	4.05
6.40	2.57
6.71	2.17
6.71	2.34
7.62	1.56
8.84	2.11
8.84	2.77
9.76	1.78
9.76	2.11
10.06	2.34
10.06	3.50
10.67	2.34
11.28	1.75
11.58	1.42
11.58	3.08
11.89	1.75
12.80	1.27
14.33	2.66
14.63	2.67
15.85	2.33
17.38	2.41
17.38	2.94
19.21	2.00

fitting parameters and coefficients of determination are presented in Appendix E, Tables E.1–E.6.

As stated previously, no coefficient of determination values were presented with the relationships provided in Chapter 2 (Kelley & Lutenegger, 2004; Winter et al., 2005). Cottingham (2009) conducted research that developed a relationship which used laboratory testing to predict the peak unit side resistance. The coefficient of determination ranged from 0.338 to 0.554 (Cottingham, 2009). The coefficients of determination for the clay and non-plastic silt relationships in Table 6.4 are reasobale (0.676–0.773). The coefficients of determination for the sand relationships are low (0.127–0.307) and based on a small population of data. As shown in Figures 6.7 and 6.8, the data collected for saturated sand indicates that peak f_s/σ'_v increases with increasing $N_{1,60}$ (which is a measure of sand density) since peak strength is a function of soil density, while the critical-state $f_s/\sigma'v$ remains approximately constant at a value of 1.7 regardless of $N_{1,60}$ values since the critical-state strength is independent of density. Collection of further data would be helpful to improve these correlations for sands and to increase their coefficients of determinations. The developed relationships with low coefficients of determination should as their predictions may not be reliable.

Equation 6.3 modifies Equation 6.2 to develop a relationship which relates $N_{1,60}$ with the unit side resistance for unsaturated soils. Matric suction in unsaturated soils, which acts to increase the effective stresses, depends on the degree of saturation. The unit side resistance will increase with increasing effective stresses. Therefore, an inverse relationship exists

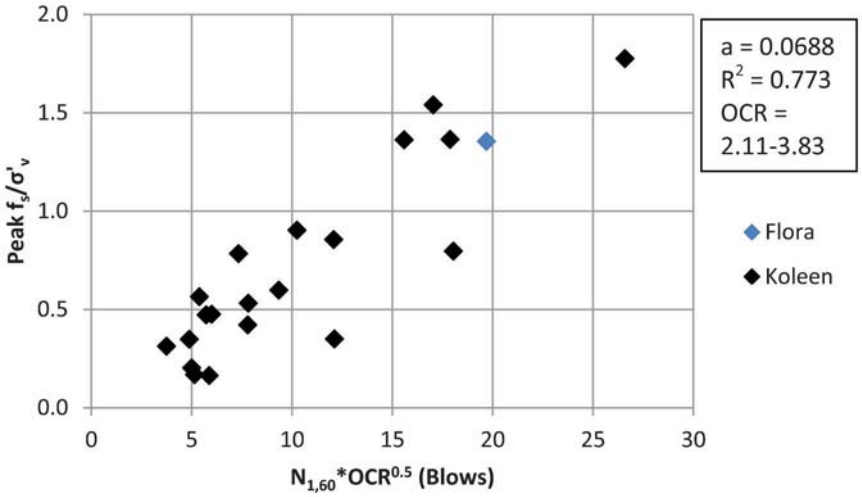

Figure 6.3 Peak unit side resistance versus $N_{1,60}$ values for saturated clay.

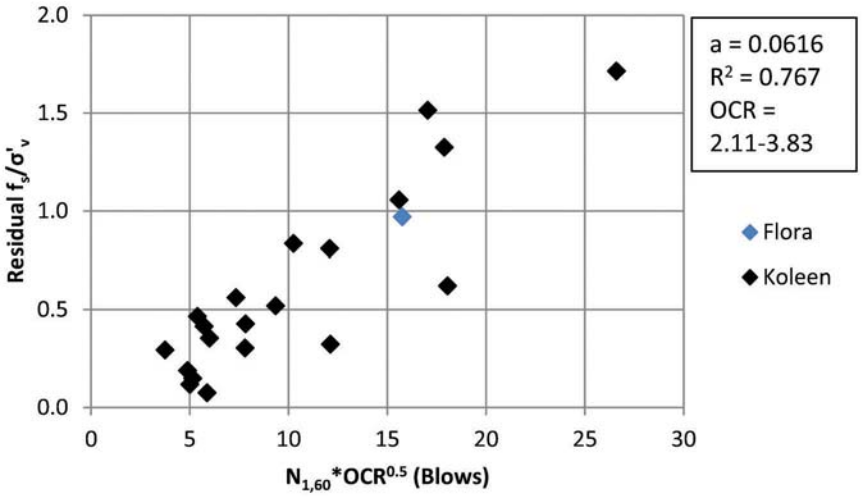

Figure 6.4 Residual unit side resistance versus $N_{1,60}$ values for saturated clay.

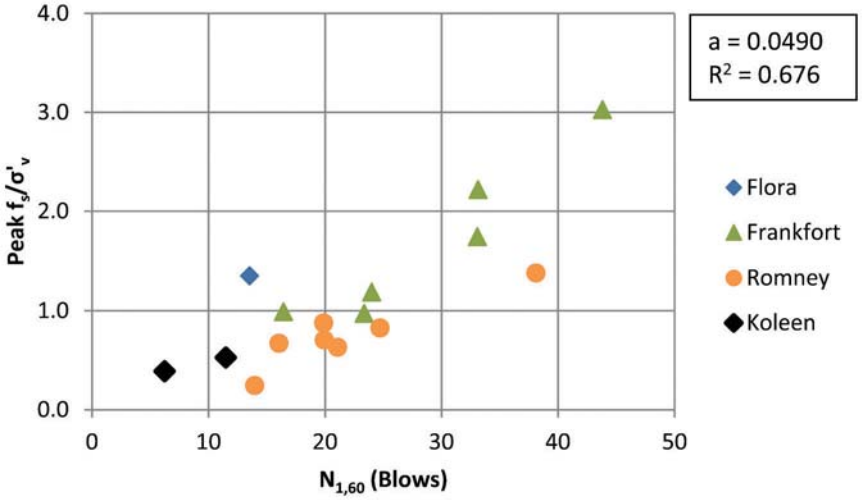

Figure 6.5 Peak unit side resistance versus $N_{1,60}$ values for saturated non-plastic silt.

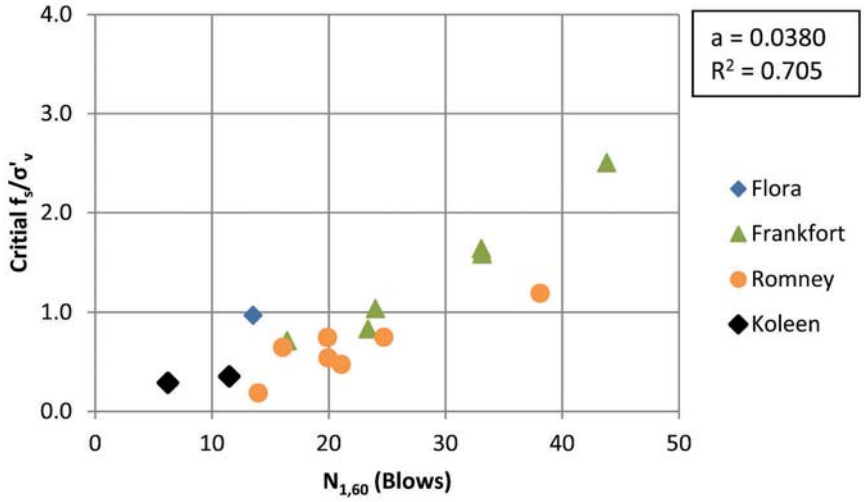

Figure 6.6 Critical unit side resistance versus $N_{1,60}$ values for saturated non-plastic silt.

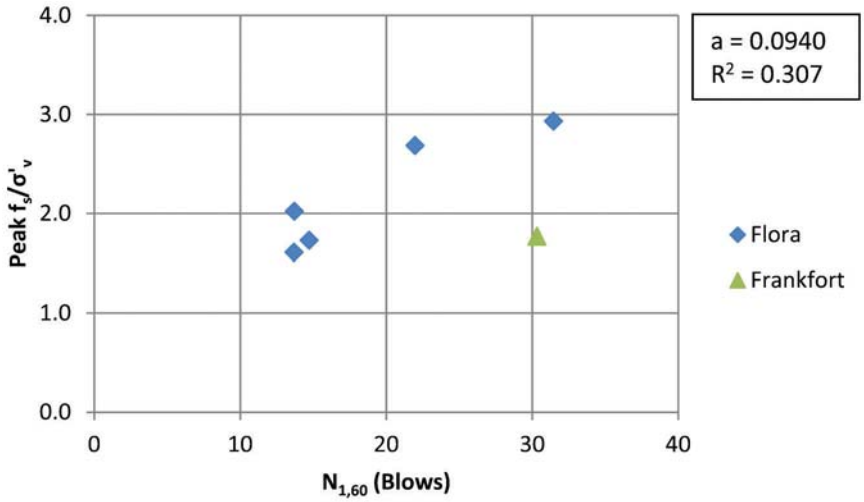

Figure 6.7 Peak unit side resistance versus $N_{1,60}$ values for saturated sand.

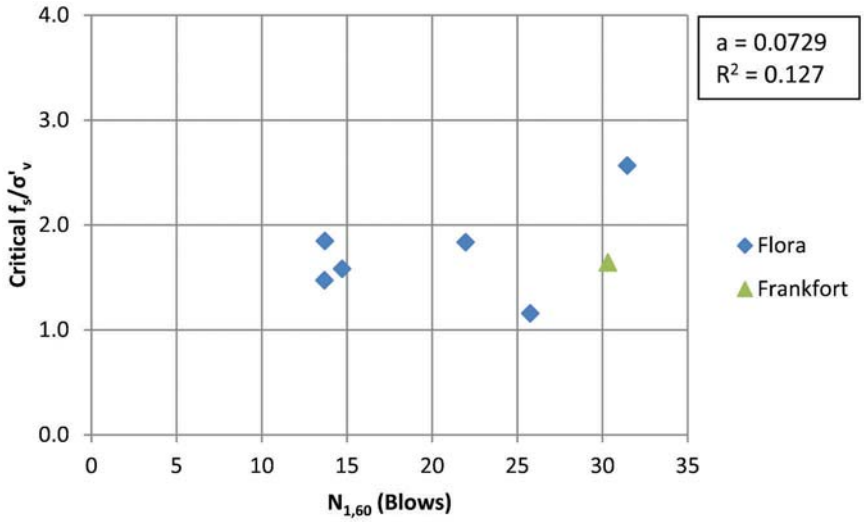

Figure 6.8 Critical unit side resistance versus $N_{1,60}$ values for saturated sand.

TABLE 6.4
Fitting parameter, a, and coefficient of determination relating $N_{1,60}$ and f_s shown in Equation 6.2 for various soils

	Fitting Parameter, a	Coefficient of Determination, R^2	OCR Range
Clay-Peak f_s	0.0688	0.773	2.11–3.83
Clay-Residual f_s	0.0616	0.767	2.11–3.83
Non-Plastic Silt-Peak f_s	0.0490	0.676	N/A
Non-Plastic Silt-Critical f_s	0.0380	0.705	N/A
Sand-Peak f_s	0.0940	0.307	N/A
Sand-Critical f_s	0.0739	0.127	N/A

between the degree of saturation and the unit side resistance:

$$\frac{f_s}{\sigma'_v} = a\frac{N_{1,60}}{S} \tag{6.3a}$$

where f_s = unit side resistance (kPa), σ'_v = vertical effective stress (kPa), a = fitting parameter (unitless), $N_{1,60}$ = normalized blow count for 60 percent hammer energy efficiency (Blows) and S = degree of saturation (percent) and:

$$\frac{f_s}{\sigma'_v} = a\frac{N_{1,60}}{S}\sqrt{OCR} \tag{6.3b}$$

where OCR = overconsolidation ratio.

Figure 6.9 presents the developed relationship between $N_{1,60}$ and peak unit side resistance for unsaturated clay. Figure 6.10 presents the developed relationship between $N_{1,60}$ and residual unit side resistance for unsaturated clay. Figure 6.11 presents the developed relationship between $N_{1,60}$ and peak unit side resistance for unsaturated non-plastic silt and Figure 6.12 presents the developed relationship between $N_{1,60}$ and critical unit side resistance for unsaturated non-plastic silt. Figure 6.13 presents the developed relationship between $N_{1,60}$ and peak unit side resistance for unsaturated sand and Figure 6.14 presents the developed relationship between $N_{1,60}$ and critical unit side resistance for unsaturated sand. Table 6.5 presents a summary of the fitting parameter, a, and the coefficient of determination for the six plots shown in Figures 6.9–6.14. The data used to develop the relationships and determine the respective fitting parameters and coefficients of determination are presented in Appendix E, Tables E.7–E.12.

The coefficients of determination for the clay relationships in Table 6.5 are reasonable (0.551–0.710). The coefficients of determination for the non-plastic silt relationships are low (0.115–0.232) and based on a small population of data. The coefficients of determination for the sand relationship fall between the stated values for non-plastic silt and clay. The developed relationships with low coefficients of determination should not be used as their predictions may not be reliable.

6.3.2 CPT Tip Resistance versus Unit Side Resistance Relationships

Cone resistance q_c can be normalized with respect to the vertical effective stress as:

$$q_{c,1} = q_c\sqrt{\frac{P_a}{\sigma'_v}} \tag{6.4}$$

where $q_{c,1}$ = normalized CPT tip resistance (kPa), q_c = CPT tip resistance (kPa), σ'_v = vertical effective stress (kPa), and Pa = reference stress (100 kPa).

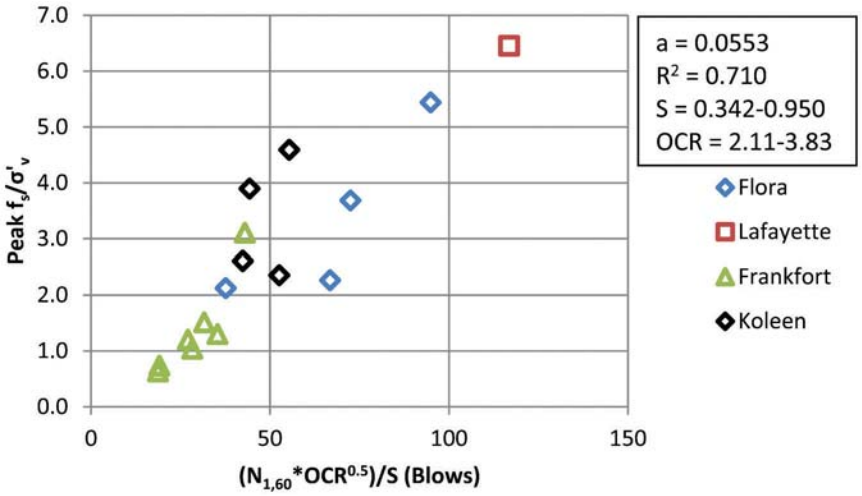

Figure 6.9 Peak unit side resistance versus $N_{1,60}$ values for unsaturated clay.

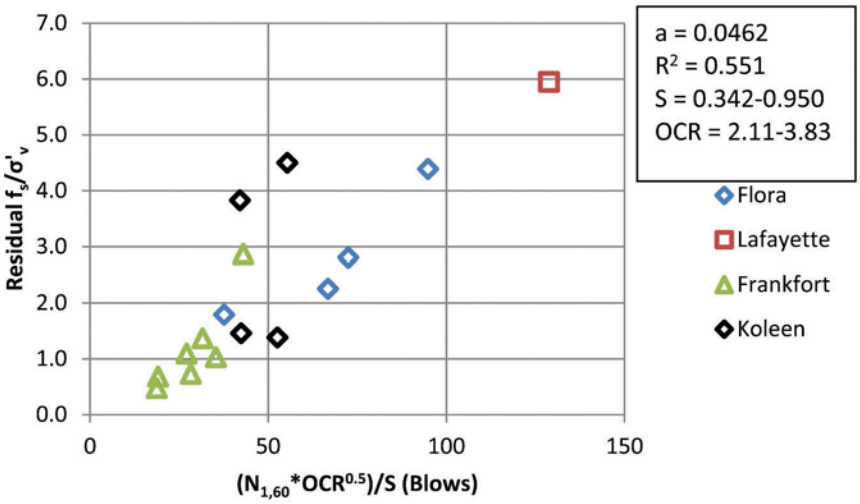

Figure 6.10 Residual unit side resistance versus $N_{1,60}$ values for unsaturated clay.

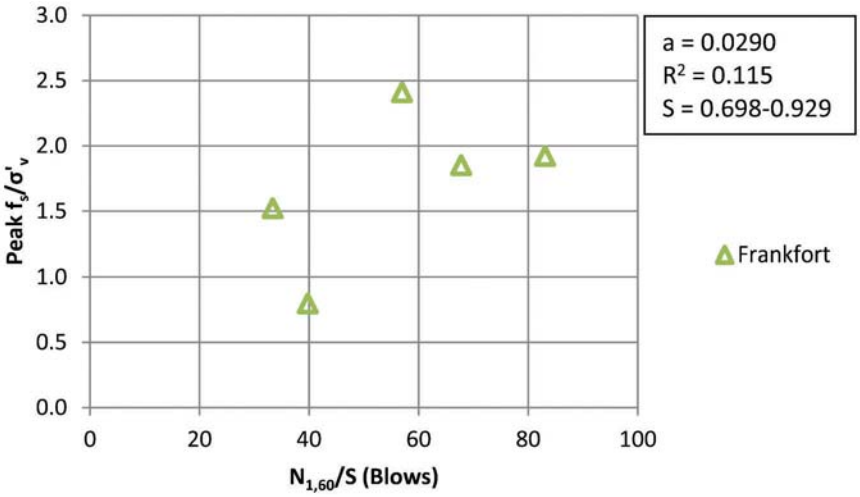

Figure 6.11 Peak unit side resistance $N_{1,60}$ values for unsaturated non-plastic silt.

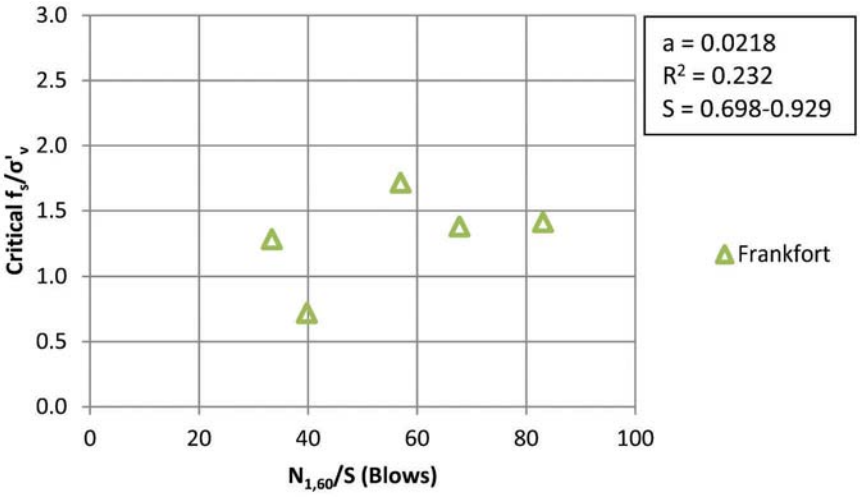

Figure 6.12 Critical unit side resistance $N_{1,60}$ values for unsaturated non-plastic silt.

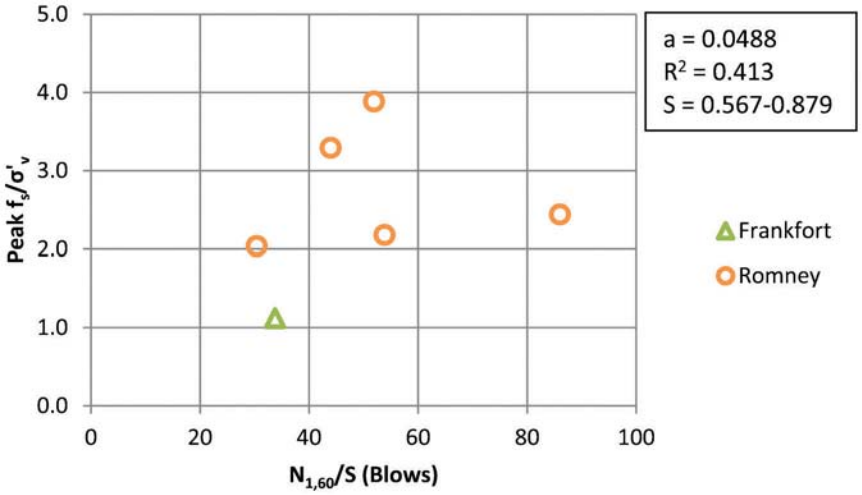

Figure 6.13 Peak unit side resistance $N_{1,60}$ values for unsaturated sand.

The relationship between unit side resistance and CPT tip resistance was normalized by the effective vertical stress and atmospheric pressure to develop a unitless equation for non-plastic silt and sand:

$$\frac{f_s}{\sigma'_v} = a\frac{q_{c,1}}{P_a} \tag{6.5a}$$

where f_s = unit side resistance (kPa), σ'_v = vertical effective stress (kPa), a = fitting parameter (unitless), $q_{c,1}$ = normalized CPT tip resistance (kPa) and P_a = atmospheric pressure (100 kPa) and a unitless equation for clay:

$$\frac{f_s}{\sigma'_v} = a\frac{q_{c,1}}{P_a}\sqrt{OCR} \tag{6.5b}$$

where OCR= over-consolidation ratio.

Figure 6.15 presents the developed relationship between $q_{c,1}$ and peak unit side resistance for saturated clay and Figure 6.16 presents the developed relationship between $q_{c,1}$ and residual unit side resistance for saturated clay. Figure 6.17 presents the developed relationship between $q_{c,1}$ and peak unit side resistance for saturated non-plastic silt and Figure 6.18 presents the developed relationships between $q_{c,1}$ and the critical unit side resistance for saturated non-plastic silt. Figure 6.19 presents the developed relationship between $q_{c,1}$ and peak unit side resistance for saturated sand, and Figure 6.20 presents the developed relationship between $q_{c,1}$ and critical unit side resistance for saturated sand. No published relationships using tip resistance to predict the unit side resistance were found in the literature. Table 6.6 summarizes the fitting parameter, a, and the coefficient of determination for the six plots shown in Figures 6.15–6.20. The data used to develop the relationships and determine the respective fitting parameters and coefficients of determination are presented in Appendix E in Tables E.13–E.18.

As stated previously, no published relationships relating CPT tip resistance and unit side resistance exist in the literature. The coefficients of determination for the clay and non-plastic silt relationships in

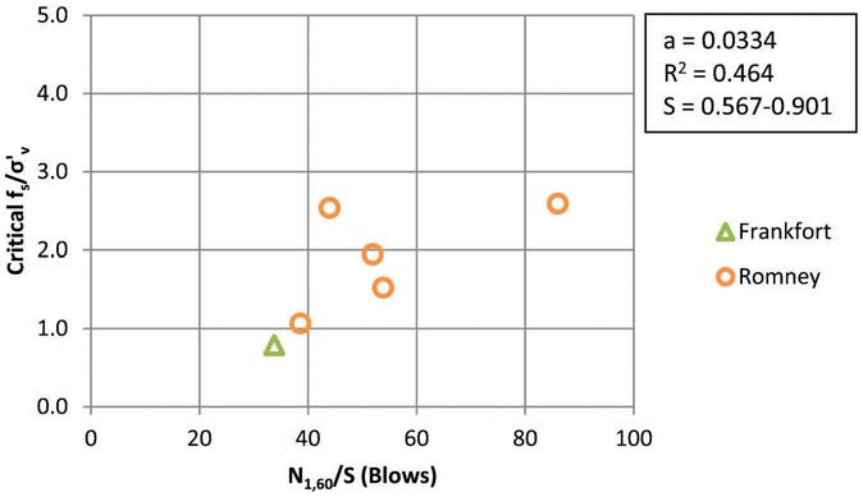

Figure 6.14 Critical unit side resistance $N_{1,60}$ values for unsaturated sand.

TABLE 6.5
Fitting Parameter, a, and coefficient of determination relating $N_{1,60}$ and f_s shown in Equation 6.3 for various soils

	Fitting Parameter, a	Coefficient of Determination, R^2	Degree of Saturation	OCR Range
Clay-Peak f_s	0.0553	0.710	0.342–0.950	2.11–3.83
Clay-Residual f_s	0.0462	0.551	0.342–0.950	2.11–3.83
Non-Plastic Silt-Peak f_s	0.0290	0.115	0.698–0.929	N/A
Non-Plastic Silt-Critical f_s	0.0218	0.232	0.698–0.929	N/A
Sand-Peak f_s	0.0488	0.413	0.567–0.879	N/A
Sand-Critical f_s	0.0334	0.464	0.567–0.901	N/A

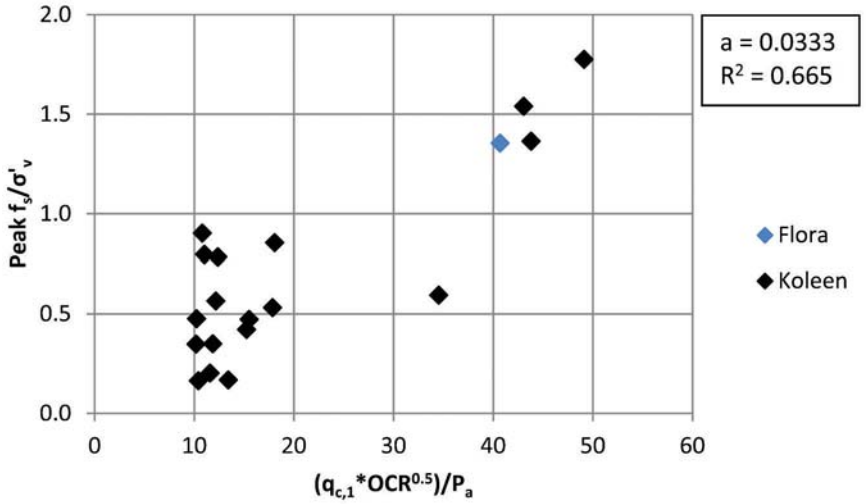

Figure 6.15 Peak unit side resistance versus $q_{c,1}$ values for saturated clay.

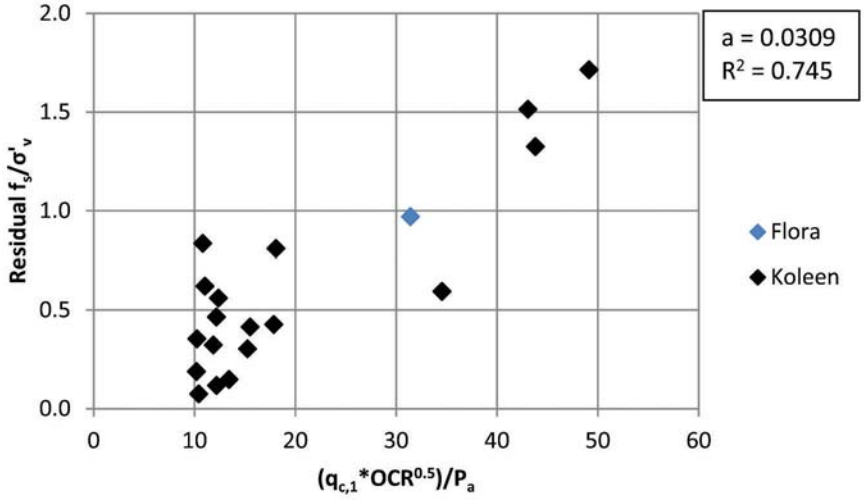

Figure 6.16 Residual unit side resistance versus $q_{c,1}$ values for saturated clay.

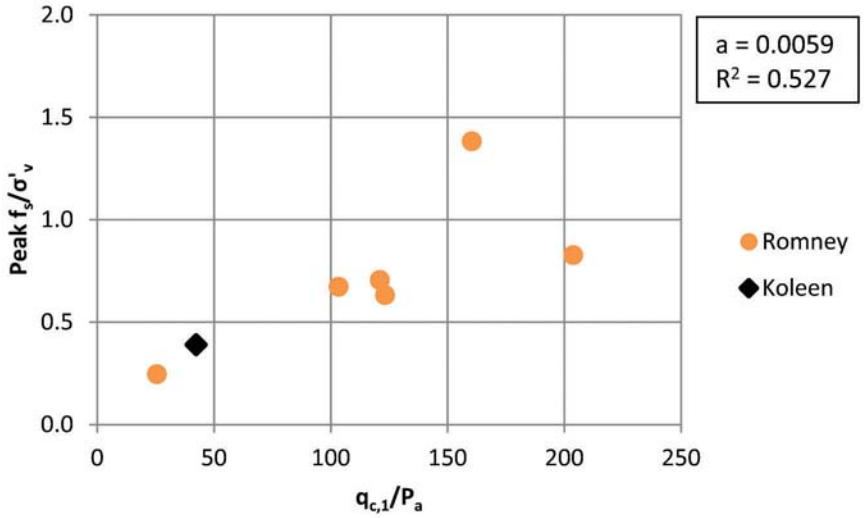

Figure 6.17 Peak unit side resistance versus $q_{c,1}$ values for saturated non-plastic silt.

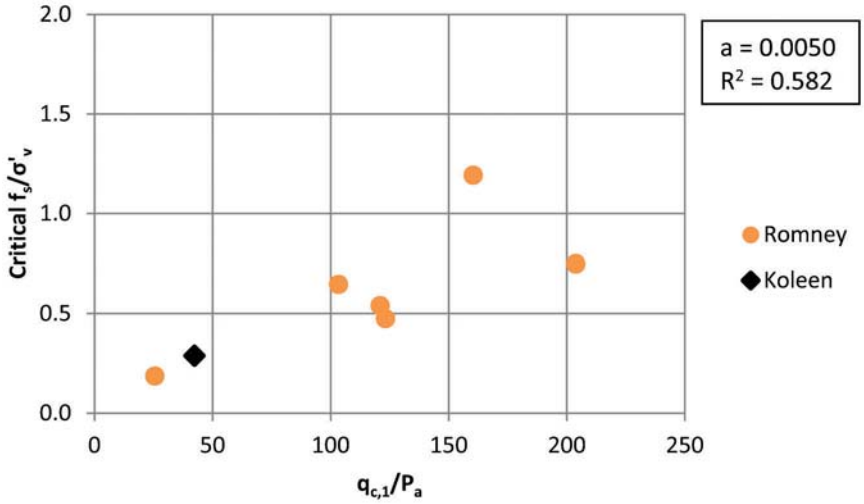

Figure 6.18 Critical unit side resistance versus $q_{c,1}$ values for saturated non-plastic silt.

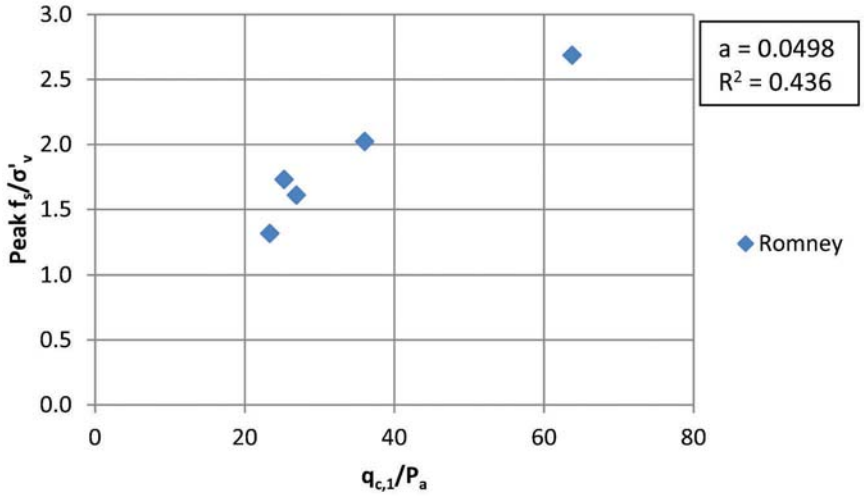

Figure 6.19 Peak unit side resistance versus $q_{c,1}$ values for saturated sand.

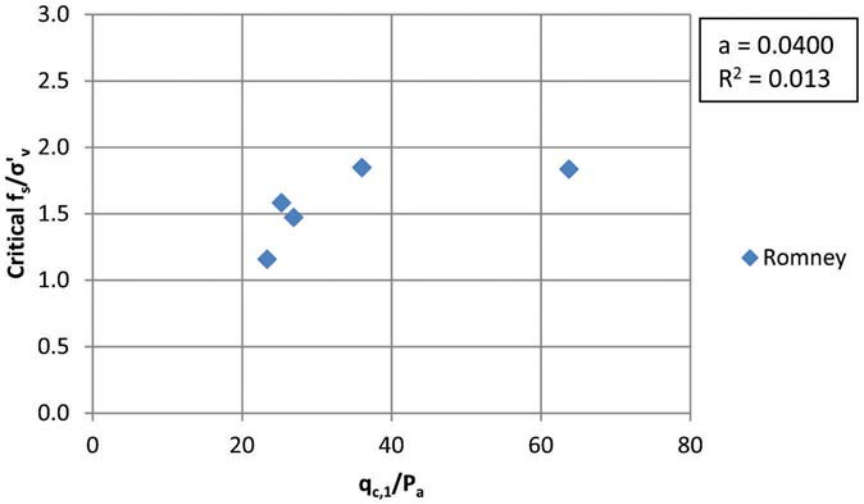

Figure 6.20 Critical unit side resistance versus $q_{c,1}$ values for saturated sand.

Table 6.6 are reasonably high (0.527–0.745). The coefficients of determination for the sand relationships are low (0.013–0.436) and based on a small population of data. The developed relationships based on low coefficients of determination should not be used.

The relationship between unit side resistance and undrained shear strength was normalized by the effective vertical stress and atmospheric pressure to develop a unitless equation:

$$\frac{f_s}{\sigma'_v} = a\frac{s_u}{\sigma'_v} \tag{6.6}$$

where f_s = unit side resistance (kPa), σ'_v = vertical effective stress (kPa), a = fitting parameter (unitless), s_u = undrained shear strength (kPa). The undrained shear strength was estimated using Equation 2.4 with cone factors equal to 10 and 14. Then Equation 6.6 was used to relate the unit side resistance with the undrained shear strength for saturated clays. Figure 6.21 presents the upper bound relationship between the peak unit side resistance and the undrained shear strength. Figure 6.22 presents the lower bound relationship between the peak unit side resistance and the undrained shear strength. Figure 6.23 presents the upper bound relationship between the residual unit side resistance and the undrained shear strength. Figure 6.24 presents the lower bound relationship between the residual unit side resistance and the undrained shear strength. Table 6.7 summarizes the upper and lower bounds with the cone factors used and the fitting parameter, a, with the coefficients of determination for Figures 6.21–6.24. The data used to develop the relationships and determine the respective fitting parameters and coefficients of determination are presented in Appendix E, Tables E.13–E.18.

The relationship between unit side resistance and undrained shear strength can also be expressed as:

$$\frac{f_s}{\sigma'_v} = a\frac{s_u}{\sigma'_v}OCR^b \tag{6.7}$$

where f_s = unit side resistance (kPa), σ'_v = vertical effective stress (kPa), a = fitting parameter (unitless), s_u = undrained shear strength (kPa), OCR = over-consolidation ratio, b = fitting parameter (unitless). In Equation 6.7 the end-of-test undrained shear strength determined from direct shear tests and the OCR determined from 1-D consolidation tests were used to obtain the fitting parameters a and b.

Figure 6.25 presents a relationship between the residual unit side resistance and the end-of-test undrained shear strength normalized using vertical effective stress. Table 6.8 summarizes the values of fitting parameters, a and b, together with the coefficient of determination. The data used to determine the fitting parameters and coefficients of determination are presented in Appendix E, Table E.19.

TABLE 6.6
Fitting parameter, a, and coefficient of determination relating $q_{c,1}$ and f_s shown in Equation 6.5 for various soils

	Fitting Parameter, a	Coefficient of Determination, R^2	OCR Range
Clay-Peak f_s	0.0333	0.665	1.79–4.23
Clay-Residual f_s	0.0309	0.745	1.79–4.23
Non-Plastic Silt-Peak f_s	0.0059	0.527	N/A
Non-Plastic Silt-Critical f_s	0.0050	0.582	N/A
Sand-Peak f_s	0.0498	0.436	N/A
Sand-Critical f_s	0.0400	0.013	N/A

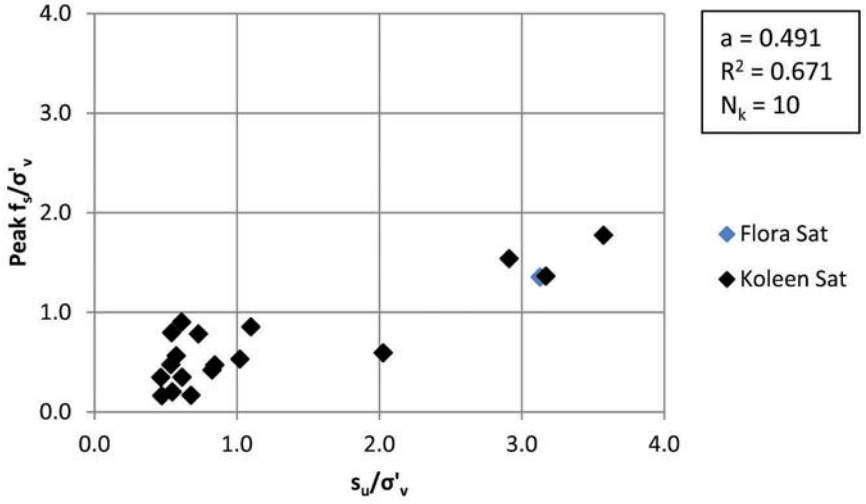

Figure 6.21 Upper bound relating peak unit side resistance to undrained shear strength.

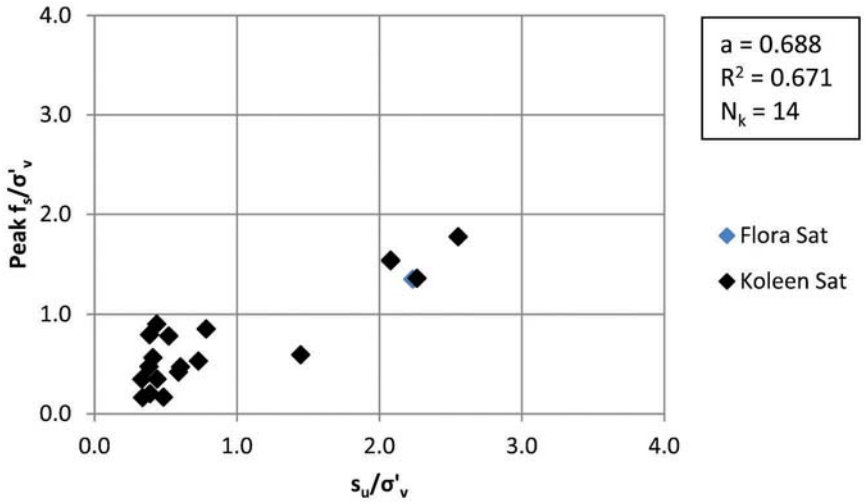

Figure 6.22 Lower bound relating peak unit side resistance to undrained shear strength.

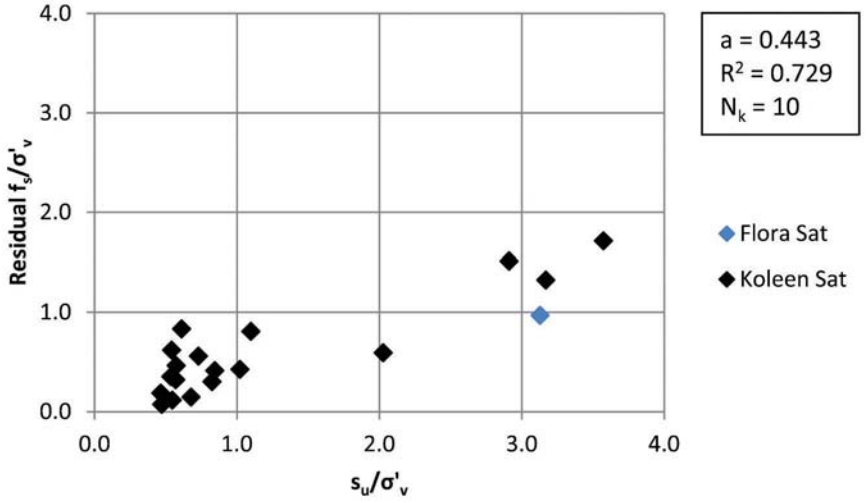

Figure 6.23 Upper bound relating residual unit side resistance to undrained shear strength.

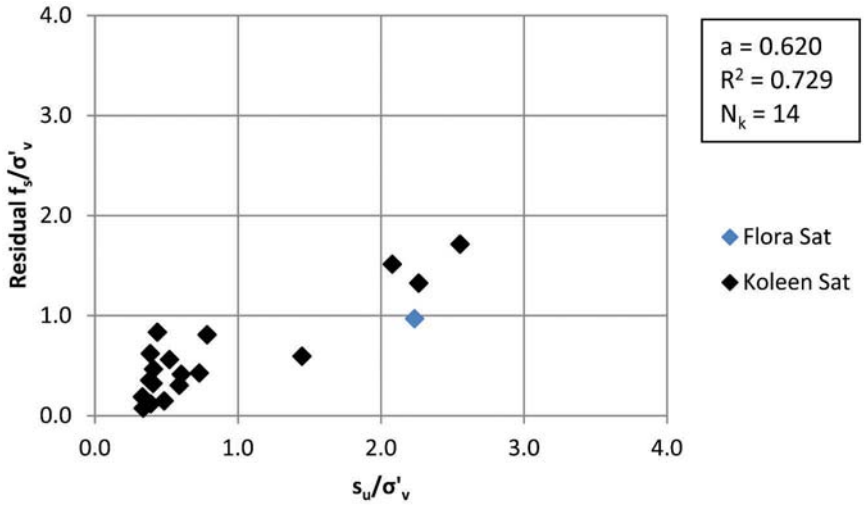

Figure 6.24 Lower bound relating residual unit side resistance to undrained shear strength.

TABLE 6.7
Cone factor, fitting parameter, and coefficient of determination for upper and lower bounds relating s_u and f_s shown in Equation 6.6 for clay soils

Bound	Cone Factor, N_k	Fitting Parameter, a	Coefficient of Determination, R^2
Upper Bound-Peak f_s	10	0.491	0.671
Lower Bound-Peak f_s	14	0.688	0.671
Upper Bound-Residual f_s	10	0.443	0.729
Lower Bound-Residual f_s	14	0.620	0.729

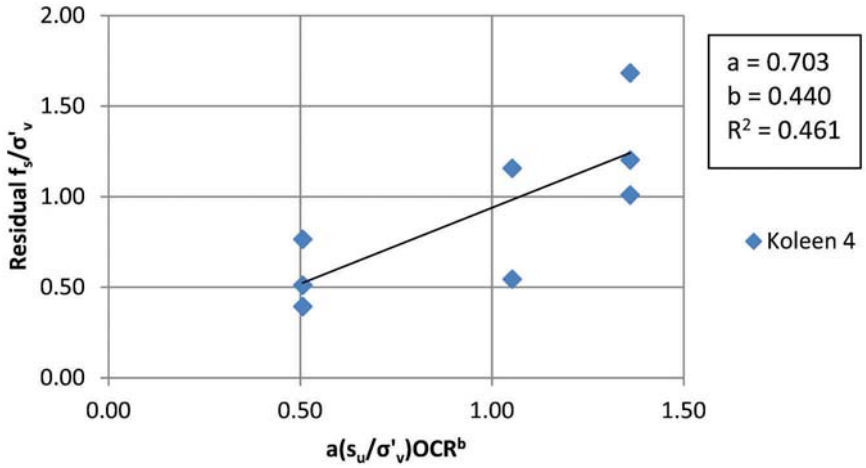

Figure 6.25 Residual unit side resistance versus end-of-test undrained shear strength for saturated clay normalized with vertical effective stress.

TABLE 6.8
Fitting parameters, and coefficient of determination relating s_u and f_s shown in Equation 6.7 for clay soils

Normalization	Fitting Parameter, a	Fitting Parameter, b	Coefficient of Determination, R^2
Vertical effective stress	0.703	0.440	0.461

As previously done with Equations 6.2 and 6.3, Equation 6.5 was modified to develop Equations 6.8 which capture the inverse relationship between the degree of saturation and unit side resistance due to matric suction occurring in unsaturated soils:

$$\frac{f_s}{\sigma'_v} = a\frac{q_{c,1}}{S(P_a)} \tag{6.8a}$$

where f_s = unit side resistance (kPa), σ'_v = vertical effective stress (kPa), a = fitting parameter (unitless), $q_{c,1}$ = CPT tip resistance (kPa), S = degree of saturation (percent) and P_a = atmospheric pressure (100 kPa) and:

$$\frac{f_s}{\sigma'_v} = a\frac{q_{c,1}}{S(P_a)}\sqrt{OCR} \tag{6.8b}$$

where OCR = over-consolidation ratio.

Figure 6.26 presents the developed relationship between $q_{c,1}$ and peak unit side resistance for unsaturated clay, and Figure 6.27 presents the developed relationship between $q_{c,1}$ and residual unit side resistance for unsaturated clay. Figure 6.28 presents the developed relationship between $q_{c,1}$ and peak unit side resistance for unsaturated non-plastic silt, and Figure 6.29 presents the developed relationships between $q_{c,1}$ and the critical unit side resistance for unsaturated non-plastic silt. Figure 6.30 presents the developed relationship between $q_{c,1}$ and peak unit side resistance for unsaturated sand and Figure 6.31 presents the developed relationship between $q_{c,1}$ and critical unit side resistance for unsaturated sand. No published relationships using tip resistance to predict the unit side resistance were found in the literature. Table 6.9 presents a summary of the fitting parameter a and the coefficient of determination for the six plots (Figures 6.26–6.31). The data used to develop the relationships and determine the respective fitting parameters and coefficient of determinations are presented in Appendix E, Tables E.20–E.25.

As stated previously, no published relationships relating CPT tip resistance and unit side resistance exist in the literature. The coefficients of determination for the clay-unit side resistance relationship in Table 6.6 need to be improved with more data. The coefficients of determination for the non-plastic silt and sand relationships are low (0.018–0.272) and based on a small population of data.

6.4 Chapter Summary

Chapter 6 presented two new relationships relating $N_{1,60}$ and $q_{c,1}$ to the unit side resistance measured in saturated and unsaturated soils and a new relationship relating s_u to the unit side resistance measured in saturated clay soils. The relationship using $N_{1,60}$ to predict the *in situ* unit side resistance is shown in Equation 6.2 for saturated soils and in Equation 6.3 for unsaturated soils. Equation 6.2 is a unitless relationship between $N_{1,60}$ and the unit side resistance normalized by the vertical effective stress. The relationship was developed based on the data collected for clay, non-plastic silt, and sand groupings shown in Figures 6.3–6.8. Table 6.4 summarizes the fitting parameters and coefficients of determination for dataset. Equation 6.3 builds on the form of Equation 6.2 by incorporating the inverse relationship between the degree of saturation

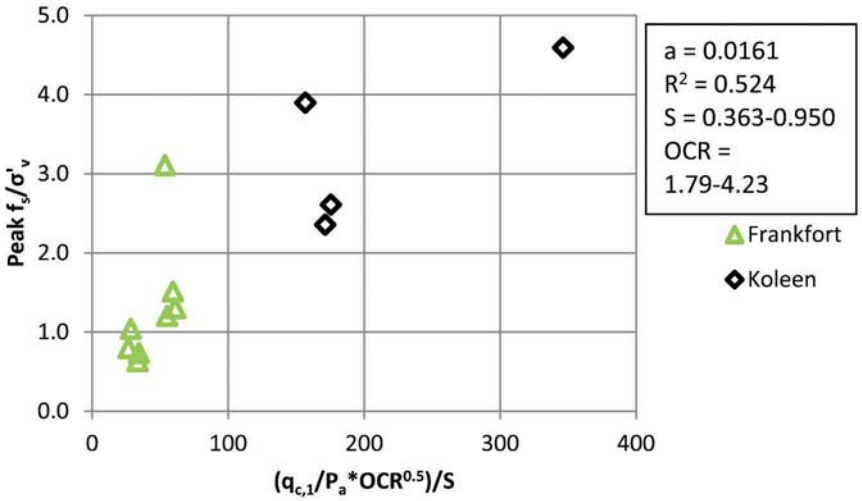

Figure 6.26 Peak unit side resistance versus $q_{c,1}$ values for unsaturated clay.

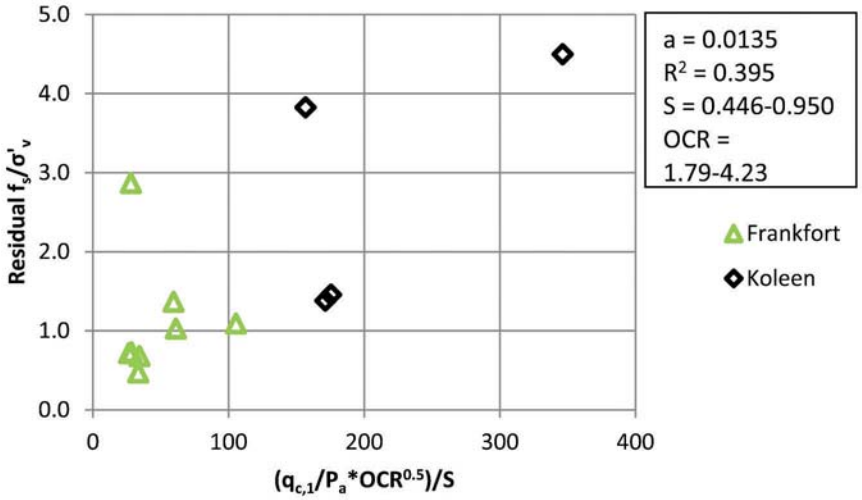

Figure 6.27 Residual unit side resistance versus $q_{c,1}$ values for unsaturated clay.

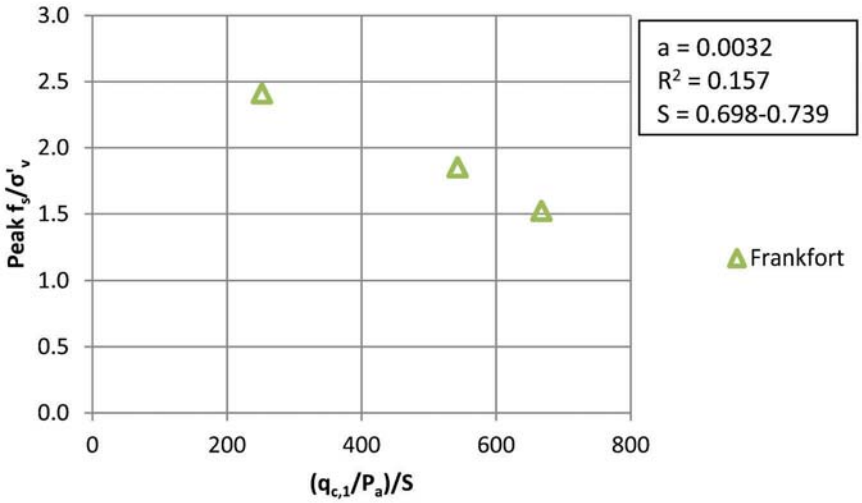

Figure 6.28 Peak unit side resistance versus $q_{c,1}$ values for unsaturated non-plastic silt.

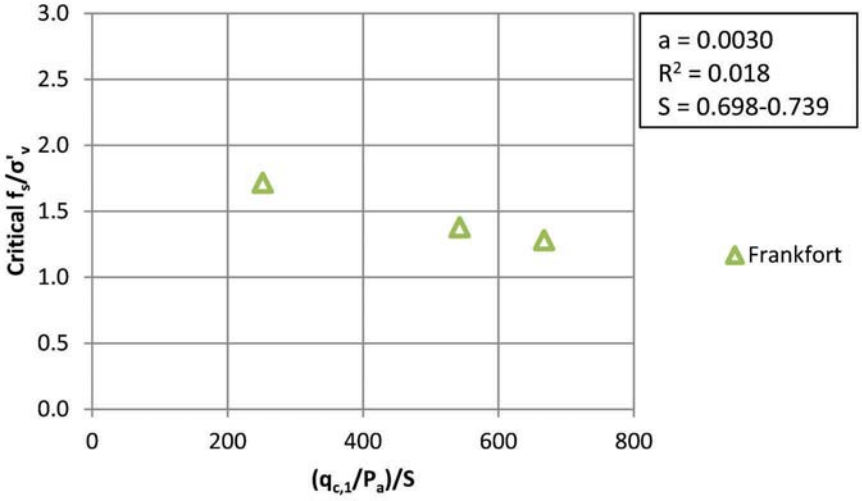

Figure 6.29 Critical unit side resistance versus $q_{c,1}$ values for unsaturated non-plastic silt.

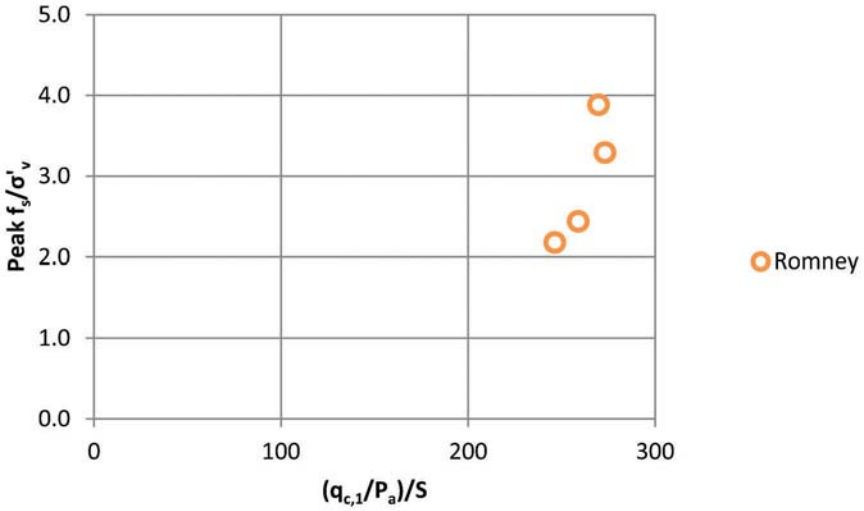

Figure 6.30 Peak unit side resistance versus $q_{c,1}$ values for unsaturated sand.

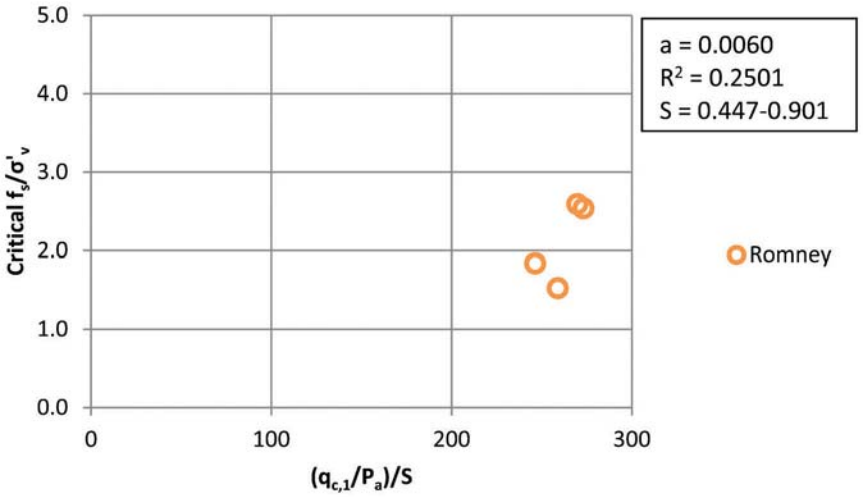

Figure 6.31 Critical unit side resistance versus $q_{c,1}$ values for unsaturated sand.

TABLE 6.9
Fitting parameter, a, and coefficient of determination relating $q_{c,1}$ and f_s shown in Equation 6.8 for various soils

	Fitting Parameter, a	Coefficient of Determination, R^2	Degree of Saturation	OCR Range
Clay-Peak f_s	0.0161	0.524	0.363–0.950	1.79-4.23
Clay-Residual f_s	0.0135	0.395	0.446–0.950	1.79-4.23
Non-Plastic Silt-Peak f_s	0.0032	0.157	0.698–0.739	N/A
Non-Plastic Silt-Critical f_s	0.0030	0.018	0.698–0.739	N/A
Sand-Peak f_s	0.0102	0.272	0.447–0.901	N/A
Sand-Critical f_s	0.0060	0.250	0.447–0.901	N/A

and the unit side resistance. The relationship was developed based on the data collected for clay, non-plastic silt and sand groupings shown in Figures 6.9–6.14. Table 6.5 summarizes the fitting parameters and coefficients of determination for each dataset.

No relationships for $q_{c,1}$ and unit side resistance were found in the literature. This research is the first to develop relationships between CPT and SPT-T measurements. Equation 6.5 is a unitless relationship that relates normalized q_c and unit side resistance for saturated soils. The relationship was developed based on the data presented for clay, non-plastic silt, and sand groupings shown in Figures 6.15–6.20. Table 6.6 summarizes the fitting parameters and coefficients of determination for each dataset. Equation 6.6 relates the unit side resistance with the undrained shear strength of saturated clays. Equation 6.8 captures the inverse relationship between the degree of saturation and the unit side resistance for unsaturated soils. The relationship was developed based on the clay, non-plastic silt, and sand data presented in Figures 6.27–6.32. Table 6.9 presents the fitting parameters and coefficients of determination for each dataset.

In general, the coefficients of determination for the relationships proposed in this report are reasonably high for clay, but low for non-plastic silt and sand. The relationships for non-plastic silt and sand were developed based on limited data. Further data needs to be collected to improve the preliminary relationships proposed in this report. In addition, the process of determining the degree of saturation for silty and sandy soils is difficult due to the sensitive nature of the soil structure. The volume can be destroyed during sample extraction, opening of the split-spoon sampler, placement in the sample jars or extraction from the jars in the laboratory. Any of these activities can change the volume thus changing the unit weight which leads to incorrect estimates of the degree of saturation.

7. CONCLUSIONS AND RECOMMENDATIONS

7.1 Conclusions

The method of calculating a torque ratio is a simple process for data analysis; however, the method does not provide results that lead to distinct relationships with soil types. The ranges of torque ratios for various soils overlap each other leading to unclear results. The torque ratios may be valid for specific sites but do not provide useable data relating to soil behavior classification. To better understand if using torque ratios for soil classification is feasible, more data need to be collected. Additionally, other variables need to be explored to determine if a classification system that uses normalized variables can be developed for soil behavior classification. This process would be similar to that used in the development of the normalized tip resistance and friction ratio relations which are used for soil behavior classification based on CPT results.

Table 7.1 provides all the correlations developed in this research project. Two different equations were developed for saturated and unsaturated soils that relate blow count to unit side resistance. Both equations are normalized equations that directly relate $N_{1,60}$ to unit side resistance; however, the equation for unsaturated soil has the degree of saturation as a variable. Two other equations were developed for saturated and unsaturated soils that relate CPT tip resistance to unit side resistance. Both equations are normalized equations that relate $q_{c,1}$ directly to unit side resistance. The equation for unsaturated soils has the degree of saturation as a variable as well. One additional equation was developed that indirectly relates s_u estimated from CPT measurements with unit side resistance.

As stated previously, published relationships for $N_{1,60}$-unit side resistance did not provide a coefficient of determination (Kelley & Lutenegger, 2004; Winter et al., 2005). Cottingham (2009) published coefficients of determination for relationships between laboratory testing and unit side resistance ranging from 0.338 to 0.554. Reasonably good correlations were developed for saturated clay data and non-plastic silt. More data need to be collected for sand and non-plastic silt to improve the preliminary relationships proposed in this report. This occurred for two reasons: first, small data populations used in the development of the relationships and secondly, difficulty with adequately determining the degree of saturation for non-plastic soils due to soil structure destruction. The relationships based on low coefficients of determination should not be used due to the unpredictable outcome.

Overall, four equations that relate SPT and CPT measurements with unit side resistance ($N_{1,60}$-f_s and q_c-f_s equations) were developed based on sets of data collected for clay, non-plastic silt and sand. One additional equation was developed that can be used to estimate the s_u of saturated clay from unit side resistance. These proposed equations account for the *in situ* saturated/unsaturated soil state; coefficients of determination are provided to allow for the end user to assess the strength of the relationships. The developed relationships between CPT tip resistance and unit side resistance were the first of their nature. Similar to the method used for developing the two $N_{1,60}$-f_s equations, the q_c-f_s equations account for the saturated/unsaturated soil state and provide the coefficients of determination for assessment of relationship strength.

7.2 Recommendations

Use of the SPT-T equipment is recommended in connection with SPT site investigations done by INDOT for sites with fine-grained soils for which the developed correlations between torque measurements and shear strength are reliable. Additional data can be collected in the context of INDOT projects to verify and refine the correlations provided in this report. If fabrication of other SPT-T hardware is required by INDOT, improvements can be made to the current

TABLE 7.1
Summary of correlations developed for clay, silt and sand

Soil	f_s Condition	Saturation	Equations	Fitting Parameter, a	Coefficient of Determination, R^2
Clay	Peak	Saturated	$\frac{f_s}{\sigma'_v} = aN_{1,60}\sqrt{OCR}$	0.0688	0.773
			$\frac{f_s}{\sigma'_v} = a\frac{q_{c,1}}{P_a}\sqrt{OCR}$	0.0333	0.665
			$\frac{f_s}{\sigma'_v} = a\frac{s_u}{\sigma'_v}$	0.491	0.671
			$\frac{f_s}{\sigma'_v} = a\frac{s_u}{\sigma'_v}$	0.688	0.671
		Unsaturated	$\frac{f_s}{\sigma'_v} = a\frac{N_{1,60}}{S}\sqrt{OCR}$	0.0553	0.710
			$\frac{f_s}{\sigma'_v} = a\frac{q_{c,1}}{S(P_a)}\sqrt{OCR}$	0.0161	0.524
	Critical	Saturated	$\frac{f_s}{\sigma'_v} = aN_{1,60}\sqrt{OCR}$	0.0616	0.767
			$\frac{f_s}{\sigma'_v} = a\frac{q_{c,1}}{P_a}\sqrt{OCR}$	0.0309	0.745
			$\frac{f_s}{\sigma'_v} = a\frac{s_u}{\sigma'_v}$	0.443	0.729
			$\frac{f_s}{\sigma'_v} = a\frac{s_u}{\sigma'_v}$	0.620	0.729
			$\frac{f_s}{\sigma'_v} = a\frac{s_u}{\sigma'_v}OCR^b$	a=0.703 b=0.440	0. 461
		Unsaturated	$\frac{f_s}{\sigma'_v} = a\frac{N_{1,60}}{S}\sqrt{OCR}$	0.0462	0.551
			$\frac{f_s}{\sigma'_v} = a\frac{q_{c,1}}{S(P_a)}\sqrt{OCR}$	0.0135	0.395
Silt	Peak	Saturated	$\frac{f_s}{\sigma'_v} = aN_{1,60}$	0.0490	0.676
			$\frac{f_s}{\sigma'_v} = a\frac{q_{c,1}}{P_a}$	0.0059	0.527
		Unsaturated	$\frac{f_s}{\sigma'_v} = a\frac{N_{1,60}}{S}$	0.0290	0.115
			$\frac{f_s}{\sigma'_v} = a\frac{q_{c,1}}{S(P_a)}$	0.0032	0.157
	Critical	Saturated	$\frac{f_s}{\sigma'_v} = aN_{1,60}$	0.0380	0.705
			$\frac{f_s}{\sigma'_v} = a\frac{q_{c,1}}{P_a}$	0.0050	0.582
		Unsaturated	$\frac{f_s}{\sigma'_v} = a\frac{N_{1,60}}{S}$	0.0218	0.232
			$\frac{f_s}{\sigma'_v} = a\frac{q_{c,1}}{S(P_a)}$	0.0030	0.018
Sand	Peak	Saturated	$\frac{f_s}{\sigma'_v} = aN_{1,60}$	0.0940	0.307
			$\frac{f_s}{\sigma'_v} = a\frac{q_{c,1}}{P_a}$	0.0498	0.436
		Unsaturated	$\frac{f_s}{\sigma'_v} = a\frac{N_{1,60}}{S}$	0.0488	0.413
			$\frac{f_s}{\sigma'_v} = a\frac{q_{c,1}}{S(P_a)}$	0.0102	0.272
	Critical	Saturated	$\frac{f_s}{\sigma'_v} = aN_{1,60}$	0.0739	0.127
			$\frac{f_s}{\sigma'_v} = a\frac{q_{c,1}}{P_a}$	0.0400	0.013
		Unsaturated	$\frac{f_s}{\sigma'_v} = a\frac{N_{1,60}}{S}$	0.0334	0.464
			$\frac{f_s}{\sigma'_v} = a\frac{q_{c,1}}{S(P_a)}$	0.0060	0.250

SPT-Torque prototype. Use of a more expensive but lighter alloy material can be explored in order to reduce the current size and weight of the hardware while at the same time keeping it sturdy. A storage box could be fabricated to safely transport and store the hardware when not in use by the INDOT drilling crew. A cost-benefit analysis could be done to determine the cost of production of additional SPT-T units versus benefits due to better site investigations and geotechnical design.

REFERENCES

ASTM. (2007a). *Standard test method for particle-size analysis of soils*. ASTM D422-63 (Reapproved 2007). West Conshohocken, PA: ASTM International.

ASTM. (2007b). *Standard test method for standard penetration test (SPT) and split-barrel sampling of soils.* ASTM D1586-08a. West Conshohocken, PA: ASTM International.

ASTM. (2009c). *Standard test methods for particle-size distribution (graduation) of soils using sieve analysis.* ASTM D6913-04 (Reapproved 2009). West Conshohocken, PA: ASTM International.

ASTM. (2010a). *Standard test methods for laboratory determination of water (moisture) content of soil and rock by mass*. ASTM D2216-10. West Conshohocken, PA: ASTM International.

ASTM. (2010b). *Standard practice for classification of soils for engineering purposes (unified soil classification system)*. ASTM D2487-10. West Conshohocken, PA: ASTM International.

ASTM. (2010c). *Standard test methods for liquid limit, plastic limit, and plasticity index of soils.* ASTM D4318-10. West Conshohocken, PA: ASTM International.

Bleuer, N. K. (1991). The Lafayette Bedrock Valley System of Indiana; Concept, form and fill stratigraphy. In W. N. Melhorn & J. P. Kempton (Eds.), *Geology and hydrology of the Teays-Mahomet Bedrock Valley System: Boulder, Colo., Geological Society of America Special Paper 258* (pp. 51–77).

Bullock, P. J. (1999). *Pile friction freeze: A field and laboratory study* (Unpublished doctoral dissertation). Gainesville: University of Florida.

Bullock, P. J., & Schmertmann, J. H. (2003). *Determining the effect of stage testing on the dimensionless pile side shear setup factor.* (Florida Department of Transportation Publication No. BC-354, RPWO 27). Tallahassee: University of Florida.

Bullock, P. J., Schmertmann, J. H., McVay, M. C., & Townsend, F. C. (2005a). Side shear setup. I: Test piles driven in Florida. *Journal of Geotechnical and Geoenvironmental Engineering*, *131*(3), 292–300.

Bullock, P. J., Schmertmann, J. H., McVay, M. C. & Townsend, F. C. (2005b). Side shear setup. II: Results from Florida test piles. *Journal of Geotechnical and Geoenvironmental Engineering*, *131*(3), 301–310.

Cottingham, M. A. (2009). *In situ determination of residual soil shear strength parameters using the standard penetration test with torque* (Doctoral dissertation). Charlotte: University of North Carolina at Charlotte.

Decourt, L., & Quaresma Filho, A. R. (1991). The SPT-CF: An improved SPT. In *Proceedings from SEFE II, Vol. I, Sao Paulo* (pp. 106–110).

Decourt, L., & Quaresma Filho, A. R. (1994). Practical applications of the standard penetration test complemented by torque measurements, SPT-T: Present stage and future trends. In *Proceedings of the International Conference on Soil Mechanics and Foundation Engineering* (pp. 143–146).

Hicks, J. M. (2001). Determining the effect of stage testing on the dimensionless pile side shear setup factor (Master's thesis). Gainesville: University of Florida.

Hara, A., Ohta, T., Niwa, M., Tanaka, S., & Banno, T. (1974). Shear modulus and shear strength of cohesive soils. *Soils and Foundation*, *14*(3), 1–12.

Kelley, S. P., & Lutenegger, A. J. (1999). Enhanced site characterization in residual soils using the SPT-T and drive cone tests. In B. Edelen (Ed.), *Behavioral characteristics of residual soils* (Geotechnical Special Publication No. 92 (88–100)). New York, NY: American Society of Civil Engineers.

Kelley, S. P., & Lutenegger, A. J. (2004). Unit skin friction from the standard penetration test supplemented with the measurement of torque. *Journal of Geotechnical and Geoenvironmental Engineering*, *130*(5), 540–543.

Komurka, V. E., Wagner, A. B., & Edil, T. B. (2003). *Estimating soil/pile set-up* (Wisconsin Highway Research Program Publication No. 0092-00-14). Madison, WI: Wisconsin Department of Transportation.

Kulhawy, F. H., & Mayne, P. W. (1990). *Manual on estimating soil properties for foundation design*. Palo Alto, CA: Electric Power Research Institute.

Lutenegger, A. J. (2008). The standard penetration test—More than just a one number test. In A-B. Huang & P. W. Mayne (Eds.), *Geotechnical and geophysical site characterization* (pp. 481–485). London, UK: Taylor and Francis Group.

Lutenegger, A. J. (2009). Estimating driven pile side resistance from SPT-Torque tests. In M. Iskander, D. F. Laefer & M. H. Hussein (Eds.), *Contemporary topics in in situ testing, analysis, and reliability of foundations* (Geotechnical Special Publication No. 186) (pp. 9–17). New York, NY: American Society of Civil Engineers. http://dx.doi.org/10.1061/41022(336)2

Lutenegger, A. J., & Kelley, S. P. (1998). Standard penetration tests with torque measurements. In *Proceedings of the International Symposium on Site Characterization*, *Vol. 2* (pp. 939–945).

Peixoto, A. S. P., Albequerque, P. J. R., & de Carvalho, D. (2000). Utilization of SPT-T, CPT and DMT tests to predict the ultimate bearing capacity of precast concrete pile in Brazilian unsaturated residual soil. In C. D. Shackelford, S. L. Houston, & N=Y Chang (Eds.), *Proceedings: Advances in Unsaturated Geotechnics* (pp. 32–39). http://dx.doi.org/10.1061/40510(287)3

Peixoto, A. S. P., Antenor, V. B., Montanha, R. K., Nogueira, J. D. F., & de Oliveria Neto, L. (2008). Influence factors in torque measurements of SPT-T test. In A-B Huang & P. W. Mayne (Eds.), *Proceedings of the 3rd International Conference on Site Characterization*.

Peixoto, A. S. P., Antenor, V. B., Ramos, T. M., & David, R. (2007). Rod length influence in torque measurement of SPT-T test. In *Proceedings of sessions of Geo-Denver 2007 Congress: Problematic soils and rocks and in situ characterization*, *Vol. 225* (pp. 162–170).

Peixoto, A. S. P., & de Carvalho, D. (1999). Standard penetration test with torque measurement (SPT-T) and some factors that affect the T/N ratio. In *Panamerican Conference on Soil Mechanics and Geotechnical Engineering*, *XI, Vol. 3* (pp. 1605–1612).

Peixoto, A. S. P., de Carvalho, D., & Giacheti, H. L. (2003). SPT-T and CPT tests to predict bearing capacity of piles in Brazilian

practice. In *Panamerican Conference on Soil Mechanics and Geotechnical Engineering*, *Vol. 1* (pp. 381–386).
Peixoto, A. S. P., & de Oliveria Neto, L. (2010). Theoretical and experimental evaluation of the influence of the length of drill rods in the SPT-T tests. *Soils & Rocks*, *33*, 23–31.
Ranzini, S. M. T. (1988). SPTF. Technical note. *Solos e Rochas*, *11*, 29–30.
Ranzini, S. M. T. (1994). SPTF: 2ª parte. *Solos e Rochas*, *17*, 189–190.
Rausche, F., Thendean, G., Abou-matar, H., Likins, G. E., & Gobel, G. G. (1995). *Investigation of dynamic and static pile behavior from modified standard penetration tests*. Presented at the 1995 PDA Users Day, Heidelberg, Germany. Retrieved from http://www.pile.com/reference/PDAUsersDay1995Cleve/InvestigationOfDynamicAndStaticPileBehaviorFromModifiedStandardPenetrationTests.pdf.
Salgado, R. (2008). *The engineering of foundations*. New York, NY: McGraw-Hill.
Terzaghi, K., & Peck, R. B. (1967). *Soil mechanics in engineering practice* (2nd ed.). New York, NY: John Wiley & Sons.
West, T. R. (1995). *Geology applied to engineering*, Upper Saddle River, NJ: Prentice Hall.
Winter, C. J., Wagner, A. B., & Komurka, V. E. (2005). *Investigation of standard penetration torque testing (SPT-T) to predict pile performance* (Wisconsin Highway Research Program Publication No. 0092-04-09). Madison, WI: Wisconsin Department of Transportation.

APPENDIX A. SPT-TORQUE CALIBRATION

Table A.1 presents the data for the calibration process of the strain gages located on the SPT-Torque shaft.

TABLE A.1
SPT-Torque calibration data

Dead Load	Load (lb)	Load (kg)	Distance (m)	Torque (N.m)	Total Dead Torque (N.m)
Bucket	2.14	0.97	0.51	4.86	6.62
Lever Arm	9.44	4.28	0.23	1.76	

Trial	Recorded Strain	Loading/Unloading Sequence (lb)	Total Net Load (kg)	Lever Arm Distance (m)	Applied Torque (N.m)	Total Net Torque (N.m)
1	−5.04E-05	2.52	1.14	0.51	5.72	12.33
2	−5.76E-05	2.52	2.29	0.51	11.44	18.05
3	−7.50E-05	8.90	6.32	0.51	31.63	38.25
4	−9.16E-05	7.95	9.93	0.51	49.68	56.29
5	−1.08E-04	7.94	13.53	0.51	67.70	74.31
6	−1.43E-04	16.55	21.04	0.51	105.25	111.87
7	−1.68E-04	12.17	26.56	0.51	132.87	139.49
8	−1.93E-04	11.61	31.82	0.51	159.22	165.83
9	−2.18E-04	12.05	37.29	0.51	186.56	193.18
10	−2.43E-04	12.04	42.75	0.51	213.89	220.50
11	−2.67E-04	12.05	48.22	0.51	241.23	247.85
12	−2.45E-04	−12.05	42.75	0.51	213.89	220.50
13	−2.20E-04	−12.04	37.29	0.51	186.56	193.18
14	−1.94E-04	−12.05	31.82	0.51	159.22	165.83
15	−1.70E-04	−11.61	26.56	0.51	132.87	139.49
16	−1.45E-04	−12.17	21.04	0.51	105.25	111.87
17	−1.08E-04	−16.55	13.53	0.51	67.70	74.31
18	−9.16E-05	−7.94	9.93	0.51	49.68	56.29
19	−7.68E-05	−7.95	6.32	0.51	31.63	38.25
20	−5.77E-05	−8.90	2.29	0.51	11.44	18.05
21	−5.41E-05	−2.52	1.14	0.51	5.72	12.33
22	−4.92E-05	−2.52	0.00	0.51	0.00	6.62

Figure A.1 presents the calibration data presented in Table A.1 with a calibration factor of 1,088,433.87.

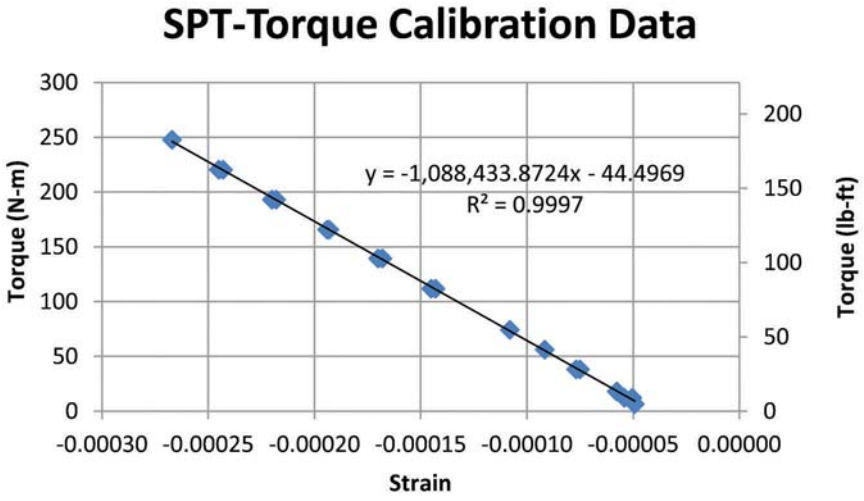

Figure A.1 Plot of the calibration data.

APPENDIX B. SPT-TORQUE PLOTS

FIGURES B.1 THROUGH B.12

Figures B.1 through B.12 present SPT-Torque test data from the Flora Maintenance Unit (Carroll County, Indiana) collected on August 9, 2011.

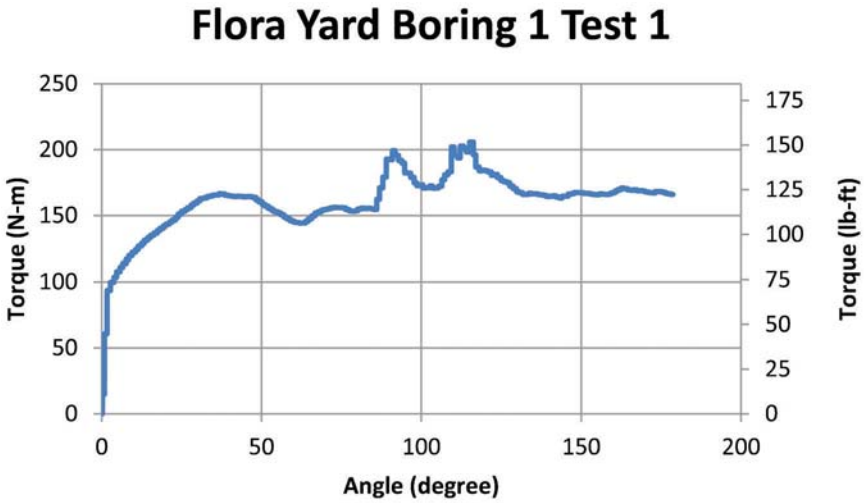

Figure B.1 Flora yard boring 1 test performed at a depth of 1.07–1.52 meters.

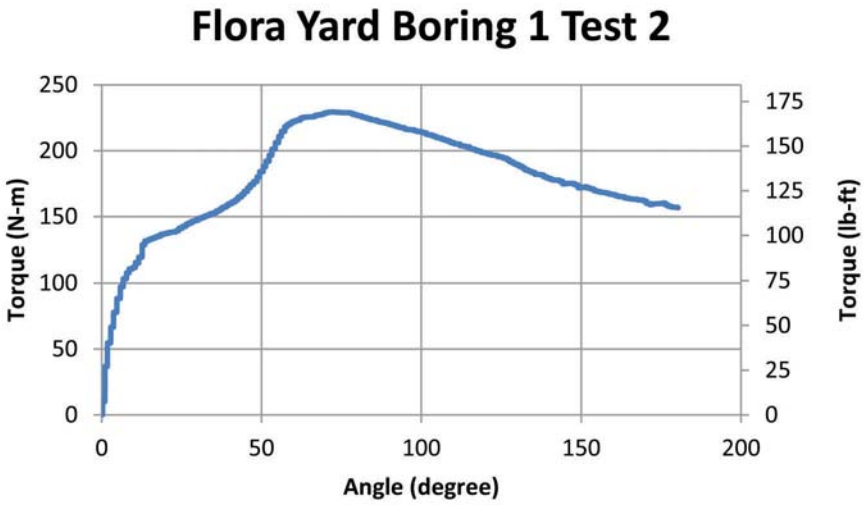

Figure B.2 Flora yard boring 1 test performed at a depth of 2.59–3.05 meters.

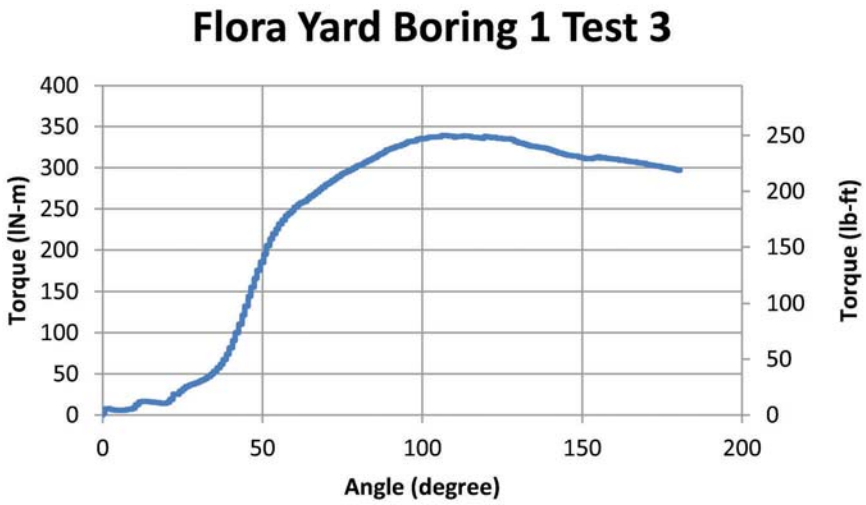

Figure B.3 Flora yard boring 1 test performed at a depth of 4.12–4.57 meters.

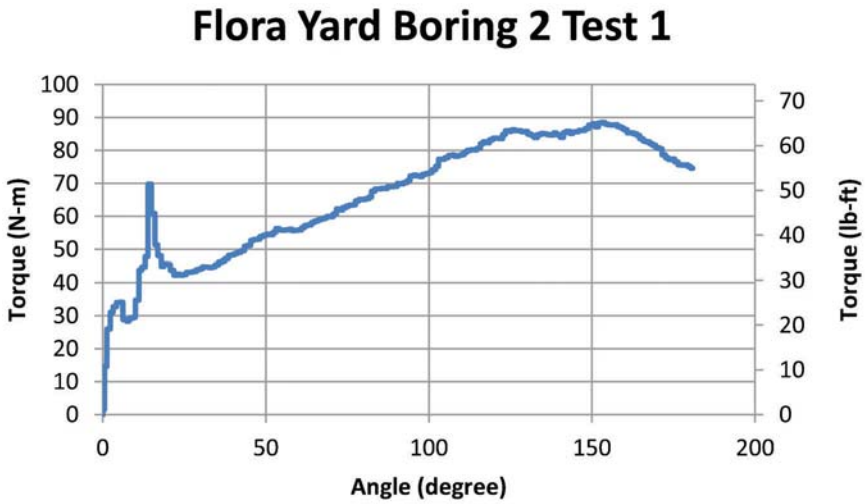

Figure B.4 Flora yard boring 2 test performed at a depth of 1.07–1.52 meters.

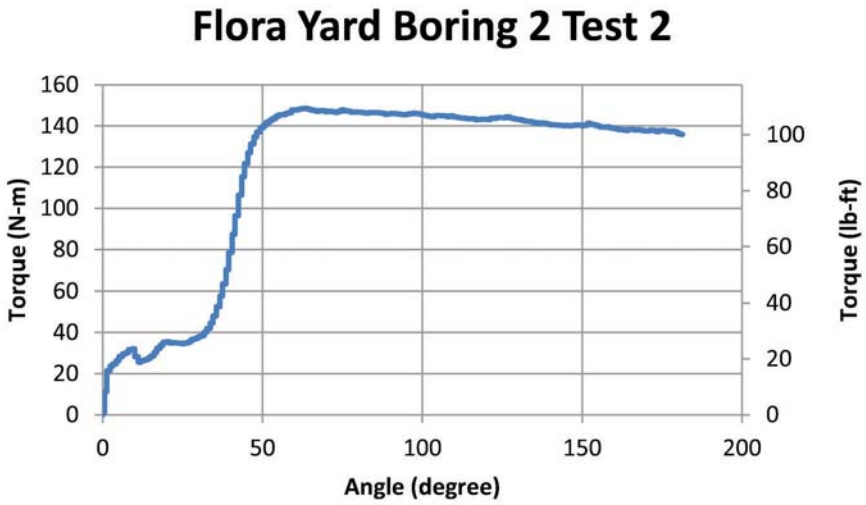

Figure B.5 Flora yard boring 2 test performed at a depth of 2.59–3.05 meters.

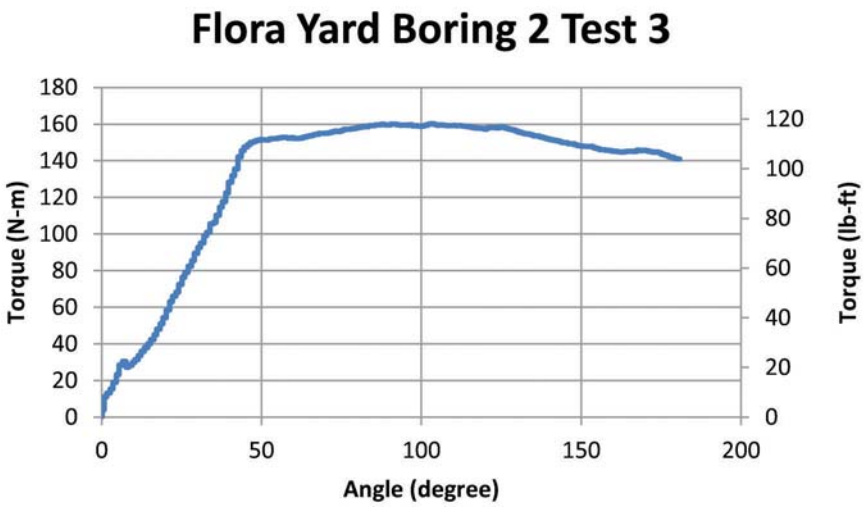

Figure B.6 Flora yard boring 2 test performed at a depth of 4.12–4.57 meters.

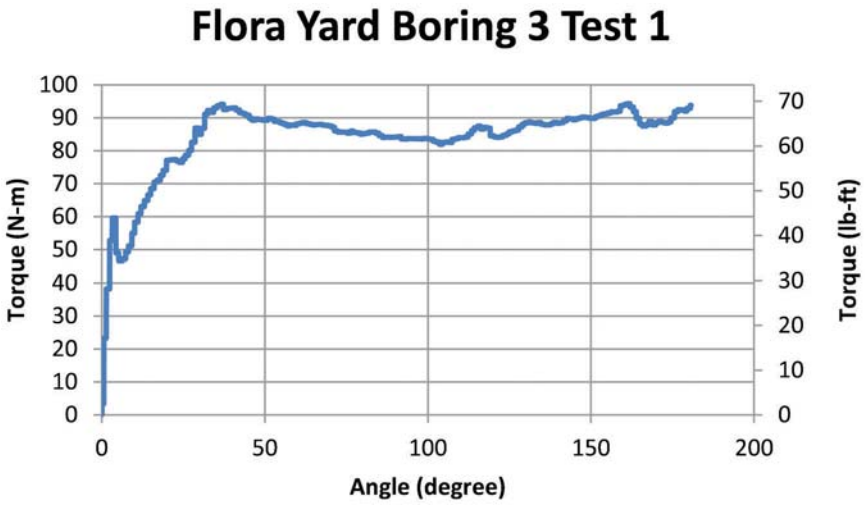

Figure B.7 Flora yard boring 3 test performed at a depth of 1.07–1.52 meters.

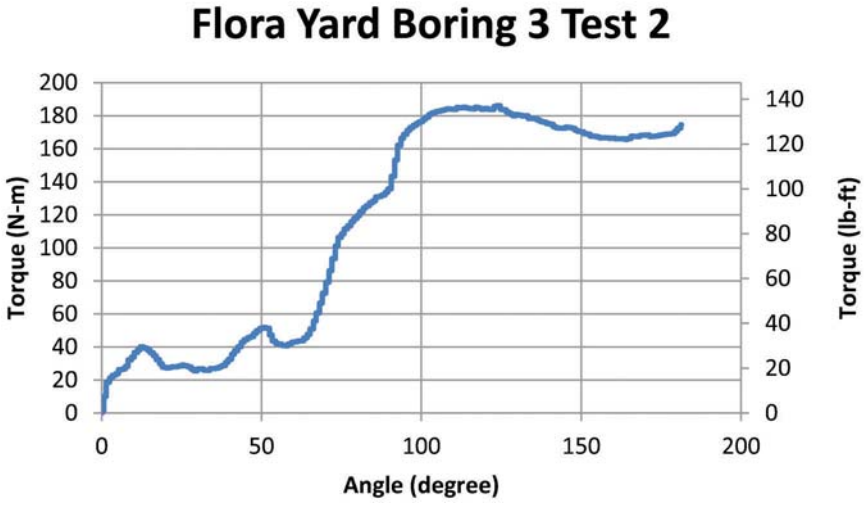

Figure B.8 Flora yard boring 3 test performed at a depth of 2.59–3.05 meters.

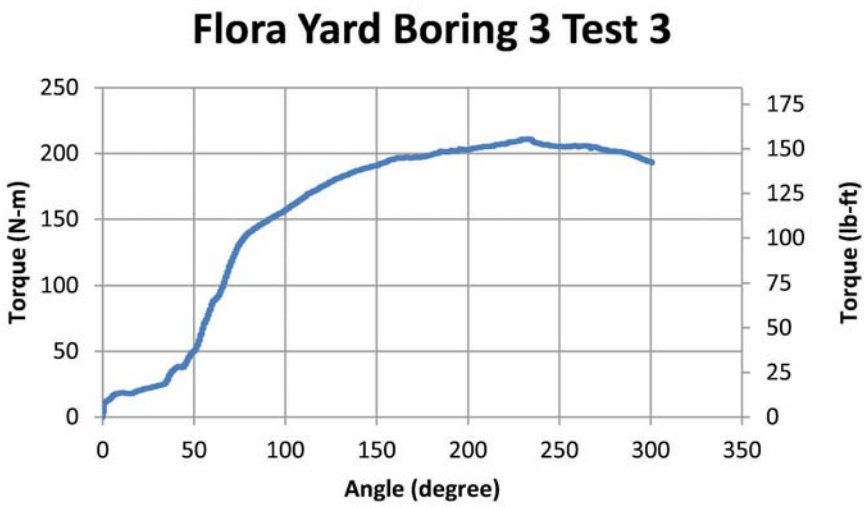

Figure B.9 Flora yard boring 3 test performed at a depth of 4.12–4.57 meters.

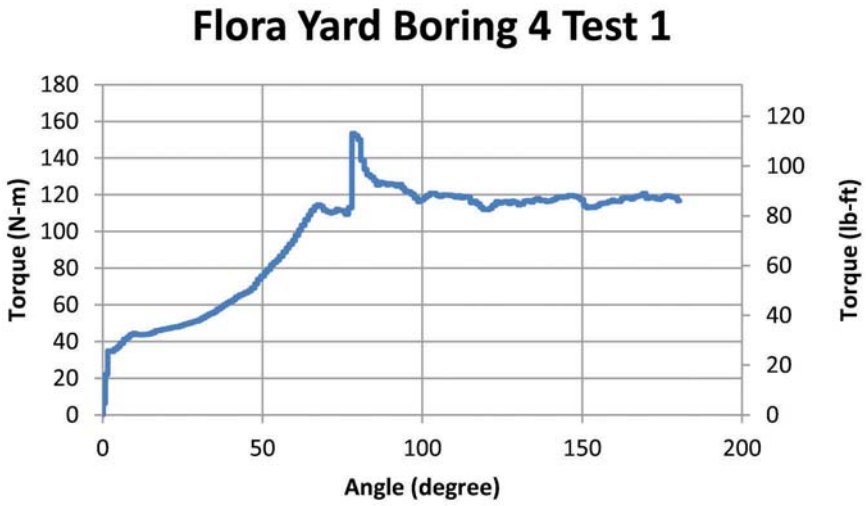

Figure B.10 Flora yard boring 4 test performed at a depth of 1.07–1.52 meters.

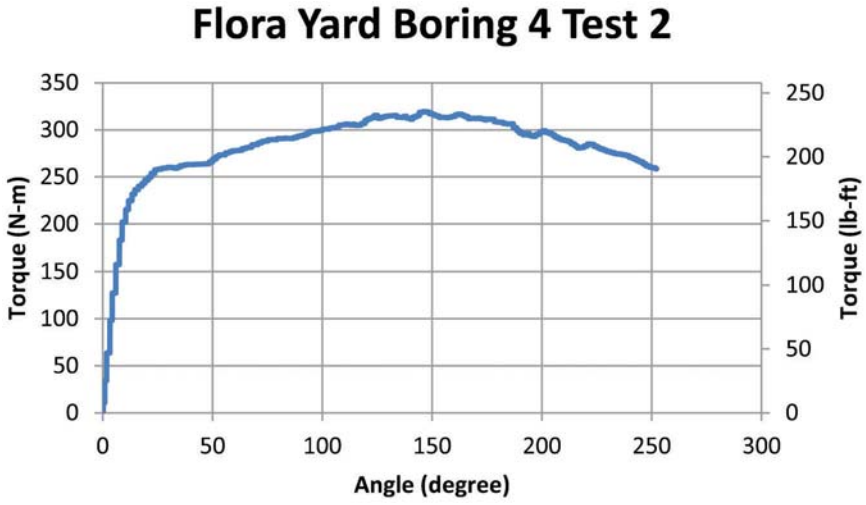

Figure B.11 Flora yard boring 4 test performed at a depth of 2.59–3.05 meters.

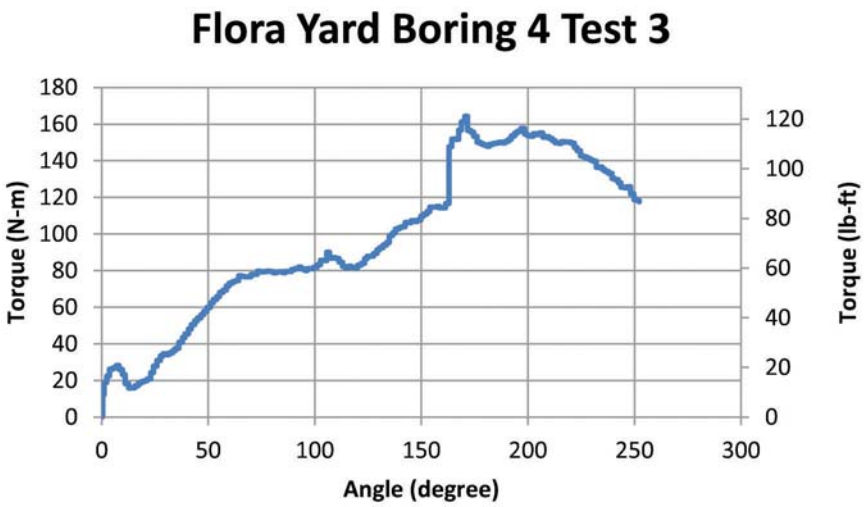

Figure B.12 Flora yard boring 4 test performed at a depth of 4.12–4.57 meters.

FIGURES B.13 THROUGH B.18

Figures B.13 through B.18 present SPT-Torque test data from the Lafayette Maintenance Unit (Tippecanoe County, Indiana) collected on September 1, 2011.

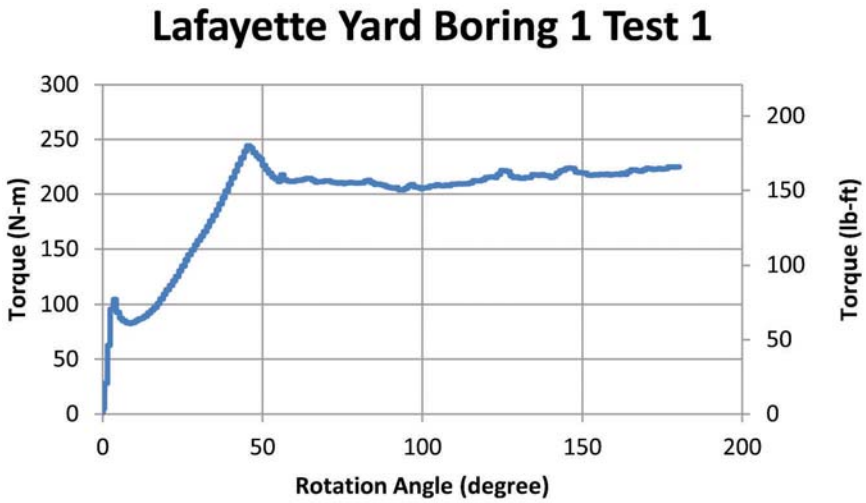

Figure B.13 Lafayette yard boring 1 test performed at a depth of 1.07–1.52 meters.

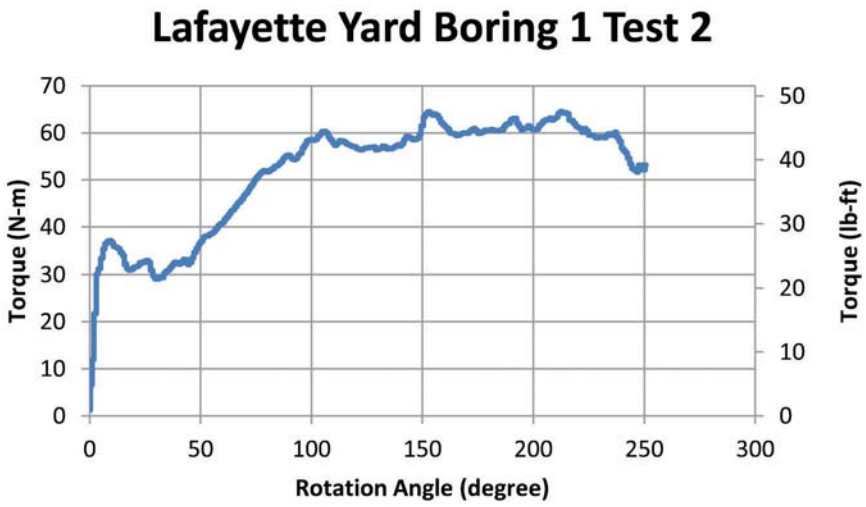

Figure B.14 Lafayette yard boring 1 test performed at a depth of 2.59–3.05 meters.

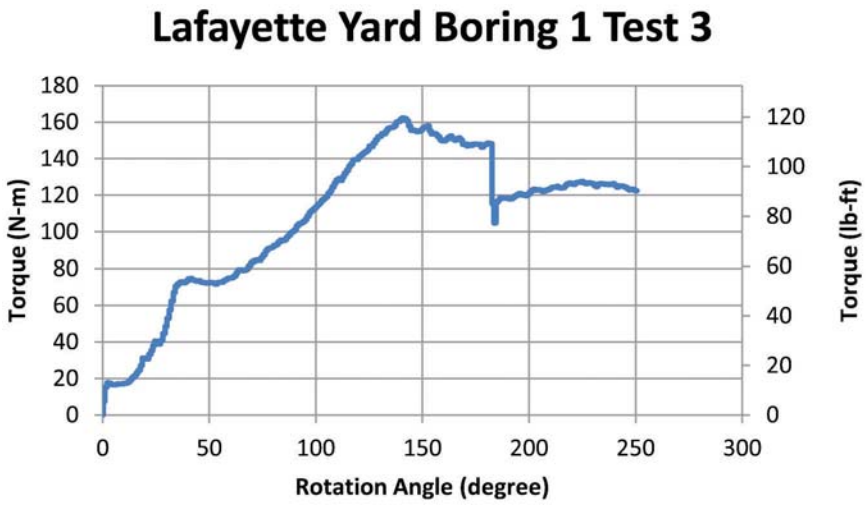

Figure B.15 Lafayette yard boring 1 test performed at a depth of 4.12–4.57 meters.

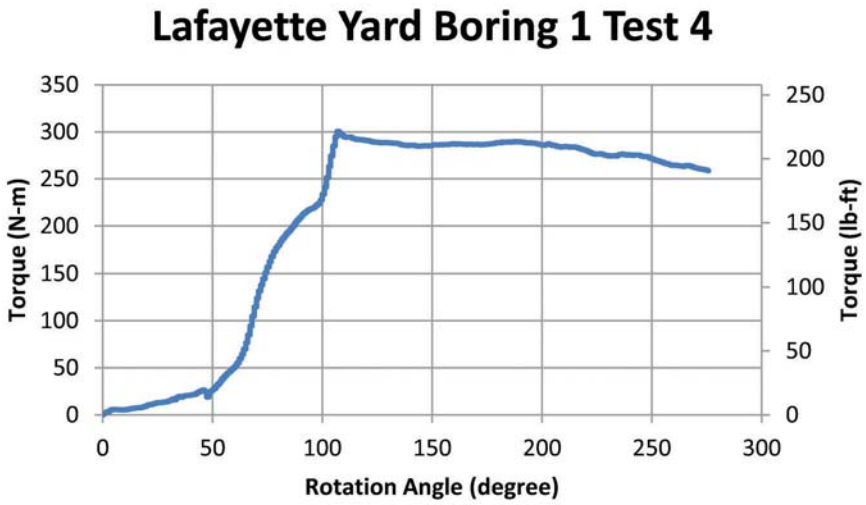

Figure B.16 Lafayette yard boring 1 test performed at a depth of 5.64–6.10 meters.

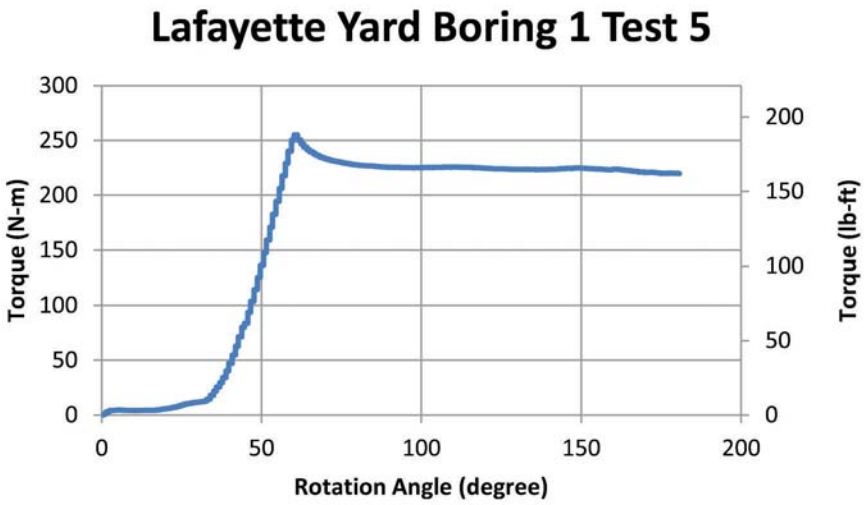

Figure B.17 Lafayette yard boring 1 test performed at a depth of 7.16–7.62 meters.

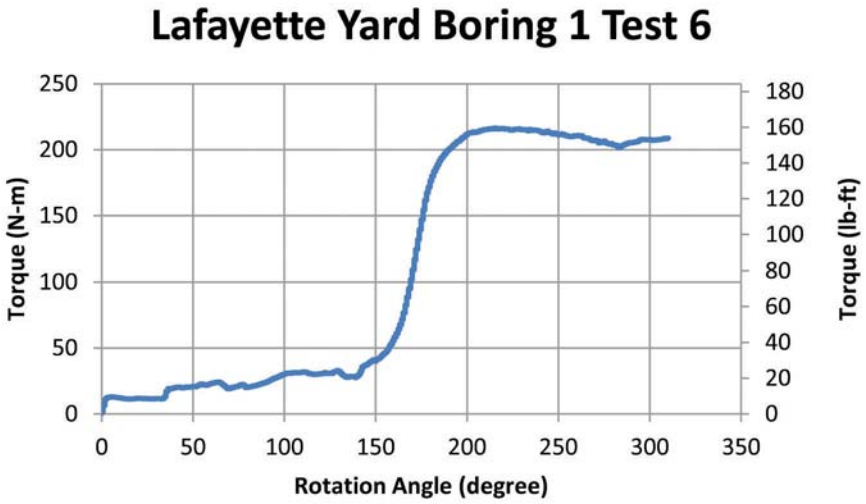

Figure B.18 Lafayette yard boring 1 test performed at a depth of 8.69–9.15 meters.

FIGURES B.19 THROUGH B.41

Figures B.19 through B.41 present SPT-Torque test data from the Frankfort Maintenance Unit (Clinton County, Indiana) collected from January 4–6, 2012.

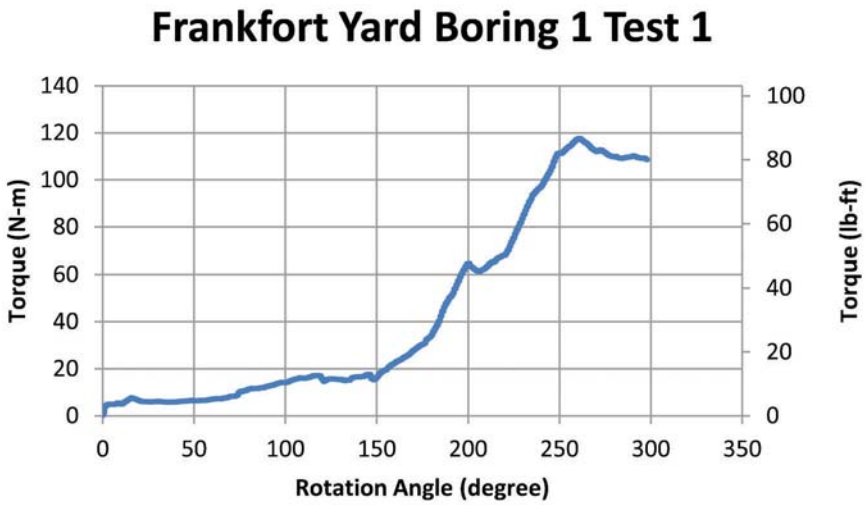

Figure B.19 Frankfort yard boring 1 test performed at a depth of 1.07–1.52 meters.

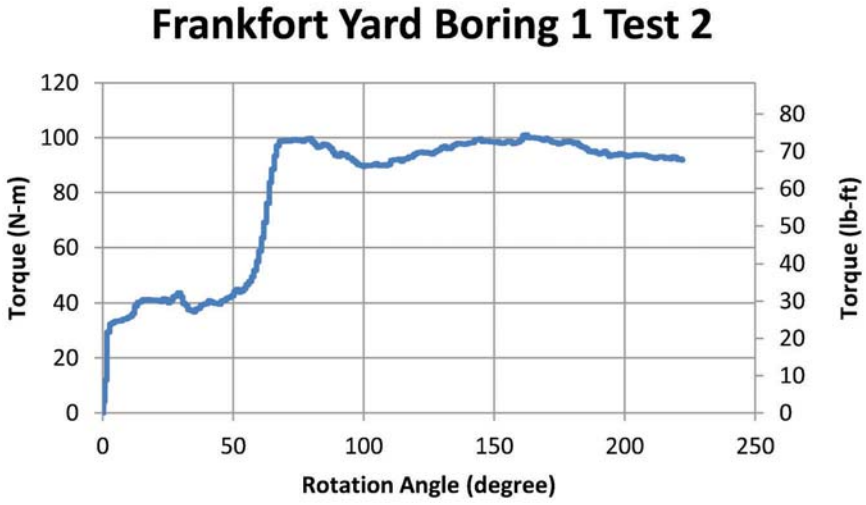

Figure B.20 Frankfort yard boring 1 test performed at a depth of 2.59–3.05 meters.

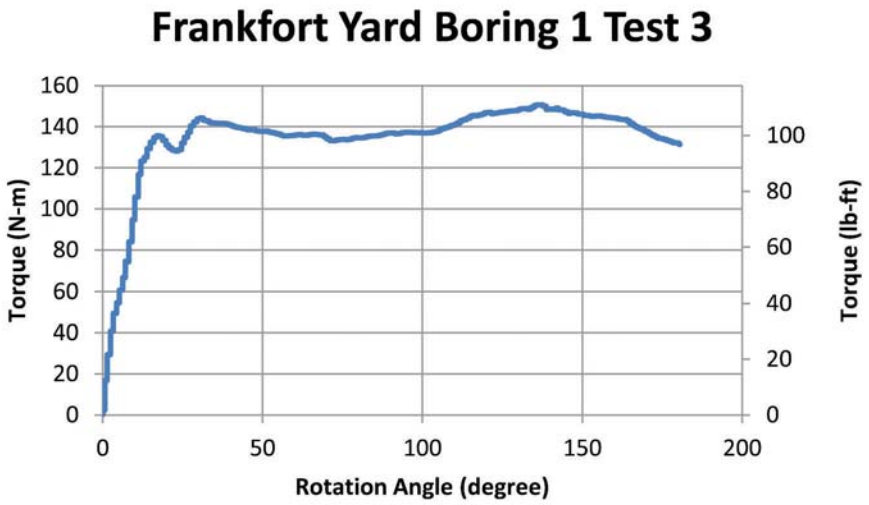

Figure B.21 Frankfort yard boring 1 test performed at a depth of 4.12–4.57 meters.

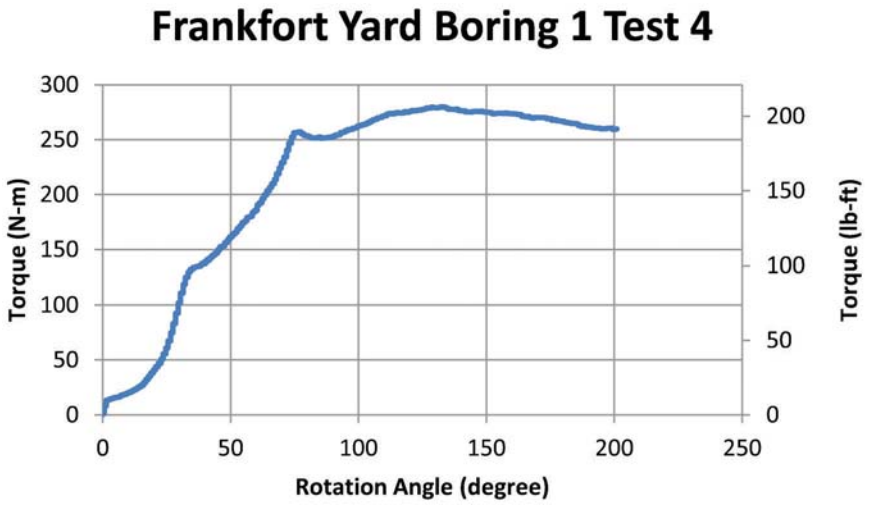

Figure B.22 Frankfort yard boring 1 test performed at a depth of 5.64–6.10 meters.

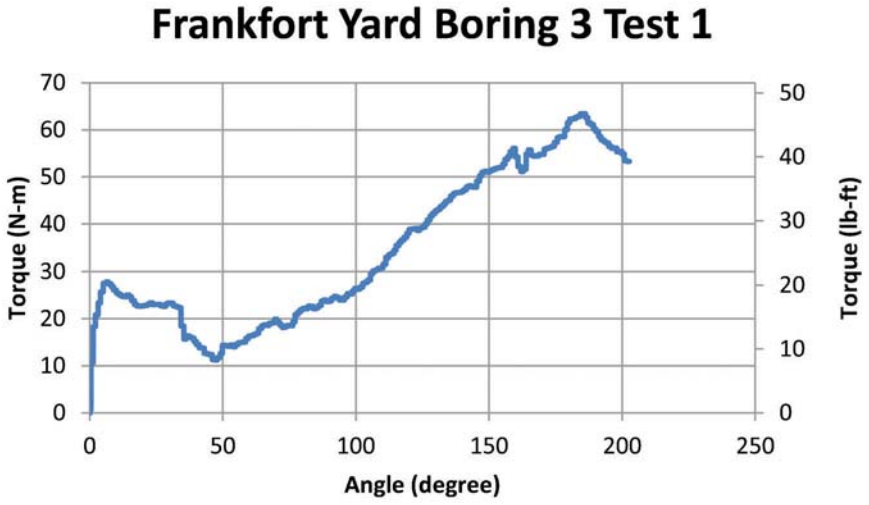

Figure B.23 Frankfort yard boring 3 test performed at a depth of 1.07–1.52 meters.

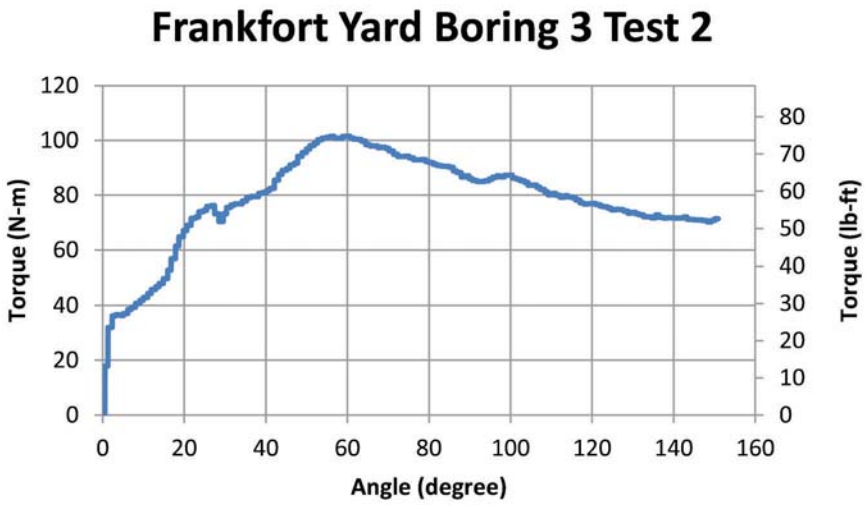

Figure B.24 Frankfort yard boring 3 test performed at a depth of 2.59–3.05 meters.

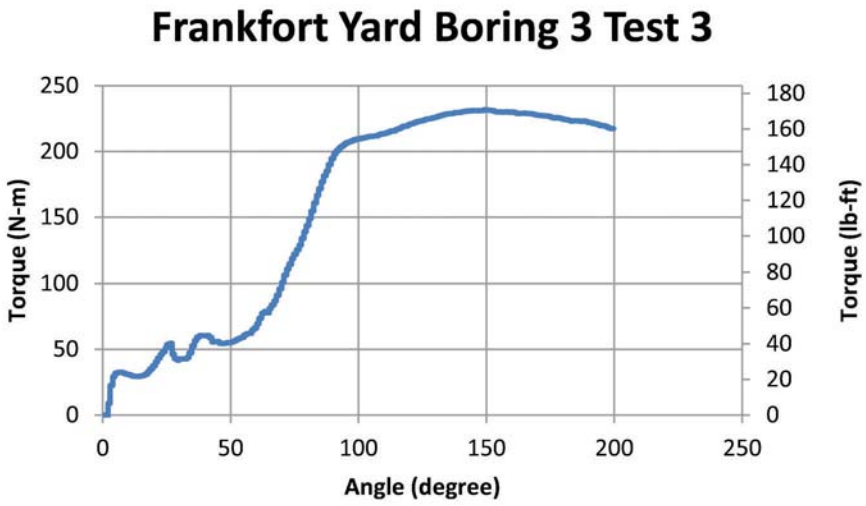

Figure B.25 Frankfort yard boring 3 test performed at a depth of 4.12–4.57 meters.

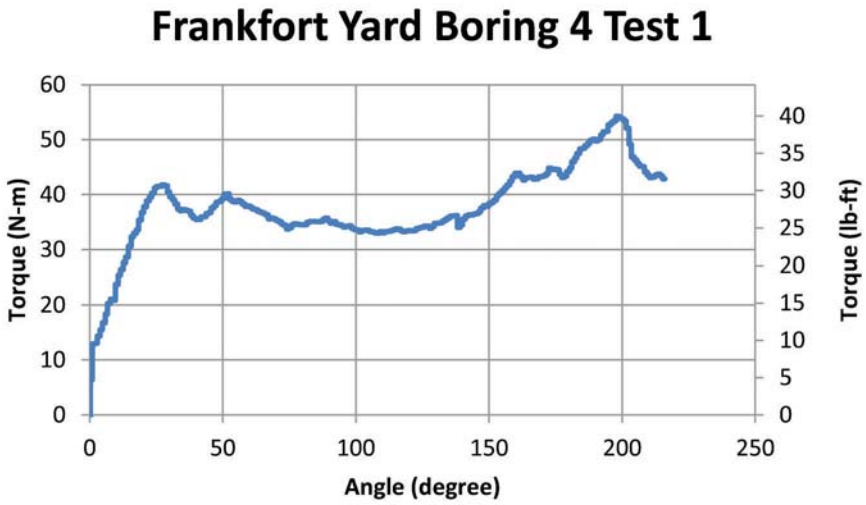

Figure B.26 Frankfort yard boring 4 test performed at a depth of 1.07–1.52 meters.

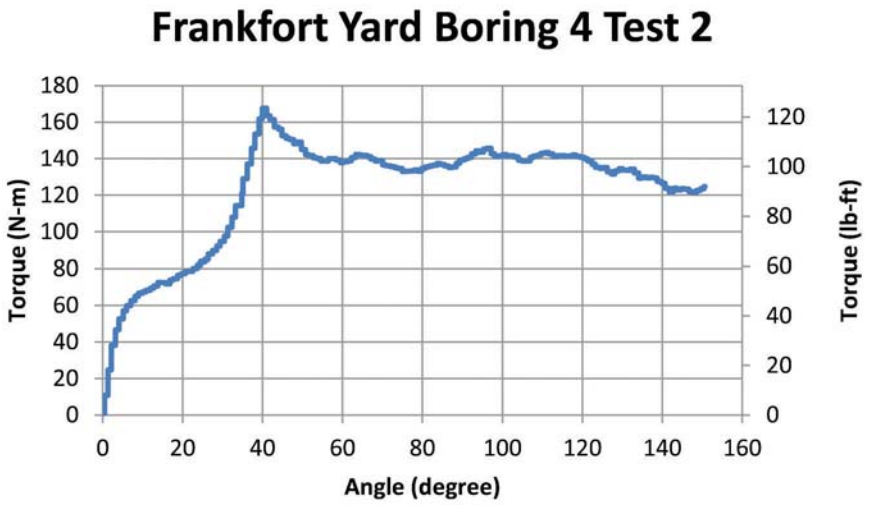

Figure B.27 Frankfort yard boring 4 test performed at a depth of 2.59–3.05 meters.

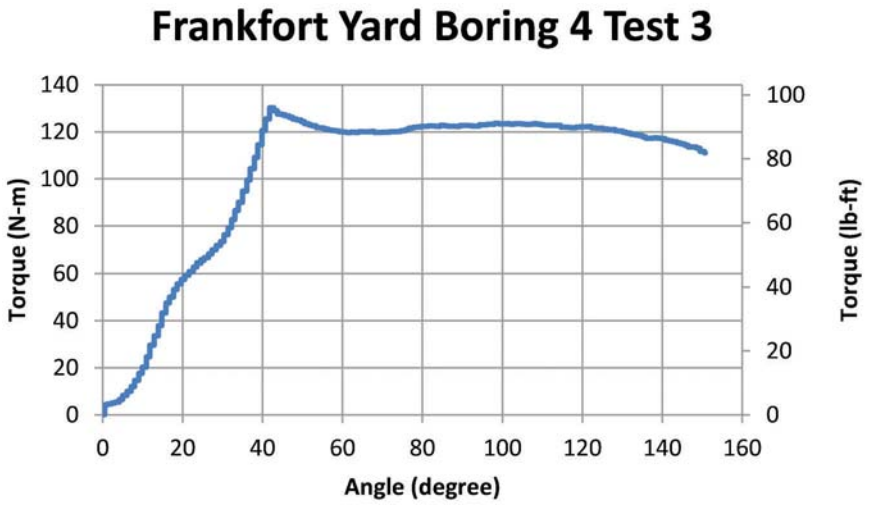

Figure B.28 Frankfort yard boring 4 test performed at a depth of 4.12–4.57 meters.

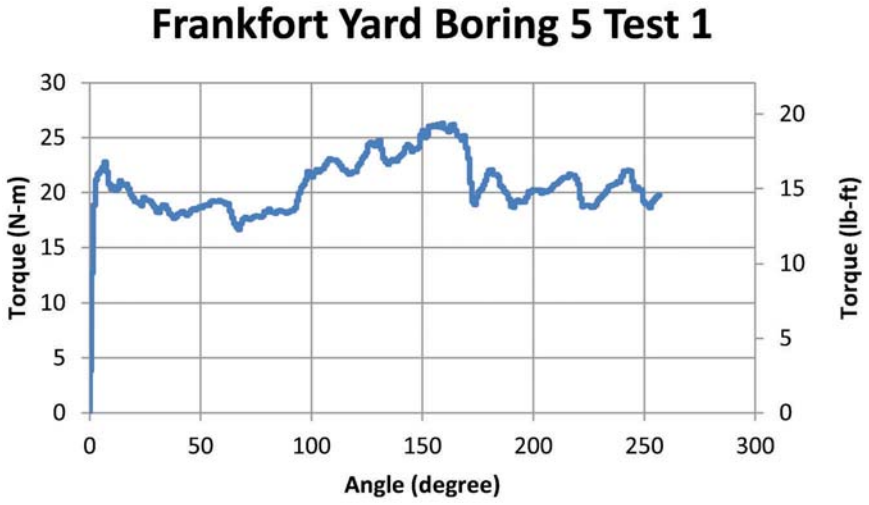

Figure B.29 Frankfort yard boring 5 test performed at a depth of 1.07–1.52 meters.

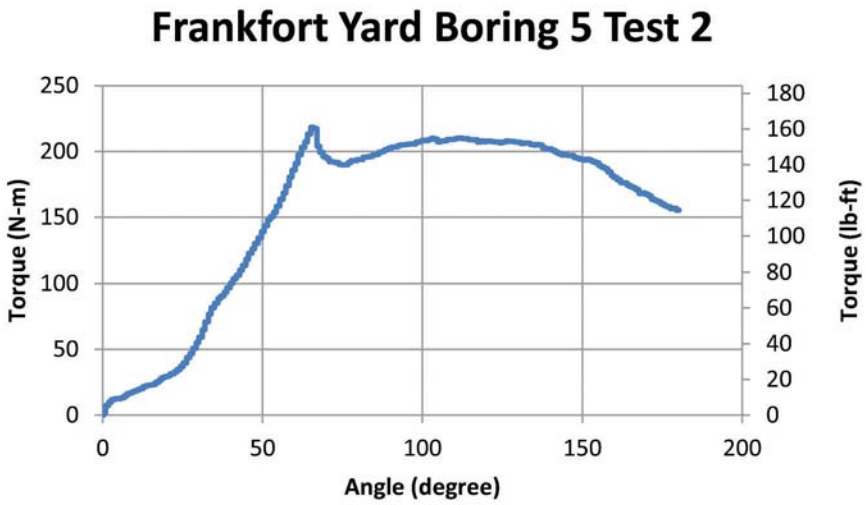

Figure B.30 Frankfort yard boring 5 test performed at a depth of 2.59–3.05 meters.

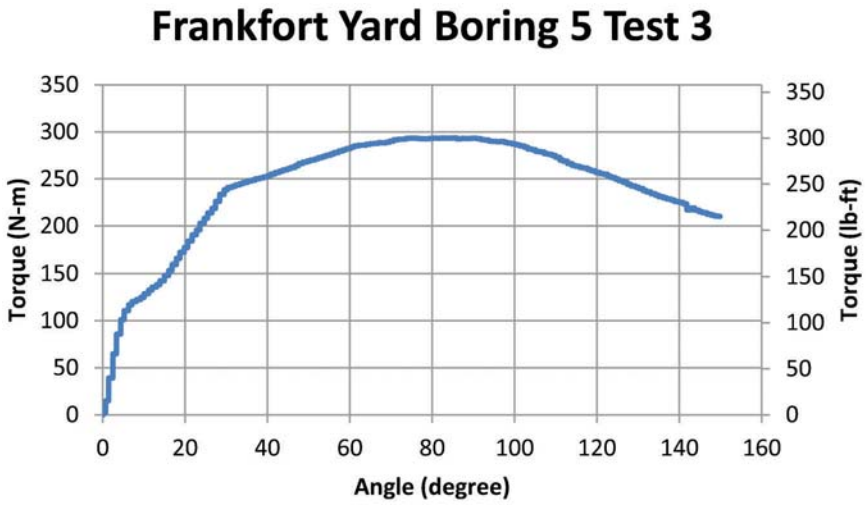

Figure B.31 Frankfort yard boring 5 test performed at a depth of 4.12–4.57 meters.

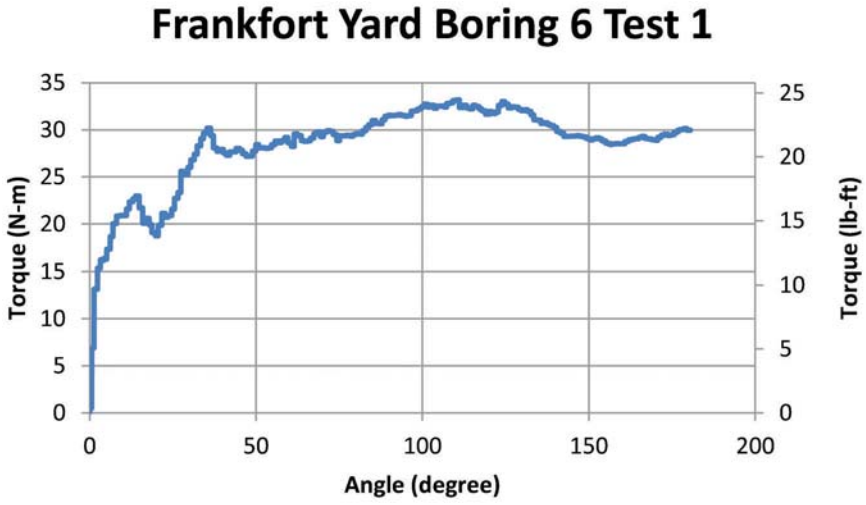

Figure B.32 Frankfort yard boring 6 test performed at a depth of 1.07–1.52 meters.

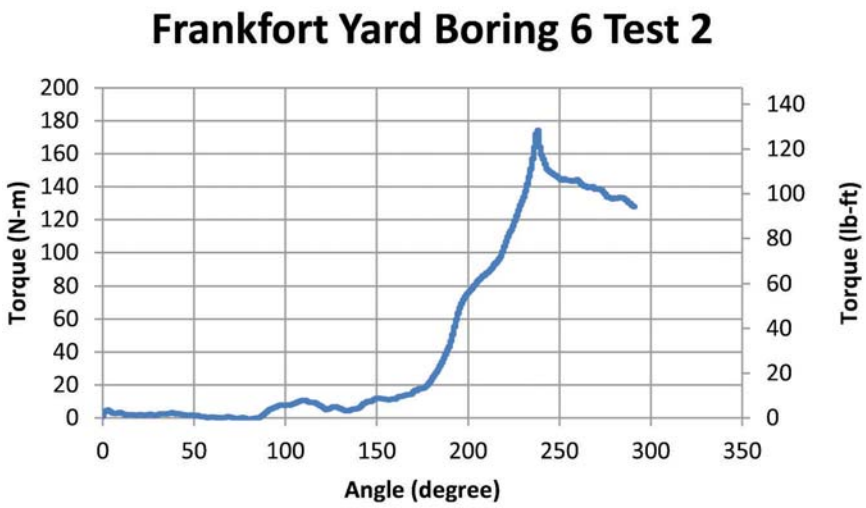

Figure B.33 Frankfort yard boring 6 test performed at a depth of 2.59–3.05 meters.

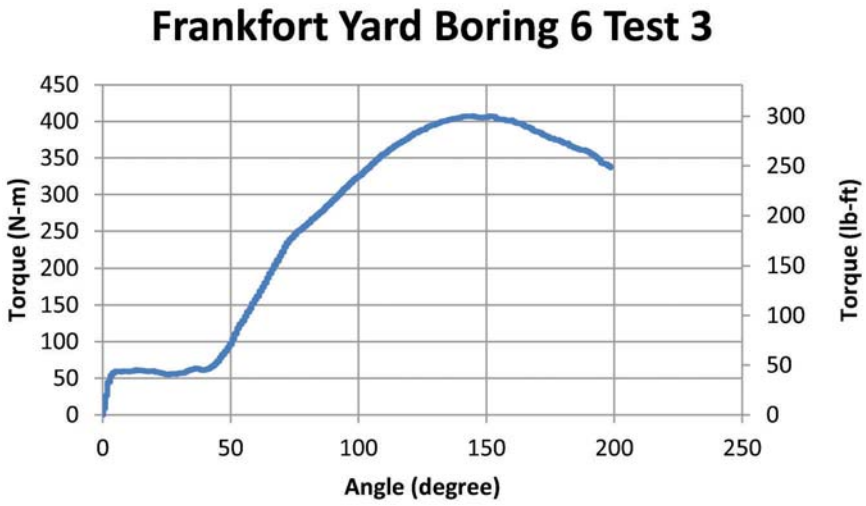

Figure B.34 Frankfort yard boring 6 test performed at a depth of 4.12–4.57 meters.

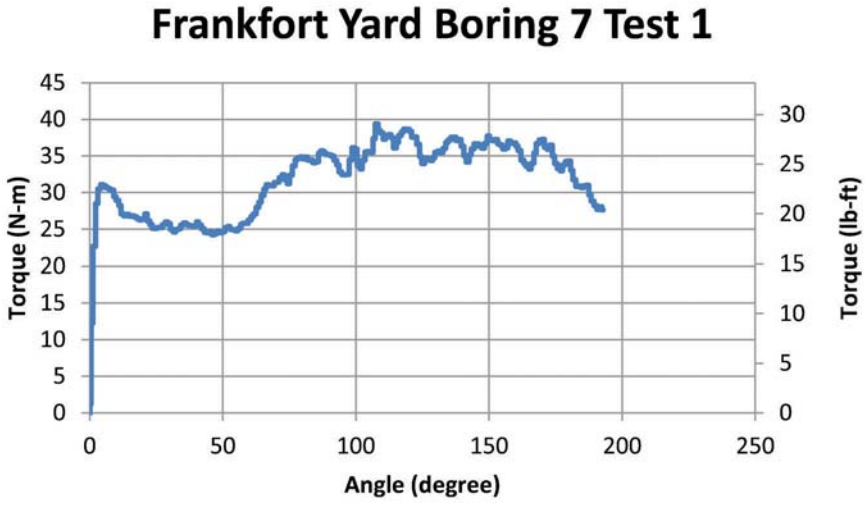

Figure B.35 Frankfort yard boring 7 test performed at a depth of 1.07–1.52 meters.

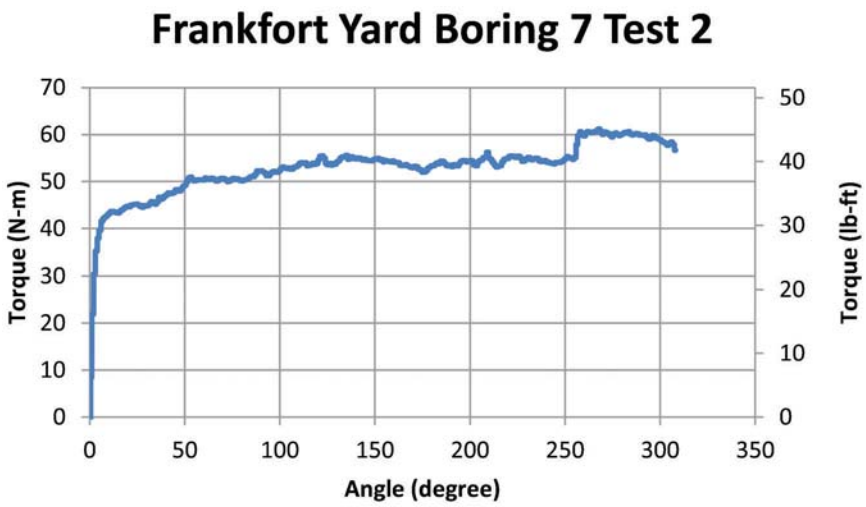

Figure B.36 Frankfort yard boring 7 test performed at a depth of 2.59–3.05 meters.

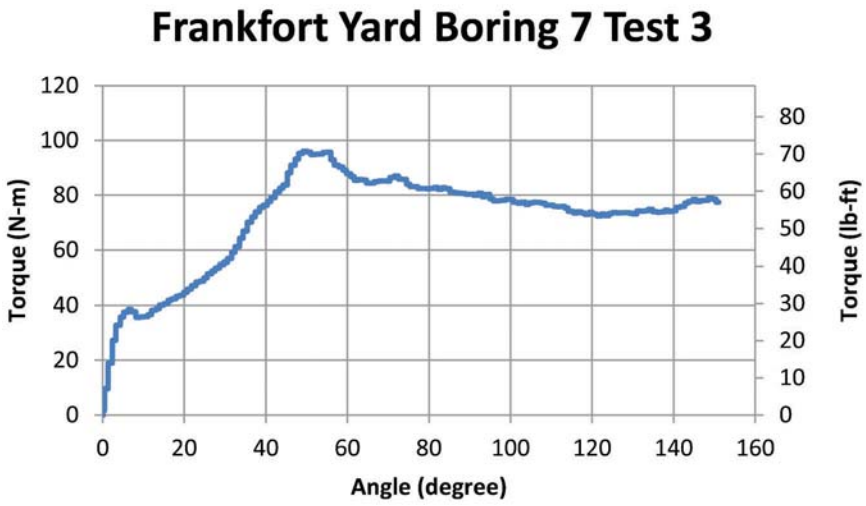

Figure B.37 Frankfort yard boring 7 test performed at a depth of 4.12–4.57 meters.

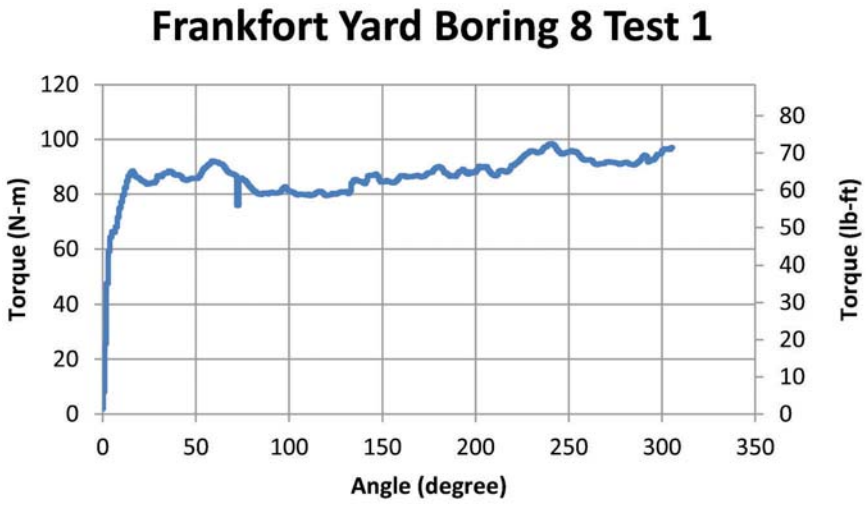

Figure B.38 Frankfort yard boring 8 test performed at a depth of 1.07–1.52 meters.

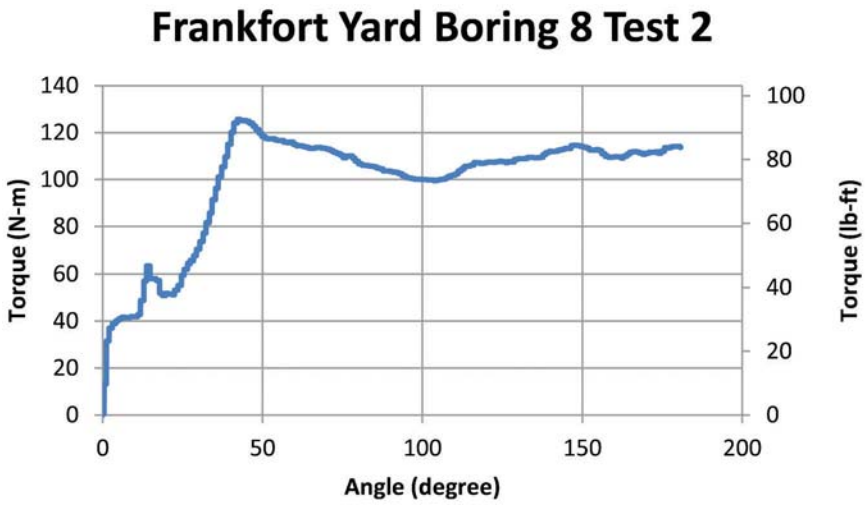

Figure B.39 Frankfort yard boring 8 test performed at a depth of 2.59–3.05 meters.

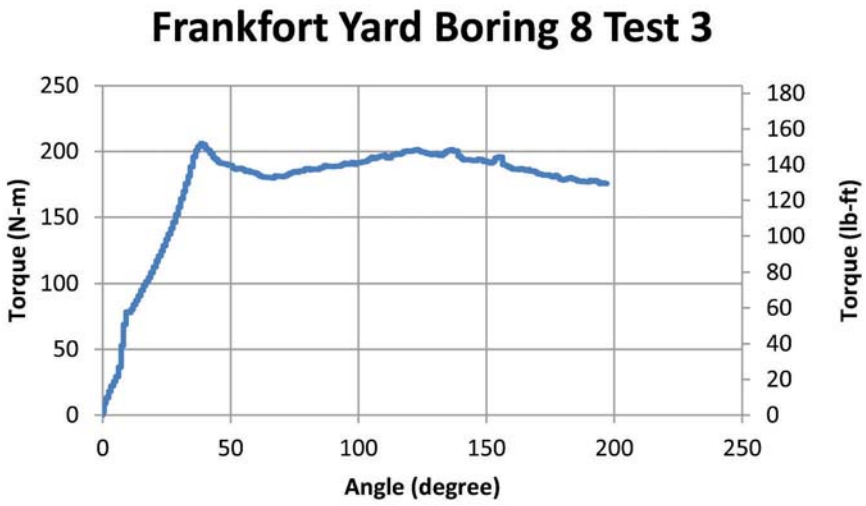

Figure B.40 Frankfort yard boring 8 test performed at a depth of 4.12–4.57 meters.

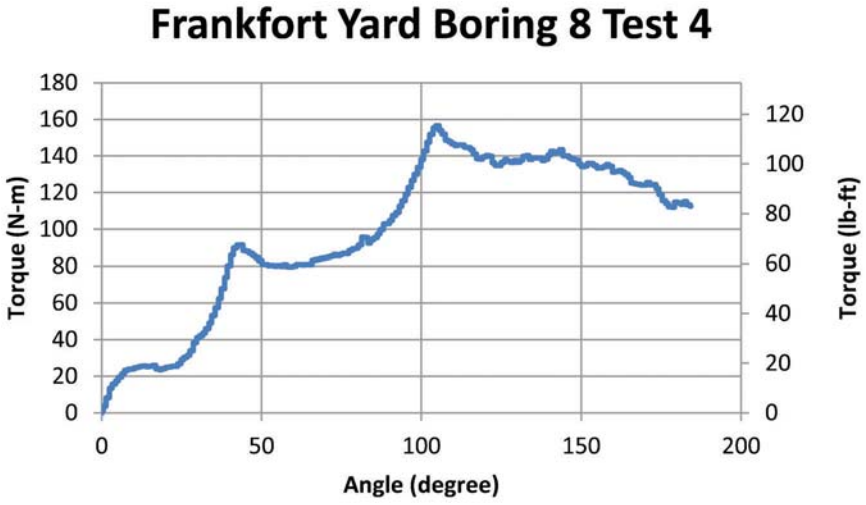

Figure B.41 Frankfort yard boring 8 test performed at a depth of 5.64–6.10 meters.

FIGURES B.42 THROUGH B.66

Figures B.42 through B.66 present SPT-Torque test data from the Romney Maintenance Unit (Tippecanoe County, Indiana) collected from January 9–10, 2012.

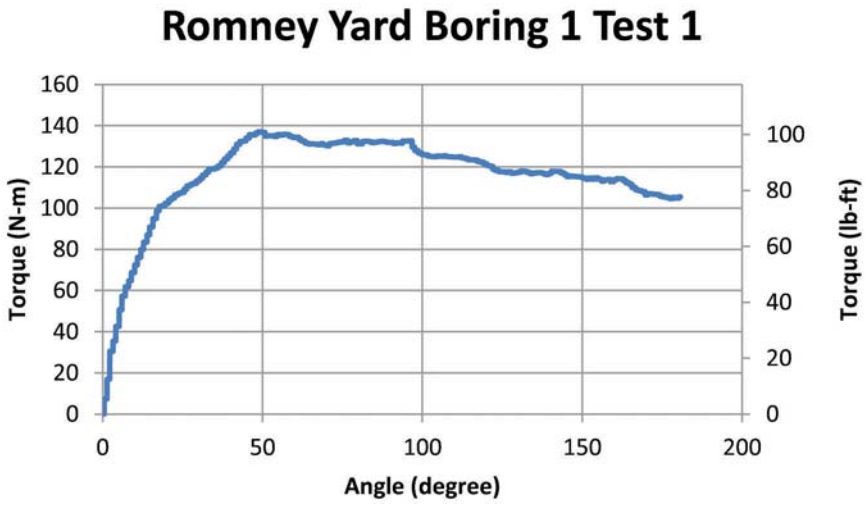

Figure B.42 Romney yard boring 1 test performed at a depth of 1.07–1.52 meters.

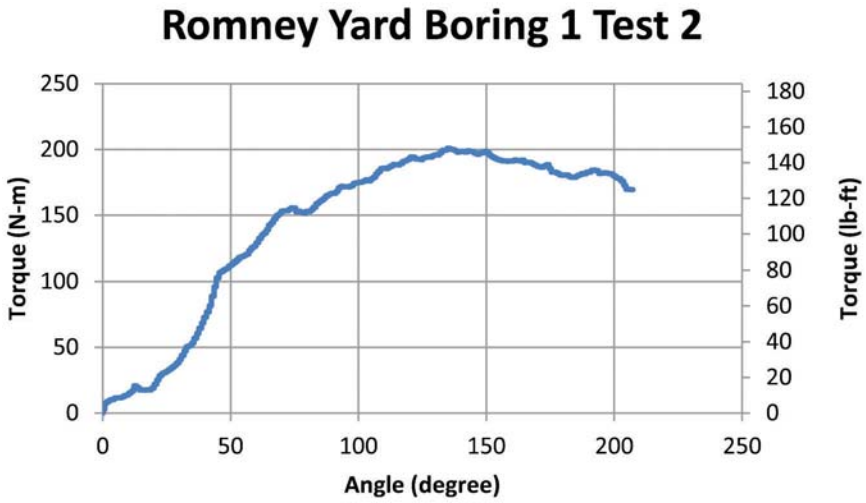

Figure B.43 Romney yard boring 1 test performed at a depth of 2.59–3.05 meters.

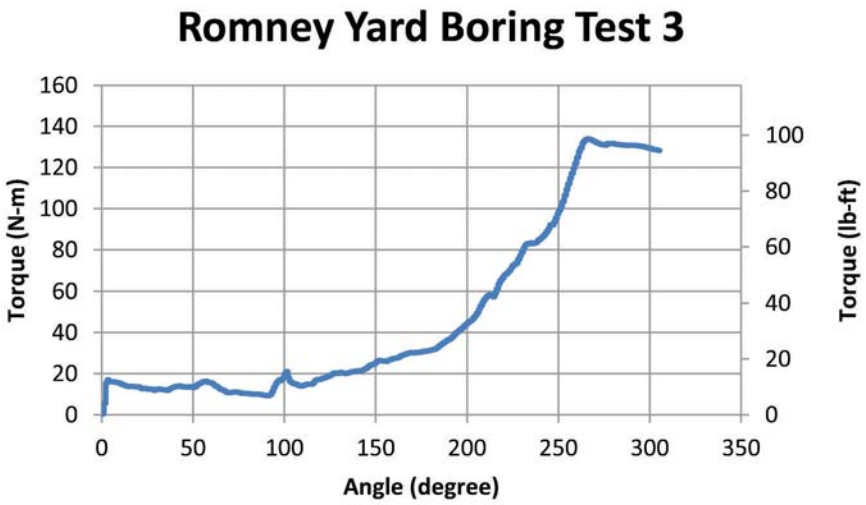

Figure B.44 Romney yard boring 1 test performed at a depth of 4.12–4.57 meters.

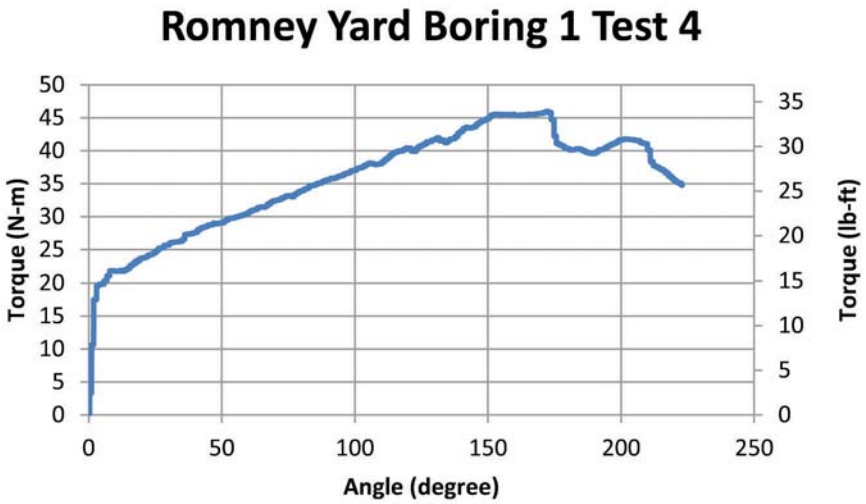

Figure B.45 Romney yard boring 1 test performed at a depth of 5.64–6.10 meters.

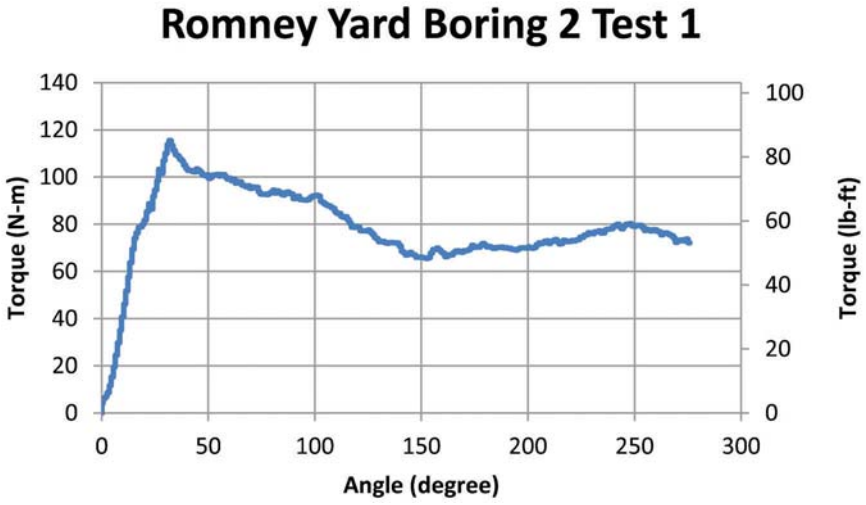

Figure B.46 Romney yard boring 2 test performed at a depth of 1.07–1.52 meters.

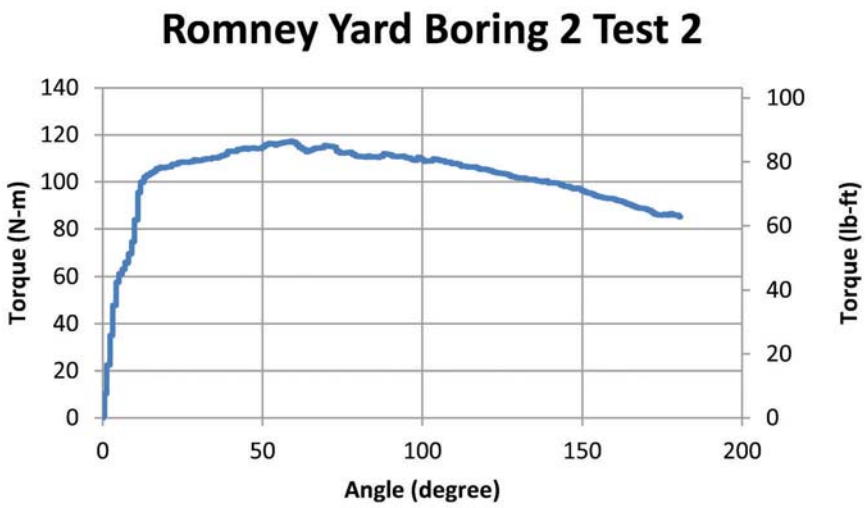

Figure B.47 Romney yard boring 2 test performed at a depth of 2.59–3.05 meters.

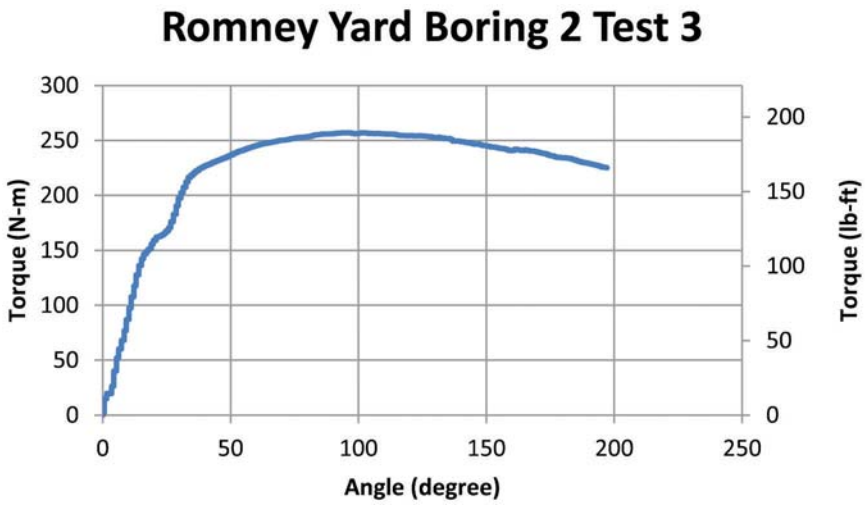

Figure B.48 Romney yard boring 2 test performed at a depth of 4.12–4.57 meters.

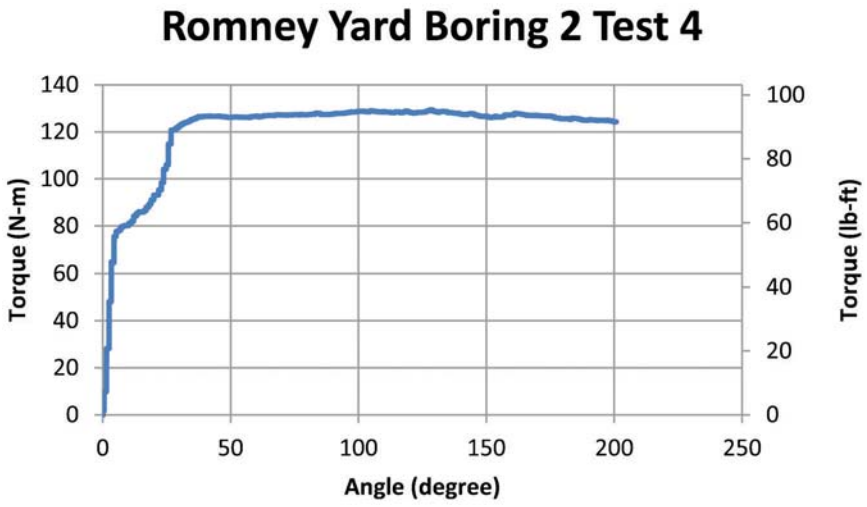

Figure B.49 Romney yard boring 2 test performed at a depth of 5.64–6.10 meters.

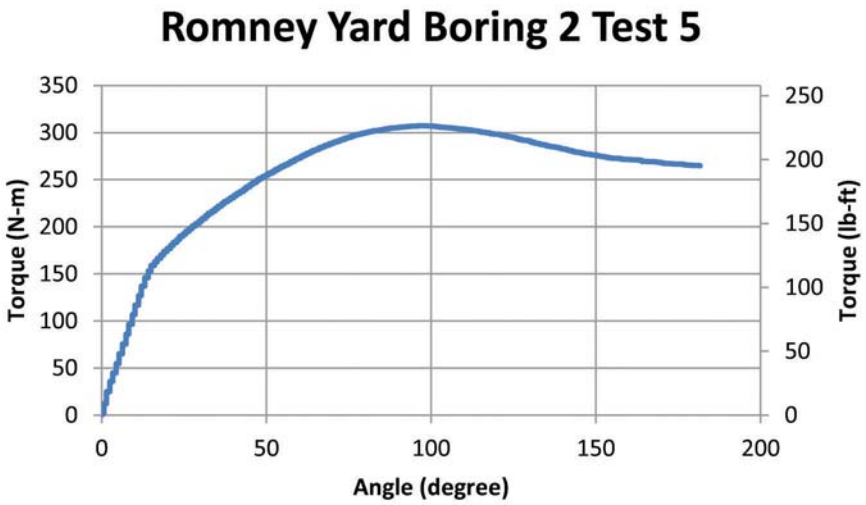

Figure B.50 Romney yard boring 2 test performed at a depth of 7.16–7.62 meters.

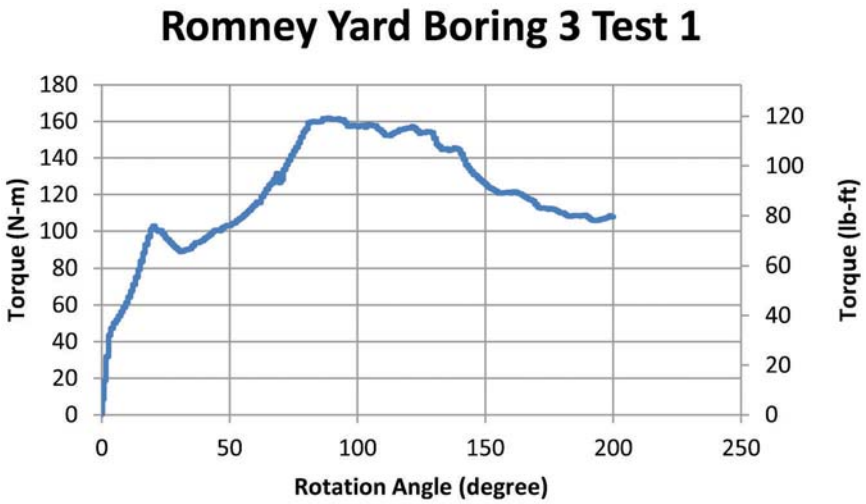

Figure B.51 Romney yard boring 3 test performed at a depth of 1.07–1.52 meters.

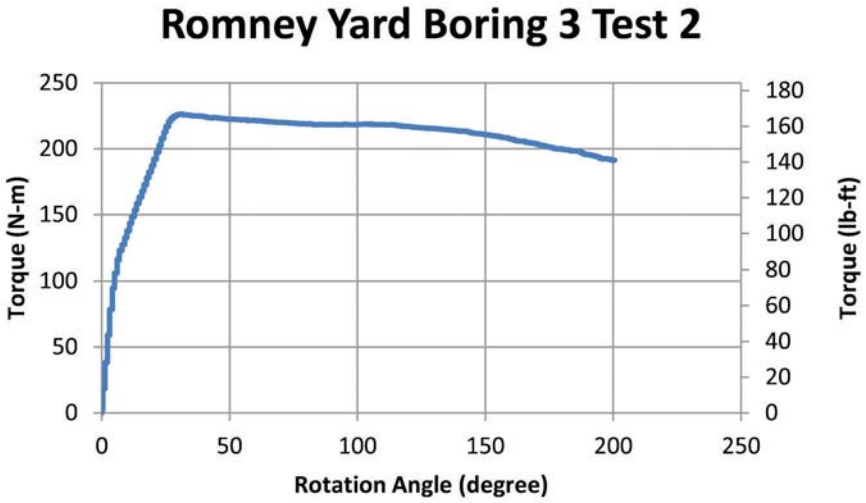

Figure B.52 Romney yard boring 3 test performed at a depth of 2.59–3.05 meters.

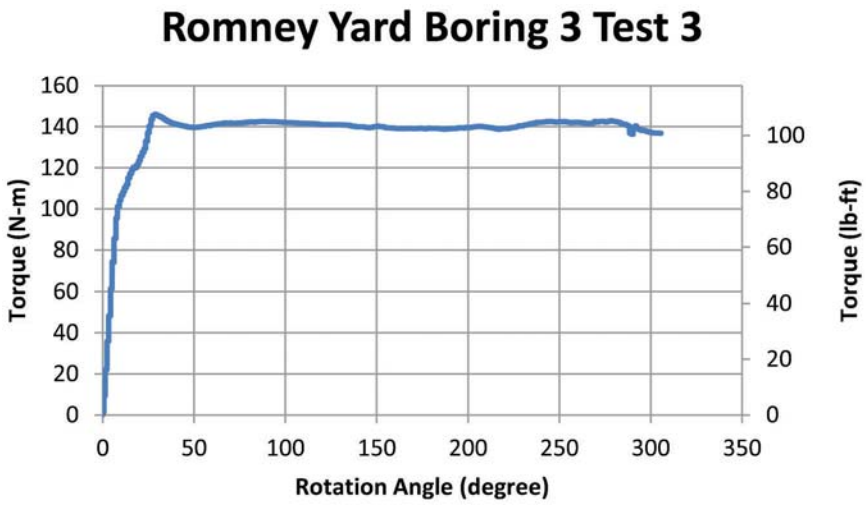

Figure B.53 Romney yard boring 3 test performed at a depth of 4.12–4.57 meters.

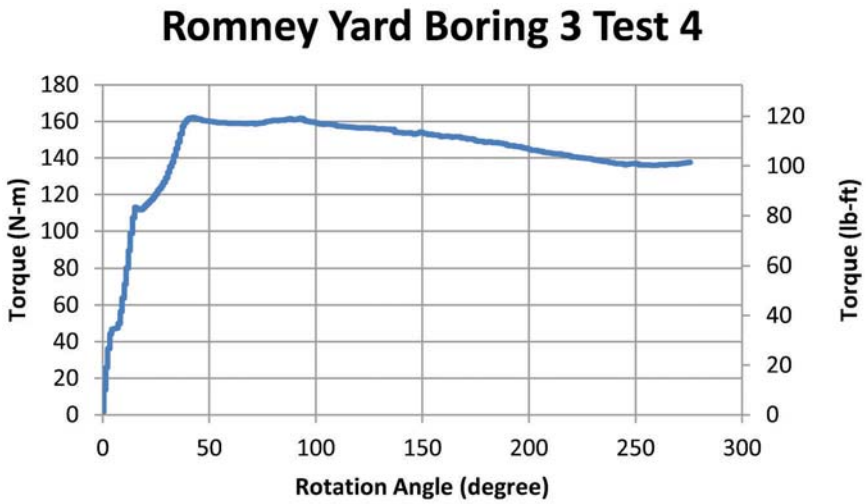

Figure B.54 Romney yard boring 3 test performed at a depth of 5.64–6.10 meters.

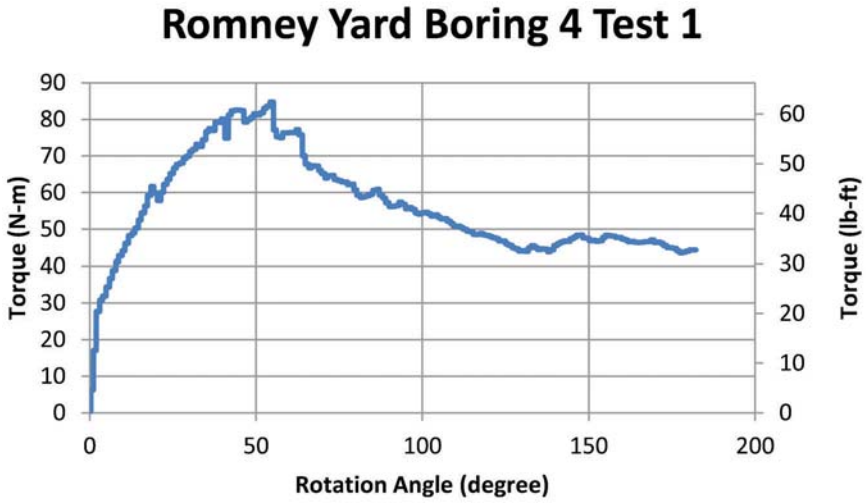

Figure B.55 Romney yard boring 4 test performed at a depth of 1.07–1.52 meters.

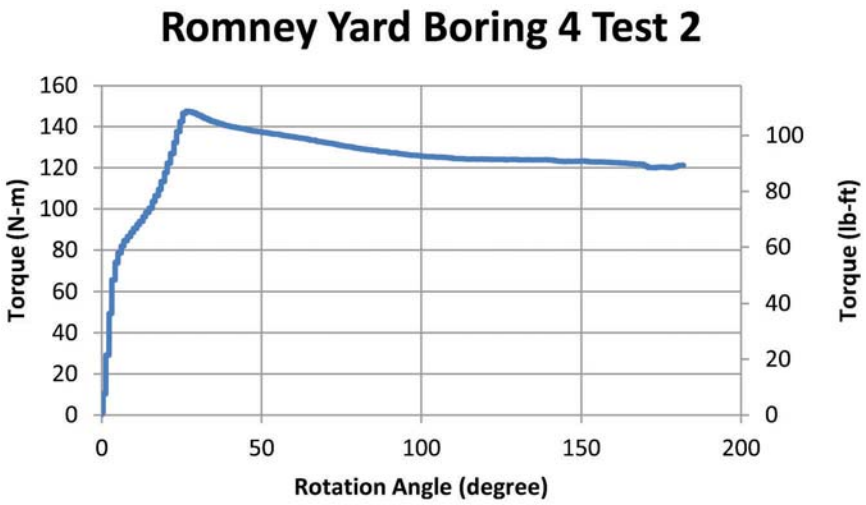

Figure B.56 Romney yard boring 4 test performed at a depth of 2.59–3.05 meters.

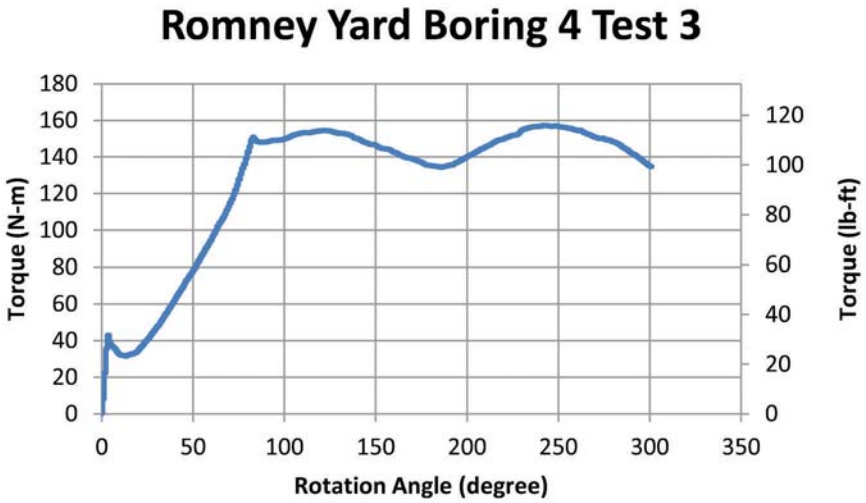

Figure B.57 Romney yard boring 4 test performed at a depth of 4.12–4.57 meters.

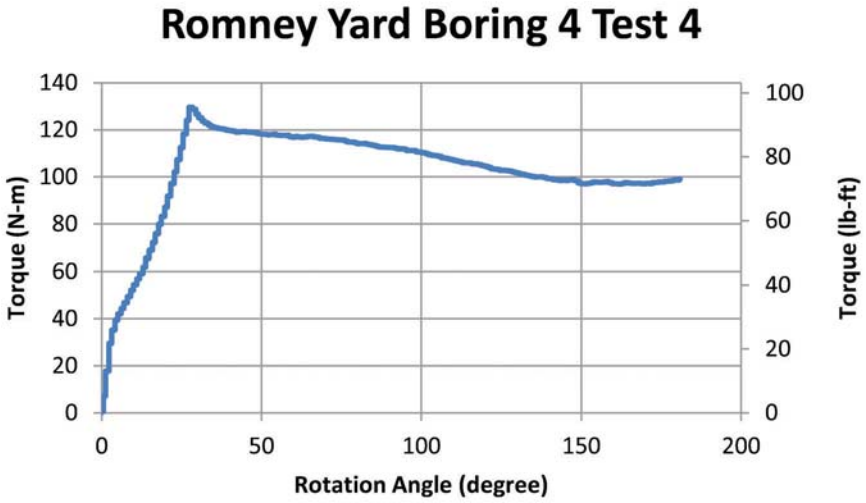

Figure B.58 Romney yard boring 4 test performed at a depth of 5.64–6.10 meters.

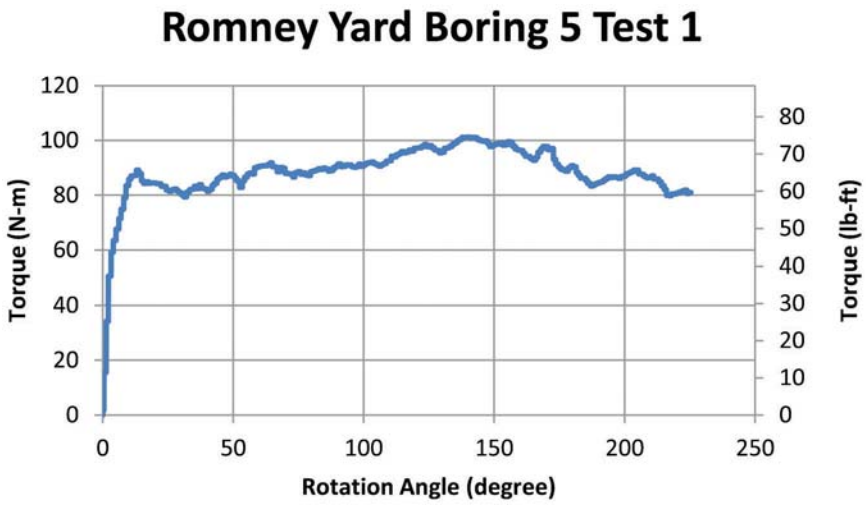

Figure B.59 Romney yard boring 5 test performed at a depth of 1.07–1.52 meters.

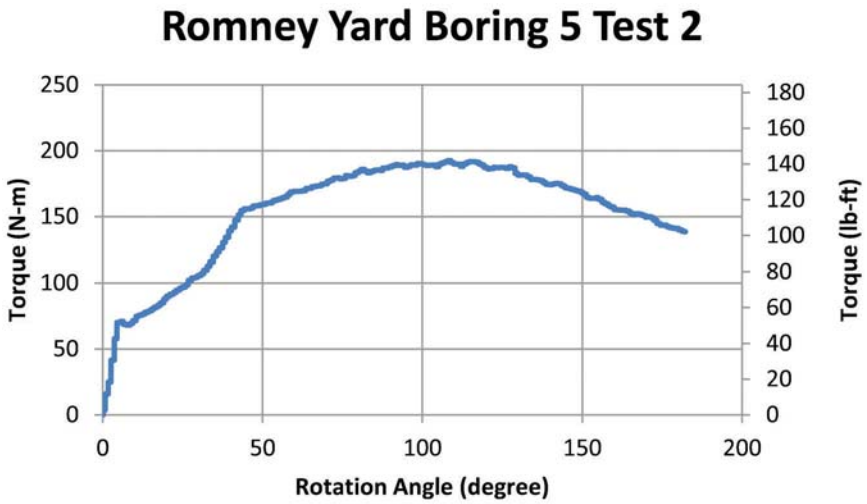

Figure B.60 Romney yard boring 5 test performed at a depth of 2.59–3.05 meters.

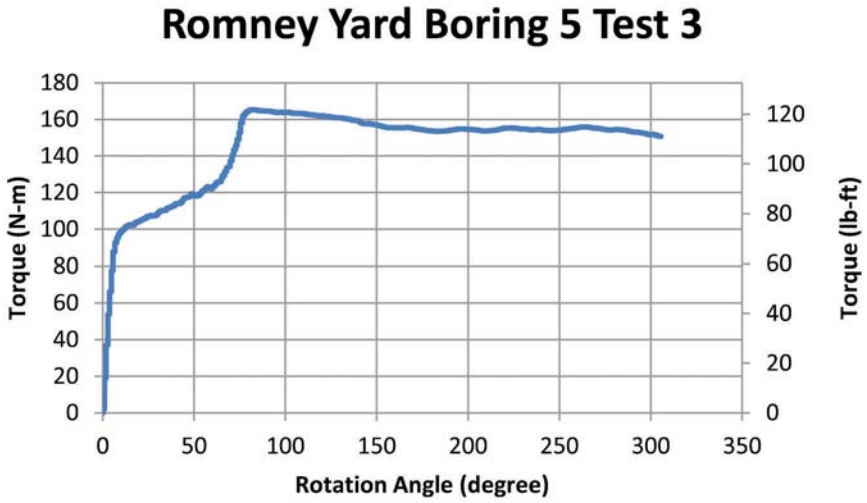

Figure B.61 Romney yard boring 5 test performed at a depth of 4.12–4.57 meters.

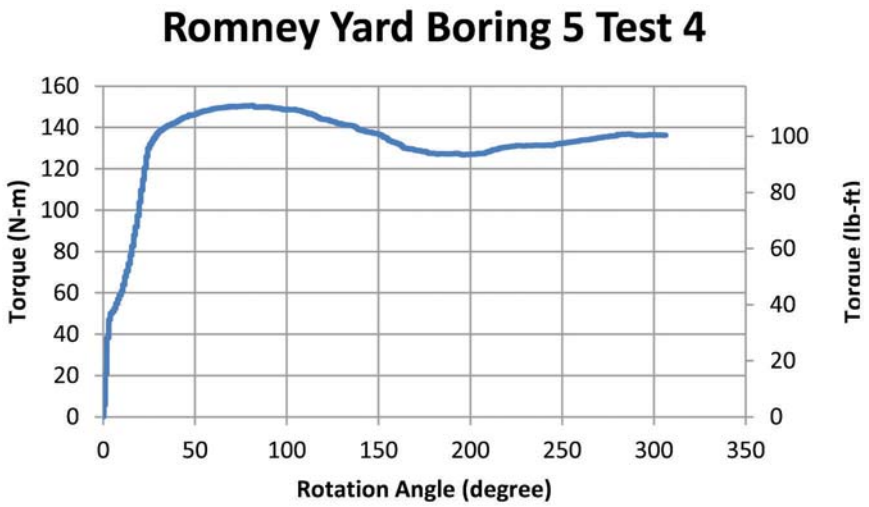

Figure B.62 Romney yard boring 5 test performed at a depth of 5.64–6.10 meters.

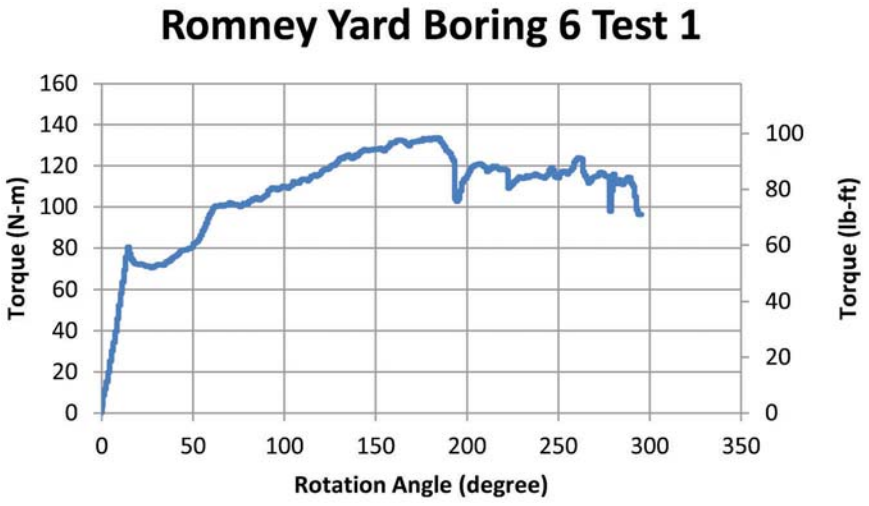

Figure B.63 Romney yard boring 6 test performed at a depth of 1.07–1.52 meters.

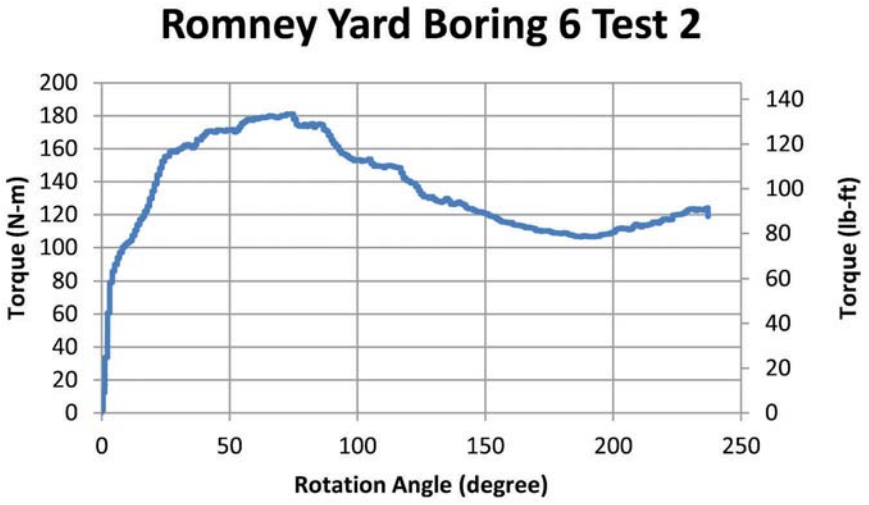

Figure B.64 Romney yard boring 6 test performed at a depth of 2.59–3.05 meters.

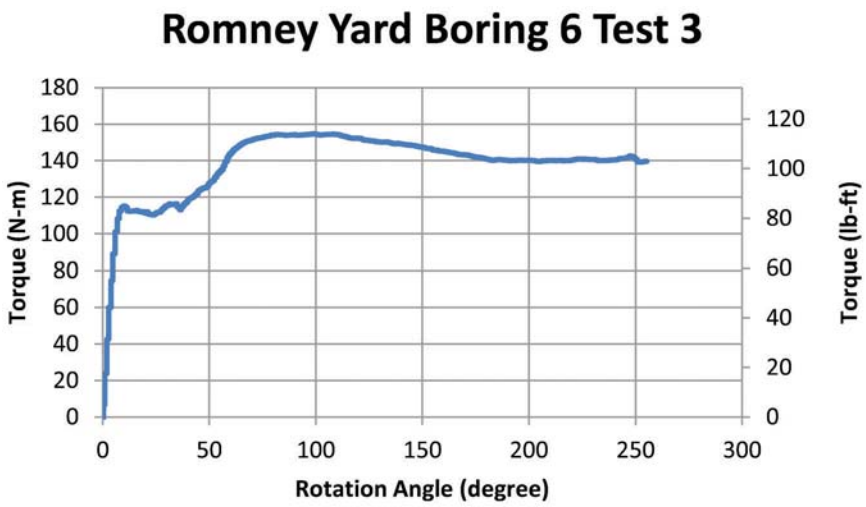

Figure B.65 Romney yard boring 6 test performed at a depth of 4.12–4.57 meters.

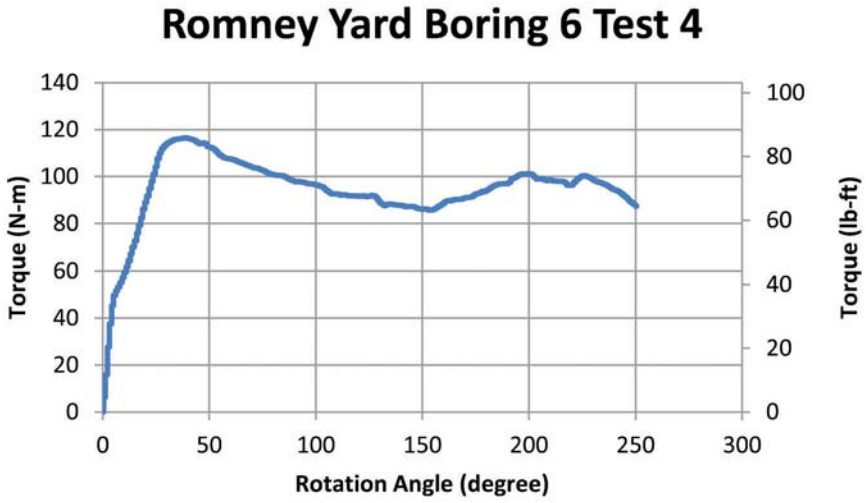

Figure B.66 Romney yard boring 6 test performed at a depth of 5.64–6.10 meters.

FIGURES B.67 THROUGH B.94

Figures B.67 through B.94 present SPT-Torque test data from the Koleen Interstate 69 expansion site (Greene County, Indiana) collected on July 16–19, 2012.

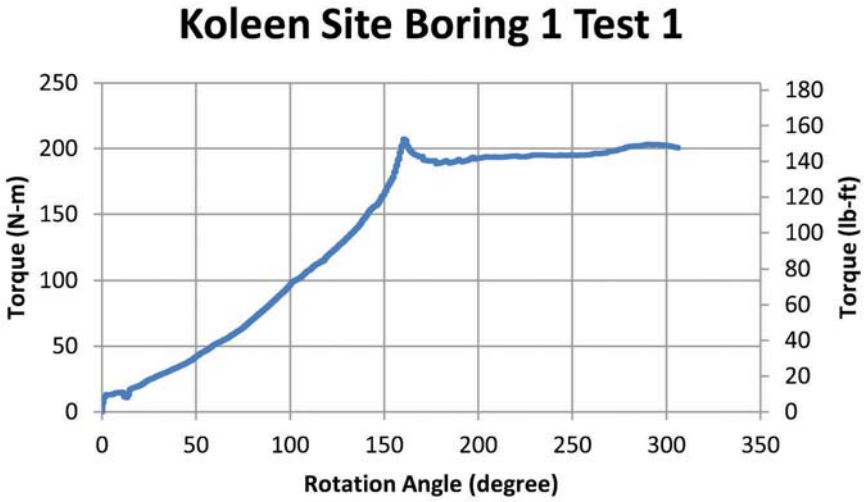

Figure B.67 Koleen site boring 1 test performed at a depth of 1.07–1.52 meters.

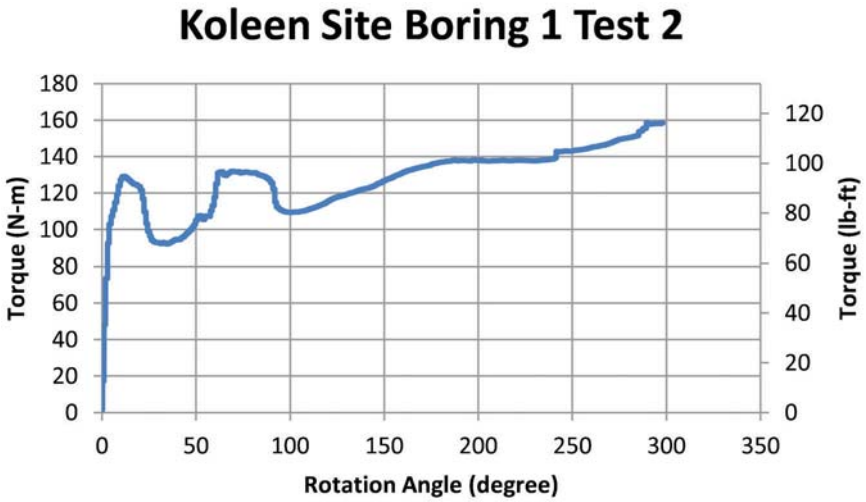

Figure B.68 Koleen site boring 1 test performed at a depth of 2.59–3.05 meters.

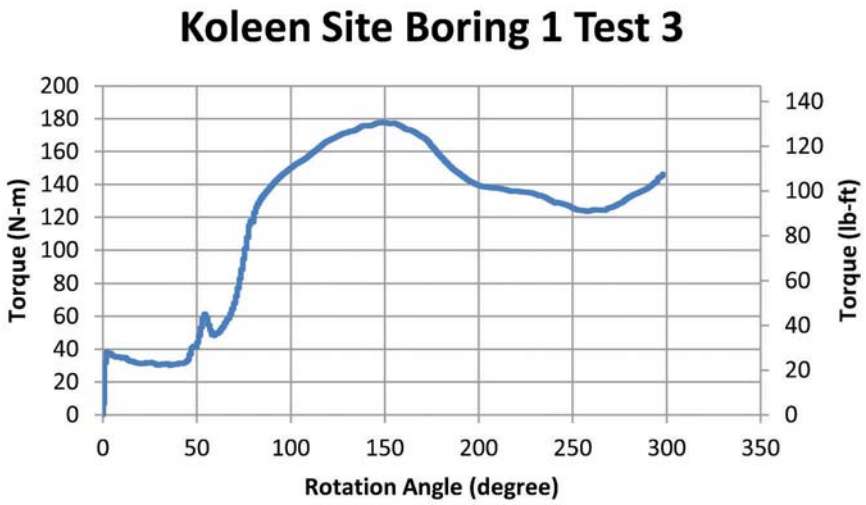

Figure B.69 Koleen site boring 1 test performed at a depth of 4.12–4.57 meters.

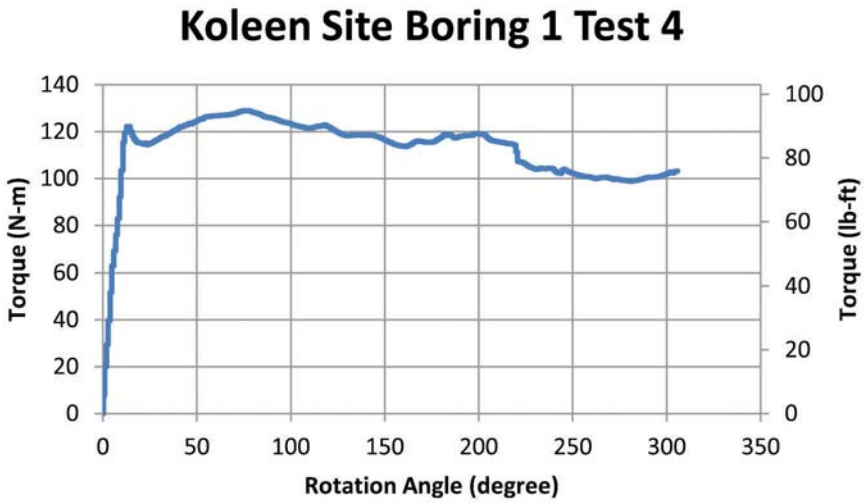

Figure B.70 Koleen site boring 1 test performed at a depth of 5.64–6.10 meters.

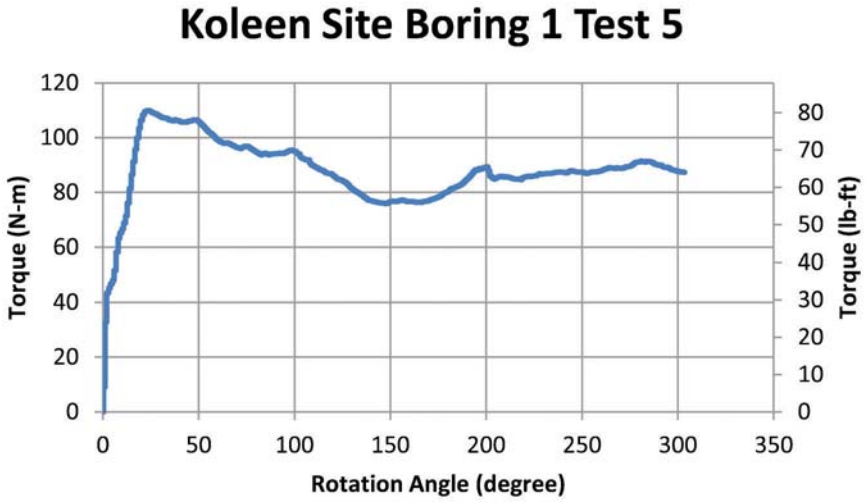

Figure B.71 Koleen site boring 1 test performed at a depth of 7.16–7.62 meters.

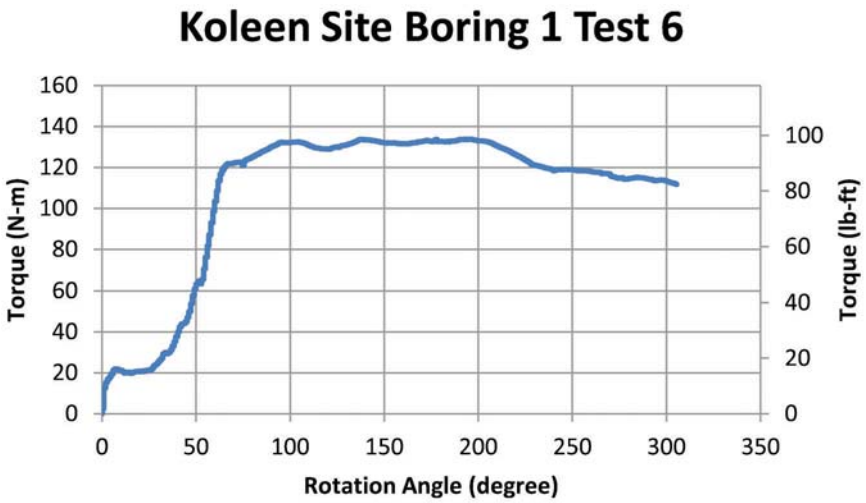

Figure B.72 Koleen site boring 1 test performed at a depth of 8.69–9.15 meters.

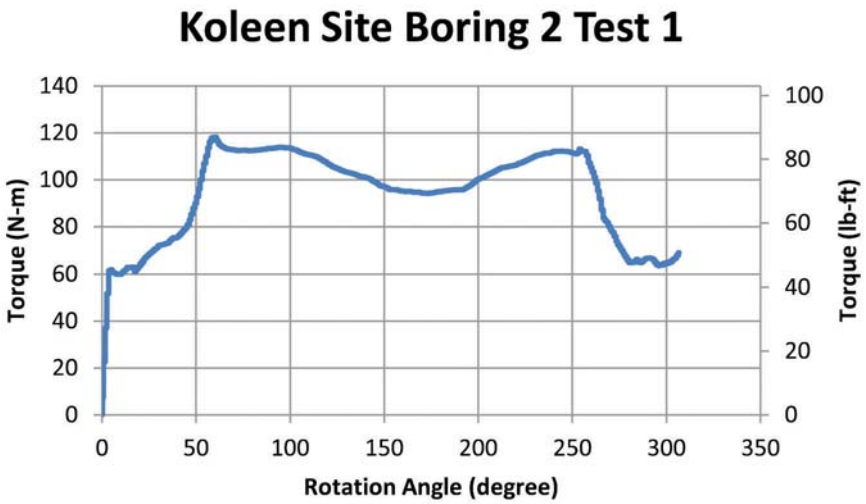

Figure B.73 Koleen site boring 2 test performed at a depth of 1.07–1.52 meters.

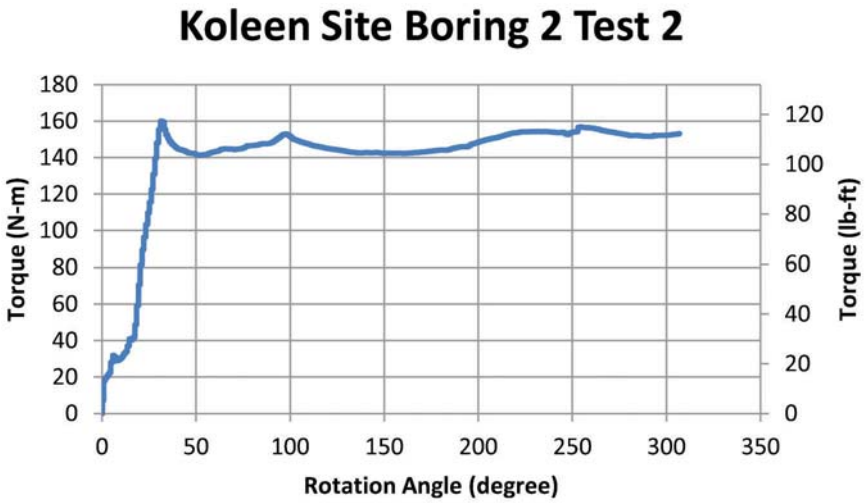

Figure B.74 Koleen site boring 2 test performed at a depth of 2.59–3.05 meters.

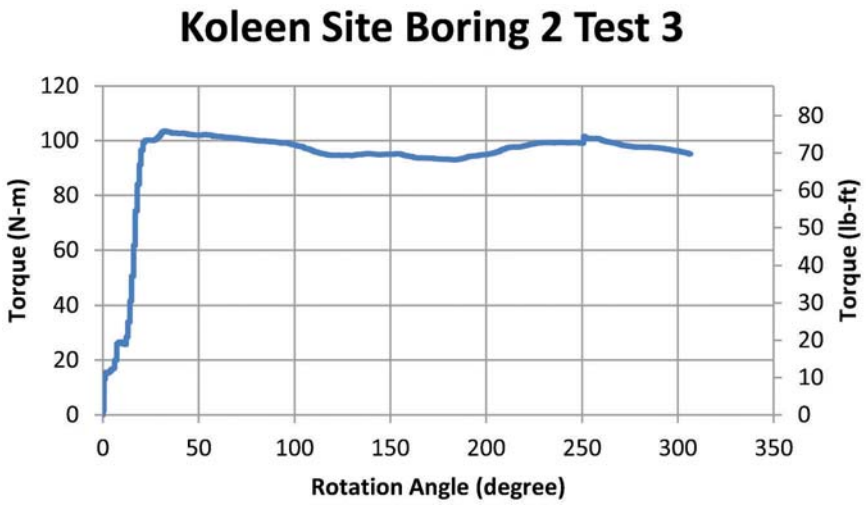

Figure B.75 Koleen site boring 2 test performed at a depth of 4.12–4.57 meters.

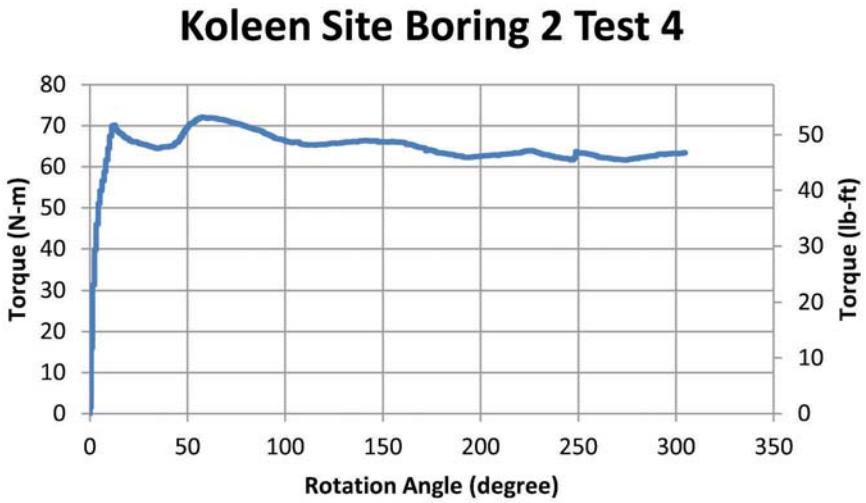

Figure B.76 Koleen site boring 2 test performed at a depth of 5.64–6.10 meters.

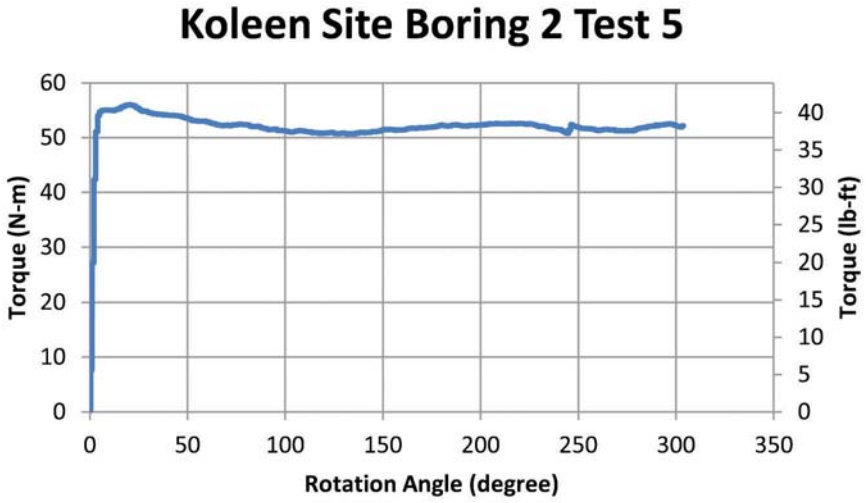

Figure B.77 Koleen site boring 2 test performed at a depth of 7.16–7.62 meters.

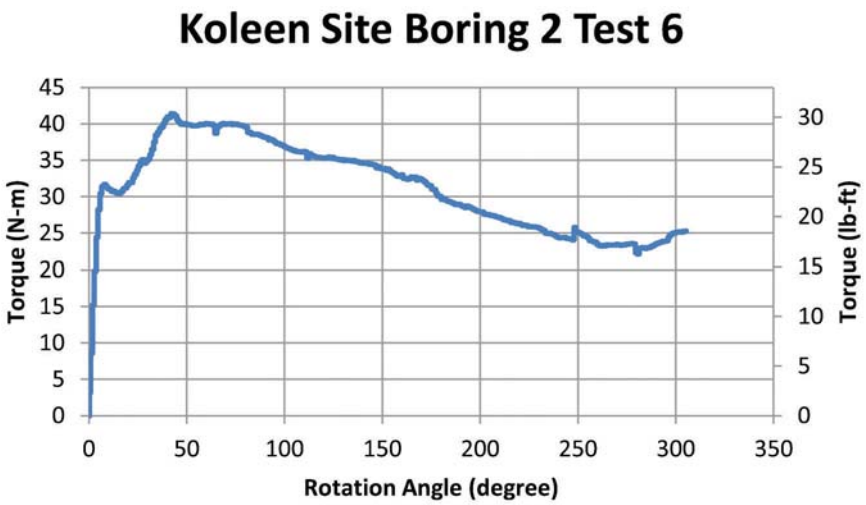

Figure B.78 Koleen site boring 2 test performed at a depth of 8.69–9.15 meters.

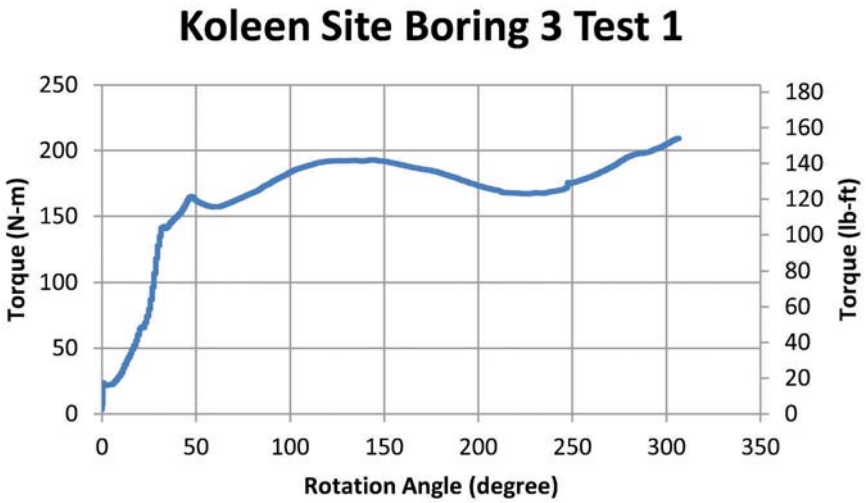

Figure B.79 Koleen site boring 3 test performed at a depth of 1.07–1.52 meters.

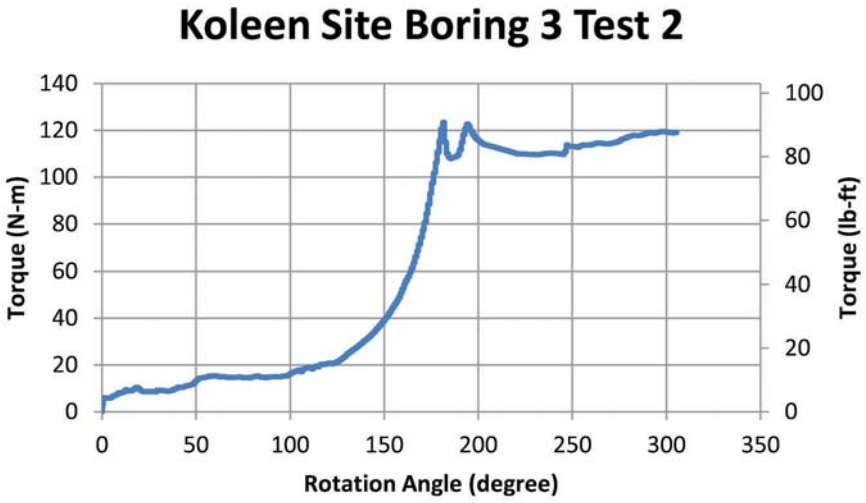

Figure B.80 Koleen site boring 3 test performed at a depth of 2.59–3.05 meters.

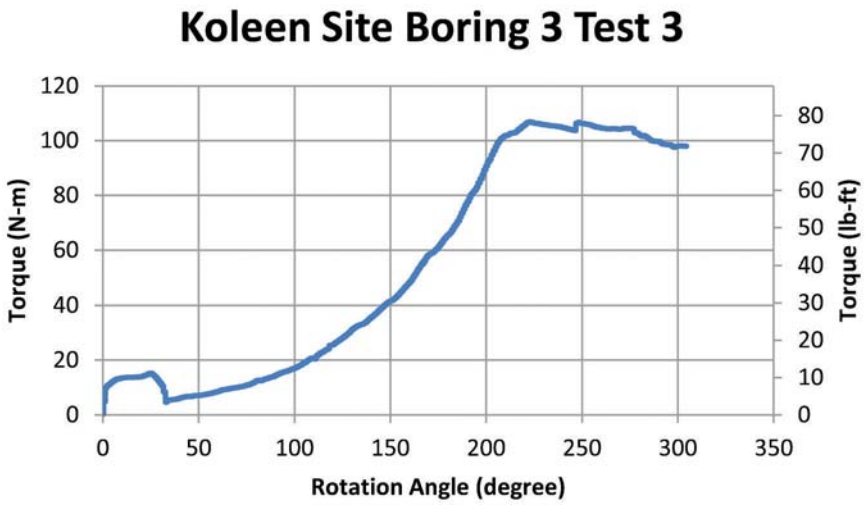

Figure B.81 Koleen site boring 3 test performed at a depth of 4.12–4.57 meters.

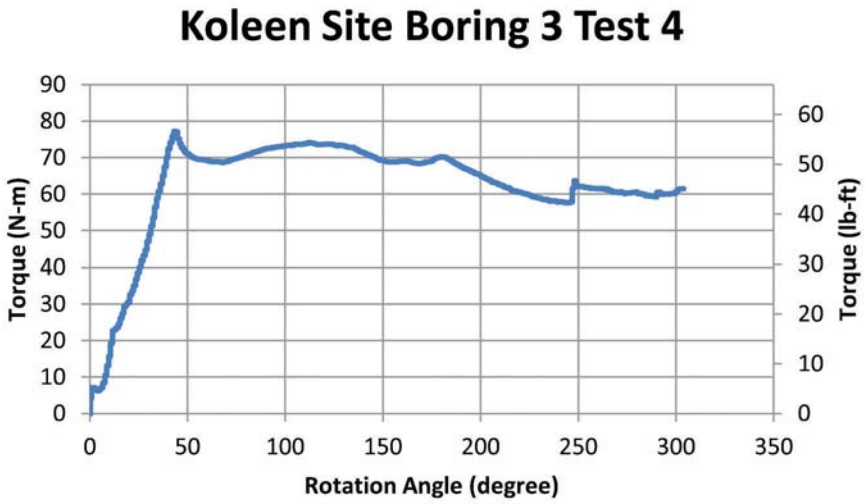

Figure B.82 Koleen site boring 3 test performed at a depth of 5.64–6.10 meters.

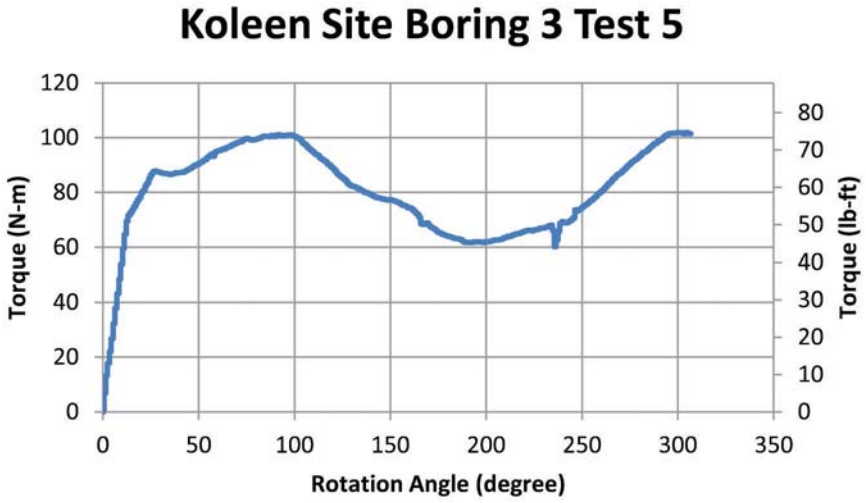

Figure B.83 Koleen site boring 3 test performed at a depth of 7.16–7.62 meters.

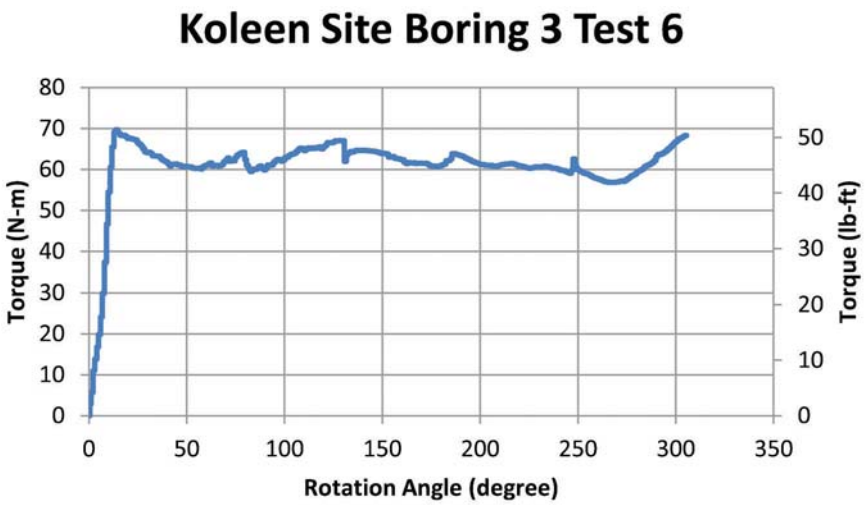

Figure B.84 Koleen site boring 3 test performed at a depth of 8.69–9.15 meters.

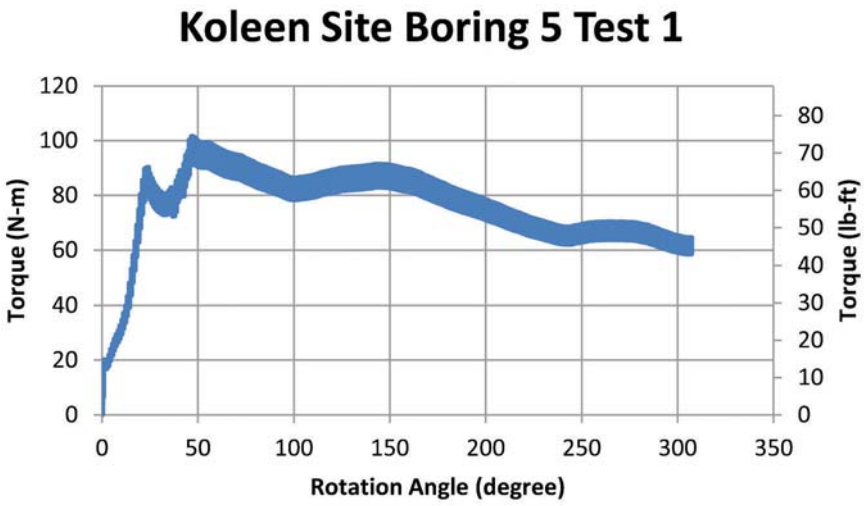

Figure B.85 Koleen site boring 5 test performed at a depth of 1.07–1.52 meters.

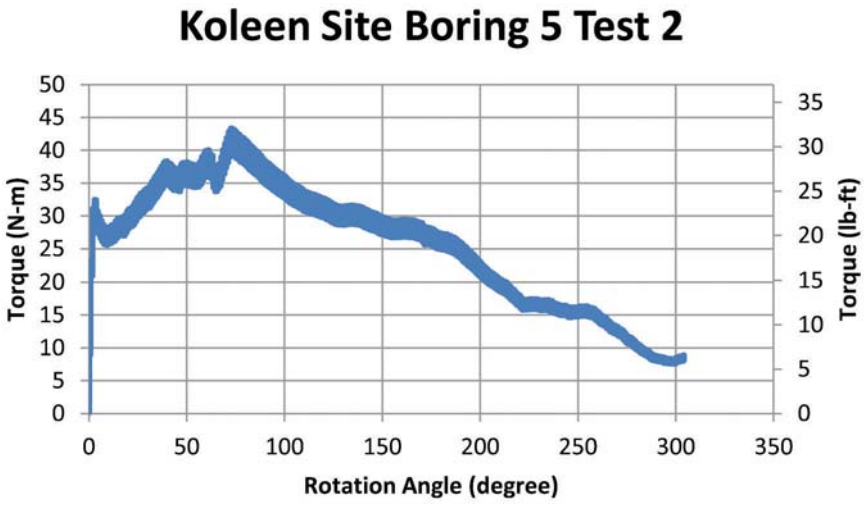

Figure B.86 Koleen site boring 5 test performed at a depth of 2.59–3.05 meters.

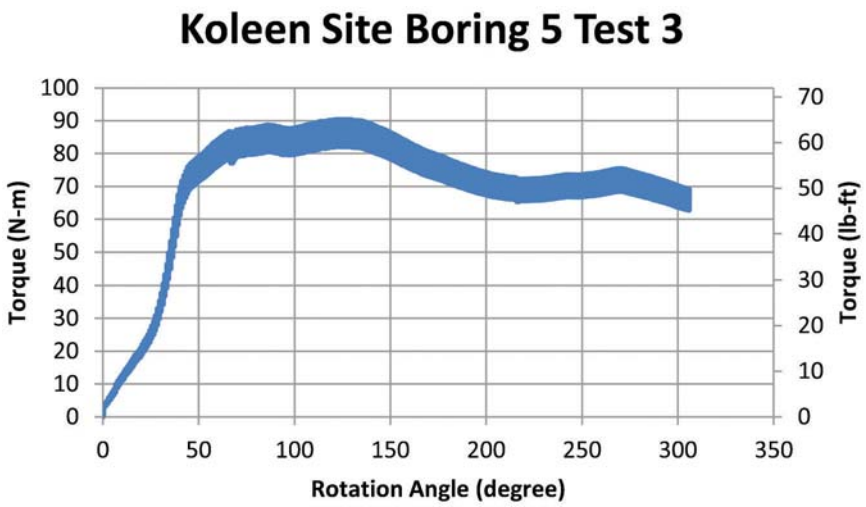

Figure B.87 Koleen site boring 5 test performed at a depth of 4.12–4.57 meters.

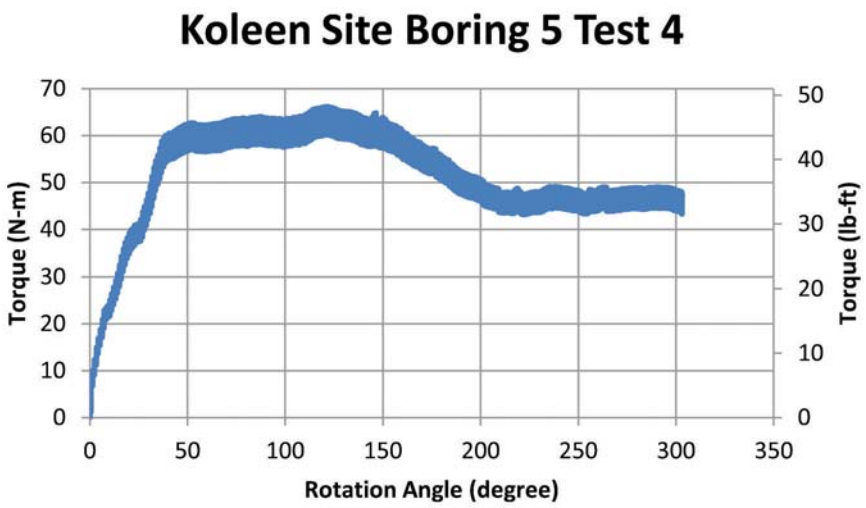

Figure B.88 Koleen site boring 5 test performed at a depth of 5.64–6.10 meters.

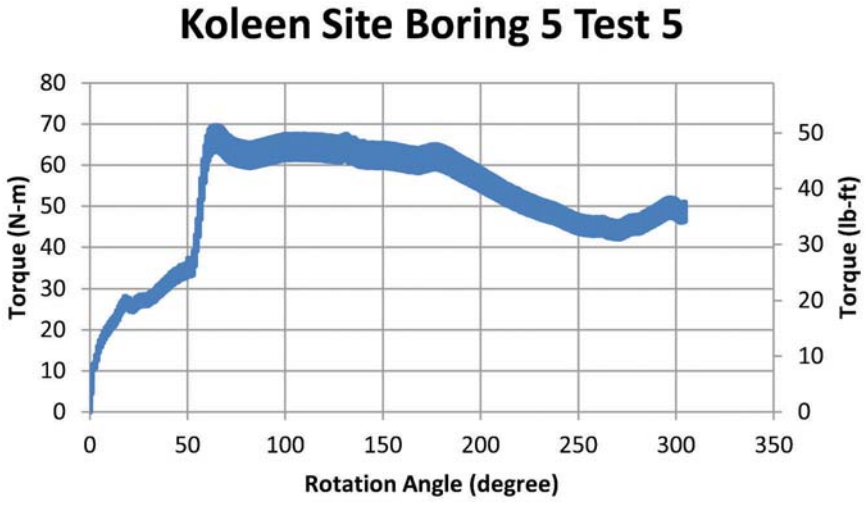

Figure B.89 Koleen site boring 5 test performed at a depth of 7.16–7.62 meters.

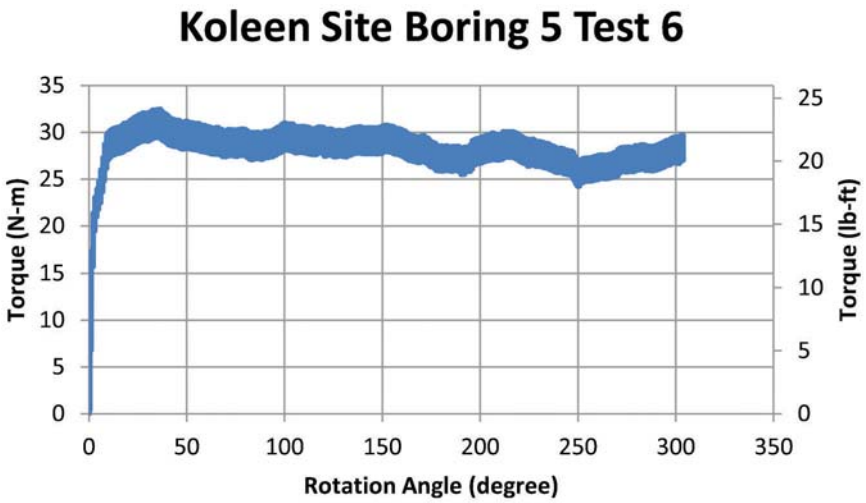

Figure B.90 Koleen site boring 5 test performed at a depth of 8.69–9.15 meters.

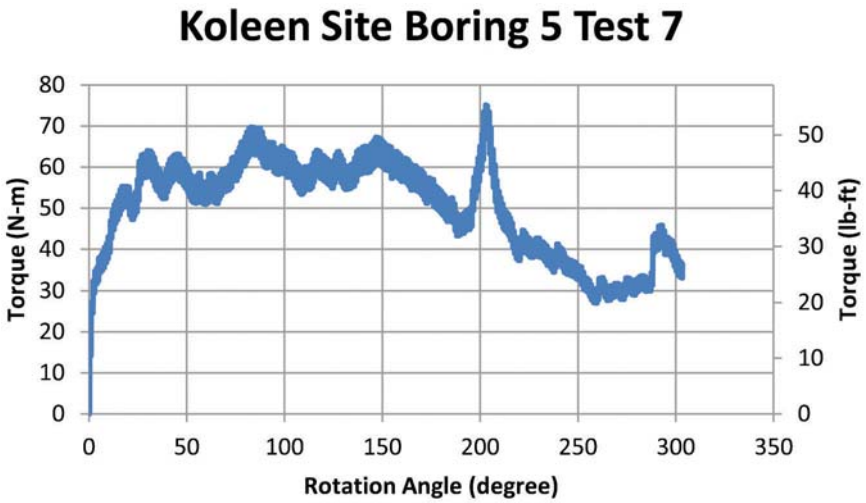

Figure B.91 Koleen site boring 5 test performed at a depth of 10.21–10.67 meters.

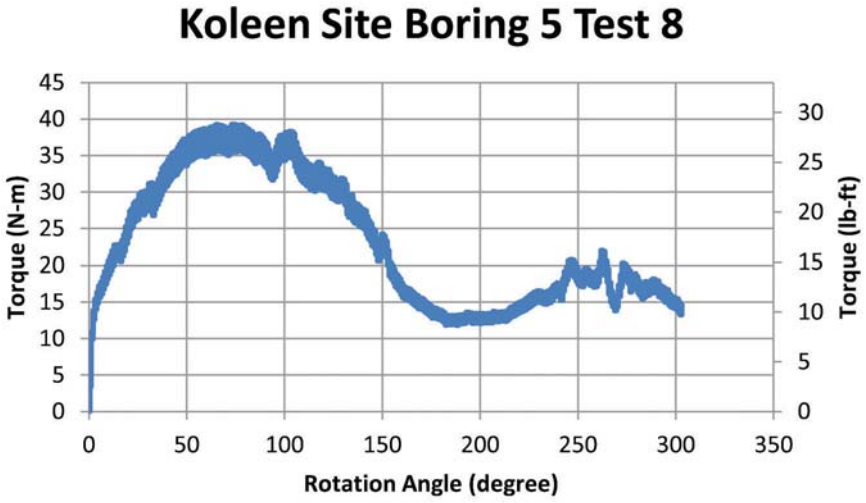

Figure B.92 Koleen site boring 5 test performed at a depth of 11.74–12.20 meters.

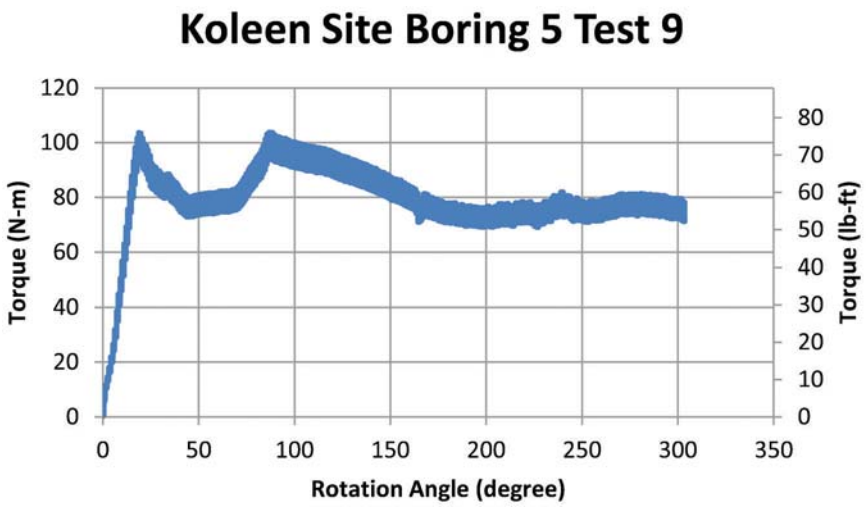

Figure B.93 Koleen site boring 5 test performed at a depth of 13.26–13.72 meters.

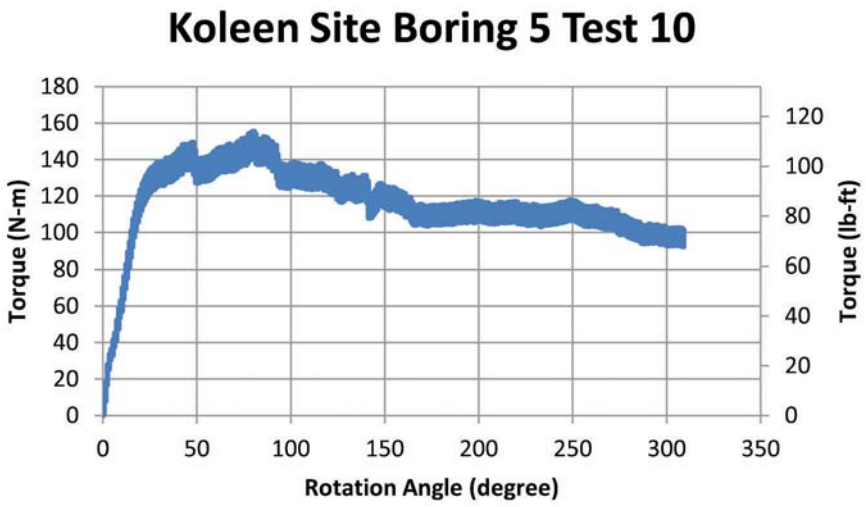

Figure B.94 Koleen site boring 5 test performed at a depth of 14.79–15.24 meters.

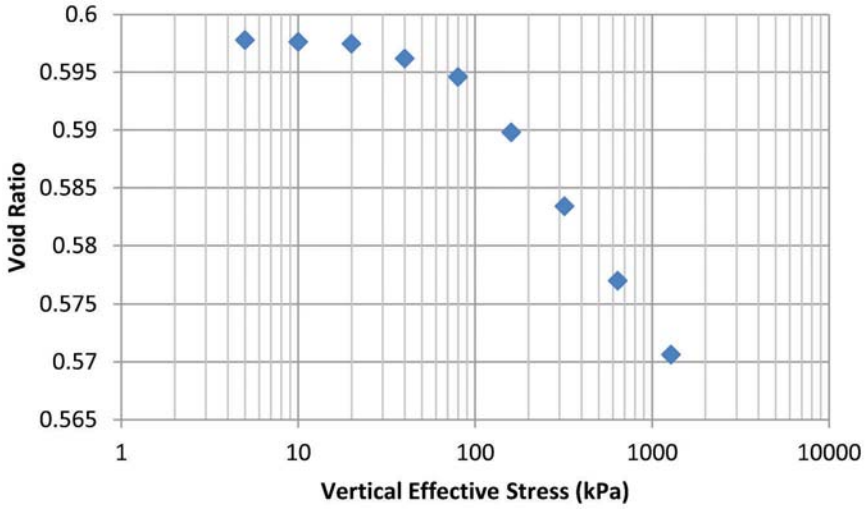

Figure C.1 1-D consolidation test for Flora 6 with a depth of 2.08 meters.

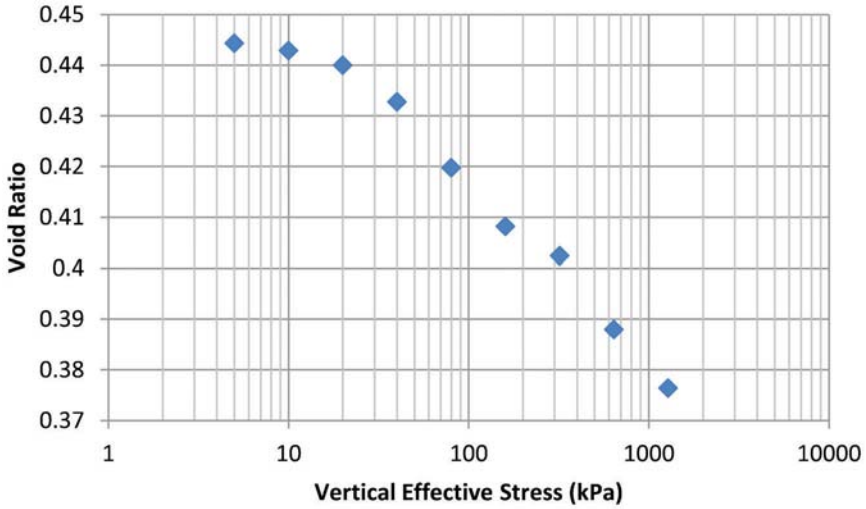

Figure C.2 1-D consolidation test for Flora 6 with a depth of 2.95 meters.

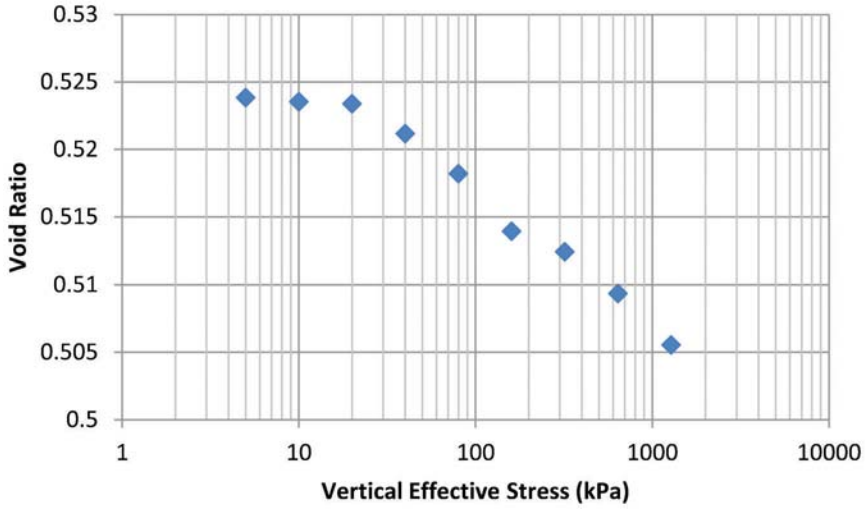

Figure C.3 1-D consolidation test for Frankfort 9 with a depth of 1.55 meters.

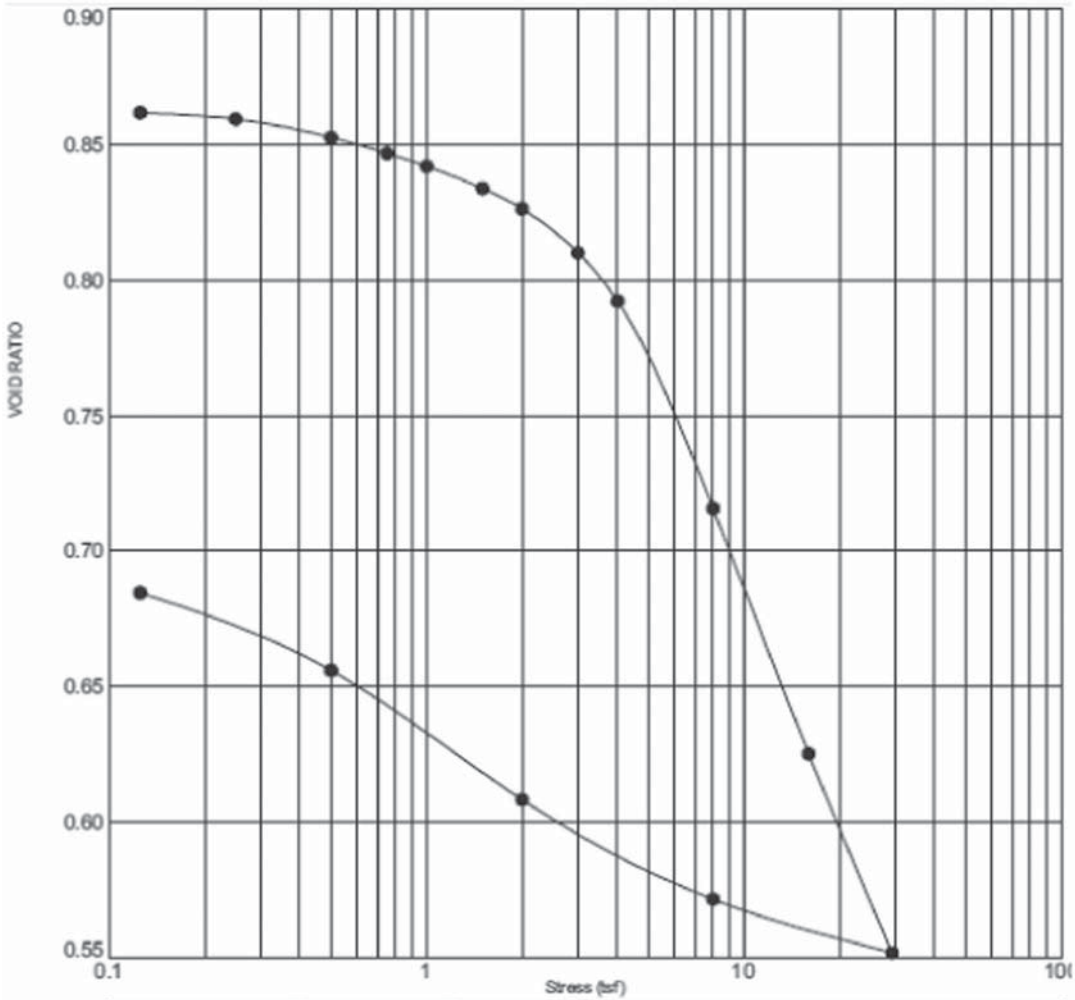

Boring	Sample	Depth	Soil Description
S2-CB-4A	ST-2	16.5 - 17	Silty Clay with some marl A-7-6 (35)

Initial Wet Density (pcf)	Initial Dry Density (pcf)	Initial Moisture (%)	Final Dry Density (pcf)	Final Moisture (%)	Specific Gravity
119.0	91.0	30.8	100.4	25.3	2.712

Initial Void Ratio	Cc	Cr	Cv (in2/sec)	Po (tsf)	Pmax (tsf)
0.86	0.29	0.058		1	3.8

Figure C.4 1-D consolidation test from the Koleen site performed by INDOT.

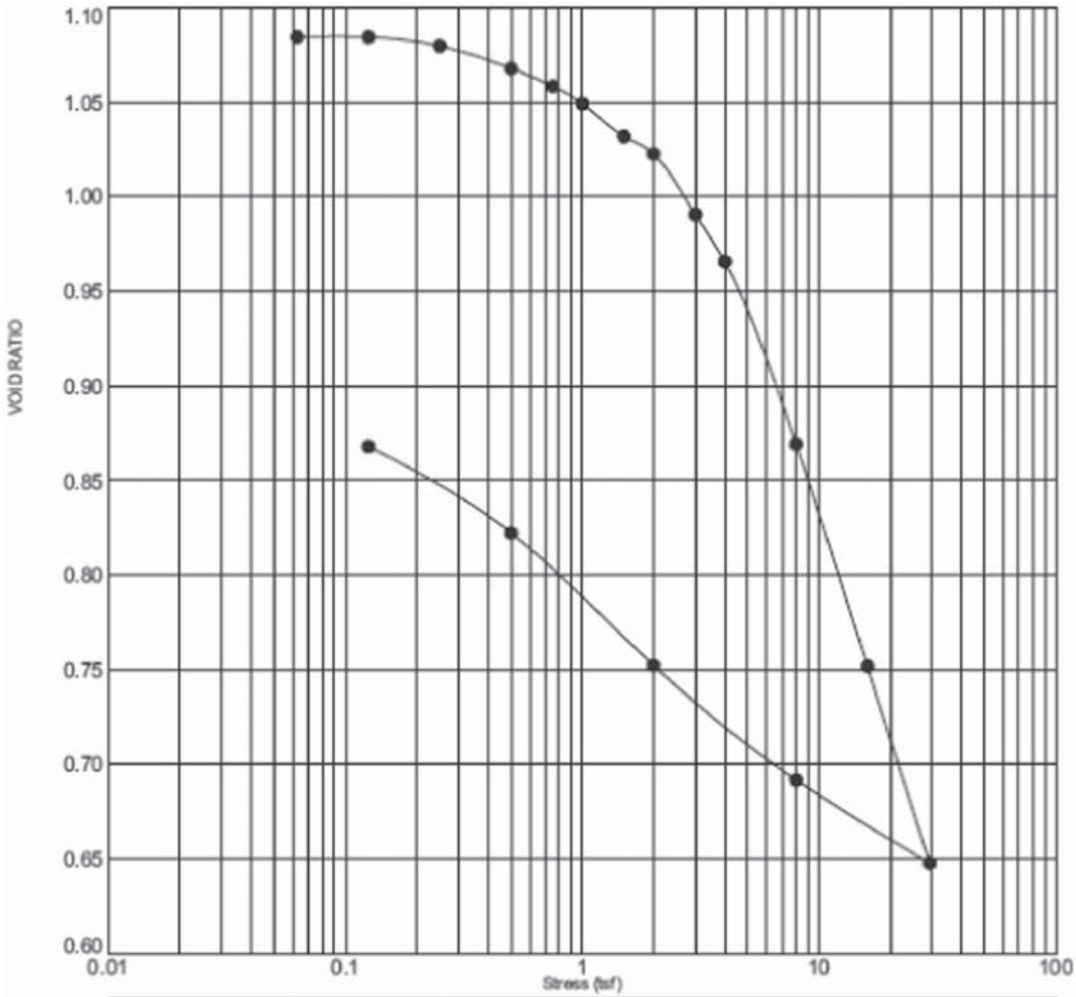

Boring	Sample	Depth	Soil Description
S2-CB-4A	ST-5	29 - 29.5	Clay with little marl A-7-6 (47)

Initial Wet Density (pcf)	Initial Dry Density (pcf)	Initial Moisture (%)	Final Dry Density (pcf)	Final Moisture (%)	Specific Gravity
111.8	79.9	39.8	89.3	32.5	2.671

Initial Void Ratio	Cc	Cr	Cv (in2/sec)	Po (tsf)	Pmax (tsf)
1.08	0.39	0.093		1.3	3.6

Figure C.5 1-D consolidation test from the Koleen site performed by INDOT.

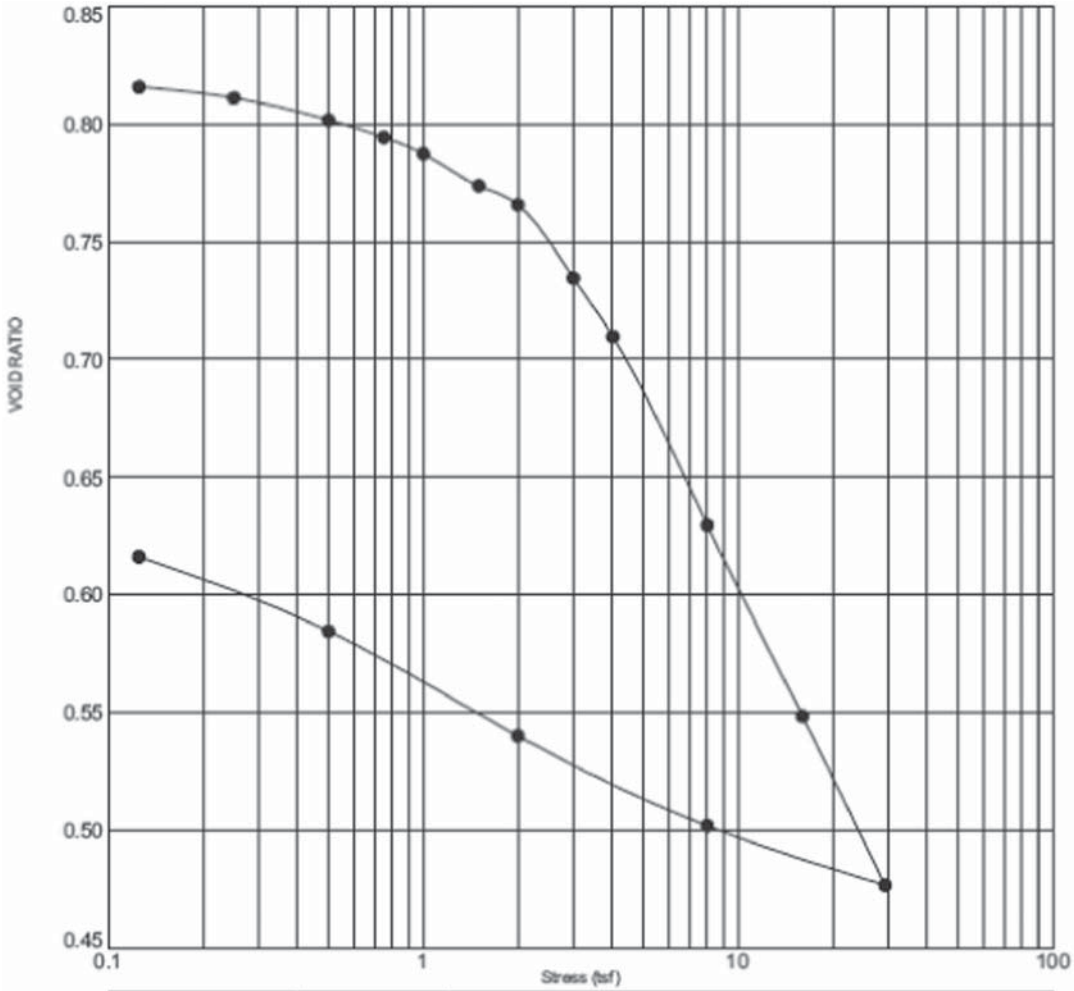

Boring	Sample	Depth	Soil Description
S2-CB-5A	ST-1	14 - 14.5	Silty Clay with some marl A-7-6 (33)

Initial Wet Density (pcf)	Initial Dry Density (pcf)	Initial Moisture (%)	Final Dry Density (pcf)	Final Moisture (%)	Specific Gravity
118.8	91.0	30.5	102.3	23.3	2.650

Initial Void Ratio	Cc	Cr	Cv (in2/sec)	Po (tsf)	Pmax (tsf)
0.82	0.27	0.05		0.8	2.5

Figure C.6 1-D consolidation test from the Koleen site performed by INDOT.

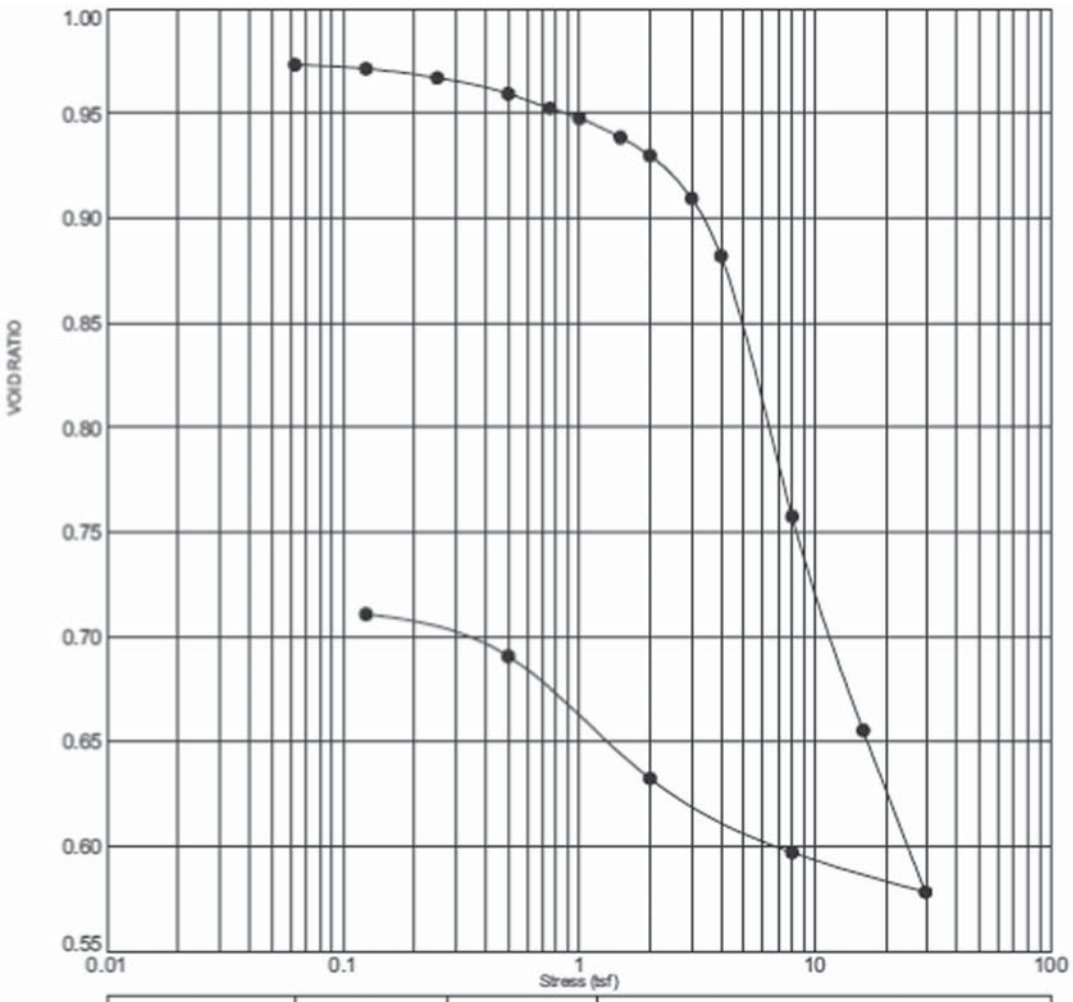

Boring	Sample	Depth	Soil Description
S2-CB-5A	ST-2	21 - 21.5	Silty Clay with little marl A-7-6 (23)

Initial Wet Density (pcf)	Initial Dry Density (pcf)	Initial Moisture (%)	Final Dry Density (pcf)	Final Moisture (%)	Specific Gravity
111.3	81.6	36.5	94.3	27.4	2.584

Initial Void Ratio	Cc	Cr	Cv (in2/sec)	Po (tsf)	Pmax (tsf)
0.98	0.36	0.054		1.2	3.2

Figure C.7 1-D consolidation test from the Koleen site performed by INDOT.

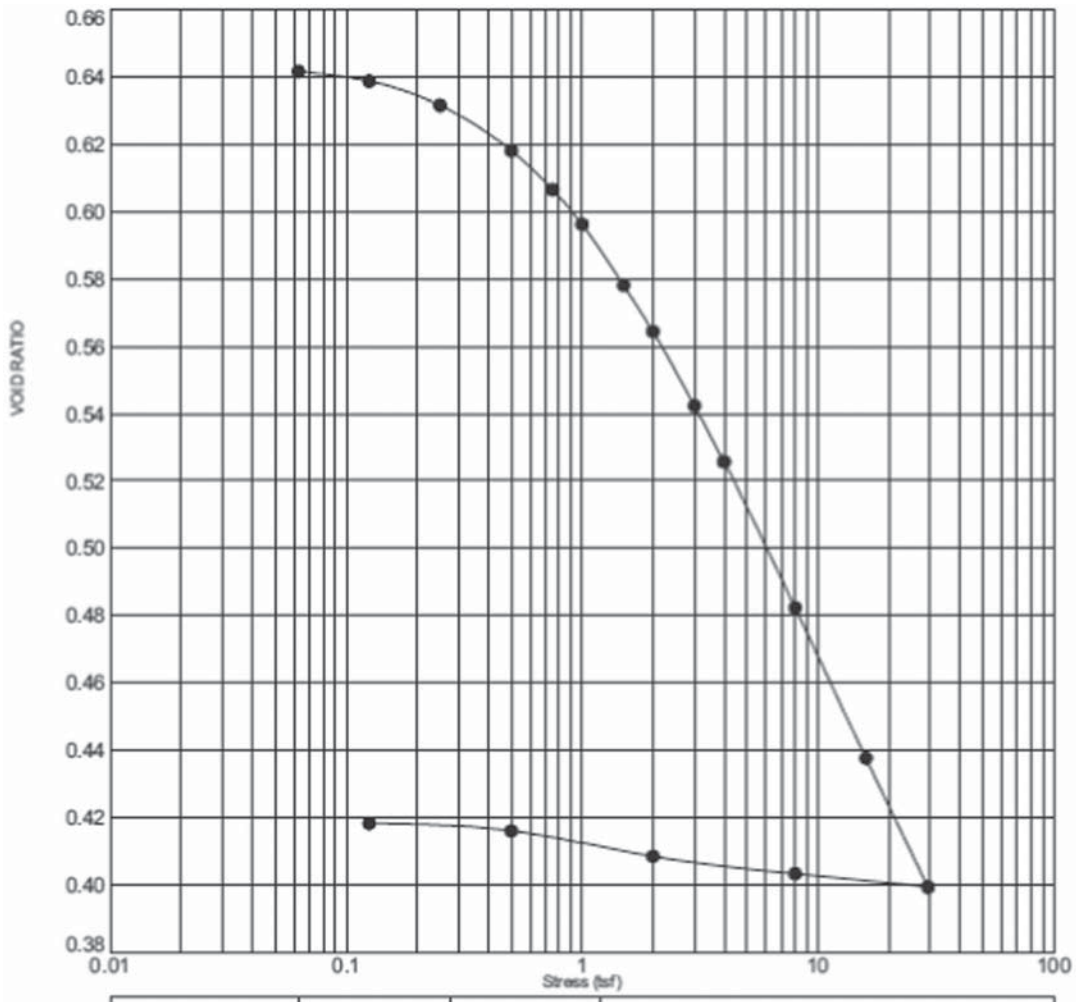

Boring	Sample	Depth	Soil Description
S2-CB-6	ST-2	25 - 25.5	Silty Loam A-6 (7)

Initial Wet Density (pcf)	Initial Dry Density (pcf)	Initial Moisture (%)	Final Dry Density (pcf)	Final Moisture (%)	Specific Gravity
122.6	98.9	24.0	114.8	16.1	2.607

Initial Void Ratio	Cc	Cr	Cv (in2/sec)	Po (tsf)	Pmax (tsf)
0.72	0.15	0.0093		0.9	1.4

Figure C.8 1-D consolidation test from the Koleen site performed by INDOT.

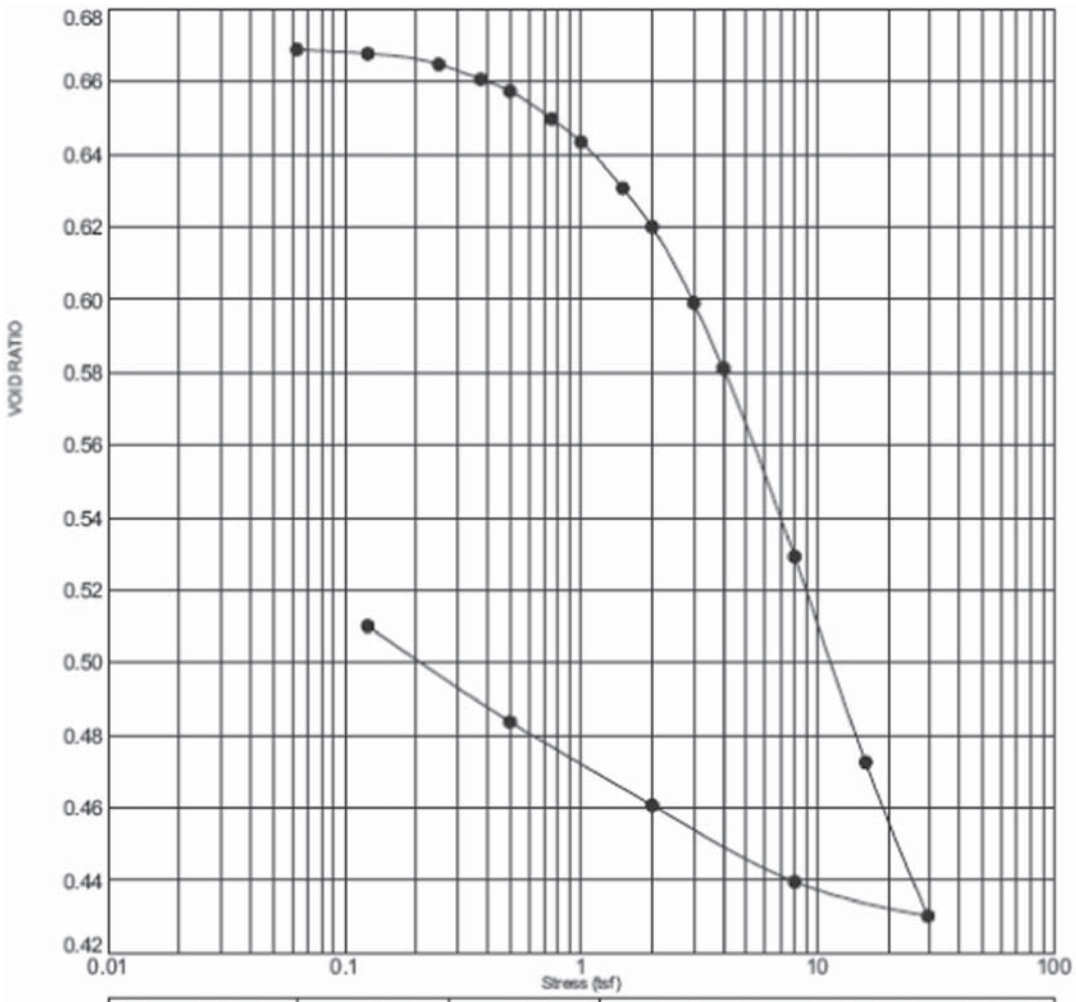

Boring	Sample	Depth	Soil Description
S2-RB-44	ST-2	31 - 33	Silty Clay Loam A-7-6 (22)

Initial Wet Density (pcf)	Initial Dry Density (pcf)	Initial Moisture (%)	Final Dry Density (pcf)	Final Moisture (%)	Specific Gravity
121.4	98.3	23.5	108.7	19.3	2.629

Initial Void Ratio	Cc	Cr	Cv (in2/sec)	Po (tsf)	Pmax (tsf)
0.62	0.18	0.039		1.2	2.1

Figure C.9 1-D consolidation test from the Koleen site performed by INDOT.

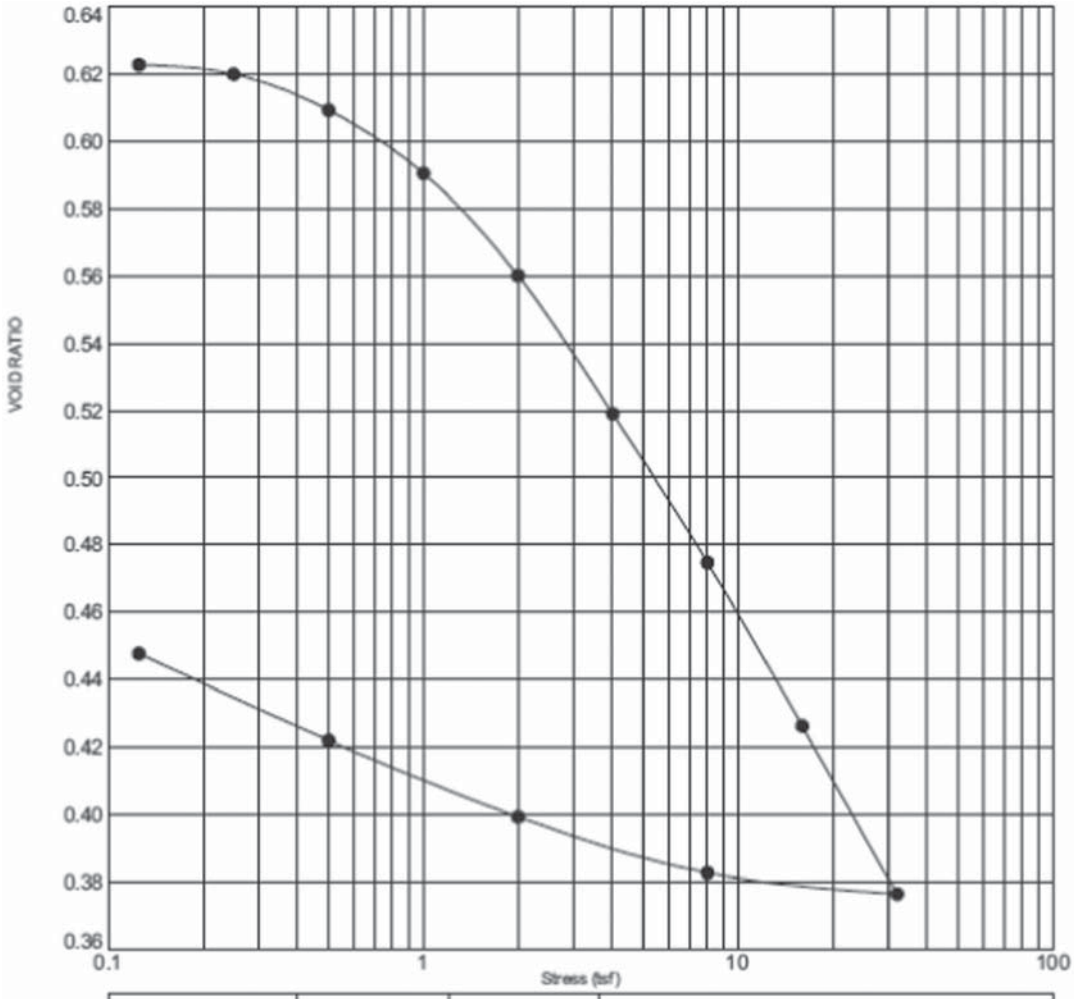

Boring	Sample	Depth	Soil Description
S2-RB-44	ST-3	41.5 - 42	Silty Clay Loam A-6 (24)

Initial Wet Density (pcf)	Initial Dry Density (pcf)	Initial Moisture (%)	Final Dry Density (pcf)	Final Moisture (%)	Specific Gravity
126.2	102.4	23.2	116.6	17.8	2.664

Initial Void Ratio	Cc	Cr	Cv (in2/sec)	Po (tsf)	Pmax (tsf)
0.62	0.16	0.031		1.5	1.9

Figure C.10 1-D consolidation test from the Koleen site performed by INDOT.

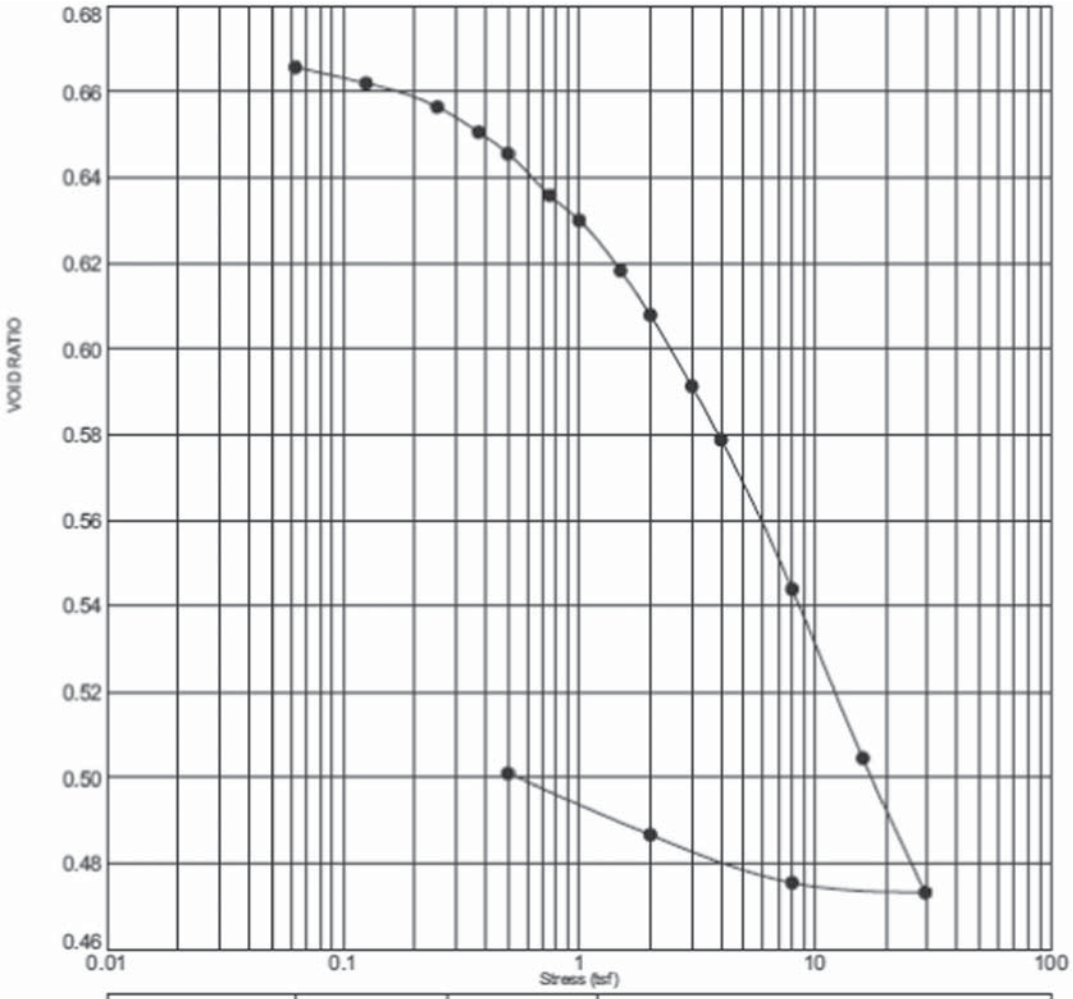

Boring	Sample	Depth	Soil Description
S2-RB-46	ST-4	38 - 40	Silty Clay Loam A-6 (18)

Initial Wet Density (pcf)	Initial Dry Density (pcf)	Initial Moisture (%)	Final Dry Density (pcf)	Final Moisture (%)	Specific Gravity
123.1	98.3	25.2	109.1	19.2	2.633

Initial Void Ratio	Cc	Cr	Cv (in2/sec)	Po (tsf)	Pmax (tsf)
0.62	0.13	0.017		1.2	1.7

Figure C.11 1-D consolidation test from the Koleen site performed by INDOT.

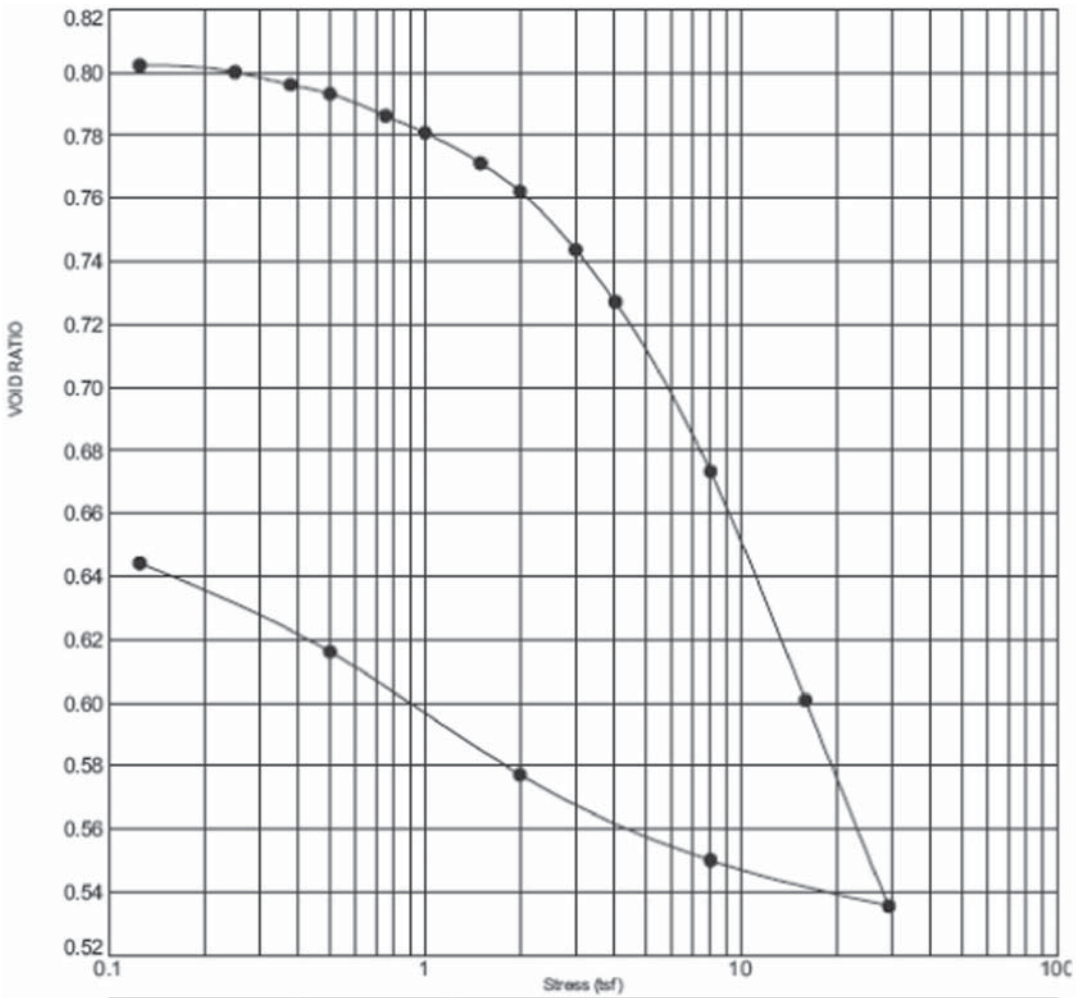

Boring	Sample	Depth	Soil Description
S2-RB-46	ST-5	48 - 50	Silty Clay A-7-6 (28)

Initial Wet Density (pcf)	Initial Dry Density (pcf)	Initial Moisture (%)	Final Dry Density (pcf)	Final Moisture (%)	Specific Gravity
117.9	91.7	28.6	100.3	24.4	2.641

Initial Void Ratio	Cc	Cr	Cv (in2/sec)	Po (tsf)	Pmax (tsf)
0.76	0.24	0.047		1.5	4

Figure C.12 1-D consolidation test from the Koleen site performed by INDOT.

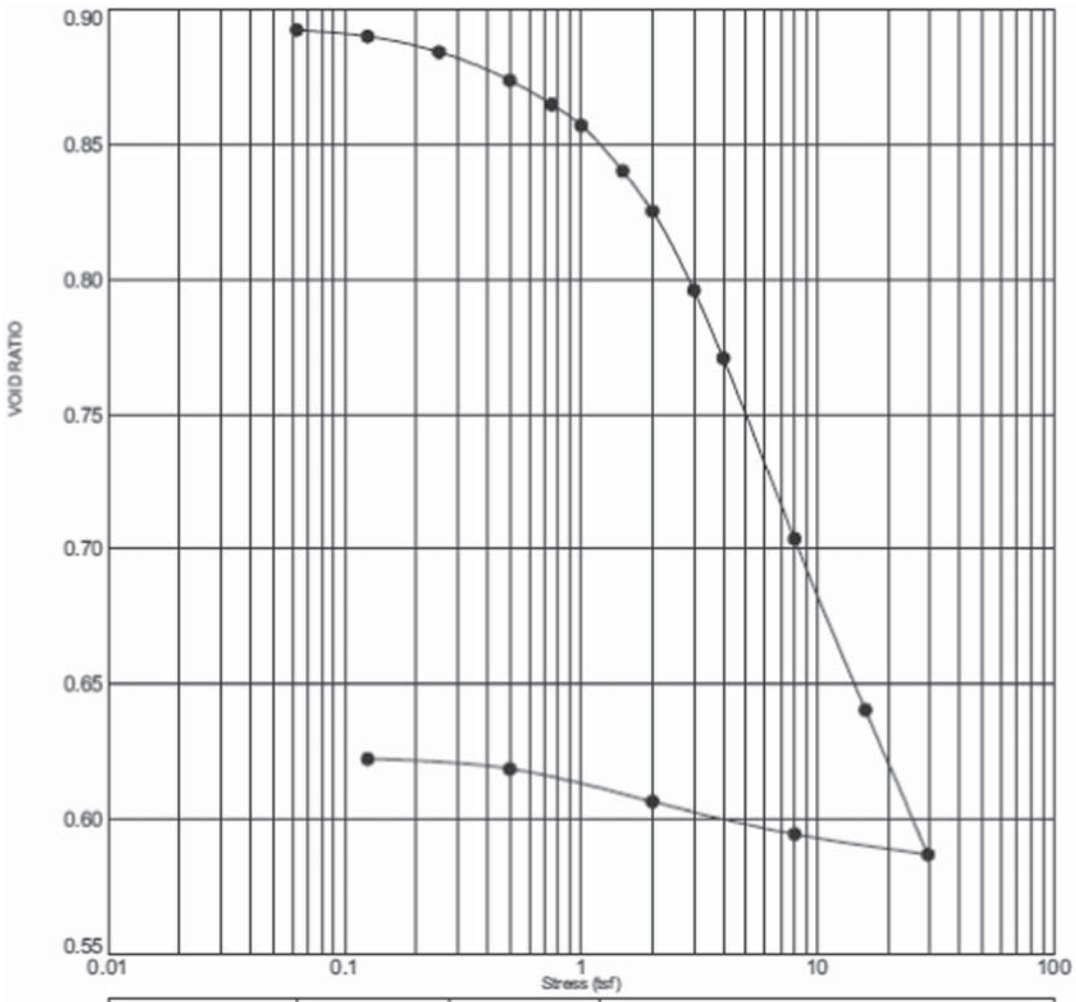

Boring	Sample	Depth	Soil Description
S2-RB-47	ST-1	21.5 - 22	Silty Loam A-7-6 (22)

Initial Wet Density (pcf)	Initial Dry Density (pcf)	Initial Moisture (%)	Final Dry Density (pcf)	Final Moisture (%)	Specific Gravity
115.8	87.5	32.3	102.1	23.4	2.655

Initial Void Ratio	Cc	Cr	Cv (in2/sec)	Po (tsf)	Pmax (tsf)
0.89	0.22	0.018		0.6	1.3

Figure C.13 1-D consolidation test from the Koleen site performed by INDOT.

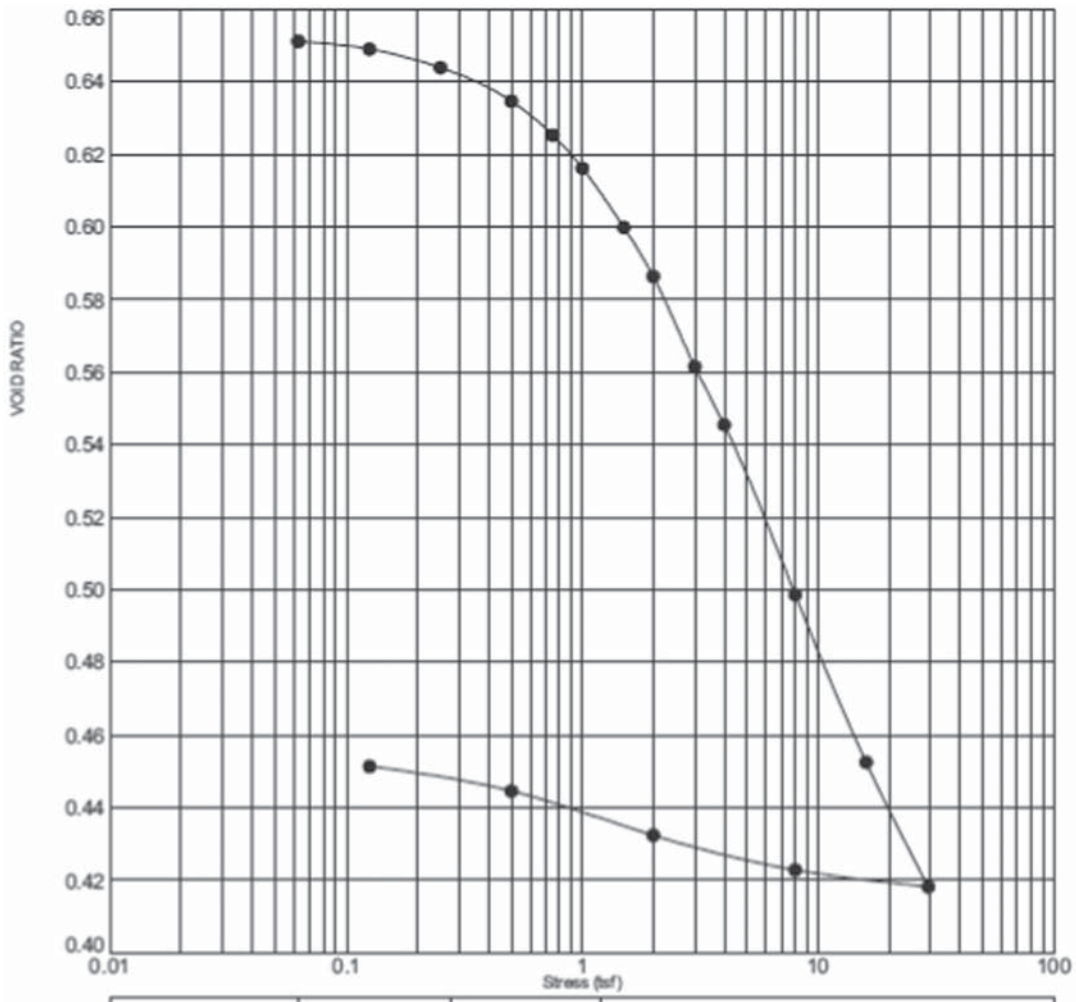

Boring	Sample	Depth	Soil Description
S2-RB-47	ST-3	36.5 - 38	Loam A-6 (4)

Initial Wet Density (pcf)	Initial Dry Density (pcf)	Initial Moisture (%)	Final Dry Density (pcf)	Final Moisture (%)	Specific Gravity
122.1	99.7	22.4	113.6	17.1	2.642

Initial Void Ratio	Cc	Cr	Cv (in2/sec)	Po (tsf)	Pmax (tsf)
0.65	0.15	0.015		1.1	1.2

Figure C.14 1-D consolidation test from the Koleen site performed by INDOT.

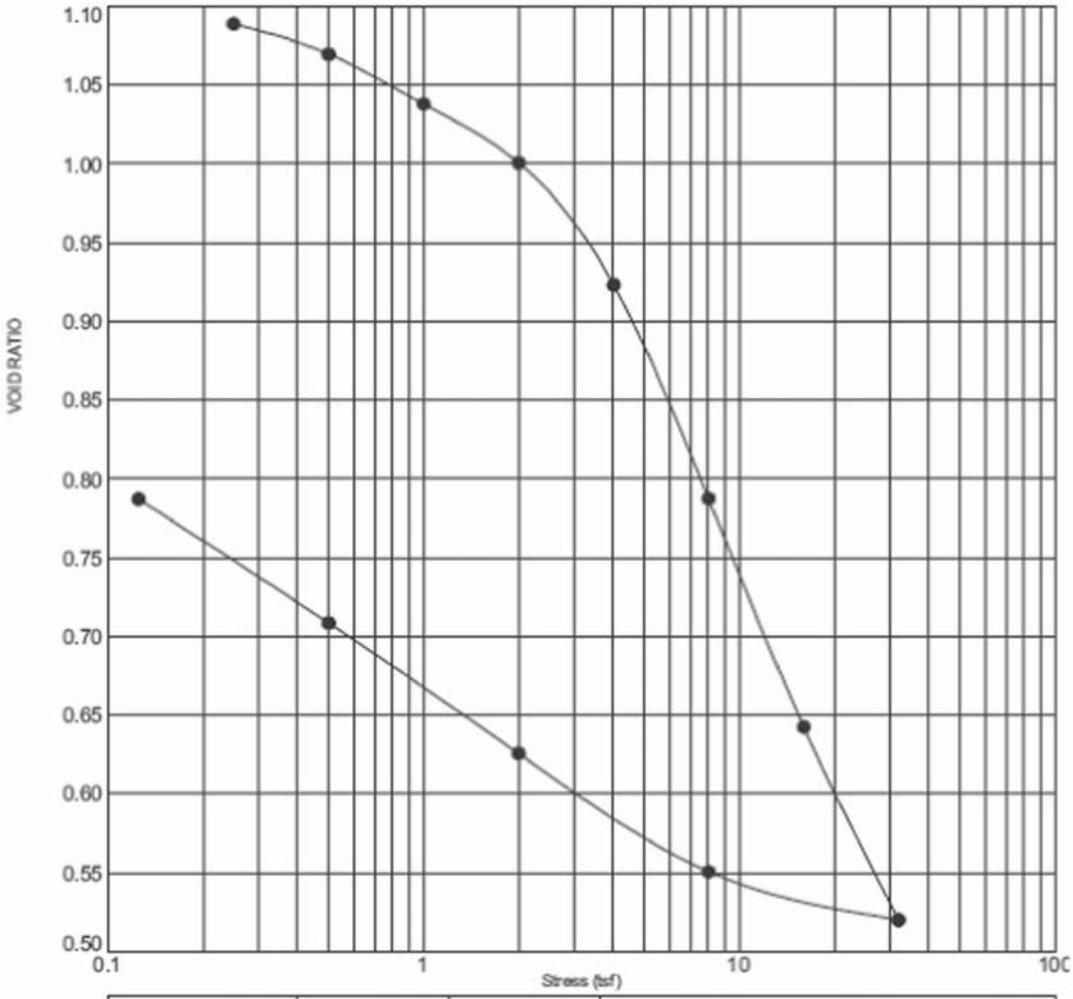

Boring	Sample	Depth	Soil Description
S2-RB-47	ST-4	46.5 - 47	Clay A-7-6 (49)

Initial Wet Density (pcf)	Initial Dry Density (pcf)	Initial Moisture (%)	Final Dry Density (pcf)	Final Moisture (%)	Specific Gravity
111.3	78.8	41.3	108.6	33.7	2.644

Initial Void Ratio	Cc	Cr	Cv (in2/sec)	Po (tsf)	Pmax (tsf)
1.09	0.47	0.085		1.2	3.2

Figure C.15 1-D consolidation test from the Koleen site performed by INDOT.

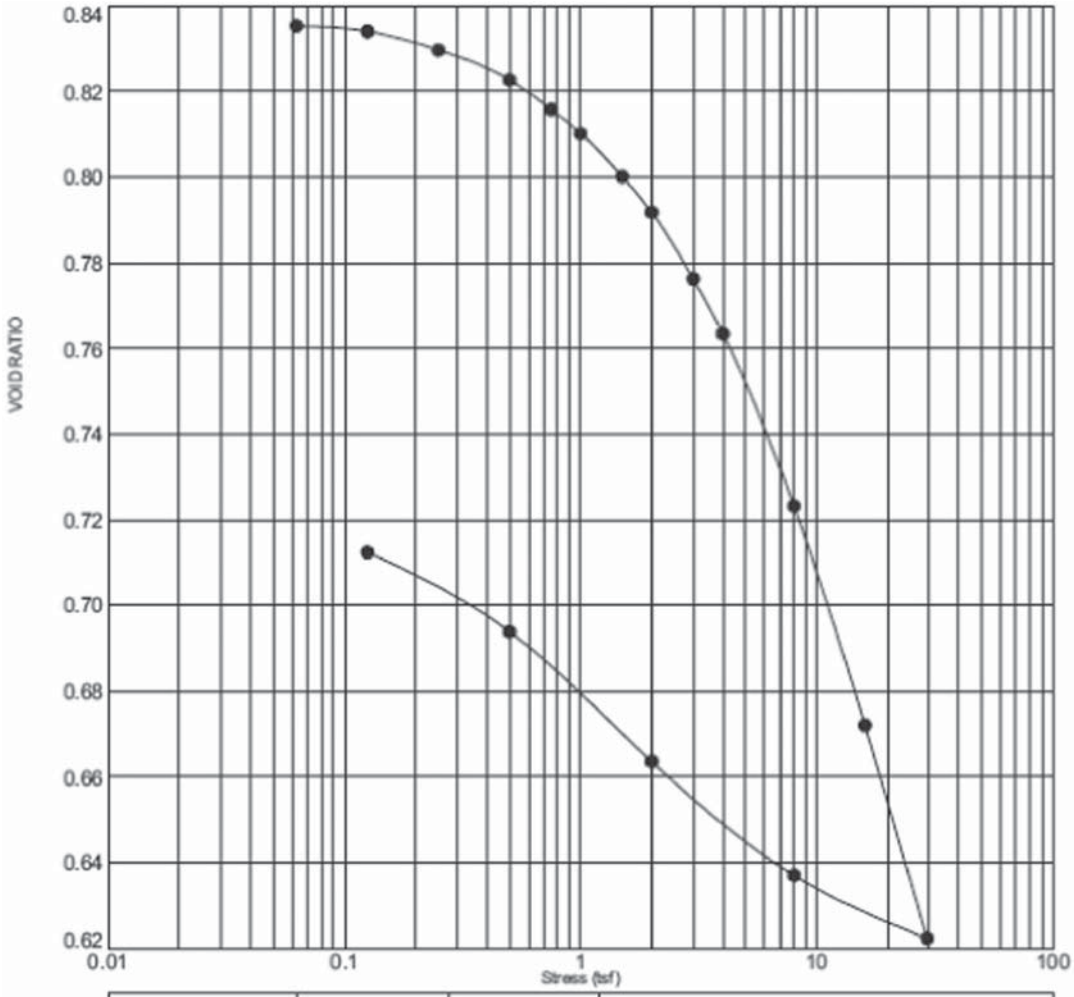

Boring	Sample	Depth	Soil Description
S2-RB-47	ST-5	56.5 - 57	Clay A-7-6 (36)

Initial Wet Density (pcf)	Initial Dry Density (pcf)	Initial Moisture (%)	Final Dry Density (pcf)	Final Moisture (%)	Specific Gravity
118.2	90.8	30.2	97.4	26.7	2.672

Initial Void Ratio	Cc	Cr	Cv (in2/sec)	Po (tsf)	Pmax (tsf)
0.84	0.18	0.039		1.6	3

Figure C.16 1-D consolidation test from the Koleen site performed by INDOT.

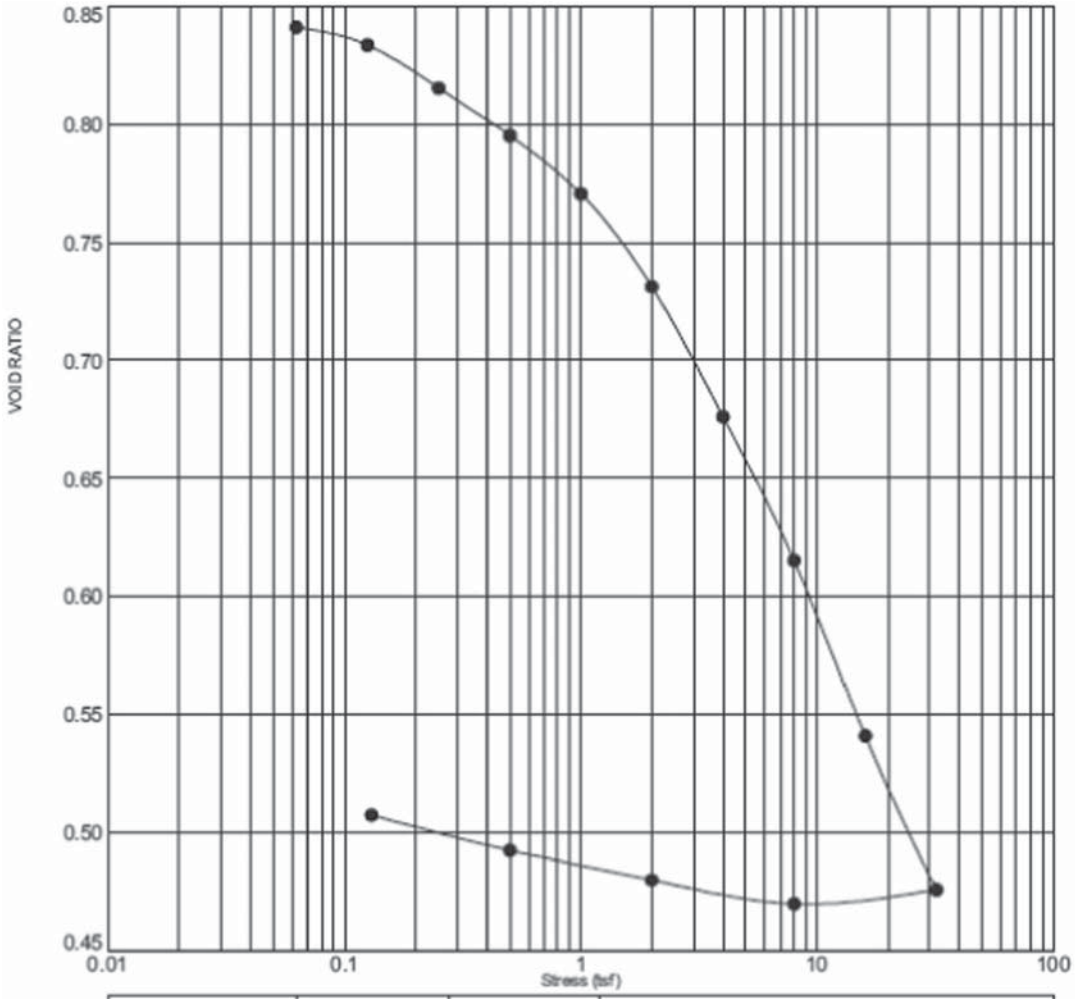

Boring	Sample	Depth	Soil Description
S2-RB-48	ST-3	31.5 - 32	Silt A-4 (9)

Initial Wet Density (pcf)	Initial Dry Density (pcf)	Initial Moisture (%)	Final Dry Density (pcf)	Final Moisture (%)	Specific Gravity
117.9	91.2	29.4	104.2	23.2	2.697

Initial Void Ratio	Cc	Cr	Cv (in2/sec)	Po (tsf)	Pmax (tsf)
0.85	0.22	0.021		0.9	1.6

Figure C.17 1-D consolidation test from the Koleen site performed by INDOT.

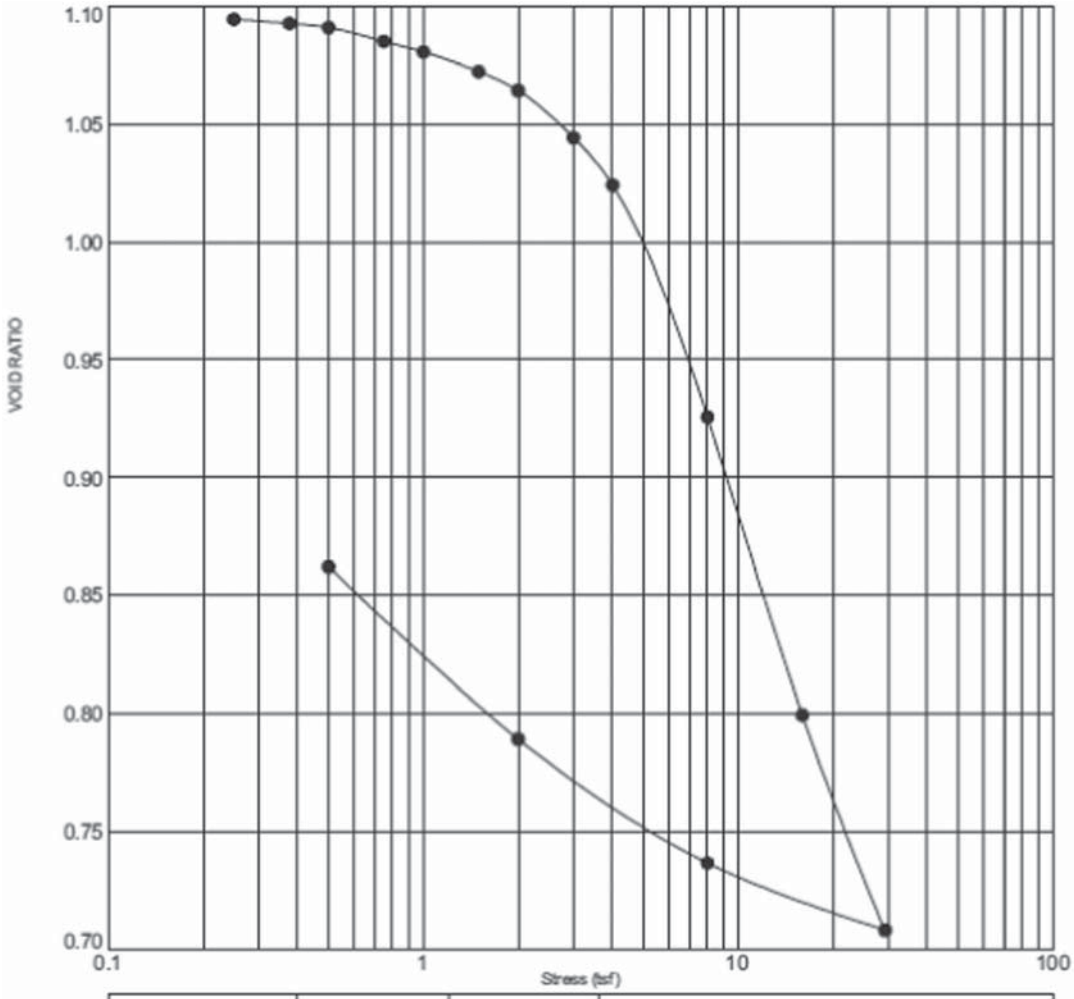

Boring	Sample	Depth	Soil Description
S2-S-3-11	ST-2	62.5 - 63	Silty Clay A-7-6 (41)

Initial Wet Density (pcf)	Initial Dry Density (pcf)	Initial Moisture (%)	Final Dry Density (pcf)	Final Moisture (%)	Specific Gravity
108.6	80.9	34.2	95.5	28.4	2.715

Initial Void Ratio	Cc	Cr	Cv (in2/sec)	Po (tsf)	Pmax (tsf)
1.00	0.4	0.087		2	4

Figure C.18 1-D consolidation test from the Koleen site performed by INDOT.

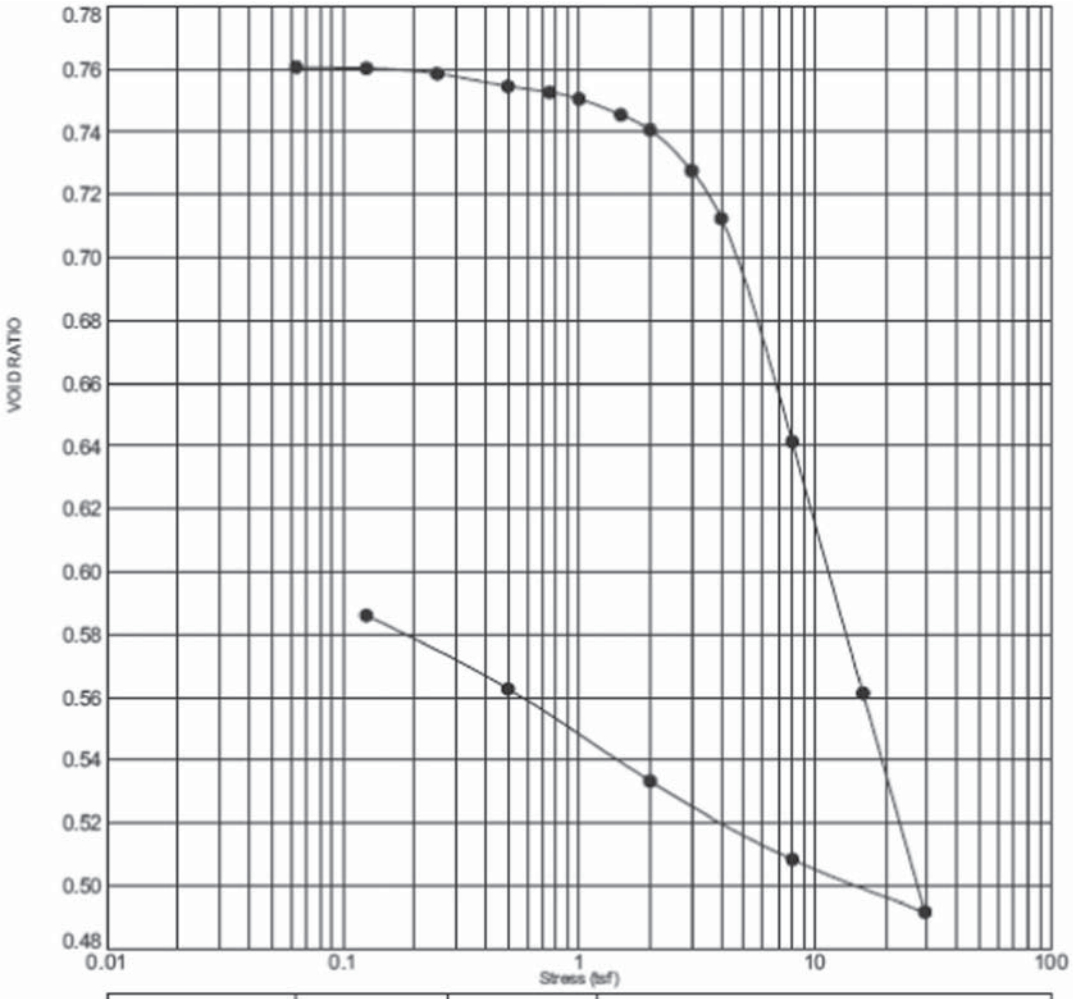

Boring	Sample	Depth	Soil Description
S2-ST-9	ST-7	38 - 40	Silty Clay A-7-6 (26)

Initial Wet Density (pcf)	Initial Dry Density (pcf)	Initial Moisture (%)	Final Dry Density (pcf)	Final Moisture (%)	Specific Gravity
119.7	95.7	25.1	106.2	19.8	

Initial Void Ratio	Cc	Cr	Cv (in2/sec)	Po (tsf)	Pmax (tsf)
0.76	0.27	0.043		1.2	3.7

Figure C.19 1-D consolidation test from the Koleen site performed by INDOT.

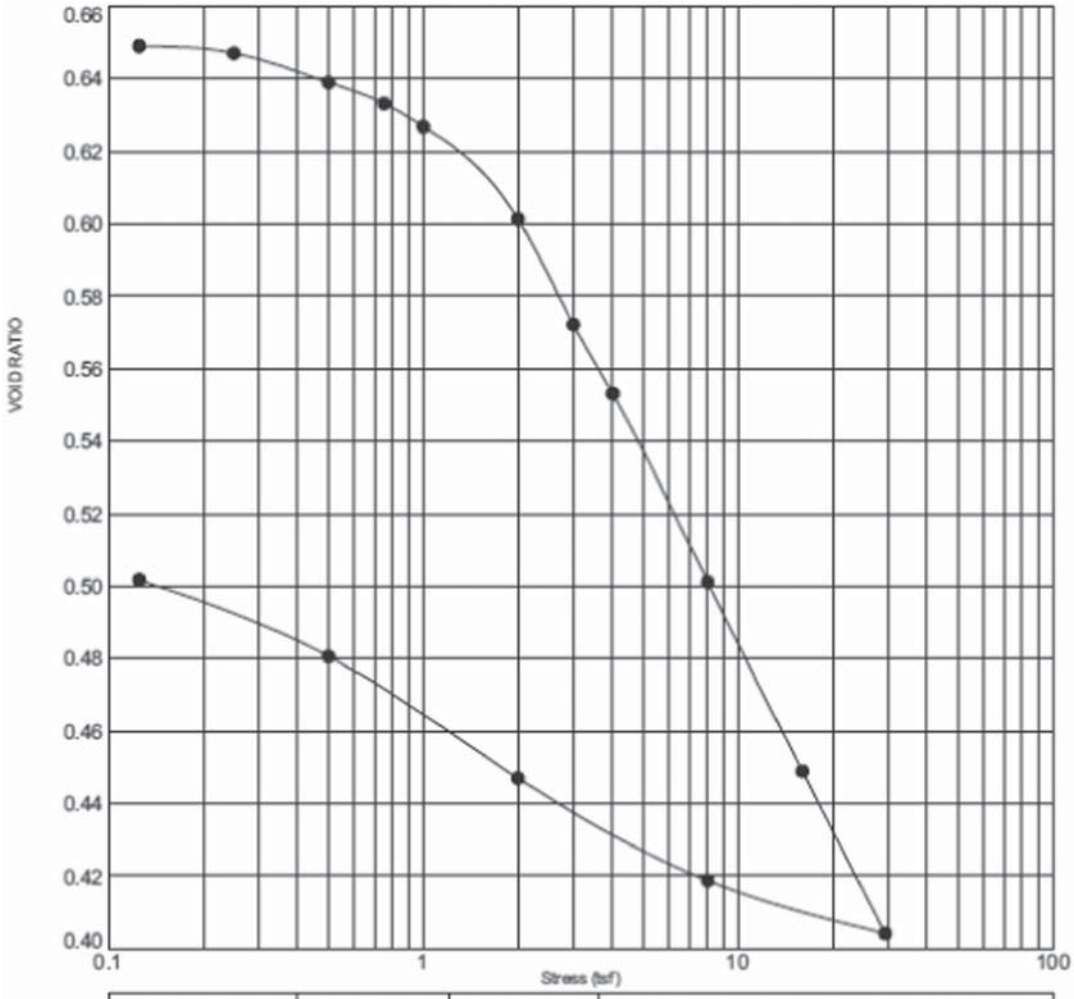

Boring	Sample	Depth	Soil Description
S2-ST-15A	ST-2	35 - 35.5	

Initial Wet Density (pcf)	Initial Dry Density (pcf)	Initial Moisture (%)	Final Dry Density (pcf)	Final Moisture (%)	Specific Gravity
123.9	100.1	23.8	110.0	19.0	2.647

Initial Void Ratio	Cc	Cr	Cv (in2/sec)	Po (tsf)	Pmax (tsf)
0.68	0.17	0.05		1	1.7

Figure C.20 1-D consolidation test from the Koleen site performed by INDOT.

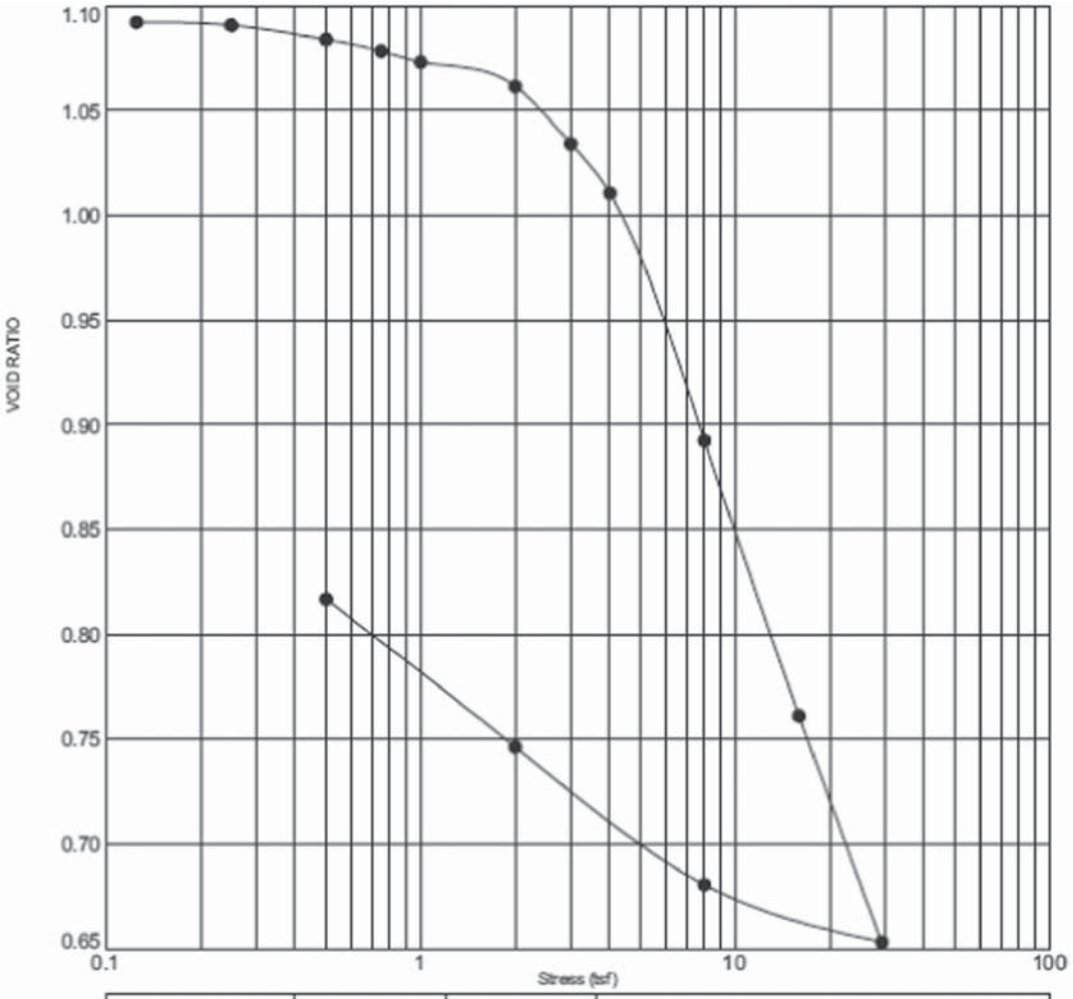

Boring	Sample	Depth	Soil Description
S2-ST-15A	ST-5	52 - 52.5	Clay A-7-6 (43)

Initial Wet Density (pcf)	Initial Dry Density (pcf)	Initial Moisture (%)	Final Dry Density (pcf)	Final Moisture (%)	Specific Gravity
109.3	78.0	40.2	87.8	32.7	2.615

Initial Void Ratio	Cc	Cr	Cv (in2/sec)	Po (tsf)	Pmax (tsf)
1.09	0.43	0.12		1.5	3.5

Figure C.21 1-D consolidation test from the Koleen site performed by INDOT.

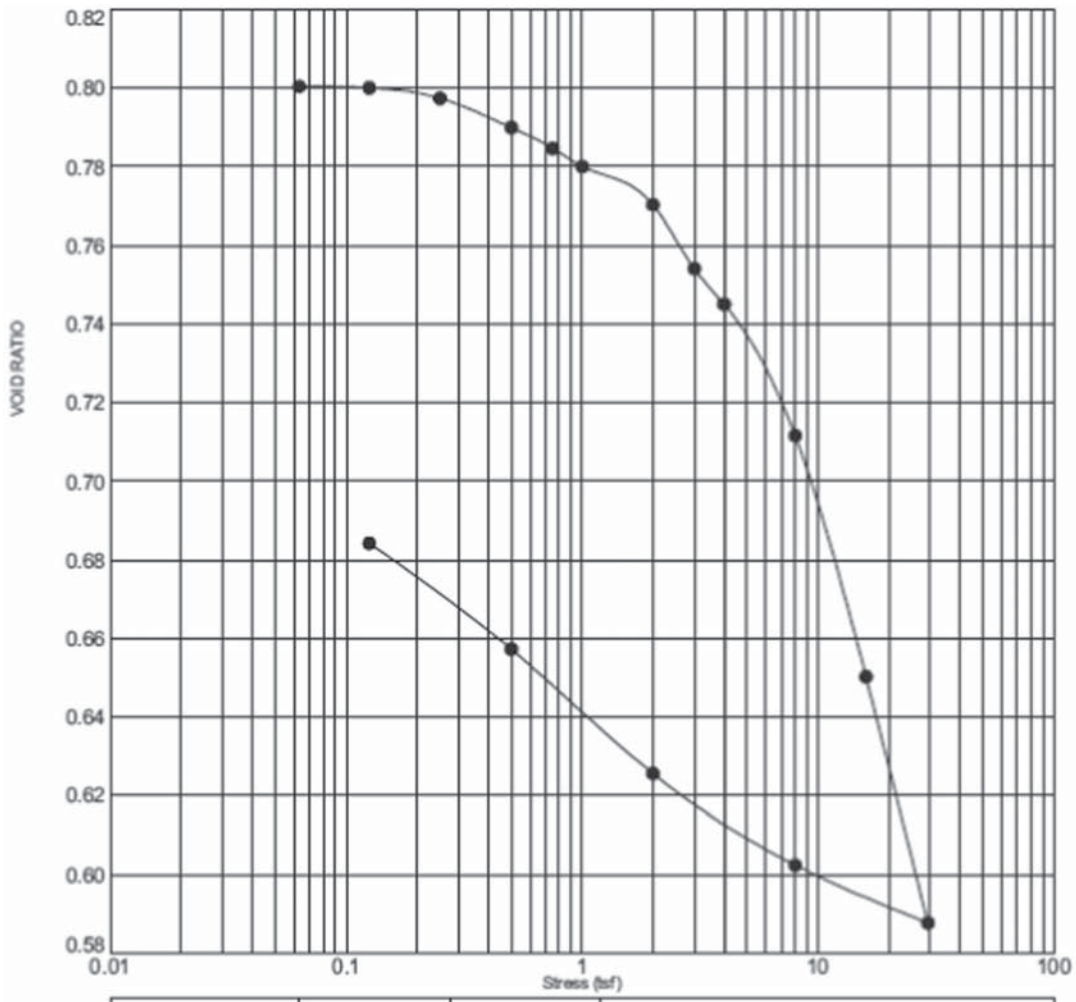

Boring	Sample	Depth	Soil Description
S2-ST-17	ST-10	56.5 - 57	Silty Clay Loam A-6 (15)

Initial Wet Density (pcf)	Initial Dry Density (pcf)	Initial Moisture (%)	Final Dry Density (pcf)	Final Moisture (%)	Specific Gravity
120.1	93.5	28.4	100.0	25.3	

Initial Void Ratio	Cc	Cr	Cv (in2/sec)	Po (tsf)	Pmax (tsf)
0.80	0.23	0.042		1.7	5

Figure C.22 1-D consolidation test from the Koleen site performed by INDOT.

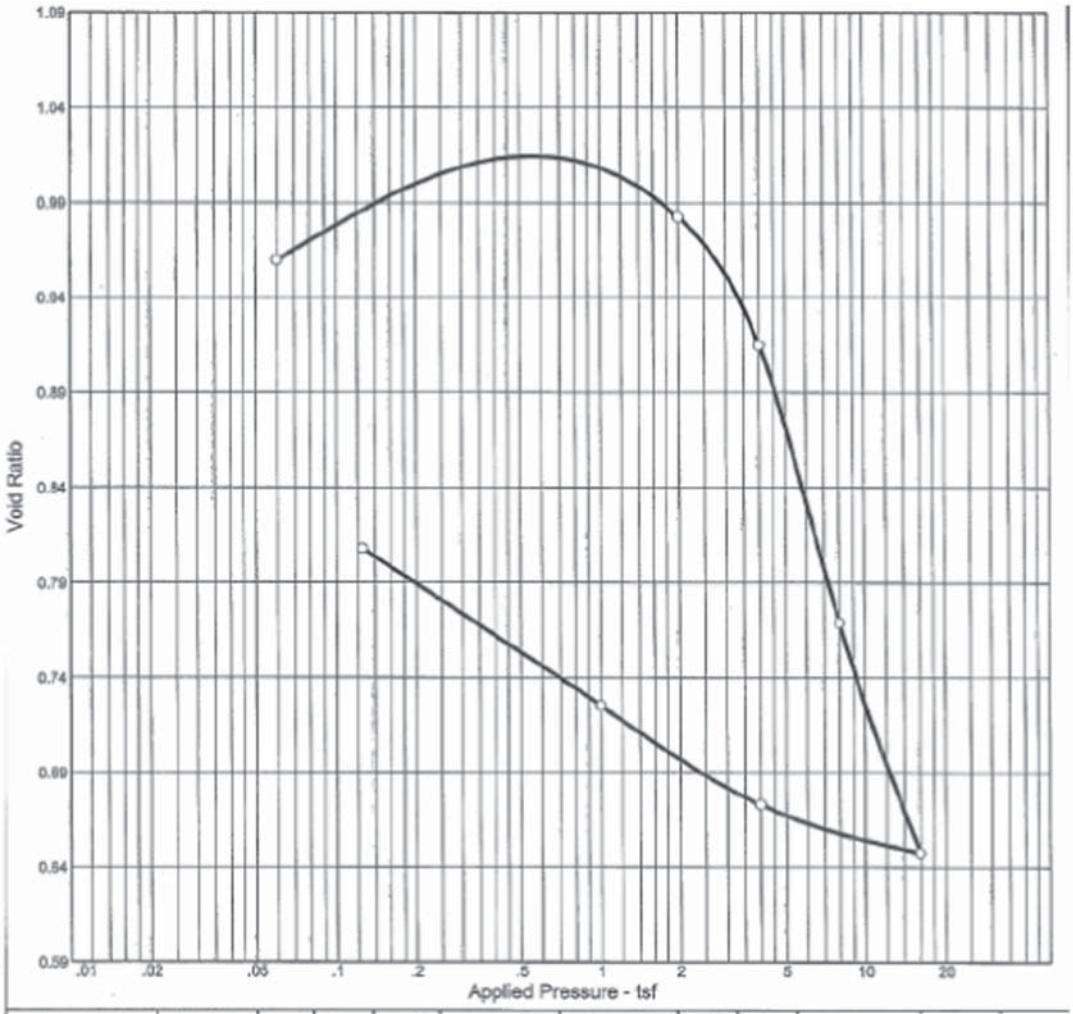

Natural		Dry Dens. (pcf)	LL	PI	Sp. Gr.	Overburden (tsf)	P_c (tsf)	C_c	C_r	Swell Press. (tsf)	Swell %	e_o
Sat.	Moist.											
97.2 %	36.8 %	82.8	47	25	2.66	0.7	3.0	0.45	0.09			1.006

MATERIAL DESCRIPTION	USCS	AASHTO
GRAY CLAY, MOIST - STIFF	CL	A-7-6(29)

Project No. N1125115 **Client:** ATC ASSOCIATES, INC

Project: INDOT - I-69

Source: S2-ST-9 **Elev./Depth:** 19'

Remarks:
Lab No. 4263
SWELLED

Figure C.23 1-D consolidation test from the Koleen site performed by INDOT.

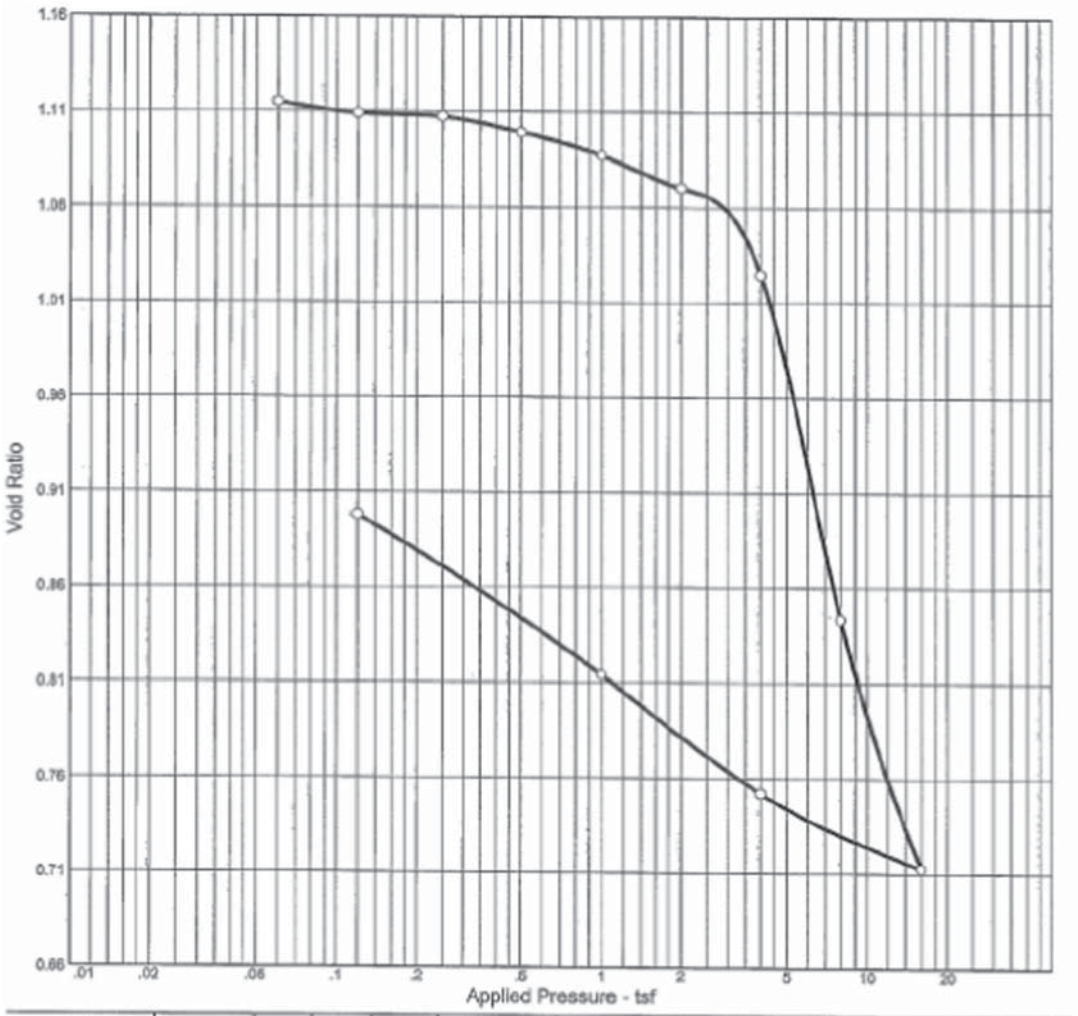

Natural Sat.	Natural Moist.	Dry Dens. (pcf)	LL	PI	Sp. Gr.	Overburden (tsf)	P_c (tsf)	C_c	C_r	Swell Press. (tsf)	Swell %	e_o
97.6 %	40.9 %	78.6	55	29	2.664	1.0	3.5	0.51	0.09			1.115

MATERIAL DESCRIPTION	USCS	AASHTO
GRAY CLAY, MOIST - STIFF	CH	A-7-6(34)

Project No. N1125115 **Client:** ATC ASSOCIATES, INC
Project: INDOT - I-69
Source: S2-ST-9 **Elev./Depth:** 33'

Remarks:
Lab No. 4264

Figure C.24 1-D consolidation test from the Koleen site performed by INDOT.

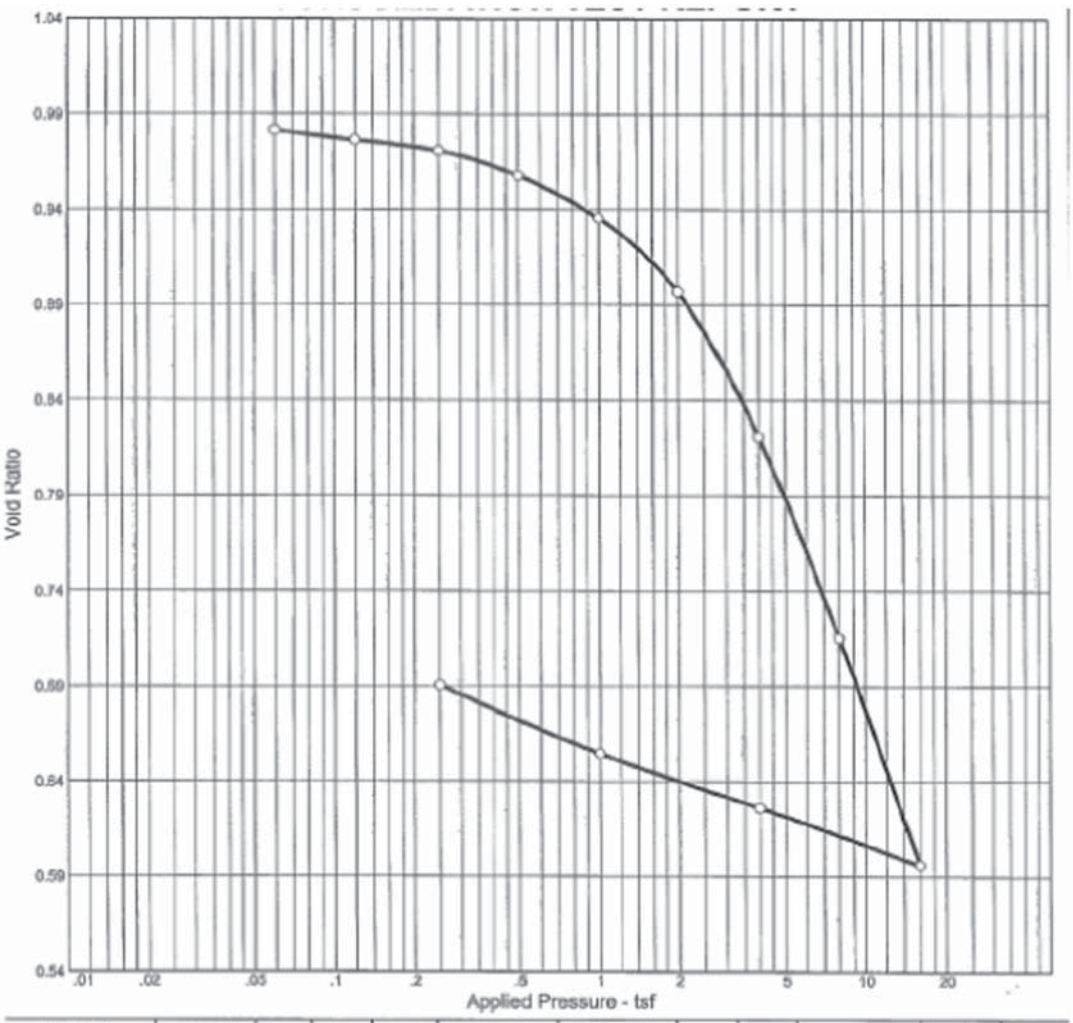

Natural Sat.	Natural Moist.	Dry Dens. (pcf)	LL	PI	Sp. Gr.	Overburden (tsf)	P_c (tsf)	C_c	C_r	Swell Press. (tsf)	Swell %	e_o
99.4 %	36.0 %	85.3	42	20	2.708	1.0	2.6	0.40	0.05			0.982

MATERIAL DESCRIPTION	USCS	AASHTO
BROWNISH GRAY SILTY CLAY, MOIST - STIFF	CL	A-7-6(22)

Project No. N1125115 **Client:** ATC ASSOCIATES, INC
Project: INDOT - I-69
Source: S2-ST-22 **Elev./Depth:** 32'
Remarks:
Lab No. 4369

Figure C.25 1-D consolidation test from the Koleen site performed by INDOT.

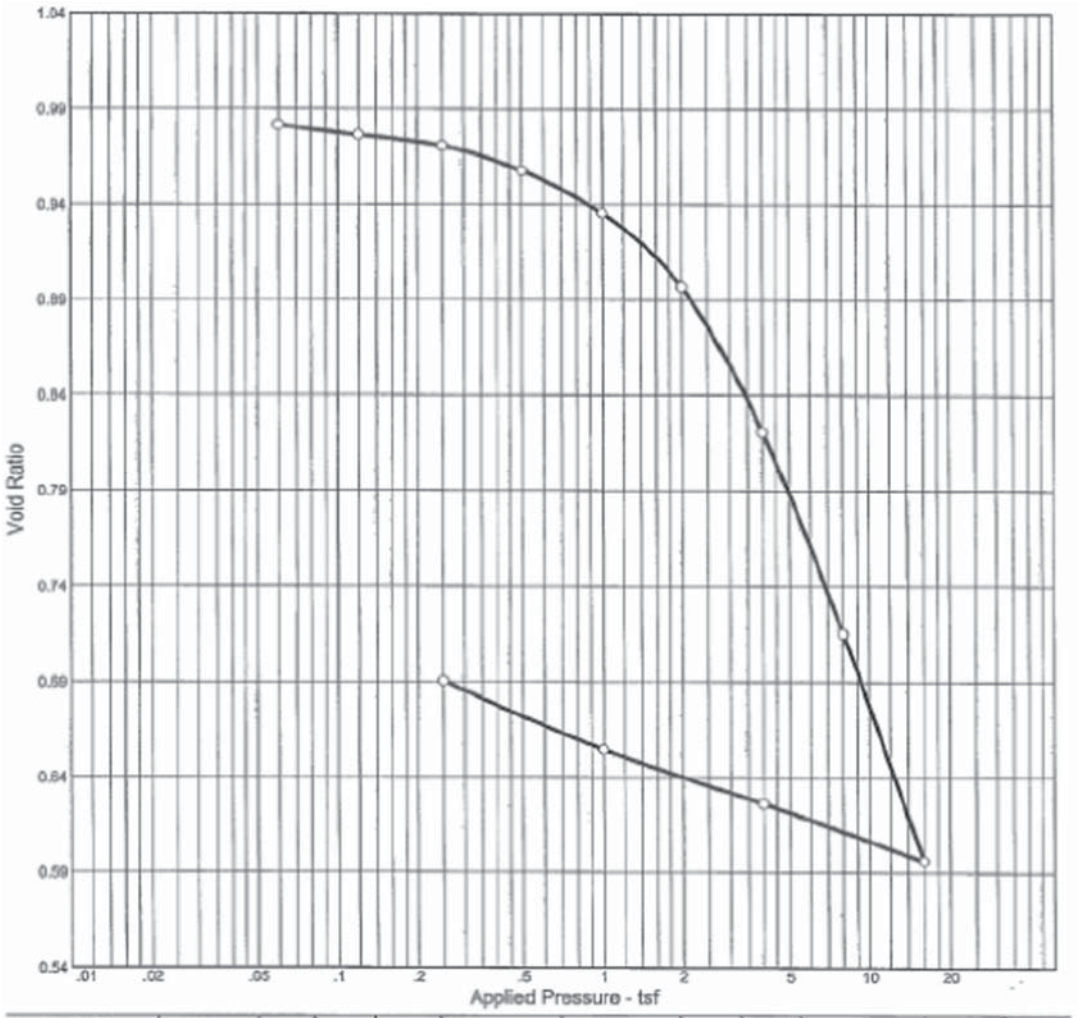

Natural Sat.	Natural Moist.	Dry Dens. (pcf)	LL	PI	Sp. Gr.	Overburden (tsf)	P_c (tsf)	C_C	C_r	Swell Press. (tsf)	Swell %	e_o
99.4 %	36.0 %	85.3	42	20	2.708	1.0	2.6	0.40	0.05			0.982

MATERIAL DESCRIPTION	USCS	AASHTO
BROWNISH GRAY SILTY CLAY, MOIST - STIFF	CL	A-7-6(22)

Project No. N1125115 **Client:** ATC ASSOCIATES, INC
Project: INDOT - I-69
Source: S2-ST-22 **Elev./Depth:** 32'

Remarks:
Lab No. 4369

Figure C.26 1-D consolidation test from the Koleen site performed by INDOT.

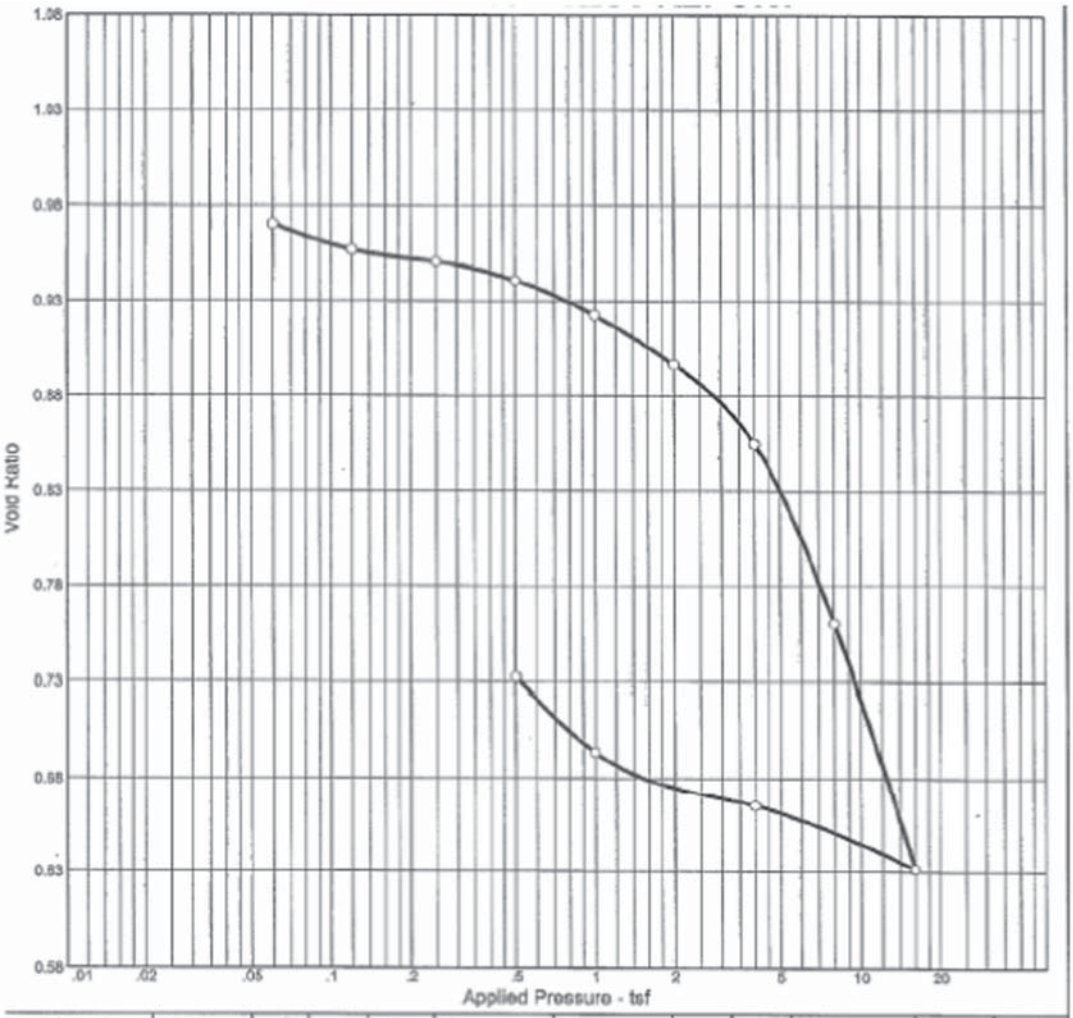

Natural Sat.	Natural Moist.	Dry Dens. (pcf)	LL	PI	Sp. Gr.	Overburden (tsf)	P_c (tsf)	C_c	C_r	Swell Press. (tsf)	Swell %	e_o
96.5 %	34.3 %	86.4	42	20	2.728	1.6	4.5	0.43	0.08			0.971

MATERIAL DESCRIPTION	USCS	AASHTO
BROWNISH GRAY SILTY CLAY	CL	A-7-6(22)

Project No. N1125115 **Client:** ATC ASSOCIATES, INC

Project: INDOT - I-69

Source: S2-ST-22 **Elev./Depth:** 52'

Remarks:
Lab No. 4365

Figure C.27 1-D consolidation test from the Koleen site performed by INDOT.

APPENDIX D. FIELD AND LABORATORY TESTING RESULTS

TABLE D.1
SPT, CPT and laboratory testing results from Flora Maintenance Unit boring 1

Depth (m)	Soil Type	$N_{1,60}$	$q_{c,1}$ (kPa)	w_c (%)	LL (%)	PL (%)	Sand (%)	Silt (%)	Clay (%)
1.07–1.52	CL	15.5	428.9	29.1	45.1	27.1	40.0	33.0	27.0
2.59–3.05	SP-SC	22.0	6375.2	20.9	N/A	N/A	92.2	6.4	1.4
4.12–4.57	SP	31.5	19976.6	16.7	N/A	N/A	97.8	~1	~1

TABLE D.2
SPT, CPT and laboratory testing results from Flora Maintenance Unit boring 2

Depth (m)	Soil Type	$N_{1,60}$	$q_{c,1}$ (kPa)	w_c (%)	LL (%)	PL (%)	Sand (%)	Silt (%)	Clay (%)
1.07–1.52	CL	13.0	469.4	17.0	29.1	17.9	52.1	30.8	17.1
2.59–3.05	SP	13.7	2689.1	19.8	N/A	N/A	99.5	~0	~0
4.12–4.57	SP	25.8	2333.6	21.3	N/A	N/A	97.7	~1	~1

TABLE D.3
SPT, CPT and laboratory testing results from Flora Maintenance Unit boring 3

Depth (m)	Soil Type	$N_{1,60}$	$q_{c,1}$ (kPa)	w_c (%)	LL (%)	PL (%)	Sand (%)	Silt (%)	Clay (%)
1.07–1.52	SC-SM	18.5	1269.5	17.5	23.6	18.5	54.6	30.1	15.3
2.59–3.05	SP-SC	13.7	3602.8	21.6	28.7	21.6	94.1	~3	~3
4.12–4.57	SP	14.7	2525.3	17.6	N/A	N/A	95.2	~2.5	~2.5

TABLE D.4
SPT, CPT and laboratory testing results from Flora Maintenance Unit boring 4

Depth (m)	Soil Type	$N_{1,60}$	$q_{c,1}$ (kPa)	w_c (%)	LL (%)	PL (%)	Sand (%)	Silt (%)	Clay (%)
1.07–1.52	SC-SM	14.8	222.8	13.5	23.9	18.0	64.6	25.6	9.8
2.59–3.05	SP-SC	13.7	1355.4	21.6	N/A	N/A	89.8	7.3	2.9
4.12–4.57	SC-SM	13.5	2570.0	20.9	N/A	N/A	83.2	12.5	4.3

TABLE D.5
SPT, CPT and laboratory testing results from Lafayette Maintenance Unit boring 1

Depth (m)	Soil Type	$N_{1,60}$	$q_{c,1}$ (kPa)	w_c (%)	LL (%)	PL (%)	Gravel (%)	Sand (%)	Silt (%)	Clay (%)
1.07–1.52	CL	25.2	3623.5	16.0	46.7	25.7	N/A	45.0	28.0	27.0
2.59–3.05	SP-SC	9.1	991.7	6.8	N/A	N/A	N/A	89.6	~5	~5
4.12–4.57	SP-SC	19.9	1857.8	5.8	N/A	N/A	26.4	61.7	8.0	3.9
5.64–6.10	SP-SC	26.8	N/A	3.9	N/A	N/A	N/A	91.1	8.0	0.9
7.16–7.62	CL-ML	21.1	N/A	23.4	21.8	16.8	N/A	10.7	78.1	11.2
8.69–9.15	ML	50.1	N/A	20.5	NP	NP	N/A	46.6	49.1	4.2

TABLE D.6
SPT, CPT and laboratory testing results from Frankfort Maintenance Unit boring 1

Depth (m)	Soil Type	$N_{1,60}$	$q_{c,1}$ (kPa)	w_c (%)	LL (%)	PL (%)	Gravel (%)	Sand (%)	Silt (%)	Clay (%)
1.07–1.52	CL	13.7	1698.0	26.5	34.7	13.7	N/A	35.5	52.0	12.5
2.59–3.05	SC-SM	16.8	3423.5	11.0	15.5	11.0	N/A	52.7	41.0	6.3
4.12–4.57	ML	24.0	4789.2	18.2	19.1	17.0	N/A	31.0	61.7	7.3
5.64–6.10	SW-SM	30.3	28744.7	15.4	NP	NP	9.9	78.3	10.5	1.3

TABLE D.7
SPT, CPT and laboratory testing results from Frankfort Maintenance Unit boring 3

Depth (m)	Soil Type	$N_{1,60}$	$q_{c,1}$ (kPa)	w_c (%)	LL (%)	PL (%)	Gravel (%)	Sand (%)	Silt (%)	Clay (%)
1.07–1.52	SM	26.1	4148.0	12.7	NP	NP	N/A	54.3	40.5	5.2
2.59–3.05	SP-SC	19.1	17119.1	16.8	19.2	12.3	19.3	70.5	8.4	1.8
4.12–4.57	SM	33.1	N/A	20.4	NP	NP	N/A	53.1	44.5	2.4

TABLE D.8
SPT, CPT and laboratory testing results from Frankfort Maintenance Unit boring 4

Depth (m)	Soil Type	$N_{1,60}$	$q_{c,1}$ (kPa)	w_c (%)	LL (%)	PL (%)	Sand (%)	Silt (%)	Clay (%)
1.07–1.52	SC-SM	19.6	3382.6	13.6	18.5	12.0	51.9	40.7	7.4
2.59–3.05	SM	50.1	49304.7	8.5	17.6	N/A	51.7	41.0	7.3
4.12–4.57	SM	23.4	N/A	16.2	NP	NP	68.0	26.7	5.3

TABLE D.9
SPT, CPT and laboratory testing results from Frankfort Maintenance Unit boring 5

Depth (m)	Soil Type	$N_{1,60}$	$q_{c,1}$ (kPa)	w_c (%)	LL (%)	PL (%)	Gravel (%)	Sand (%)	Silt (%)	Clay (%)
1.07–1.52	SC-SM	13.0	2327.0	14.6	19.2	14.7	N/A	54.1	36.7	9.2
2.59–3.05	SM	39.8	27870.8	11.7	14.8	N/A	17.6	55.9	22.5	4.0
4.12–4.57	SM	33.1	N/A	23.4	15.5	N/A	N/A	64.6	33.4	2.0

TABLE D.10
SPT, CPT and laboratory testing results from Frankfort Maintenance Unit boring 6

Depth (m)	Soil Type	$N_{1,60}$	$q_{c,1}$ (kPa)	w_c (%)	LL (%)	PL (%)	Gravel (%)	Sand (%)	Silt (%)	Clay (%)
1.07–1.52	SM	36.9	1845.8	18.7	20.3	17.6	3.1	56.1	33.8	7.0
2.59–3.05	SM	58.9	17848.0	12.9	15.1	N/A	N/A	71.7	25.1	3.2
4.12–4.57	ML	43.8	N/A	12.1	11.4	N/A	N/A	47.9	44.4	7.7

TABLE D.11
SPT, CPT and laboratory testing results from Frankfort Maintenance Unit boring 7

Depth (m)	Soil Type	$N_{1,60}$	$q_{c,1}$ (kPa)	w_c (%)	LL (%)	PL (%)	Gravel (%)	Sand (%)	Silt (%)	Clay (%)
1.07–1.52	CL	18.2	1829.9	15.3	25.4	16.8	N/A	48.0	41.3	10.7
2.59–3.05	CL-ML	13.8	2485.2	19.1	21.6	16.3	5.1	42.1	41.9	10.9
4.12–4.57	CL-ML	46.9	20129.7	14.4	21.2	15.6	N/A	43.1	46.6	10.3

TABLE D.12
SPT, CPT and laboratory testing results from Frankfort Maintenance Unit boring 8

Depth (m)	Soil Type	$N_{1,60}$	$q_{c,1}$ (kPa)	w_c (%)	LL (%)	PL (%)	Gravel (%)	Sand (%)	Silt (%)	Clay (%)
1.07–1.52	CL	18.2	2262.0	21.4	28.0	19.7	N/A	14.7	68.4	16.9
2.59–3.05	CL	16.9	3176.8	18.4	27.9	20.7	N/A	47.6	42.3	10.1
4.12–4.57	CL-ML	59.6	12093.6	13.0	19.6	15.8	1.5	42.8	47.9	7.8
5.64–6.10	SM	16.4	2557.3	13.4	17.3	14.0	3.5	49.7	40.6	6.2

TABLE D.13
SPT, CPT and laboratory testing results from Romney Maintenance Unit boring 1

Depth (m)	Soil Type	$N_{1,60}$	$q_{c,1}$ (kPa)	w_c (%)	LL (%)	PL (%)	Gravel (%)	Sand (%)	Silt (%)	Clay (%)
1.07–1.52	SP-SC	30.4	1117.0	4.5	N/A	N/A	24.1	69.1	~3.5	~3.5
2.59–3.05	SW-SC	45.3	6126.0	4.7	N/A	N/A	35.3	55.5	~4.5	~4.5
4.12–4.57	ML	18.6	2624.7	21.7	NP	NP	N/A	31.2	66.2	2.6
5.64–6.10	SM	14.0	2548.6	22.2	NP	NP	N/A	77.4	21.7	0.9

TABLE D.14
SPT, CPT and laboratory testing results from Romney Maintenance Unit boring 2

Depth (m)	Soil Type	$N_{1,60}$	$q_{c,1}$ (kPa)	w_c (%)	LL (%)	PL (%)	Gravel (%)	Sand (%)	Silt (%)	Clay (%)
1.07–1.52	GW	42.8	21710.5	6.6	N/A	N/A	52.0	45.7	~1	~1
2.59–3.05	ML	16.8	20630.8	22.4	NP	NP	N/A	4.1	88.4	7.5
4.12–4.57	SM	20.9	11304.8	20.6	NP	NP	N/A	75.1	23.4	1.5
5.64–6.10	ML	16.0	10328.5	22.0	NP	NP	0.5	31.5	64.5	3.5
7.16–7.62	ML	38.1	16033.1	15.7	NP	NP	N/A	30.7	65.7	3.6

TABLE D.15
SPT, CPT and laboratory testing results from Romney Maintenance Unit boring 3

Depth (m)	Soil Type	$N_{1,60}$	$q_{c,1}$ (kPa)	w_c (%)	LL (%)	PL (%)	Gravel (%)	Sand (%)	Silt (%)	Clay (%)
1.07–1.52	SP-SM	50.0	11009.3	5.1	NP	NP	28.8	61.0	9.1	1.1
2.59–3.05	SM	25.0	6874.5	15.2	NP	NP	N/A	66.0	32.2	1.8
4.12–4.57	SM	22.9	5268.3	20.3	NP	NP	N/A	65.4	32.8	1.8
5.64–6.10	ML	19.9	1549.7	20.9	NP	NP	N/A	39.6	55.7	4.7

TABLE D.16
SPT, CPT and laboratory testing results from Romney Maintenance Unit boring 4

Depth (m)	Soil Type	$N_{1,60}$	$q_{c,1}$ (kPa)	w_c (%)	LL (%)	PL (%)	Gravel (%)	Sand (%)	Silt (%)	Clay (%)
1.07–1.52	SP-SM	34.8	23318.7	5.3	NP	NP	28.9	63.8	~3.5	~3.5
2.59–3.05	SM	20.6	23927.8	9.4	NP	NP	N/A	59.5	37.6	2.9
4.12–4.57	SM	21.5	19459.4	19.4	NP	NP	0.3	58.8	38.0	2.9
5.64–6.10	SM	19.9	12091.2	27.3	NP	NP	N/A	63.4	34.0	2.6

TABLE D.17
SPT, CPT and laboratory testing results from Romney Maintenance Unit boring 5

Depth (m)	Soil Type	$N_{1,60}$	$q_{c,1}$ (kPa)	w_c (%)	LL (%)	PL (%)	Gravel (%)	Sand (%)	Silt (%)	Clay (%)
1.07–1.52	SP-SM	45.6	16206.0	4.9	NP	NP	25.0	68.6	~3	~3
2.59–3.05	ML	29.6	14529.1	21.5	NP	NP	11.0	19.8	65.2	4.0
4.12–4.57	SM	25.8	14399.9	19.5	NP	NP	N/A	63.8	34.3	1.9
5.64–6.10	ML	24.7	20377.3	21.9	NP	NP	N/A	8.5	84.3	7.2

TABLE D.18
SPT, CPT and laboratory testing results from Romney Maintenance Unit boring 6

Depth (m)	Soil Type	$N_{1,60}$	$q_{c,1}$ (kPa)	w_c (%)	LL (%)	PL (%)	Gravel (%)	Sand (%)	Silt (%)	Clay (%)
1.07–1.52	SP-SM	21.7	2314.2	5.6	NP	NP	17.3	73.5	~4.5	~4.5
2.59–3.05	SM	25.0	53666.2	7.6	NP	NP	37.9	48.8	11.3	2.0
4.12–4.57	SM	21.5	20968.7	20.0	NP	NP	N/A	66.1	32.6	1.3
5.64–6.10	ML	21.1	12318.4	23.3	NP	NP	N/A	28.6	68.7	2.7

TABLE D.19
SPT, CPT and laboratory testing results from Koleen site boring 1

Depth (m)	Soil Type	$N_{1,60}$	$q_{c,1}$ (kPa)
1.07–1.52	CL	20.5	7619.1
2.59–3.05	CL	8.7	2199.8
4.12–4.57	CL	8.4	618.6
5.64–6.10	CL	10.2	621.7
7.16–7.62	CL	3.2	721.3
8.69–9.15	CL	5.8	N/A

TABLE D.20
SPT, CPT and laboratory testing results from Koleen site boring 2

Depth (m)	Soil Type	$N_{1,60}$	$q_{c,1}$ (kPa)
1.07–1.52	CL	16.5	6833.1
2.59–3.05	CL	13.6	2509.5
4.12–4.57	CL*	6.5	969.5
5.64–6.10	CL*	3.2	874.5
7.16–7.62	CL*	2.2	4099.8
8.69–9.15	CL*	3.1	722.1

*Note: Visual classification during field testing (ASTM D 2488).

TABLE D.21
SPT, CPT and laboratory testing results from Koleen site boring 3

Depth (m)	Soil Type	$N_{1,60}$	$q_{c,1}$ (kPa)
1.07–1.52	CL*	22.3	13928.8
2.59–3.05	CL*	9.1	2237.7
4.12–4.57	CL*	5.5	579.7
5.64–6.10	CL*	4.4	1007.3
7.16–7.62	CL*	12.8	2048.6
8.69–9.15	CL*	7.6	739.1

*Note: Visual classification during field testing (ASTM D 2488).

TABLE D.22
SPT, CPT and laboratory testing results from Koleen site boring 5

Depth (m)	Soil Type	$N_{1,60}$	$q_{c,1}$ (kPa)
1.07–1.52	CL*	16.6	5405.7
2.59–3.05	CL*	11.4	2164.8
4.12–4.57	CL*	3.9	663.5
5.64–6.10	CL*	3.4	577.0
7.16–7.62	CL*	4.6	904.2
8.69–9.15	CL*	3.2	836.4
10.21–10.67	CL*	3.2	666.8
11.74–12.20	CL*	4.0	716.5
13.26–13.72	ML*	6.2	4227.0
14.79–15.24	ML*	11.5	N/A

*Note: Visual classification during field testing (ASTM D 2488).

TABLE D.23
Peak and critical/residual unit side resistance results and corresponding rotation angles from Flora Maintenance Unit boring 1

Depth (m)	Soil Type	Peak Unit Side Resistance (kPa)	Rotation at Peak Unit Side Resistance (deg)	Critical/Residual Unit Side Resistance (kPa)	Rotation at Critical/Residual Unit Side Resistance (deg)
1.07–1.52	CL	110.71	115.1	89.30	178.7
2.59–3.05	SP-SC	123.47	71.7	84.36	180.3
4.12–4.57	SP	182.59	106.0	159.81	180.6

TABLE D.24
Peak and critical/residual unit side resistance results and corresponding rotation angles from Flora Maintenance Unit boring 2

Depth (m)	Soil Type	Peak Unit Side Resistance (kPa)	Rotation at Peak Unit Side Resistance (deg)	Critical/Residual Unit Side Resistance (kPa)	Rotation at Critical/Residual Unit Side Resistance (deg)
1.07–1.52	CL	47.59	152.9	40.10	180.8
2.59–3.05	SP	79.95	62.9	73.14	181.3
4.12–4.57	SP	86.17	102.9	75.85	180.8

TABLE D.25
Peak and critical/residual unit side resistance results and corresponding rotation angles from Flora Maintenance Unit boring 3

Depth (m)	Soil Type	Peak Unit Side Resistance (kPa)	Rotation at Peak Unit Side Resistance (deg)	Critical/Residual Unit Side Resistance (kPa)	Rotation at Critical/Residual Unit Side Resistance (deg)
1.07–1.52	CL-ML	50.75	160.9	50.46	180.6
2.59–3.05	SP-SC	100.11	123.6	91.43	155.0
4.12–4.57	SP	113.46	233.0	103.75	300.8

TABLE D.26
Peak and critical/residual unit side resistance results and corresponding rotation angles from Flora Maintenance Unit boring 4

Depth (m)	Soil Type	Peak Unit Side Resistance (kPa)	Rotation at Peak Unit Side Resistance (deg)	Critical/Residual Unit Side Resistance (kPa)	Rotation at Critical/Residual Unit Side Resistance (deg)
1.07–1.52	SC-SM	82.49	78.0	62.82	120.0
2.59–3.05	SP-SC	171.92	145.8	139.19	252.1
4.12–4.57	SC-SM	88.38	170.4	63.30	252.3

TABLE D.27
Peak and critical/residual unit side resistance results and corresponding rotation angles from Lafayette Maintenance Unit boring 1

Depth (m)	Soil Type	Peak Unit Side Resistance (kPa)	Rotation at Peak Unit Side Resistance (deg)	Critical/Residual Unit Side Resistance (kPa)	Rotation at Critical/Residual Unit Side Resistance (deg)
1.07–1.52	CL	131.37	45.1	121.05	125.0
2.59–3.05	SP-SC	34.71	212.2	28.59	250.8
4.12–4.57	SP-SC	87.32	140.5	65.90	230.0
5.64–6.10	SP-SC	161.67	106.7	139.21	276.0
7.16–7.62	CL-ML	137.16	60.2	118.22	180.7
8.69–9.15	ML	116.34	214.6	112.27	295.0

TABLE D.28
Peak and critical/residual unit side resistance results and corresponding rotation angles from Frankfort Maintenance Unit boring 1

Depth (m)	Soil Type	Peak Unit Side Resistance (kPa)	Rotation at Peak Unit Side Resistance (deg)	Critical/Residual Unit Side Resistance (kPa)	Rotation at Critical/Residual Unit Side Resistance (deg)
1.07–1.52	CL	63.24	260.1	58.41	280.0
2.59–3.05	SC-SM	54.34	161.8	49.39	190.0
4.12–4.57	ML	81.05	136.8	70.66	180.5
5.64–6.10	SW-SM	150.57	132.0	139.69	201.0

TABLE D.29
Peak and critical/residual unit side resistance results and corresponding rotation angles from Frankfort Maintenance Unit boring 4

Depth (m)	Soil Type	Peak Unit Side Resistance (kPa)	Rotation at Peak Unit Side Resistance (deg)	Critical/Residual Unit Side Resistance (kPa)	Rotation at Critical/Residual Unit Side Resistance (deg)
1.07–1.52	SM	34.09	185.2	28.67	202.6
2.59–3.05	SP-SC	54.63	59.6	38.40	150.9
4.12–4.57	SM	124.67	149	116.91	199.7

TABLE D.30
Peak and critical/residual unit side resistance results and corresponding rotation angles from Frankfort Maintenance Unit boring 4

Depth (m)	Soil Type	Peak Unit Side Resistance (kPa)	Rotation at Peak Unit Side Resistance (deg)	Critical/Residual Unit Side Resistance (kPa)	Rotation at Critical/Residual Unit Side Resistance (deg)
1.07–1.52	SC-SM	29.16	197.7	23.06	216.0
2.59–3.05	SM	90.24	40.0	67.14	145.0
4.12–4.57	SM	7.09	41.8	59.75	150.8

TABLE D.31
Peak and critical/residual unit side resistance results and corresponding rotation angles from Frankfort Maintenance Unit boring 5

Depth (m)	Soil Type	Peak Unit Side Resistance (kPa)	Rotation at Peak Unit Side Resistance (deg)	Critical/Residual Unit Side Resistance (kPa)	Rotation at Critical/Residual Unit Side Resistance (deg)
1.07–1.52	SC-SM	14.17	158.7	10.62	250.0
2.59–3.05	SM	117.48	65.1	83.56	180.2
4.12–4.57	SM	157.94	85.1	113.10	149.8

TABLE D.32
Peak and critical/residual unit side resistance results and corresponding rotation angles from Frankfort Maintenance Unit boring 6

Depth (m)	Soil Type	Peak Unit Side Resistance (kPa)	Rotation at Peak Unit Side Resistance (deg)	Critical/Residual Unit Side Resistance (kPa)	Rotation at Critical/Residual Unit Side Resistance (deg)
1.07–1.52	SM	17.86	110.3	16.11	155.0
2.59–3.05	SM	93.69	237.9	68.79	291.2
4.12–4.57	ML	219.12	144.5	181.22	198.7

TABLE D.33
Peak and critical/residual unit side resistance results and corresponding rotation angles from Frankfort Maintenance Unit boring 7

Depth (m)	Soil Type	Peak Unit Side Resistance (kPa)	Rotation at Peak Unit Side Resistance (deg)	Critical/Residual Unit Side Resistance (kPa)	Rotation at Critical/Residual Unit Side Resistance (deg)
1.07–1.52	CL	21.16	107.3	14.86	192.9
2.59–3.05	CL-ML	32.94	267.6	30.49	308.1
4.12–4.57	CL-ML	51.66	49.1	41.66	144.0

TABLE D.34
Peak and critical/residual unit side resistance results and corresponding rotation angles from Frankfort Maintenance Unit boring 8

Depth (m)	Soil Type	Peak Unit Side Resistance (kPa)	Rotation at Peak Unit Side Resistance (deg)	Critical/Residual Unit Side Resistance (kPa)	Rotation at Critical/Residual Unit Side Resistance (deg)
1.07–1.52	CL	52.95	240.6	52.17	300.0
2.59–3.05	CL	67.65	42.1	61.18	165.0
4.12–4.57	CL-ML	110.83	38.3	94.49	197.1
5.64–6.10	SM	84.21	104.5	60.56	175.0

TABLE D.35
Peak and critical/residual unit side resistance results and corresponding rotation angles from Romney Maintenance Unit boring 1

Depth (m)	Soil Type	Peak Unit Side Resistance (kPa)	Rotation at Peak Unit Side Resistance (deg)	Critical/Residual Unit Side Resistance (kPa)	Rotation at Critical/Residual Unit Side Resistance (deg)
1.07–1.52	SP-SC	73.73	48.7	56.77	175.0
2.59–3.05	SW-SC	108.01	134.6	91.10	207.3
4.12–4.57	ML	72.05	265.8	68.99	275.0
5.64–6.10	SM	24.75	171.9	18.70	223.0

TABLE D.36
Peak and critical/residual unit side resistance results and corresponding rotation angles from Romney Maintenance Unit boring 2

Depth (m)	Soil Type	Peak Unit Side Resistance (kPa)	Rotation at Peak Unit Side Resistance (deg)	Critical/Residual Unit Side Resistance (kPa)	Rotation at Critical/Residual Unit Side Resistance (deg)
1.07–1.52	GW	62.09	31.6	38.79	270.0
2.59–3.05	ML	63.10	58.7	45.81	175.0
4.12–4.57	SM	138.31	95.3	121.16	197.1
5.64–6.10	ML	69.56	127.9	66.81	155.0
7.16–7.62	ML	165.36	95.9	142.49	165.0

TABLE D.37
Peak and critical/residual unit side resistance results and corresponding rotation angles from Romney Maintenance Unit boring 3

Depth (m)	Soil Type	Peak Unit Side Resistance (kPa)	Rotation at Peak Unit Side Resistance (deg)	Critical/Residual Unit Side Resistance (kPa)	Rotation at Critical/Residual Unit Side Resistance (deg)
1.07–1.52	SP-SM	86.99	88.3	58.00	190.0
2.59–3.05	SM	121.75	31.0	102.87	200.6
4.12–4.57	SM	78.61	28.4	73.63	145.0
5.64–6.10	ML	87.23	42.3	74.07	240.0

TABLE D.38
Peak and critical/residual unit side resistance results and corresponding rotation angles from Romney Maintenance Unit boring 4

Depth (m)	Soil Type	Peak Unit Side Resistance (kPa)	Rotation at Peak Unit Side Resistance (deg)	Critical/Residual Unit Side Resistance (kPa)	Rotation at Critical/Residual Unit Side Resistance (deg)
1.07–1.52	SP-SM	45.62	54.2	23.88	175.0
2.59–3.05	SM	79.38	26.4	65.21	170.0
4.12–4.57	SM	84.64	242.1	72.54	301.0
5.64–6.10	SM	69.71	27.4	53.29	150.0

TABLE D.39
Peak and critical/residual unit side resistance results and corresponding rotation angles from Romney Maintenance Unit boring 5

Depth (m)	Soil Type	Peak Unit Side Resistance (kPa)	Rotation at Peak Unit Side Resistance (deg)	Critical/Residual Unit Side Resistance (kPa)	Rotation at Critical/Residual Unit Side Resistance (deg)
1.07–1.52	SP-SM	54.43	139.6	43.56	220.0
2.59–3.05	ML	103.51	107.9	74.45	182.3
4.12–4.57	SM	88.95	82.3	81.10	190.0
5.64–6.10	ML	81.10	80.6	73.35	260.0

TABLE D.40
Peak and critical/residual unit side resistance results and corresponding rotation angles from Romney Maintenance Unit boring 6

Depth (m)	Soil Type	Peak Unit Side Resistance (kPa)	Rotation at Peak Unit Side Resistance (deg)	Critical/Residual Unit Side Resistance (kPa)	Rotation at Critical/Residual Unit Side Resistance (deg)
1.07–1.52	SP-SM	71.91	183.5	51.83	295.5
2.59–3.05	SM	97.38	74.2	63.93	237.3
4.12–4.57	SM	83.25	98.2	75.16	185.0
5.64–6.10	ML	62.67	38.3	47.02	250.6

TABLE D.41
Peak and critical/residual unit side resistance results and corresponding rotation angles from Koleen site boring 1

Depth (m)	Soil Type	Peak Unit Side Resistance (kPa)	Rotation at Peak Unit Side Resistance (deg)	Critical/Residual Unit Side Resistance (kPa)	Rotation at Critical/Residual Unit Side Resistance (deg)
1.07–1.52	CL	111.50	160.1	109.50	297.2
2.59–3.05	CL	85.36	289.4	83.94	289.0
4.12–4.57	CL	95.61	148.6	74.16	290.0
5.64–6.10	CL	69.32	77.3	54.05	264.4
7.16–7.62	CL	59.12	22.7	48.68	288.4
8.69–9.15	CL	72.00	192.9	62.49	270.5

TABLE D.42
Peak and critical/residual unit side resistance results and corresponding rotation angles from Koleen site boring 2

Depth (m)	Soil Type	Peak Unit Side Resistance (kPa)	Rotation at Peak Unit Side Resistance (deg)	Critical/Residual Unit Side Resistance (kPa)	Rotation at Critical/Residual Unit Side Resistance (deg)
1.07–1.52	CL	63.58	60.0	35.53	288.8
2.59–3.05	CL	86.03	31.2	83.09	271.6
4.12–4.57	CL*	55.68	31.2	52.70	285.4
5.64–6.10	CL*	38.78	57.3	34.01	183.9
7.16–7.62	CL*	30.11	19.7	28.35	209.6
8.69–9.15	CL*	22.26	41.9	12.95	255.0

*Note: Visual classification during field testing (ASTM D 2488).

TABLE D.43
Peak and critical/residual unit side resistance results and corresponding rotation angles from Koleen site boring 3

Depth (m)	Soil Type	Peak Unit Side Resistance (kPa)	Rotation at Peak Unit Side Resistance (deg)	Critical/Residual Unit Side Resistance (kPa)	Rotation at Critical/Residual Unit Side Resistance (deg)
1.07–1.52	CL*	112.60	305.6	110.32	298.3
2.59–3.05	CL*	66.35	181.2	64.45	297.2
4.12–4.57	CL*	57.55	222.4	53.21	293.5
5.64–6.10	CL*	41.51	43.0	33.36	254.1
7.16–7.62	CL*	54.82	304.0	54.82	304.0
8.69–9.15	CL*	37.49	13.7	34.62	294.6

*Note: Visual classification during field testing (ASTM D 2488).

TABLE D.44
Peak and critical/residual unit side resistance results and corresponding rotation angles from Koleen site boring 5

Depth (m)	Soil Type	Peak Unit Side Resistance (kPa)	Rotation at Peak Unit Side Resistance (deg)	Critical/Residual Unit Side Resistance (kPa)	Rotation at Critical/Residual Unit Side Resistance (deg)
1.07–1.52	CL*	54.63	46.7	32.07	299.6
2.59–3.05	CL*	21.74	72.5	4.51	296.5
4.12–4.57	CL*	48.59	122.8	34.77	296.5
5.64–6.10	CL*	35.57	121.0	26.50	204.7
7.16–7.62	CL*	37.44	63.8	26.99	289.6
8.69–9.15	CL*	17.47	35.6	15.41	289.6
10.21–10.67	CL*	40.31	202.8	21.84	293.3
11.74–12.20	CL*	21.16	73.8	9.70	288.0
13.26–13.72	ML*	55.82	86.8	41.22	158.6
14.79–15.24	ML*	83.59	79.6	55.73	288.0

*Note: Visual classification during field testing (ASTM D 2488).

APPENDIX E. ANALYSIS PLOTS DATA

TABLE E.1
Raw data used to develop relationship shown in Figure 6.3

Figure 6.3 Peak unit side resistance versus N1,60 values for saturated clay					
Site	**Depth (m)**	**Peak fs (kPa)**	**σ'$_v$ (kPa)**	**$N_{1,60}$**	**OCR**
Flora 4	4.34	88.38	65.24	13.52	2.12
Koleen 1	2.82	85.36	55.43	8.71	3.83
Koleen 1	4.34	95.61	70.16	8.37	3.47
Koleen 1	5.87	69.32	87.02	10.18	3.14
Koleen 1	7.39	59.13	104.65	3.19	2.84
Koleen 1	8.92	72.00	120.33	5.83	2.57
Koleen 2	2.82	86.03	48.46	13.59	3.83
Koleen 2	4.34	55.68	65.11	6.48	3.47
Koleen 2	5.87	38.78	82.05	3.23	3.14
Koleen 2	7.39	30.11	96.16	2.22	2.84
Koleen 2	8.92	22.26	109.78	3.12	2.57
Koleen 3	2.82	66.36	48.63	9.13	3.83
Koleen 3	4.34	57.55	63.74	5.50	3.47
Koleen 3	5.87	41.51	78.08	4.41	3.14
Koleen 3	8.92	37.49	107.12	7.56	2.57
Koleen 5	4.34	48.59	61.98	3.94	3.47
Koleen 5	5.87	35.57	74.76	3.38	3.14
Koleen 5	7.39	37.44	88.83	4.62	2.84
Koleen 5	8.92	17.47	103.70	3.21	2.57
Koleen 5	10.44	40.31	115.70	3.20	2.33
Koleen 5	11.97	21.16	128.85	4.04	2.11

TABLE E.2
Raw data used to develop relationship shown in Figure 6.4

Figure 6.4 Residual unit side resistance versus N1,60 values for saturated clay					
Site	**Depth (m)**	**Residual fs (kPa)**	**σ'$_v$ (kPa)**	**$N_{1,60}$**	**OCR**
Flora 4	4.34	63.30	65.24	13.52	2.12
Koleen 1	2.82	83.94	55.43	8.71	3.83
Koleen 1	4.34	74.16	70.16	8.37	3.47
Koleen 1	5.87	54.05	87.02	10.18	3.14
Koleen 1	7.39	48.68	104.65	3.19	2.84
Koleen 1	8.92	62.49	120.33	5.83	2.57
Koleen 2	2.82	83.09	48.46	13.59	3.83
Koleen 2	4.34	52.70	65.11	6.48	3.47
Koleen 2	5.87	34.01	82.05	3.23	3.14
Koleen 2	7.39	28.25	96.16	2.22	2.84
Koleen 2	8.92	12.95	109.78	3.12	2.57
Koleen 3	2.82	64.45	48.63	9.13	3.83
Koleen 3	4.34	53.21	63.74	5.50	3.47
Koleen 3	5.87	33.36	78.08	4.41	3.14
Koleen 3	8.92	34.62	107.12	7.56	2.57
Koleen 5	4.34	34.77	61.98	3.94	3.47
Koleen 5	5.87	26.50	74.76	3.38	3.14
Koleen 5	7.39	26.99	88.83	4.62	2.84
Koleen 5	8.92	15.41	103.70	3.21	2.57
Koleen 5	10.44	21.80	115.70	3.20	2.33
Koleen 5	11.97	9.70	128.85	4.04	2.11

TABLE E.3
Raw data used to develop relationship shown in Figure 6.5

Figure 6.5 Peak unit side resistance versus N1,60 values for saturated non-plastic silt				
Site	**Depth (m)**	**Peak fs (kPa)**	**σ'_v (kPa)**	**$N_{1,60}$**
Flora 4	4.34	88.38	65.24	11.16
Frankfort 1	4.34	81.05	68.06	20.23
Frankfort 3	4.34	124.67	71.43	28.56
Frankfort 4	4.34	70.09	71.86	20.23
Frankfort 5	4.34	157.94	71.16	28.56
Frankfort 6	4.34	219.12	72.36	38.08
Frankfort 8	4.34	84.21	84.91	15.47
Romney 1	5.87	24.75	100.28	14.28
Romney 2	5.87	69.56	103.29	16.66
Romney 2	7.39	165.36	119.49	42.56
Romney 3	5.87	87.23	99.21	20.23
Romney 4	5.87	69.71	98.66	20.23
Romney 5	5.87	81.10	97.92	24.99
Romney 6	5.87	62.67	98.99	21.42
Koleen 5	13.49	55.82	142.92	7.60
Koleen 5	15.02	83.59	147.92	14.74

TABLE E.4
Raw data used to develop relationship shown in Figure 6.6

Figure 6.6 Critical unit side resistance versus N1,60 values for saturated non-plastic silt				
Site	**Depth (m)**	**Critical fs (kPa)**	**σ'_v (kPa)**	**$N_{1,60}$**
Flora 4	4.34	63.30	65.24	11.16
Frankfort 1	4.34	70.66	68.06	20.23
Frankfort 3	4.34	116.91	71.43	28.56
Frankfort 4	4.34	59.75	71.86	20.23
Frankfort 5	4.34	113.10	71.16	28.56
Frankfort 6	4.34	181.22	72.36	38.08
Frankfort 8	4.34	60.56	84.91	15.47
Romney 1	5.87	18.70	100.28	14.28
Romney 2	5.87	66.81	103.29	16.66
Romney 2	7.39	142.49	119.49	42.56
Romney 3	5.87	74.07	99.21	20.23
Romney 4	5.87	53.29	98.66	20.23
Romney 5	5.87	73.35	97.92	24.99
Romney 6	5.87	47.02	98.99	21.42
Koleen 5	13.49	41.22	142.92	7.60
Koleen 5	15.02	55.73	147.92	14.74

TABLE E.5
Raw data used to develop relationship shown in Figure 6.7

Figure 6.7 Peak unit side resistance versus N1,60 values for saturated sand				
Site	**Depth (m)**	**Peak fs (kPa)**	**σ'_v (kPa)**	**$N_{1,60}$**
Flora 1	2.82	123.47	45.94	21.96
Flora 1	4.34	182.60	62.25	31.45
Flora 2	2.82	79.95	49.63	13.67
Flora 3	2.82	100.11	49.47	13.70
Flora 3	4.34	113.46	65.54	14.71
Frankfort 1	5.87	150.57	85.00	30.31

TABLE E.6
Raw data used to develop relationship shown in Figure 6.8

Figure 6.8 Critical unit side resistance versus N1,60 values for saturated sand				
Site	**Depth (m)**	**Critical fs (kPa)**	**σ'_v (kPa)**	**$N_{1,60}$**
Flora 1	2.82	84.37	45.94	21.96
Flora 1	4.34	159.81	62.25	31.45
Flora 2	2.82	73.14	49.63	13.67
Flora 2	4.34	75.85	65.48	25.75
Flora 3	2.82	91.43	49.47	13.70
Flora 3	4.34	103.75	65.54	14.71
Frankfort 1	5.87	139.69	85.00	30.31

TABLE E.7
Raw data used to develop relationship shown in Figure 6.9

Figure 6.9 Peak unit side resistance versus N1,60 values for unsaturated clay						
Site	**Depth (m)**	**Peak fs (kPa)**	**σ'_v (kPa)**	**$N_{1,60}$**	**OCR**	**S (%)**
Flora 1	1.30	110.71	20.35	15.53	4.91	36.3
Flora 2	1.30	47.59	22.38	12.96	4.47	72.8
Flora 3	1.30	50.75	22.38	18.51	4.47	58.6
Flora 4	1.30	82.49	22.38	14.81	4.47	43.2
Lafayette 1	1.30	131.37	20.35	25.24	2.50	34.2
Frankfort 1	1.30	63.24	20.35	13.67	1.97	44.6
Frankfort 1	2.82	54.34	45.122	16.83	1.88	85.3
Frankfort 4	1.30	29.16	22.38	19.55	1.79	74.0
Frankfort 5	1.30	14.17	22.38	13.03	1.79	93.2
Frankfort 7	1.30	21.16	20.35	18.22	1.97	90.4
Frankfort 7	2.83	32.94	44.70	13.83	1.90	95.0
Frankfort 8	2.83	67.65	44.70	16.90	1.90	73.8
Koleen 1	1.30	111.50	28.61	20.45	4.23	95.0
Koleen 2	1.30	63.58	24.36	16.51	4.23	80.1
Koleen 3	1.30	112.60	24.52	22.29	4.23	82.9
Koleen 5	1.30	54.63	23.12	16.59	4.23	64.9

TABLE E.8
Raw data used to develop relationship shown in Figure 6.10

Figure 6.10 Residual unit side resistance versus N1,60 values for unsaturated clay						
Site	**Depth (m)**	**Residual fs (kPa)**	**σ'_v (kPa)**	**$N_{1,60}$**	**OCR**	**S (%)**
Flora 1	1.30	89.30	20.35	15.53	4.91	36.3
Flora 2	1.30	40.10	22.38	12.96	4.47	72.8
Flora 3	1.30	50.46	22.38	18.51	4.47	58.6
Flora 4	1.30	62.82	22.38	14.81	4.47	43.2
Lafayette 1	1.30	121.05	20.35	25.24	2.50	34.2
Frankfort 1	1.30	58.41	20.35	13.67	1.97	44.6
Frankfort 1	2.82	49.39	45.122	16.83	1.88	85.3
Frankfort 4	1.30	23.06	22.38	19.55	1.79	74.0
Frankfort 5	1.30	10.62	22.38	13.03	1.79	93.2
Frankfort 7	1.30	14.86	20.35	18.22	1.97	90.4
Frankfort 7	2.83	30.49	44.70	13.83	1.90	95.0
Frankfort 8	2.83	61.18	44.70	16.90	1.90	73.8
Koleen 1	1.30	109.50	28.61	20.45	4.23	95.0
Koleen 2	1.30	35.53	24.36	16.51	4.23	80.1
Koleen 3	1.30	110.32	24.52	22.29	4.23	82.9
Koleen 5	1.30	32.07	23.12	16.59	4.23	64.9

TABLE E.9
Raw data used to develop relationship shown in Figure 6.11

Figure 6.11 Peak unit side resistance N1,60 values for unsaturated non-plastic silt					
Site	**Depth (m)**	**Peak fs (kPa)**	**σ'_v (kPa)**	**$N_{1,60}$**	**S (%)**
Frankfort 3	1.30	34.09	22.38	26.06	78.2
Frankfort 4	2.82	90.24	48.71	50.05	73.9
Frankfort 5	2.82	117.49	48.71	39.75	69.8
Frankfort 6	1.30	17.86	22.38	36.72	92.9
Frankfort 6	2.82	93.69	48.71	58.88	70.9

TABLE E.10
Raw data used to develop relationship shown in Figure 6.12

Figure 6.12 Critical unit side resistance N1,60 values for unsaturated non-plastic silt					
Site	**Depth (m)**	**Critical fs (kPa)**	**σ'_v (kPa)**	**$N_{1,60}$**	**S (%)**
Frankfort 3	1.30	28.67	22.38	26.06	78.2
Frankfort 4	2.82	67.14	48.71	50.05	73.9
Frankfort 5	2.82	83.56	48.71	39.75	69.8
Frankfort 6	1.30	16.11	22.38	36.72	92.9
Frankfort 6	2.82	68.79	48.71	58.88	70.9

TABLE E.11
Raw data used to develop relationship shown in Figure 6.13

Figure 6.13 Peak unit side resistance N1,60 values for unsaturated sand					
Site	**Depth (m)**	**Peak fs (kPa)**	**σ'_v (kPa)**	**$N_{1,60}$**	**S (%)**
Frankfort 3	2.82	54.63	48.71	19.14	56.7
Romney 1	1.30	73.73	22.38	30.40	69.2
Romney 2	1.30	62.09	25.43	42.78	79.5
Romney 3	1.30	86.99	22.38	49.95	58.1
Romney 5	1.30	54.43	22.38	34.61	87.9
Romney 6	1.30	71.91	22.38	21.72	71.5

TABLE E.12
Raw data used to develop relationship shown in Figure 6.14

Figure 6.14 Critical unit side resistance N1,60 values for unsaturated sand					
Site	**Depth (m)**	**Critical fs (kPa)**	**σ'_v (kPa)**	**$N_{1,60}$**	**S (%)**
Frankfort 3	2.82	38.40	48.71	19.14	56.7
Romney 1	1.30	56.78	22.38	30.40	69.2
Romney 2	1.30	38.79	25.43	42.78	79.5
Romney 3	1.30	58.00	22.38	49.95	58.1
Romney 5	1.30	23.88	22.38	34.61	87.9
Romney 6	1.30	43.56	22.38	21.72	71.5

TABLE E.13
Raw data used to develop relationship shown in Figure 6.15

Figure 6.15 Peak unit side resistance versus qc,1 values for saturated clay					
Site	**Depth (m)**	**Peak fs (kPa)**	**σ'_v (kPa)**	**$q_{c,1}$ (kPa)**	**OCR**
Flora 4	4.34	88.38	65.24	2570.02	2.12
Koleen 1	2.82	85.36	55.43	2199.82	3.83
Koleen 1	5.87	69.32	87.02	621.71	3.14
Koleen 1	7.39	59.13	104.65	721.25	2.84
Koleen 2	2.83	86.03	48.46	2509.50	3.83
Koleen 2	4.34	55.68	65.11	969.54	3.47
Koleen 2	5.87	38.78	82.05	874.52	3.14
Koleen 2	8.92	22.26	109.78	722.07	2.57
Koleen 3	2.82	66.36	48.63	2237.71	3.83
Koleen 3	4.34	57.55	63.74	579.73	3.47
Koleen 3	5.87	41.51	78.08	1007.33	3.14
Koleen 3	7.39	54.82	92.20	2048.61	2.84
Koleen 3	8.92	37.49	107.12	739.14	2.57
Koleen 5	4.34	48.59	61.98	663.50	3.47
Koleen 5	5.87	35.57	74.76	577.03	3.14
Koleen 5	7.39	37.44	88.83	904.15	2.84
Koleen 5	8.92	17.47	103.70	836.36	2.57
Koleen 5	10.44	40.31	115.70	666.79	2.33
Koleen 5	11.97	21.16	128.85	716.45	2.11

TABLE E.14
Raw data used to develop relationship shown in Figure 6.16

Figure 6.16 Residual unit side resistance versus qc,1 values for saturated clay					
Site	**Depth (m)**	**Residual fs (kPa)**	**σ'_v (kPa)**	**$q_{c,1}$ (kPa)**	**OCR**
Flora 4	4.34	63.30	65.24	2570.02	2.12
Koleen 1	2.82	83.94	55.43	2199.82	3.83
Koleen 1	5.87	54.05	87.02	621.71	3.14
Koleen 1	7.39	48.68	104.65	721.25	2.84
Koleen 2	2.83	83.09	48.46	2509.50	3.83
Koleen 2	4.34	52.70	65.11	969.54	3.47
Koleen 2	5.87	34.01	82.05	874.52	3.14
Koleen 2	8.92	12.95	109.78	722.07	2.57
Koleen 3	2.82	64.45	48.63	2237.71	3.83
Koleen 3	4.34	53.21	63.74	579.73	3.47
Koleen 3	5.87	33.36	78.08	1007.33	3.14
Koleen 3	7.39	54.82	92.20	2048.61	2.84
Koleen 3	8.92	34.62	107.12	739.14	2.57
Koleen 5	4.34	34.77	61.98	663.50	3.47
Koleen 5	5.87	26.50	74.76	577.03	3.14
Koleen 5	7.39	26.99	88.83	904.15	2.84
Koleen 5	8.92	15.41	103.70	836.36	2.57
Koleen 5	10.44	21.84	115.70	666.79	2.33
Koleen 5	11.97	9.70	128.85	716.45	2.11

TABLE E.15
Raw data used to develop relationship shown in Figure 6.17

Figure 6.17 Peak unit side resistance versus qc,1 values for saturated non-plastic silt				
Site	**Depth (m)**	**Peak fs (kPa)**	**σ'_v (kPa)**	**$q_{c,1}$**
Romney 1	5.87	24.75	100.28	2548.64
Romney 1	5.87	69.56	103.29	10328.47
Romney 2	7.39	165.36	119.49	16033.11
Romney 4	5.87	69.71	98.66	12091.17
Romney 5	5.87	81.10	97.92	20377.30
Romney 6	5.87	62.67	98.99	12318.35
Koleen 5	13.49	55.82	142.92	4226.97

TABLE E.16
Raw data used to develop relationship shown in Figure 6.18

Figure 6.18 Critical unit side resistance versus qc,1 values for saturated non-plastic silt				
Site	**Depth (m)**	**Critical fs (kPa)**	**σ'_v (kPa)**	**$q_{c,1}$**
Romney 1	5.87	18.70	100.28	2548.64
Romney 1	5.87	66.81	103.29	10328.47
Romney 2	7.39	142.49	119.49	16033.11
Romney 4	5.87	53.29	98.66	12091.17
Romney 5	5.87	73.35	97.92	20377.30
Romney 6	5.87	47.02	98.99	12318.35
Koleen 5	13.49	41.22	142.92	4226.97

TABLE E.17
Raw data used to develop relationship shown in Figure 6.19

Figure 6.19 Peak unit side resistance versus qc,1 values for saturated sand				
Site	**Depth (m)**	**Peak fs (kPa)**	**σ'_v (kPa)**	**$q_{c,1}$ (kPa)**
Flora 1	2.82	123.47	45.94	6375.16
Flora 2	2.82	79.95	49.63	2689.07
Flora 2	4.34	86.18	65.48	2333.63
Flora 3	2.82	100.11	49.47	3602.82
Flora 3	4.34	113.46	65.54	2525.30

TABLE E.18
Raw data used to develop relationship shown in Figure 6.20

Figure 6.20 Critical unit side resistance versus qc,1 values for saturated sand				
Site	**Depth (m)**	**Critical fs (kPa)**	**σ'_v (kPa)**	**$q_{c,1}$ (kPa)**
Flora 1	2.82	84.37	45.94	6375.16
Flora 2	2.82	73.14	49.63	2689.07
Flora 2	4.34	75.85	65.48	2333.63
Flora 3	2.82	91.43	49.47	3602.82
Flora 3	4.34	103.75	65.54	2525.30

TABLE E.19
Raw data used to develop relationship shown in Figure 6.25

Figure 6.16 Residual unit side resistance versus qc,1 values for saturated clay					
Site	**Depth (m)**	**Residual fs (kPa)**	**σ'_v (kPa)**	**s_u (kPa)**	**OCR**
Koleen 4	9.25	66.35	53.97	56.94	3.98
Koleen 4	9.25	66.35	53.97	67.84	3.98
Koleen 4	9.25	66.35	53.97	94.93	3.98
Koleen 4	11.75	58.83	68.56	43.25	3.79
Koleen 4	11.75	58.83	68.56	91.94	3.79
Koleen 4	17.75	36.96	103.56	40.84	3.36
Koleen 4	17.75	36.96	103.56	53.02	3.36
Koleen 4	17.75	36.96	103.56	79.34	3.36

TABLE E.20
Raw data used to develop relationship shown in Figure 6.26

Figure 6.26 Peak unit side resistance versus qc,1 values for unsaturated clay						
Site	**Depth (m)**	**Peak fs (kPa)**	**σ'_v (kPa)**	**$q_{c,1}$ (kPa)**	**OCR**	**S (%)**
Frankfort 1	1.30	63.24	20.35	1698.03	1.88	44.6
Frankfort 1	2.82	54.34	45.12	3423.54	1.97	85.3
Frankfort 4	1.30	29.16	22.38	3382.59	1.79	44.6
Frankfort 5	1.30	14.17	22.38	2327.02	1.79	74.0
Frankfort 6	1.30	17.86	22.38	1845.77	1.79	93.2
Frankfort 7	1.30	21.16	20.35	1829.93	1.97	92.9
Frankfort 7	2.82	32.94	44.70	2485.24	1.90	90.4
Frankfort 8	2.82	67.65	44.70	3176.79	1.90	95.0
Koleen 1	1.30	111.50	28.61	7619.12	4.23	80.1
Koleen 2	1.30	63.58	24.36	6833.09	4.23	82.9
Koleen 3	1.30	112.60	24.52	13938.82	4.23	82.9
Koleen 5	1.30	54.63	23.18	5405.68	4.23	64.9

TABLE E.21
Raw data used to develop relationship shown in Figure 6.27

Figure 6.27 Residual unit side resistance versus qc,1 values for unsaturated clay						
Site	**Depth (m)**	**Residual fs (kPa)**	**σ'_v (kPa)**	**$q_{c,1}$ (kPa)**	**OCR**	**S (%)**
Frankfort 1	1.30	58.41	20.35	1698.03	1.88	44.6
Frankfort 1	2.82	49.39	45.12	3423.54	1.97	85.3
Frankfort 4	1.30	23.06	22.38	3382.59	1.79	44.6
Frankfort 5	1.30	10.62	22.38	2327.02	1.79	74.0
Frankfort 6	1.30	16.11	22.38	1845.77	1.79	93.2
Frankfort 7	1.30	14.86	20.35	1829.93	1.97	92.9
Frankfort 7	2.82	30.49	44.70	2485.24	1.90	90.4
Frankfort 8	2.82	61.18	44.70	3176.79	1.90	95.0
Koleen 1	1.30	109.50	28.61	7619.12	4.23	95.0
Koleen 2	1.30	35.53	24.36	6833.09	4.23	80.1
Koleen 3	1.30	110.32	24.52	13938.82	4.23	82.9
Koleen 5	1.30	32.07	23.18	5405.68	4.23	64.9

TABLE E.22
Raw data used to develop relationship shown in Figure 6.28

Figure 6.28 Peak unit side resistance versus qc,1 values for unsaturated non-plastic silt					
Site	**Depth (m)**	**Peak fs (kPa)**	**σ'_v (kPa)**	**$q_{c,1}$**	**S (%)**
Frankfort 4	2.82	90.24	48.71	49304.74	73.9
Frankfort 5	2.82	117.49	48.71	37870.76	69.8
Frankfort 6	2.82	93.69	48.71	17848.02	70.9

TABLE E.23
Raw data used to develop relationship shown in Figure 6.29

Figure 6.29 Critical unit side resistance versus qc,1 values for unsaturated non-plastic silt					
Site	**Depth (m)**	**Peak fs (kPa)**	**σ'_v (kPa)**	**$q_{c,1}$**	**S (%)**
Frankfort 4	2.82	67.14	48.71	49304.74	73.9
Frankfort 5	2.82	83.56	48.71	37870.76	69.8
Frankfort 6	2.82	68.79	48.71	17848.02	70.9

TABLE E.24
Raw data used to develop relationship shown in Figure 6.30

Figure 6.30 Peak unit side resistance versus qc,1 values for unsaturated sand					
Site	**Depth (m)**	**Peak fs (kPa)**	**σ'_v (kPa)**	**$q_{c,1}$**	**S (%)**
Romney 2	1.30	62.09	25.43	21710.46	79.5
Romney 3	1.30	86.99	22.38	11009.27	44.7
Romney 4	1.30	45.63	22.38	23318.70	90.1
Romney 5	1.30	54.43	22.38	16205.95	60.1

TABLE E.25
Raw data used to develop relationship shown in Figure 6.31

Figure 6.31 Critical unit side resistance versus qc,1 values for unsaturated sand					
Site	**Depth (m)**	**Critical fs (kPa)**	**σ'_v (kPa)**	**$q_{c,1}$**	**S (%)**
Romney 2	1.30	38.79	25.43	21710.46	79.5
Romney 3	1.30	58.00	22.38	11009.27	44.7
Romney 4	1.30	23.88	22.38	23318.70	90.1
Romney 5	1.30	43.56	22.38	16205.95	60.1

APPENDIX F. SITE SPT BORINGS AND CPT SOUNDINGS

Site: Flora Maintenance Unit
Date: 9-Aug-11
Boring: 1
Surface Elevation (m): 216.16

Final Depth (m): 4.57
Groudwater Depth (m): 2.74
Drill Rig: Truck
Drilling Method: 82.5I.D./165O.D. H.S.A.

Depth (m)	USCS	Description	N_{60} (Blows)	Remarks
1.07-1.52	CL	Moist, firm, sandy lean CLAY	7.2	
2.59-3.05	SP-SC	Wet, medium dense, poorly-graded SAND w/ silty clay	15.2	Water table encountered at 2.74 meters.
4.12-4.57	SP	Wet, medium dense, poorly-graded SAND	25.4	Sand was flowing into the hollow stem augers. The boring was terminated at 4.57 meters.

Figure F.1 Boring log for Flora Maintenance Unit boring 1.

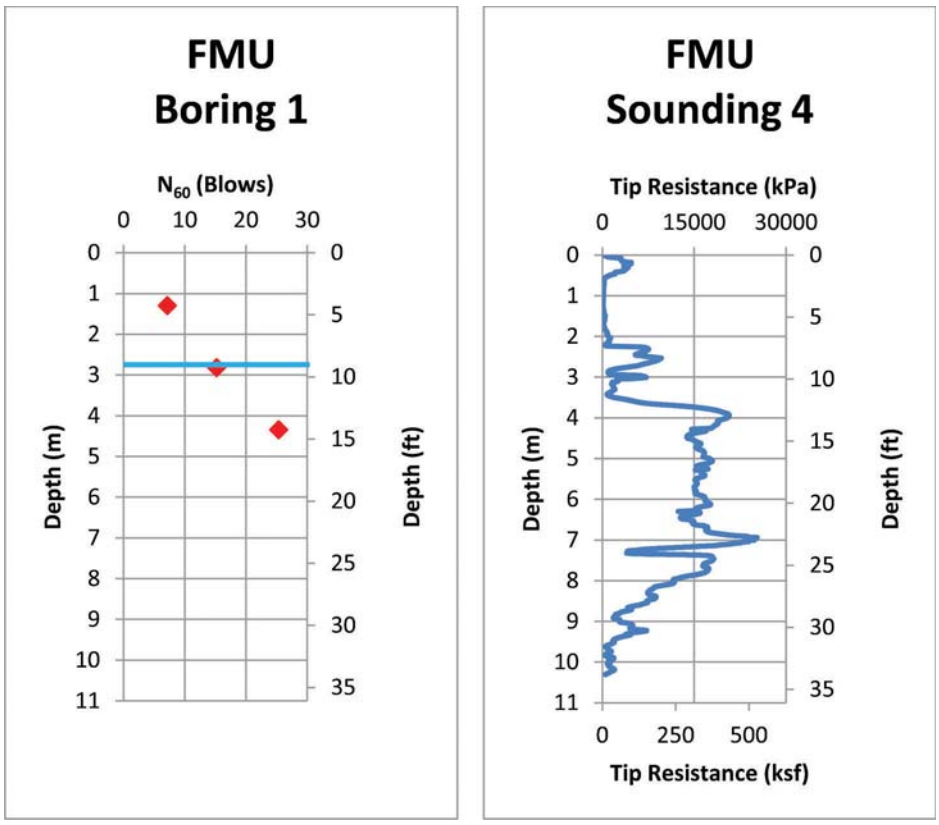

Figure F.2 Flora Maintenance Unit SPT boring 1 terminated at a depth of 4.57 meters with the adjacent CPT sounding terminated at a depth of 10.30 meters.

Site: Flora Maintenance Unit
Date: 9-Aug-11
Boring: 2
Surface Elevation (m): 216.16

Final Depth (m): 4.57
Groudwater Depth (m): 2.74
Drill Rig: Truck
Drilling Method: 82.5I.D./165O.D. H.S.A.

Depth (m)	USCS	Description	N_{60} (Blows)	Remarks
1.07-1.52	CL	Moist, stiff, sandy lean CLAY	13.0	
2.59-3.05	SP	Wet, medium dense, poorly-graded SAND	13.7	Water table encountered at 2.74 meters.
4.12-4.57		grading wet	25.8	Sand was flowing into the hollow stem augers. The boring was terminated at 4.57 meters.

Figure F.3 Boring log for Flora Maintenance Unit boring 2.

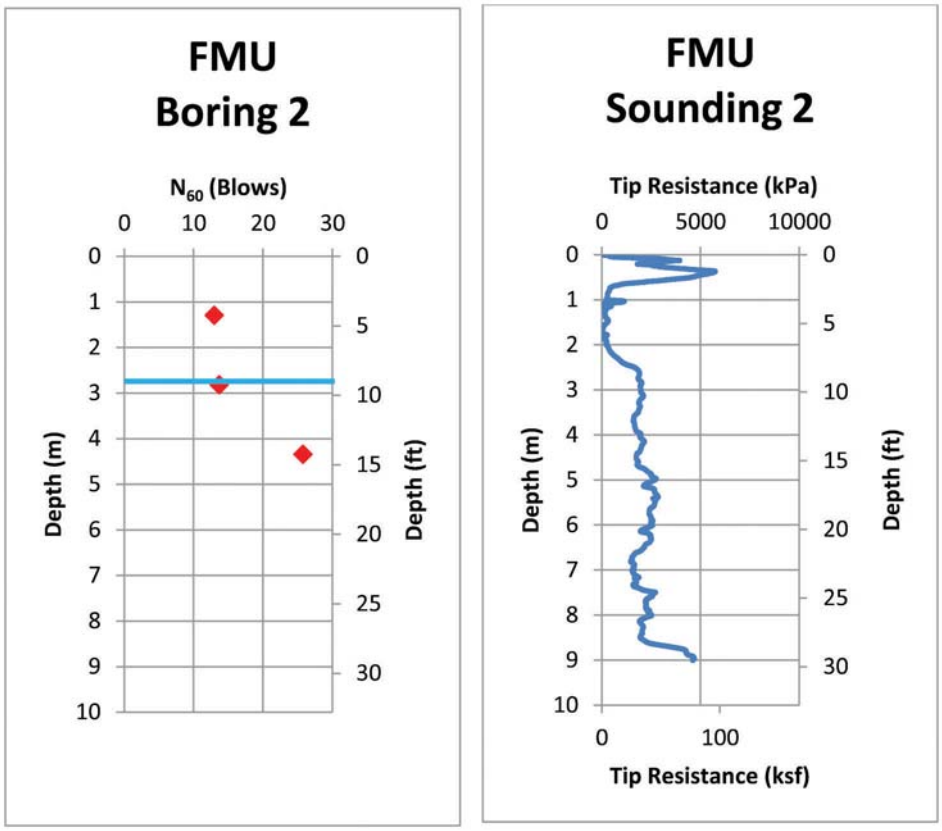

Figure F.4 Flora Maintenance Unit SPT boring 2 terminated at a depth of 4.57 meters with the adjacent CPT sounding terminated at a depth of 8.99 meters.

Site: Flora Maintenance Unit
Date: 9-Aug-11
Boring: 3
Surface Elevation (m): 216.16

Final Depth (m): 4.57
Groudwater Depth (m): 2.74
Drill Rig: Truck
Drilling Method: 82.5I.D./165O.D. H.S.A.

Depth (m)	USCS	Description	N_{60} (Blows)	Remarks
1.07-1.52	SC-SM	Moist, medium dense, silty clayey SAND	18.5	
2.59-3.05	SP-SC	Wet, medium dense, poorly-graded SAND w/ silty clay	13.7	Water table encountered at 2.74 meters.
4.12-4.57	SP	Wet, medium dense, poorly-graded SAND	14.7	Sand was flowing into the hollow stem augers. The boring was terminated at 4.57 meters.

Figure F.5 Boring log for Flora Maintenance Unit boring 3.

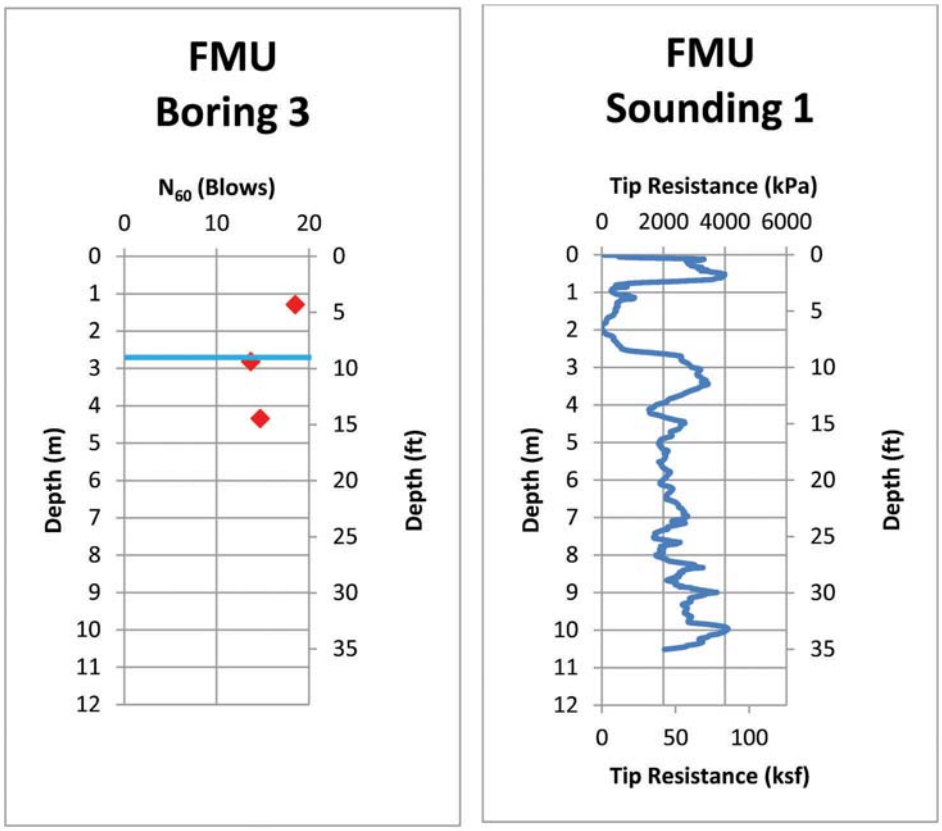

Figure F.6 Flora Maintenance Unit SPT boring 3 terminated at a depth of 4.57 meters with the adjacent CPT sounding terminated at a depth of 10.52 meters.

Site: Flora Maintenance Unit
Date: 9-Aug-11
Boring: 4
Surface Elevation (m): 216.16

Final Depth (m): 4.57
Groudwater Depth (m): 2.74
Drill Rig: Truck
Drilling Method: 82.5I.D./165O.D. H.S.A.

Depth (m)	USCS	Description	N_{60} (Blows)	Remarks
1.07-1.52	SC-SM	Moist, medium dense, silty clayey SAND	14.8	
2.59-3.05	SP-SC	Wet, medium dense, poorly-graded SAND w/ silty clay	13.7	Water table encountered at 2.74 meters.
4.12-4.57	SC-SM	Wet, medium dense, poorly-graded SAND	13.5	Sand was flowing into the hollow stem augers. The boring was terminated at 4.57 meters.

Figure F.7 Boring log for Flora Maintenance Unit boring 4.

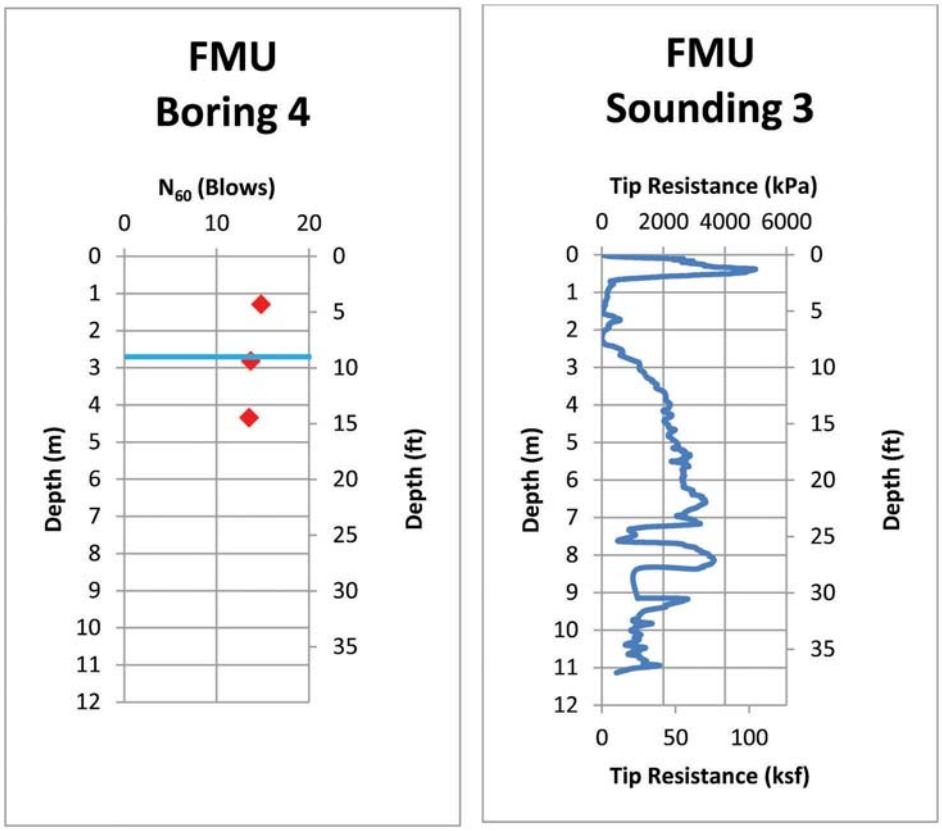

Figure F.8 Flora Maintenance Unit SPT boring 4 terminated at a depth of 4.57 meters with the adjacent CPT sounding terminated at a depth of 11.13 meters.

Site: Lafayette Maintenance Unit
Date: 1-Sep-11
Boring: 1
Surface Elevation (m): 175.91

Final Depth (m): 9.15
Groudwater Depth (m): 6.71
Drill Rig: Truck
Drilling Method: 82.5I.D./165O.D. H.S.A.

Depth (m)	USCS	Description	N_{60} (Blows)	Remarks
1.07-1.52	CL	Moist, stiff, sandy lean CLAY	25.2	
2.59-3.05	SP-SC	Moist loose, poorly-graded SAND w/ silty clay	9.1	
4.12-4.57		grading medium dense	19.9	
5.64-6.10			26.8	Water table encountered at 6.71 meters.
7.16-7.62	CL-ML	Wet, very stiff, silty CLAY	21.1	
8.69-9.15	ML	Wet, hard, sandy SILT	50.1	The boring was terminated at 9.15 meters.

Figure F.9 Boring log for Lafayette Maintenance Unit boring 1.

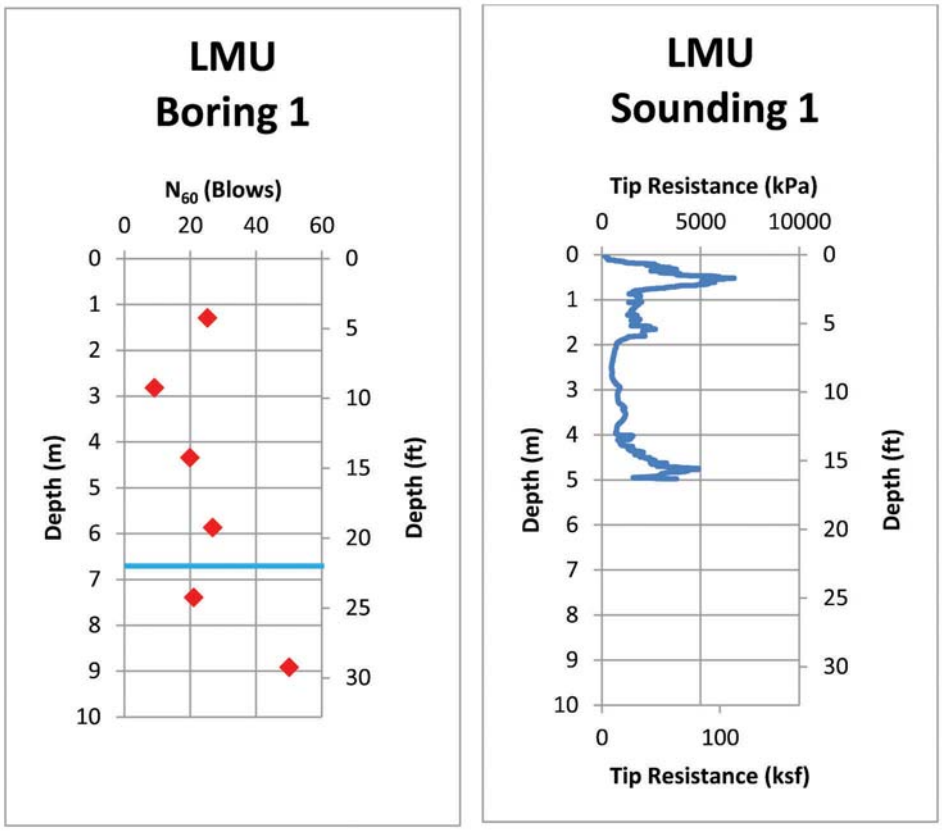

Figure F.10 Lafayette Maintenance Unit SPT boring 1 terminated at a depth of 9.15 meters with the adjacent CPT sounding terminated at a depth of 4.97 meters.

Site: Frankfort Maintenance Unit
Date: 4-Jan-12
Boring: 1
Surface Elevation (m): 264.33

Final Depth (m): 6.10
Groudwater Depth (m): 3.81
Drill Rig: ATV
Drilling Method: 82.5I.D./165O.D. H.S.A.

Depth (m)	USCS	Description	N_{60} (Blows)	Remarks
1.07-1.52	CL	Moist, stiff, sandy lean CLAY	13.7	
2.59-3.05	SC-SM	Moist, medium dense, silty clayey SAND	16.8	Water table encountered at 3.81 meters.
4.12-4.57	ML	Wet, very stiff, sandy SILT	24.0	
5.64-6.10	SW-SM	Wet, dense, well-graded SAND w/ silt	30.3	The boring was terminated at 6.10 meters.

Figure F.11 Boring log for Frankfort Maintenance Unit boring 1.

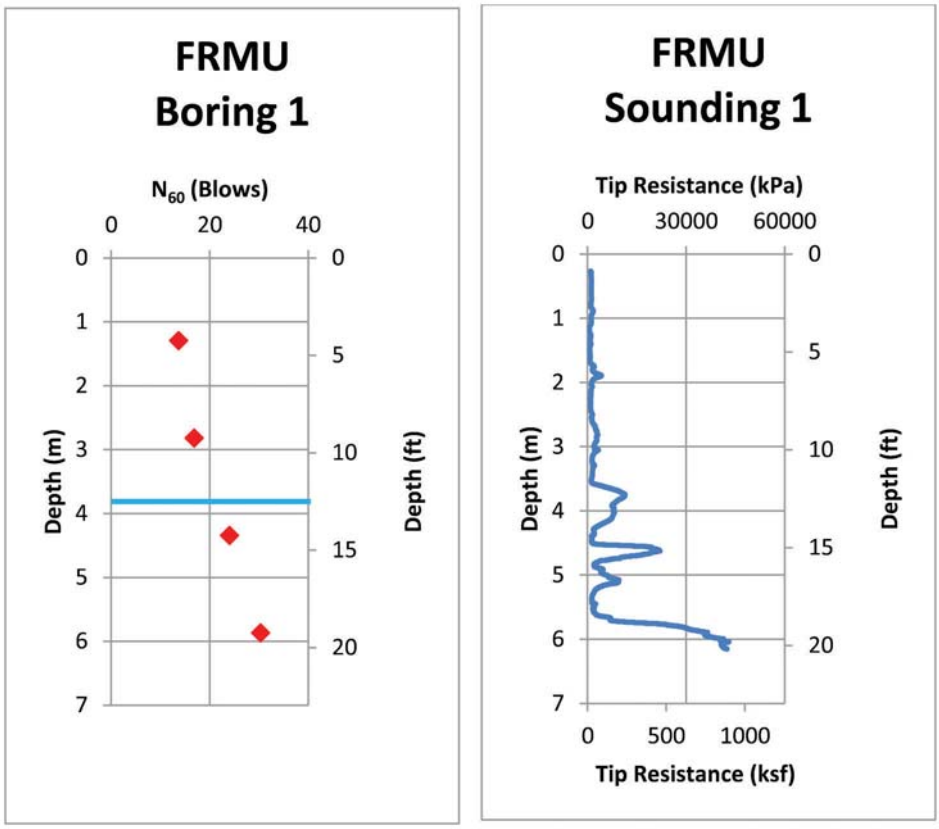

Figure F.12 Frankfort Maintenance Unit SPT boring 1 terminated at a depth of 6.10 meters with the adjacent CPT sounding terminated at a depth of 6.16 meters.

Site: Frankfort Maintenance Unit
Date: 4-Jan-12
Boring: 3
Surface Elevation (m): 264.33

Final Depth (m): 4.57
Groudwater Depth (m): 3.81
Drill Rig: ATV
Drilling Method: 82.5I.D./165O.D. H.S.A.

Depth (m)	USCS	Description	N_{60} (Blows)	Remarks
1.07-1.52	SM	Moist, medium dense, silty SAND	26.1	
2.59-3.05	SP-SC	Moist, medium dense, poorly-graded SAND w/ silty clay	19.1	Water table encountered at 3.81 meters.
4.12-4.57	SM	Wet, dense, silty SAND	33.1	The boring was terminated at 4.57 meters.

Figure F.13 Boring log for Frankfort Maintenance Unit boring 3.

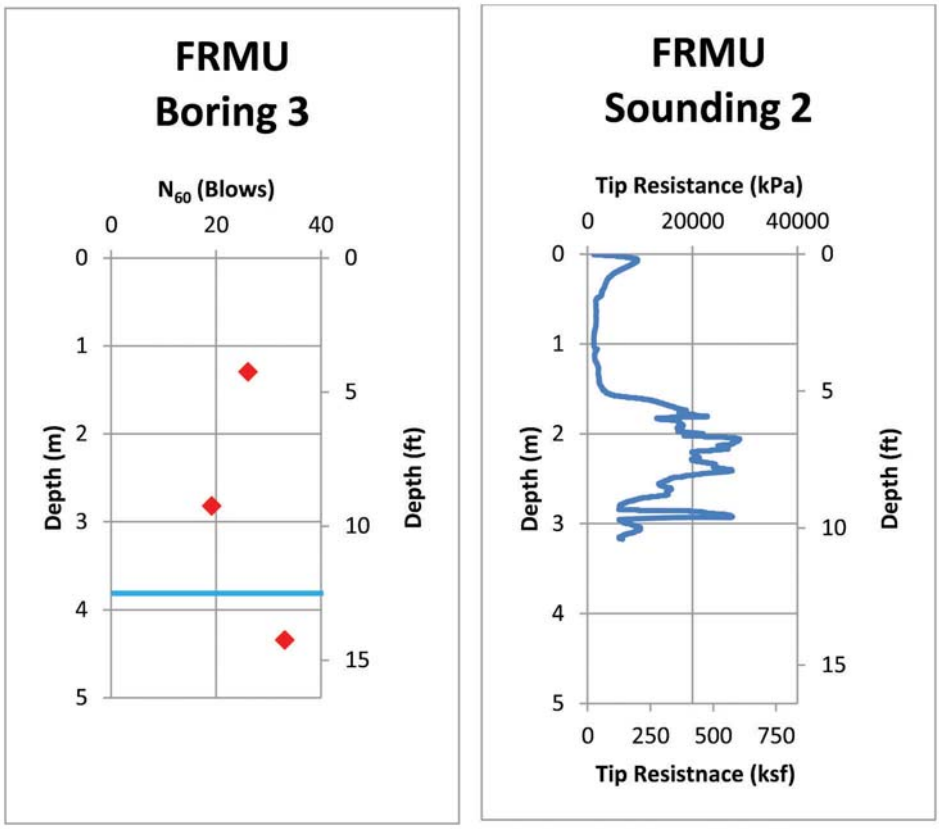

Figure F.14 Frankfort Maintenance Unit SPT boring 3 terminated at a depth of 4.57 meters with the adjacent CPT sounding terminated at a depth of 3.17 meters.

Site: Frankfort Maintenance Unit
Date: 5-Jan-12
Boring: 4
Surface Elevation (m): 264.33

Final Depth (m): 4.57
Groudwater Depth (m): 3.81
Drill Rig: ATV
Drilling Method: 82.5I.D./165O.D. H.S.A.

Depth (m)	USCS	Description	N_{60} (Blows)	Remarks
1.07-1.52	SC-SM	Moist, medium dense, silty clayey SAND	19.5	
2.59-3.05	SM	Moist, very dense, silty SAND	50.1	Water table encountered at 3.81 meters.
4.12-4.57		grading wet and medium dense	23.4	The boring was terminated at 4.57 meters.

Figure F.15 Boring log for Frankfort Maintenance Unit boring 4.

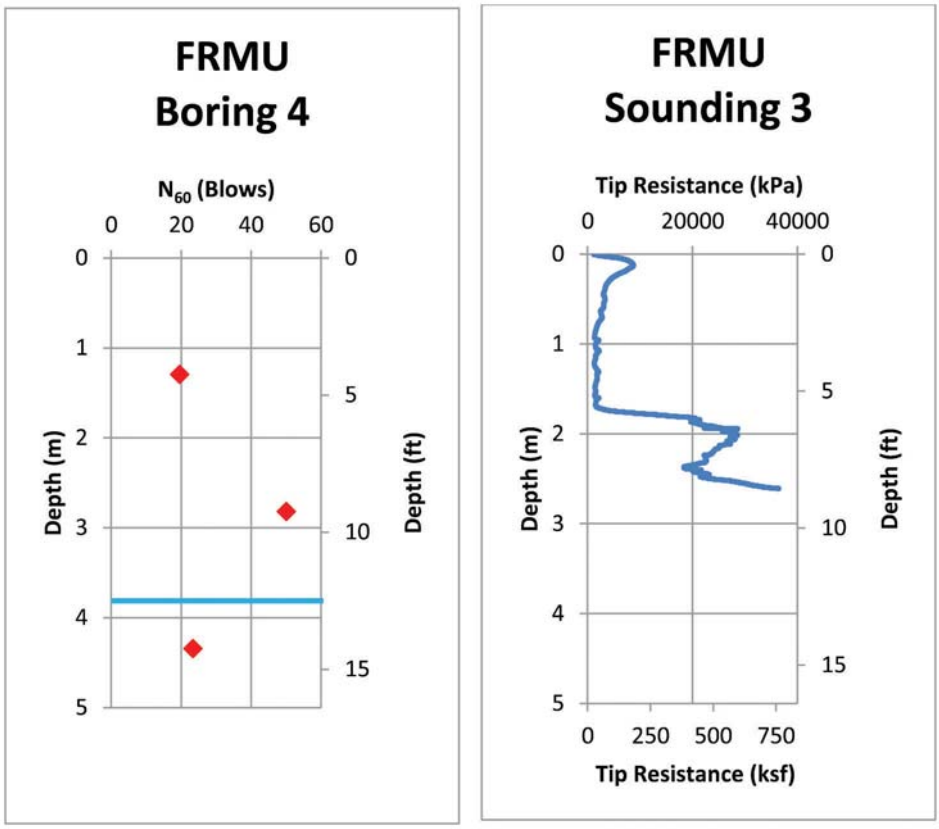

Figure F.16 Frankfort Maintenance Unit SPT boring 4 terminated at a depth of 4.57 meters with the adjacent CPT sounding terminated at a depth of 2.74 meters.

Site: Frankfort Maintenance Unit
Date: 5-Jan-12
Boring: 5
Surface Elevation (m): 264.33

Final Depth (m): 4.57
Groudwater Depth (m): 3.81
Drill Rig: ATV
Drilling Method: 82.5I.D./165O.D. H.S.A.

Depth (m)	USCS	Description	N_{60} (Blows)	Remarks
1.07-1.52	SC-SM	Moist, medium dense, silty clayey SAND	13.0	
2.59-3.05	SM	Moist, dense, silty SAND	39.7	Water table encountered at 3.81 meters.
4.12-4.57		grading wet	33.1	The boring was terminated at 4.57 meters.

Figure F.17 Boring log for Frankfort Maintenance Unit boring 5.

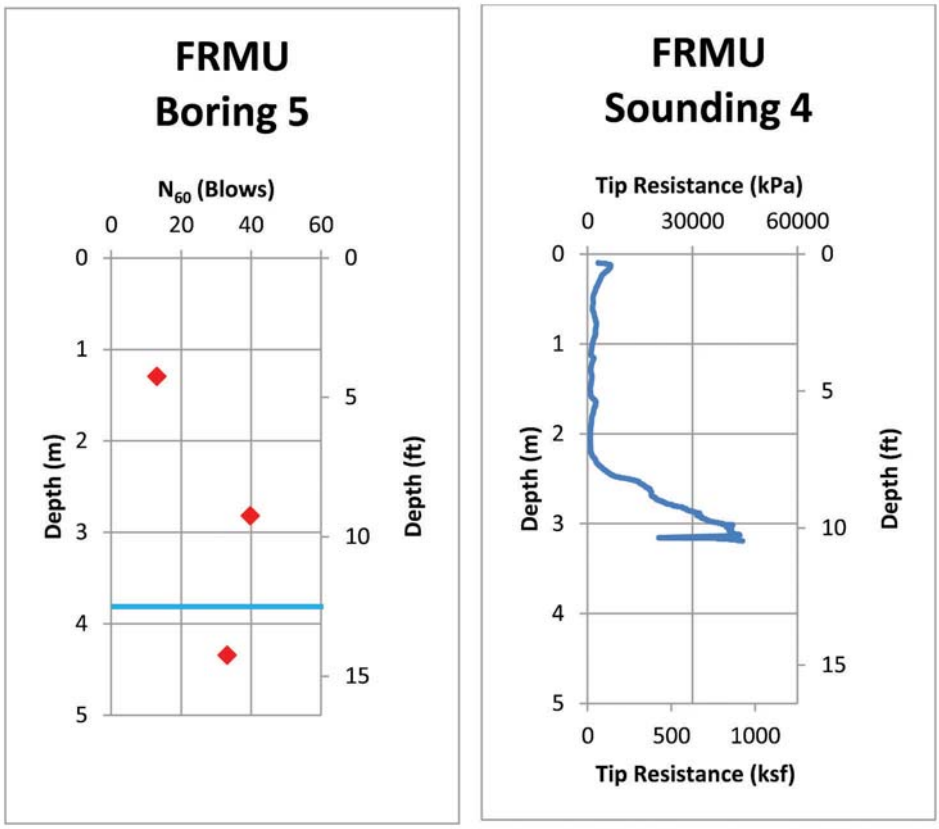

Figure F.18 Frankfort Maintenance Unit SPT boring 5 terminated at a depth of 4.57 meters with the adjacent CPT sounding terminated at a depth of 3.19 meters.

Site: Frankfort Maintenance Unit
Date: 5-Jan-12
Boring: 6
Surface Elevation (m): 264.33

Final Depth (m): 4.57
Groudwater Depth (m): 3.81
Drill Rig: ATV
Drilling Method: 82.5I.D./165O.D. H.S.A.

Depth (m)	USCS	Description	N_{60} (Blows)	Remarks
1.07-1.52	SM	Moist, dense, silty SAND	36.9	
2.59-3.05		grading very dense	58.9	Water table encountered at 3.81 meters.
4.12-4.57	ML	Wet, hard, sandy SILT	43.8	The boring was terminated at 4.57 meters.

Figure F.19 Boring log for Frankfort Maintenance Unit boring 6.

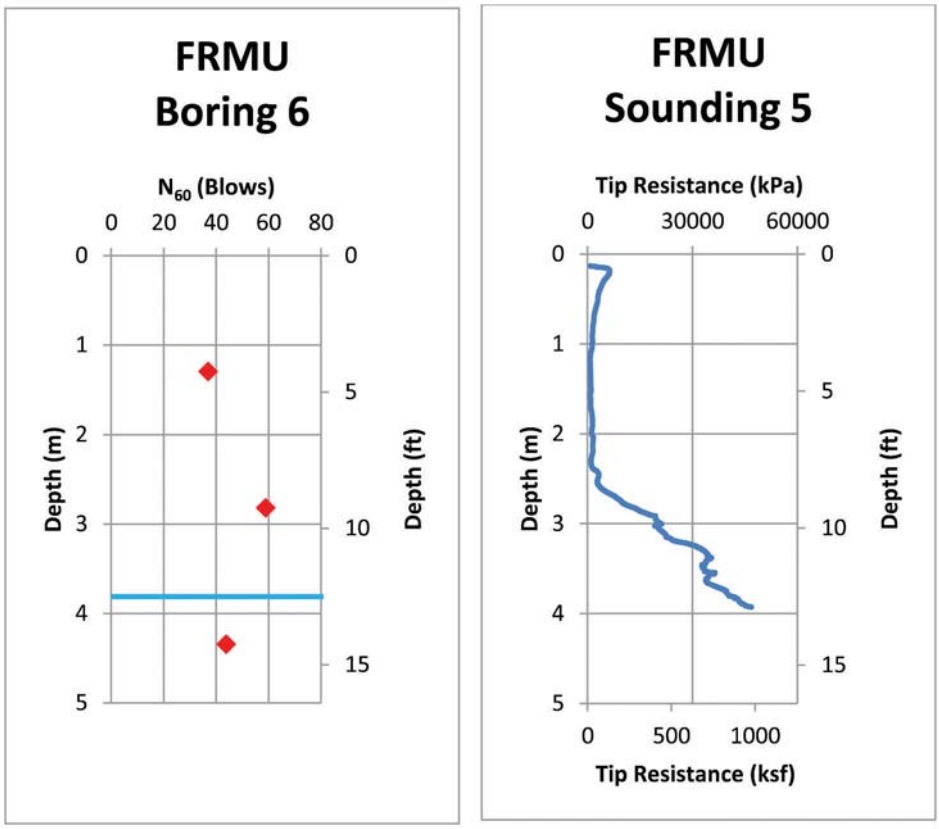

Figure F.20 Frankfort Maintenance Unit SPT boring 6 terminated at a depth of 4.57 meters with the adjacent CPT sounding terminated at a depth of 3.93 meters.

Site: Frankfort Maintenance Unit
Date: 6-Jan-12
Boring: 7
Surface Elevation (m): 264.33

Final Depth (m): 4.57
Groudwater Depth (m): 3.81
Drill Rig: ATV
Drilling Method: 82.5I.D./165O.D. H.S.A.

Depth (m)	USCS	Description	N_{60} (Blows)	Remarks
1.07-1.52	CL	Moist, very stiff, sandy lean CLAY	18.2	
2.59-3.05	CL-ML	Moist, stiff, sandy silty CLAY	13.8	Water table encountered at 3.81 meters.
4.12-4.57		grading wet and hard	46.8	The boring was terminated at 4.57 meters.

Figure F.21 Boring log for Frankfort Maintenance Unit boring 7.

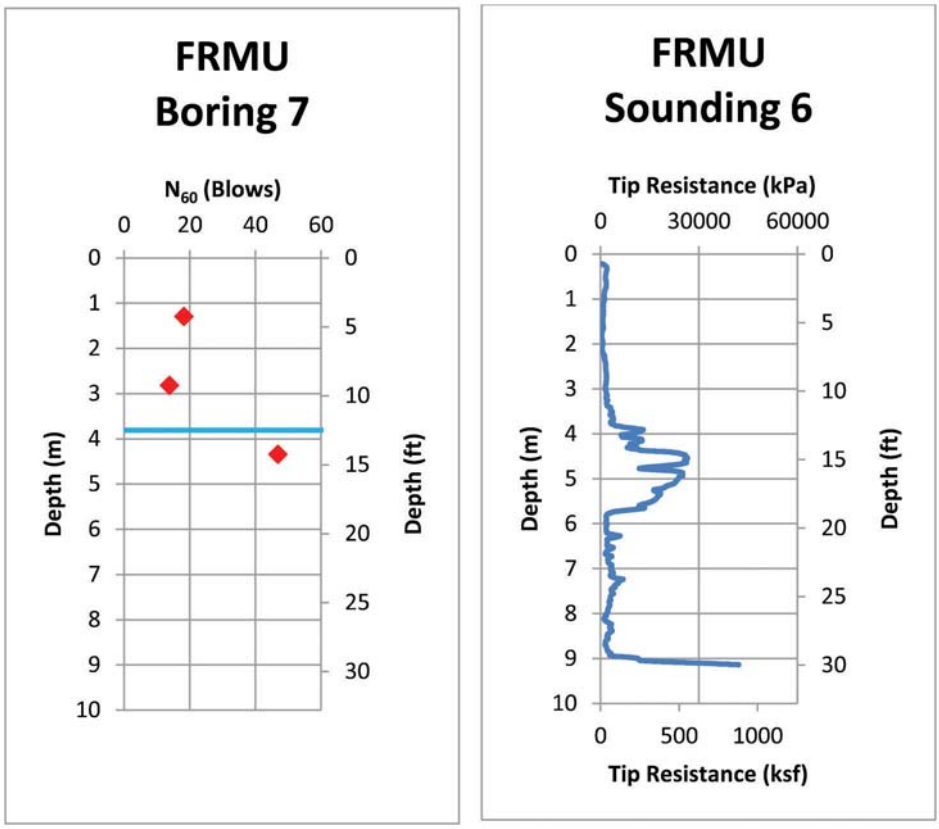

Figure F.22 Frankfort Maintenance Unit SPT boring 7 terminated at a depth of 4.57 meters with the adjacent CPT sounding terminated at a depth of 9.14 meters.

Site: Frankfort Maintenance Unit
Date: 6-Jan-12
Boring: 8
Surface Elevation (m): 264.33

Final Depth (m): 6.10
Groudwater Depth (m): 3.81
Drill Rig: ATV
Drilling Method: 82.5I.D./165O.D. H.S.A.

Depth (m)	USCS	Description	N_{60} (Blows)	Remarks
1.07-1.52	CL	Moist, very stiff, lean CLAY w/ sand	18.2	
2.59-3.05		grading sandy	16.9	Water table encountered at 3.81 meters.
4.12-4.57	CL-ML	Wet, hard, sandy silty CLAY	59.5	
5.64-6.10	SM	Wet, medium dense, silty SAND	16.4	The boring was terminated at 6.10 meters.

Figure F.23 Boring log for Frankfort Maintenance Unit boring 8.

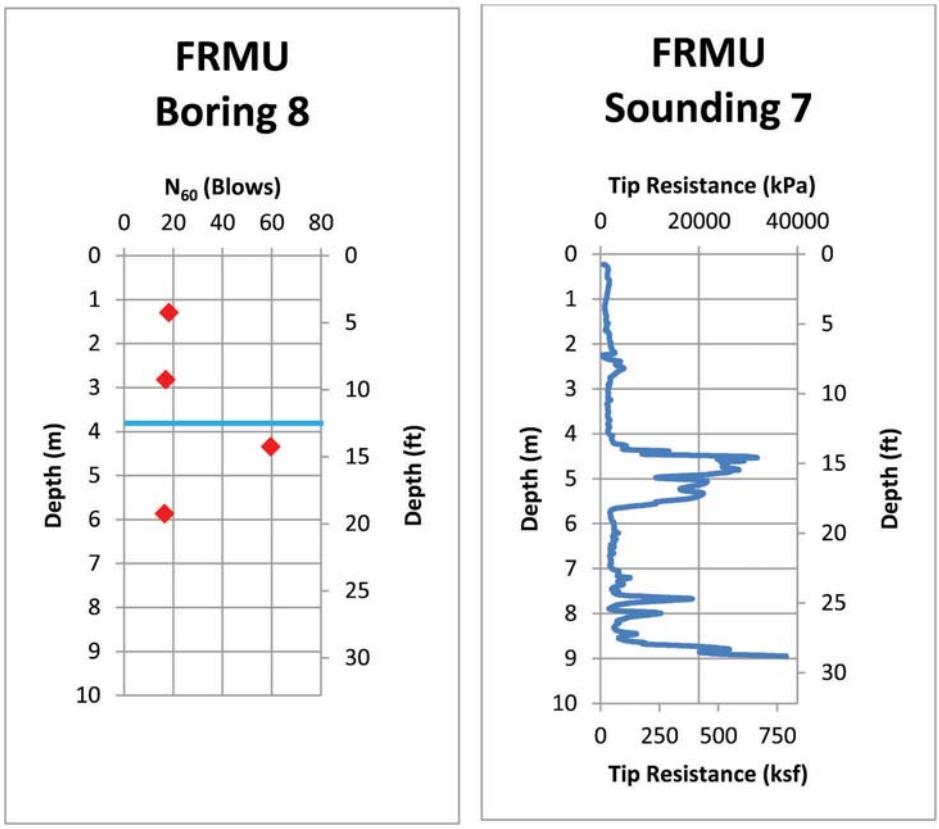

Figure F.24 Frankfort Maintenance Unit SPT boring 8 terminated at a depth of 6.10 meters with the adjacent CPT sounding terminated at a depth of 8.95 meters.

Site: Romney Maintenance Unit
Date: 9-Jan-12
Boring: 1
Surface Elevation (m): 233.23

Final Depth (m): 6.10
Groudwater Depth (m): 5.49
Drill Rig: ATV
Drilling Method: 82.5I.D./165O.D. H.S.A.

Depth (m)	USCS	Description	N_{60} (Blows)	Remarks
1.07-1.52	SP-SC	Moist, dense, poorly-graded SAND w/ silty clay and gravel	30.4	
2.59-3.05	SW-SC	Moist, dense, well-graded SAND w/ silty clay and gravel	45.2	
4.12-4.57	ML	Moist, very stiff, sandy SILT	18.6	Water table encountered at 5.49 meters.
5.64-6.10	SM	Wet, medium dense, silty SAND	14.0	The boring was terminated at 6.10 meters.

Figure F.25 Boring log for Romney Maintenance Unit boring 1.

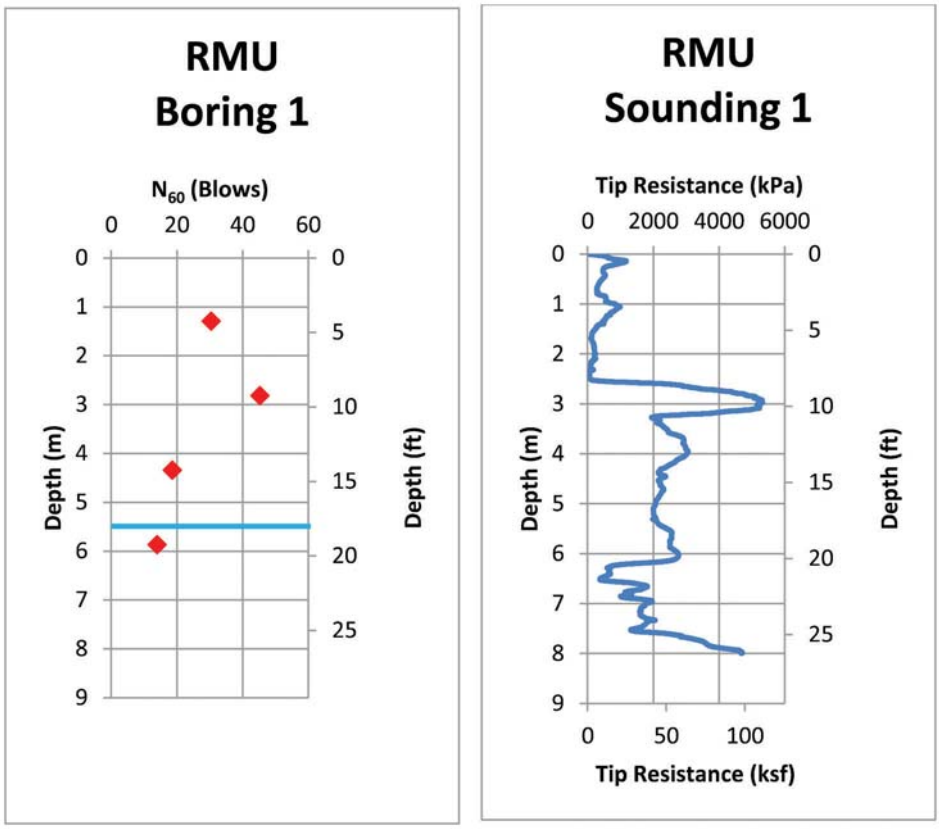

Figure F.26 Romney Maintenance Unit SPT boring 1 terminated at a depth of 6.10 meters with the adjacent CPT sounding terminated at a depth of 7.99 meters.

Site: Romney Maintenance Unit
Date: 9-Jan-12
Boring: 2
Surface Elevation (m): 233.23

Final Depth (m): 7.62
Groudwater Depth (m): 5.49
Drill Rig: ATV
Drilling Method: 82.5I.D./165O.D. H.S.A.

Depth (m)	USCS	Description	N_{60} (Blows)	Remarks
1.07-1.52	GW	Moist, dense, well-graded GRAVEL w/ sand	42.8	
2.59-3.05	ML	Moist, stiff, SILT	16.8	
4.12-4.57	SM	Moist, medium dense, silty SAND	20.9	Water table encountered at 5.49 meters.
5.64-6.10	ML	Wet, stiff, sandy SILT	16.0	
7.16-7.62		grading hard	38.1	The boring was terminated at 7.62 meters.

Figure F.27 Boring log for Romney Maintenance Unit boring 2.

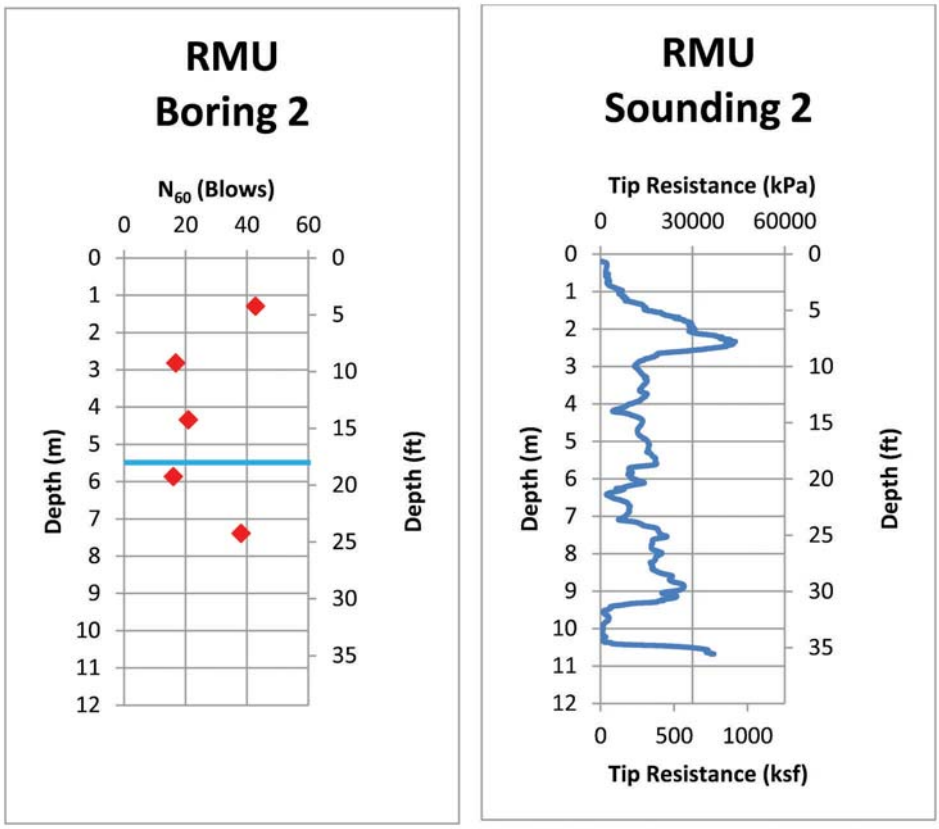

Figure F.28 Romney Maintenance Unit SPT boring 2 terminated at a depth of 7.62 meters with the adjacent CPT sounding terminated at a depth of 10.67 meters.

Site:	Romney Maintenance Unit	Final Depth (m):	6.10
Date:	9-Jan-12	Groudwater Depth (m):	5.49
Boring:	3	Drill Rig:	ATV
Surface Elevation (m):	233.23	Drilling Method:	82.5I.D./165O.D. H.S.A.

Depth (m)	USCS	Description	N_{60} (Blows)	Remarks
1.07-1.52	SP-SM	Moist, dense, poorly-graded SAND w/ silt and gravel	50.0	
2.59-3.05	SM	Moist, medium dense, silty SAND	25.0	
4.12-4.57			22.9	Water table encountered at 5.49 meters.
5.64-6.10	ML	Wet, very stiff, sandy SILT	19.9	The boring was terminated at 6.10 meters.

Figure F.29 Boring log for Romney Maintenance Unit boring 3.

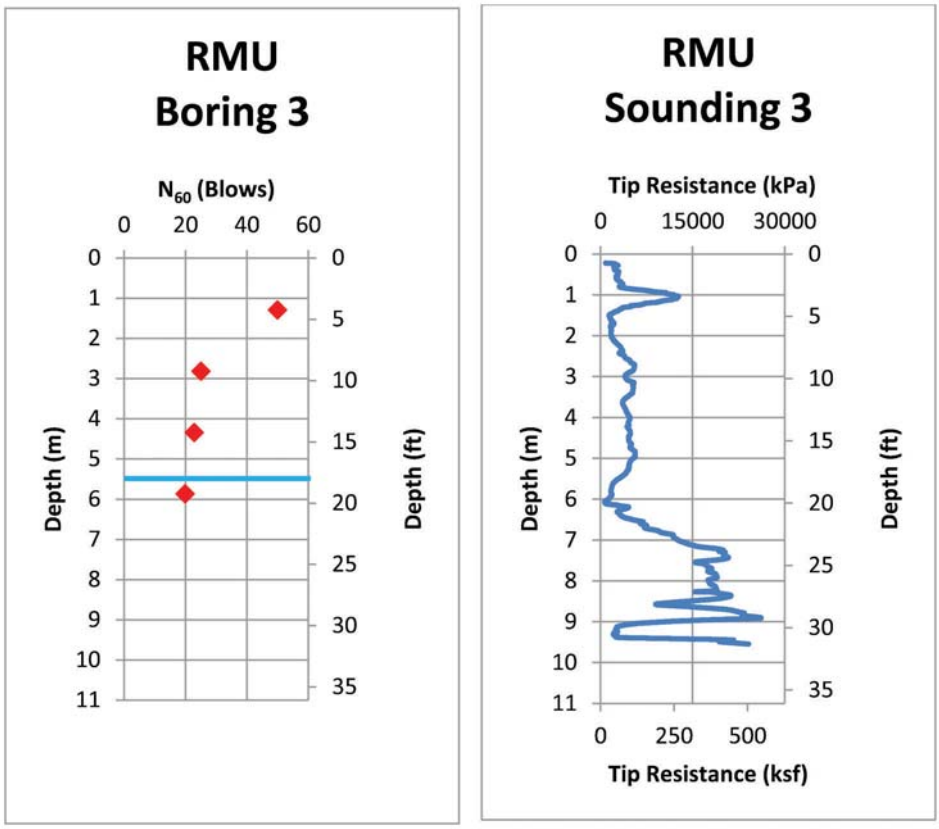

Figure F.30 Romney Maintenance Unit SPT boring 3 terminated at a depth of 6.10 meters with the adjacent CPT sounding terminated at a depth of 9.54 meters.

Site: Romney Maintenance Unit
Date: 10-Jan-12
Boring: 4
Surface Elevation (m): 233.23

Final Depth (m): 6.10
Groudwater Depth (m): 5.49
Drill Rig: ATV
Drilling Method: 82.5I.D./165O.D. H.S.A.

Depth (m)	USCS	Description	N_{60} (Blows)	Remarks
1.07-1.52	SP-SM	Moist, dense, poorly-graded SAND w/ silt and gravel	34.7	
2.59-3.05	SM	Moist, medium dense, silty SAND	20.6	
4.12-4.57			21.5	
				Water table encountered at 5.49 meters.
5.64-6.10			19.9	The boring was terminated at 6.10 meters.

Figure F.31 Boring log for Romney Maintenance Unit boring 4.

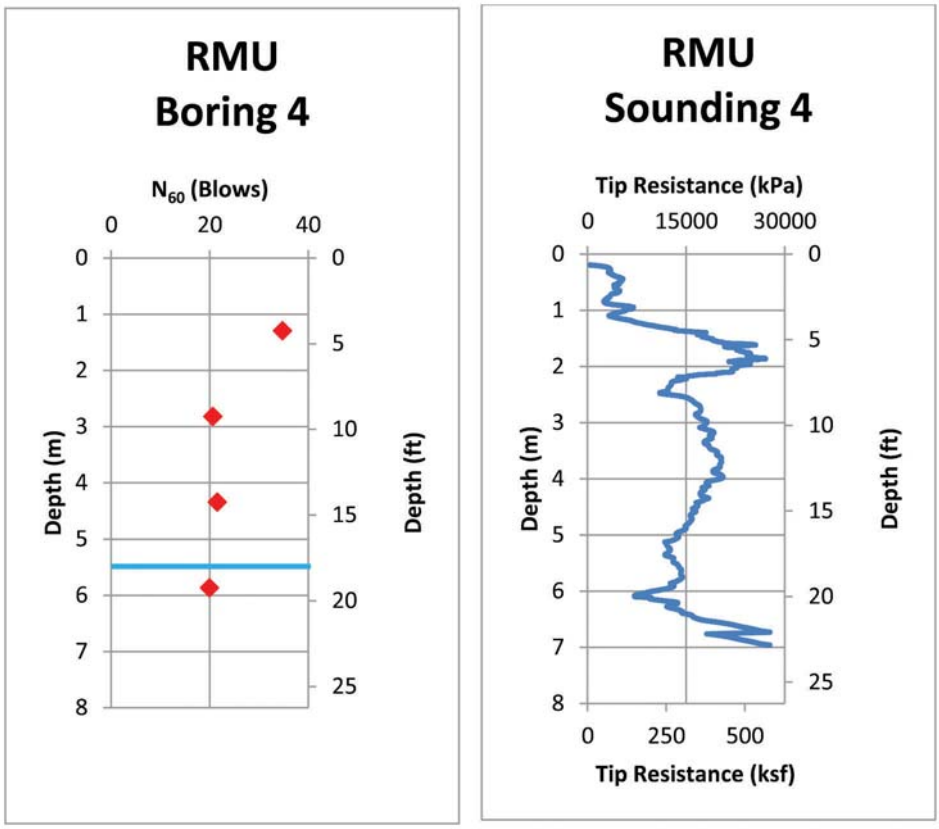

Figure F.32 Romney Maintenance Unit SPT boring 4 terminated at a depth of 6.10 meters with the adjacent CPT sounding terminated at a depth of 6.95 meters.

Site: Romney Maintenance Unit
Date: 10-Jan-12
Boring: 5
Surface Elevation (m): 233.23

Final Depth (m): 6.10
Groudwater Depth (m): 5.49
Drill Rig: ATV
Drilling Method: 82.5I.D./165O.D. H.S.A.

Depth (m)	USCS	Description	N_{60} (Blows)	Remarks
1.07-1.52	SP-SM	Moist, dense, poorly-graded SAND w/ silt and gravel	45.6	
2.59-3.05	ML	Moist, very stiff, SILT w/ sand	29.6	
4.12-4.57	SM	Moist, medium dense, silty SAND	25.7	Water table encountered at 5.49 meters.
5.64-6.10	ML	Wet, very stiff, SILT	24.7	The boring was terminated at 6.10 meters.

Figure F.33 Boring log for Romney Maintenance Unit boring 5.

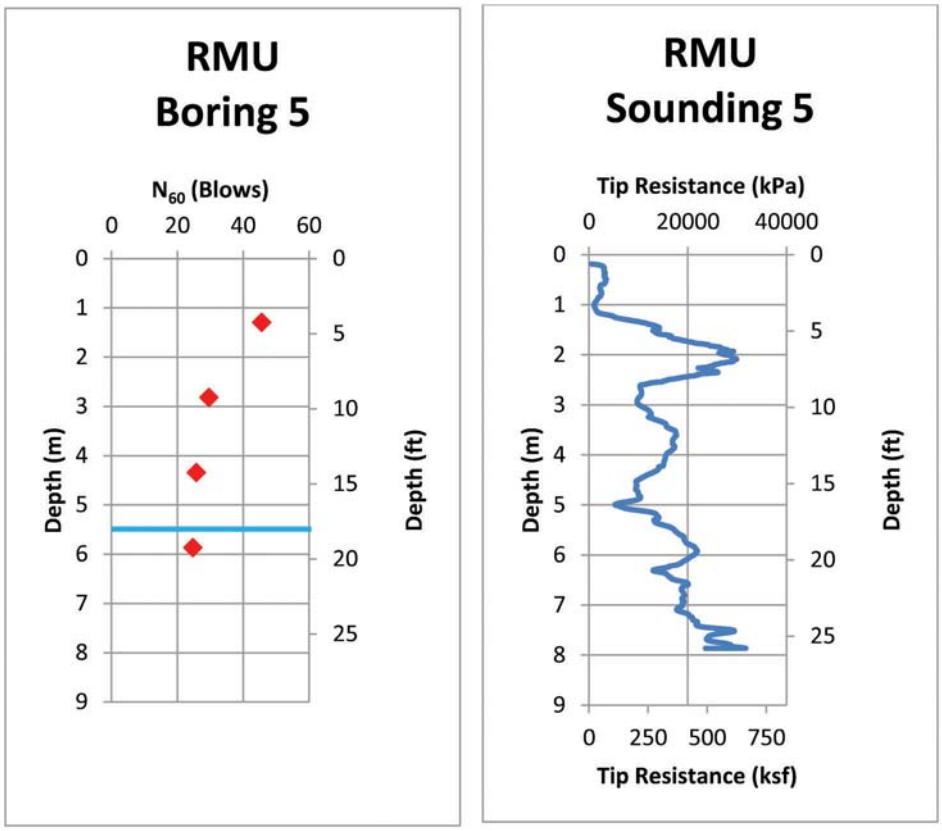

Figure F.34 Romney Maintenance Unit SPT boring 5 terminated at a depth of 6.10 meters with the adjacent CPT sounding terminated at a depth of 7.87 meters.

Site: Romney Maintenance Unit
Date: 10-Jan-12
Boring: 6
Surface Elevation (m): 233.23

Final Depth (m): 6.10
Groudwater Depth (m): 5.49
Drill Rig: ATV
Drilling Method: 82.5I.D./165O.D. H.S.A.

Depth (m)	USCS	Description	N_{60} (Blows)	Remarks
1.07-1.52	SP-SM	Moist, medium dense, poorly-graded SAND w/ silt and gravel	21.7	
2.59-3.05	SM	Moist, medium dense, silty SAND w/ gravel	25.0	
4.12-4.57		grading out gravel	21.5	Water table encountered at 5.49 meters.
5.64-6.10	ML	Wet, very stiff, sandy SILT	21.1	The boring was terminated at 6.10 meters.

Figure F.35 Boring log for Romney Maintenance Unit boring 6.

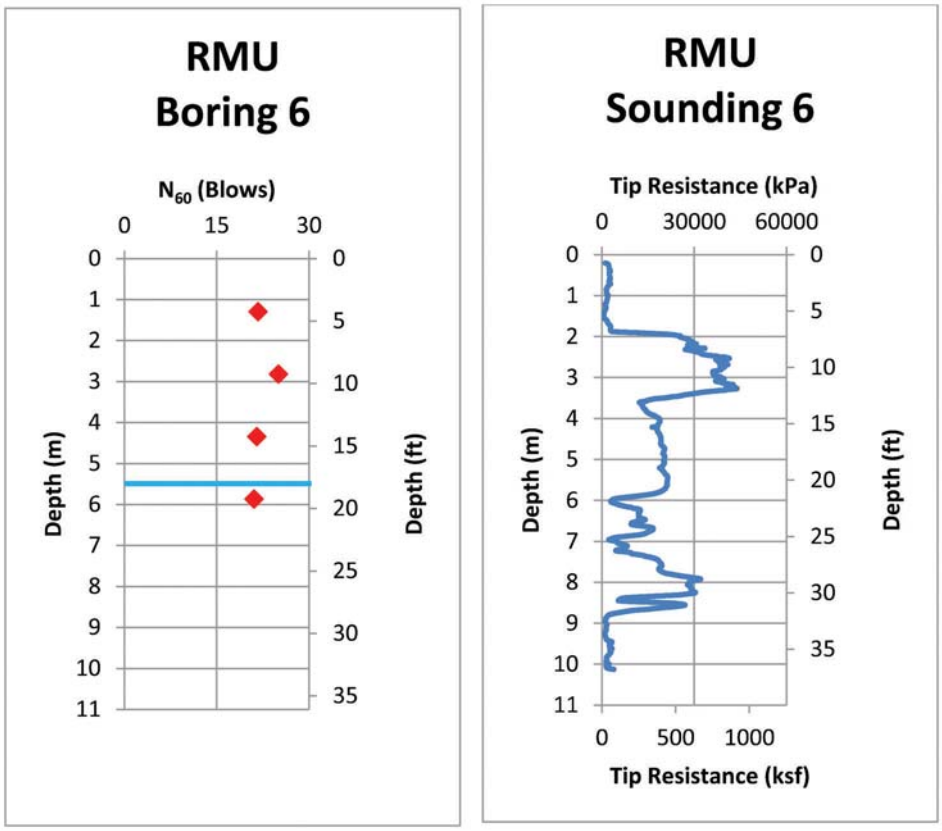

Figure F.36 Romney Maintenance Unit SPT boring 6 terminated at a depth of 6.10 meters with the adjacent CPT sounding terminated at a depth of 10.12 meters.

Site:	Koleen Interstate 69 Expansion Site	Final Depth (m):	9.15
Date:	16-Jul-12	Groudwater Depth (m):	2.18
Boring:	1	Drill Rig:	ATV
Surface Elevation (m):	158.84	Drilling Method:	82.5I.D./165O.D. H.S.A.

Depth (m)	USCS	Description	N_{60} (Blows)	Remarks
1.07-1.52	CL	Moist, stiff, lean CLAY	11.2	
2.59-3.05		grading wet and firm	6.6	
4.12-4.57			7.2	
5.64-6.10		grading stiff	9.7	
7.16-7.62		grading soft	3.3	
8.69-9.15		grading firm	6.5	The boring was terminated at 9.15 meters.

Figure F.37 Boring log for Koleen Site boring 1.

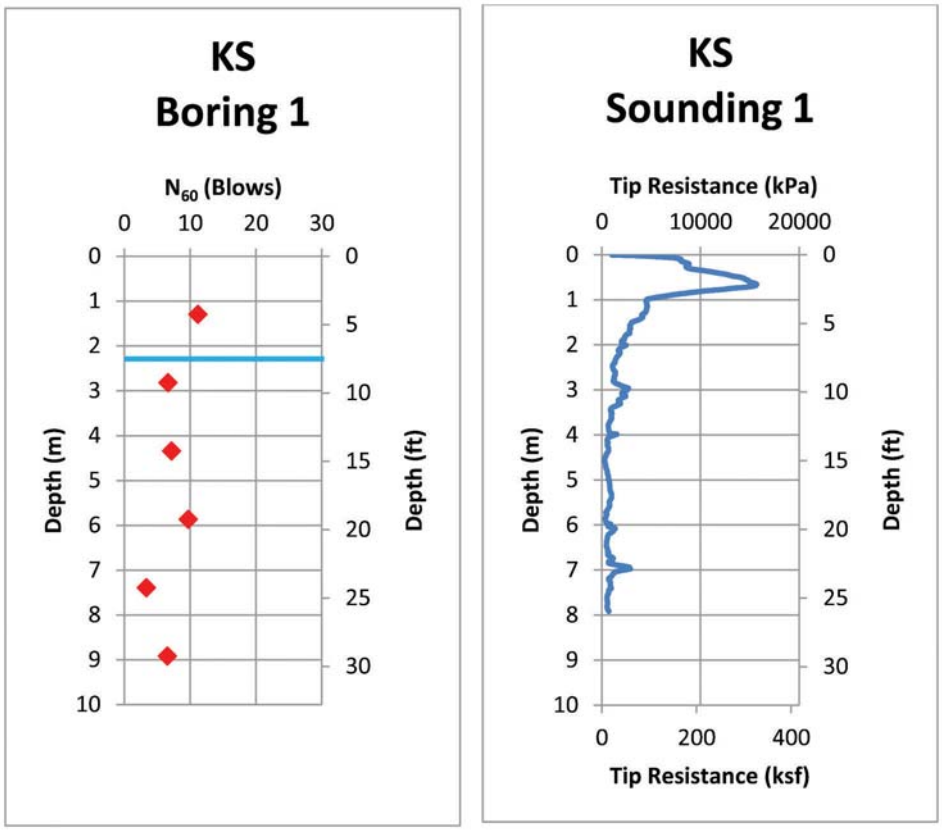

Figure F.38 Koleen site SPT boring 1 terminated at a depth of 9.15 meters with the adjacent CPT sounding terminated at a depth of 7.92 meters.

Site:	Koleen Interstate 69 Expansion Site	Final Depth (m):	9.15
Date:	16-Jul-12	Groudwater Depth (m):	2.18
Boring:	2	Drill Rig:	ATV
Surface Elevation (m):	158.84	Drilling Method:	82.5I.D./165O.D. H.S.A.

Depth (m)	USCS	Description	N_{60} (Blows)	Remarks
1.07-1.52	CL	Moist, stiff, lean CLAY	8.3	
2.59-3.05		grading wet	9.7	
4.12-4.57		grading firm	5.3	
5.64-6.10		grading soft	3.0	
7.16-7.62			2.2	
8.69-9.15			3.3	The boring was terminated at 9.15 meters.

Figure F.39 Boring log for Koleen Site boring 2.

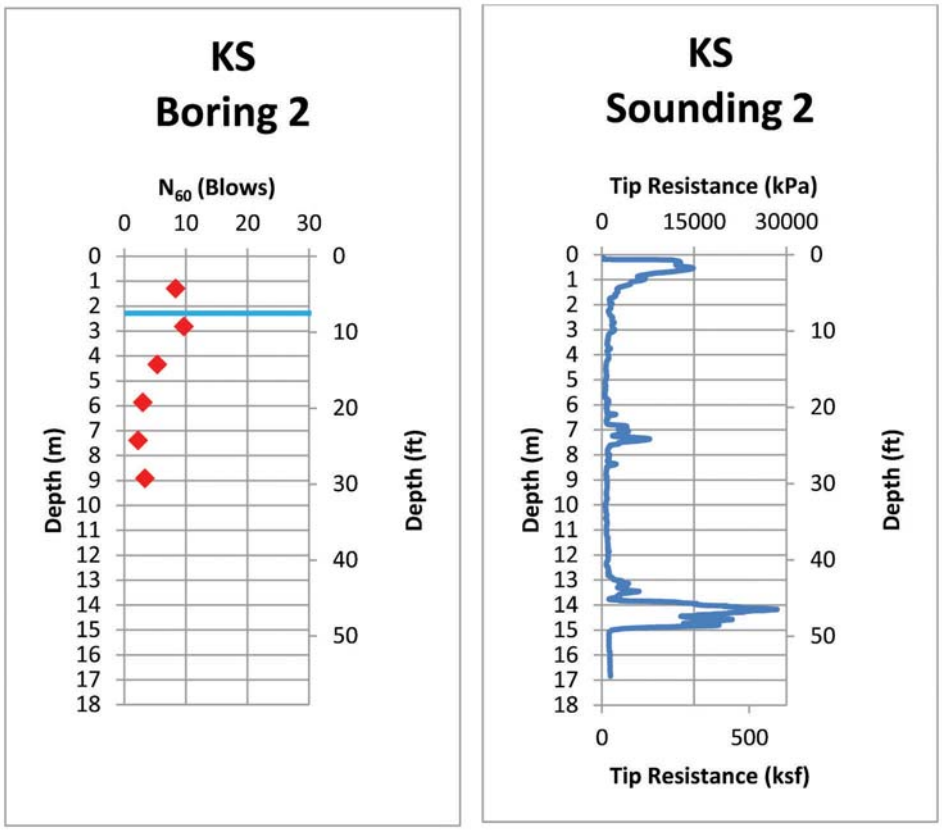

Figure F.40 Koleen site SPT boring 2 terminated at a depth of 9.15 meters with the adjacent CPT sounding terminated at a depth of 16.85 meters.

Site:	Koleen Interstate 69 Expansion Site	Final Depth (m):	9.15
Date:	17-Jul-12	Groudwater Depth (m):	2.18
Boring:	3	Drill Rig:	ATV
Surface Elevation (m):	158.84	Drilling Method:	82.5I.D./165O.D. H.S.A.

Depth (m)	USCS	Description	N_{60} (Blows)	Remarks
1.07-1.52	CL	Moist, stiff, lean CLAY	11.3	
2.59-3.05		grading wet and firm	6.5	
4.12-4.57		grading firm	4.5	
5.64-6.10			4.0	
7.16-7.62		grading stiff	12.6	
8.69-9.15			8.0	The boring was terminated at 9.15 meters.

Figure F.41 Boring log for Koleen Site boring 3.

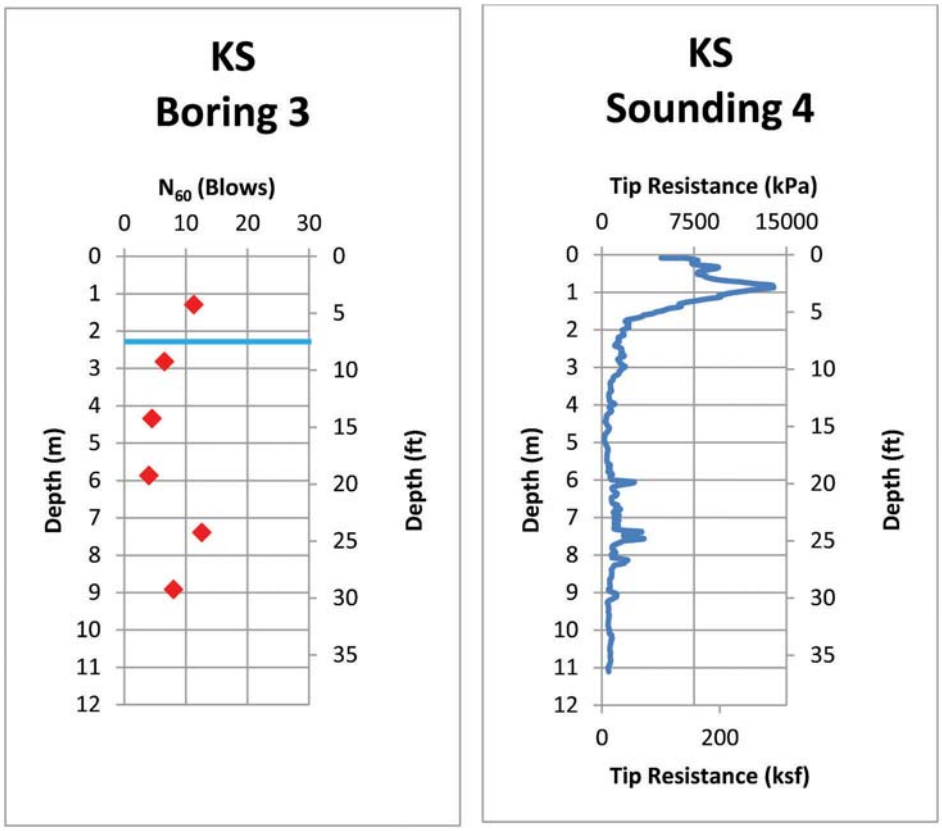

Figure F.42 Koleen site SPT boring 3 terminated at a depth of 9.15 meters with the adjacent CPT sounding terminated at a depth of 11.11 meters.

Site:	Koleen Interstate 69 Expansion Site	Final Depth (m):	15.24
Date:	19-Jul-12	Groudwater Depth (m):	2.18
Boring:	5	Drill Rig:	ATV
Surface Elevation (m):	158.84	Drilling Method:	82.5I.D./165O.D. H.S.A.

Depth (m)	USCS	Description	N_{60} (Blows)	Remarks
1.07-1.52	CL	Moist, stiff, lean CLAY	8.2	
2.59-3.05		grading wet and firm	7.9	
4.12-4.57		grading soft	3.2	
5.64-6.10			3.0	
7.16-7.62		grading firm	4.5	
8.69-9.15		grading soft	3.3	
10.21-10.67			3.5	
11.74-12.20		grading firm	4.7	
13.25-13.72	ML	Wet, firm, SILT	7.6	
14.79-15.24		grading stiff	14.7	The boring was terminated at 15.24 meters.

Figure F.43 Boring log for Koleen Site boring 5.

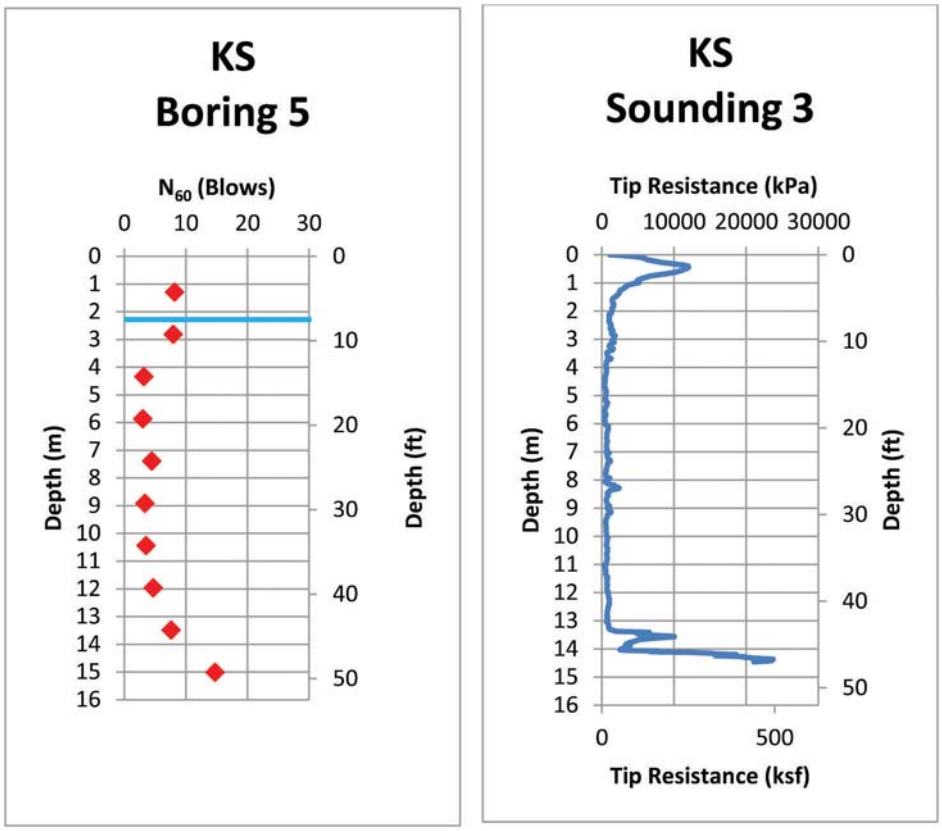

Figure F.44 Koleen site SPT boring 5 terminated at a depth of 15.24 meters with the adjacent CPT sounding terminated at a depth of 14.47 meters.

About the Joint Transportation Research Program (JTRP)

On March 11, 1937, the Indiana Legislature passed an act which authorized the Indiana State Highway Commission to cooperate with and assist Purdue University in developing the best methods of improving and maintaining the highways of the state and the respective counties thereof. That collaborative effort was called the Joint Highway Research Project (JHRP). In 1997 the collaborative venture was renamed as the Joint Transportation Research Program (JTRP) to reflect the state and national efforts to integrate the management and operation of various transportation modes.

The first studies of JHRP were concerned with Test Road No. 1—evaluation of the weathering characteristics of stabilized materials. After World War II, the JHRP program grew substantially and was regularly producing technical reports. Over 1,500 technical reports are now available, published as part of the JHRP and subsequently JTRP collaborative venture between Purdue University and what is now the Indiana Department of Transportation.

Free online access to all reports is provided through a unique collaboration between JTRP and Purdue Libraries. These are available at: http://docs.lib.purdue.edu/jtrp

Further information about JTRP and its current research program is available at: http://www.purdue.edu/jtrp

About This Report

An open access version of this publication is available online. This can be most easily located using the Digital Object Identifier (doi) listed below. Pre-2011 publications that include color illustrations are available online in color but are printed only in grayscale.

The recommended citation for this publication is:

Prezzi, M., Scheilz, S., Salgado, R., & Siddiki, N. Z. (2014). *Development of SPT-torque test correlations for glacial till* (Joint Transportation Research Program Publication No. FHWA/IN/JTRP-2014/05). West Lafayette, IN: Purdue University. http://dx.doi.org/10.5703/1288284315499